

Czech University of Life Sciences Prague
Faculty of Forestry and Wood Sciences



**Detecting the effect of non-climatic factors on climatic
sensitivity of Norway Spruce in Central Europe via a
multi-parameter approach**

Doctoral Thesis

MSc. Yumei Jiang

Supervisor: Miloš Rydval, Ph.D.

Prague 2024

Ph.D. THESIS ASSIGNMENT

MSc. Yumei Jiang

Global Change Forestry

Thesis title

Detecting the effect of non-climatic factors on climatic sensitivity of Norway Spruce in Central Europe via a multi-parameter approach

Objectives of thesis

Tree growth is influenced by both climatic and non-climatic factors. While considerable research has been performed to understand ecological and climatic relationships and signals in tree-ring datasets separately, less attention has been given to the impacts of non-climatic factors on climatic signals in widely used tree ring parameters in dendroclimatological research. Considering the characteristics of Central European forests, on the one hand, forests in the Carpathian Mountains have been subjected to disturbance events over long time periods; on the other hand, Czech forests have experienced a period of severe pollution in the late 20th century, especially in the area of the so-called Black Triangle. Moreover, these forests also experienced several extreme droughts, particularly in recent decades. The objective of this thesis is to uncover the impacts of these climatic and non-climatic factors on the growth of Norway spruce trees with a particular focus on the impacts of non-climatic factors on the climatic sensitivity of different tree-ring parameters. The specific objectives of the thesis are:

- 1) Detecting disturbance signatures in both tree-ring width and Blue Intensity chronologies on various spatial and temporal scales by applying a novel statistical method (Curve Intervention Detection), as well as exploring the extent to which temperature signals are affected by the detected disturbance signatures.
- 2) Detecting pollution signatures in tree-ring width chronologies from historically heavily polluted areas and investigating their impact on temperature signals of multiple tree-ring parameters (i.e., tree-ring width, Blue Intensity, quantitative wood anatomy) in different time periods with varying pollution intensity.
- 3) Investigating the impacts of several severe drought events in the past and a recent drought period on the growth of several major tree species in Central European forests, as well as examining the drivers of drought resistance of different species using a modeling approach.

Methodology

To achieve the objectives of this thesis, a large number of tree ring samples was collected from the studied region, which was historically influenced by a range of ecological and environmental factors. Chronologies

of several types of tree-ring parameters were generated and compared to investigate their susceptibility to the impact of these factors. The Curve Intervention Detection method was used to quantify the impacts of non-climatic factors on the structure of tree-ring chronologies. Growth-climate response analysis was conducted for all generated parameters to identify tree ring parameters with stronger temperature signals that are less impacted by non-climatic factors, and which may therefore be more suitable for dendroclimatic purposes such as the development of dendroclimatic reconstructions. Impacts of drought on tree growth as well as on their drought resistance were investigated by evaluating trends represented by both tree ring width and basal area increment.



The proposed extent of the thesis

80-150 SP

Keywords

Disturbance trend biases; Sulphur/nitrogen deposition; Drought resistance; Latewood Blue Intensity; Quantitative wood anatomy; Temperature signal; Curve Intervention Detection; Climatic extremes; Tree growth reduction

Recommended information sources

- Björklund, J., Rydval, M., Schurman, J. S., Seftigen, K., Trotsiuk, V., Janda, P., Mikoláš, M., Dušátko, M., Čada, V., Bače, R., & Svoboda, M. (2019). Disentangling the multi-faceted growth patterns of primary *Picea abies* forests in the Carpathian arc. *Agricultural and Forest Meteorology*, 271(October 2018), 214–224.
- Lloret, F., Keeling, E. G., & Sala, A. (2011). Components of tree resilience: Effects of successive low-growth episodes in old ponderosa pine forests. *Oikos*, 120(12), 1909–1920.
- Rydval, M., Druckenbrod, D., Anchukaitis, K. J., & Wilson, R. (2015). Detection and removal of disturbance trends in tree-ring series for dendroclimatology. *Canadian Journal of Forest Research*, 46(3), 387–401.
- Rydval, M., Larsson, L. Å., McGlynn, L., Gunnarson, B. E., Loader, N. J., Young, G. H. F., & Wilson, R. (2014). Blue intensity for dendroclimatology: Should we have the blues? Experiments from Scotland. *Dendrochronologia*, 32(3), 191–204.
- Seidl, R., Thom, D., Kautz, M., Martin-Benito, D., Peltoniemi, M., Vacchiano, G., Wild, J., Ascoli, D., Petr, M., Honkaniemi, J., Lexer, M. J., Trotsiuk, V., Mairota, P., Svoboda, M., Fabrika, M., Nagel, T. A., & Reyer, C. P. O. (2017). Forest disturbances under climate change. *Nature Climate Change*, 7(6), 395–402.
- Schurman, J. S., Babst, F., Björklund, J., Rydval, M., Bače, R., Čada, V., Janda, P., Mikolas, M., Saulnier, M., Trotsiuk, V., & Svoboda, M. (2019). The climatic drivers of primary *Picea* forest growth along the Carpathian arc are changing under rising temperatures. *Global Change Biology*, 25(9), 3136–3150.
- Svoboda, M., Janda, P., Bače, R., Fraver, S., Nagel, T. A., Rejzek, J., Mikoláš, M., Douda, J., Boublík, K., Šamonil, P., Čada, V., Trotsiuk, V., Teodosiu, M., Bouriaud, O., Biriş, A. I., Sýkora, O., Uzel, P., Zelenka, J., Sedlák, V., & Lehejček, J. (2014). Landscape-level variability in historical disturbance in primary *Picea abies* mountain forests of the Eastern Carpathians, Romania. *Journal of Vegetation Science*, 25(2), 386–401.
- Vacek, Z., Vacek, S., Prokúpková, A., Bulušek, D., Podrázský, V., Hůnová, I., Putalová, T., & Král, J. (2020). Long-term effect of climate and air pollution on health status and growth of *Picea abies* (L.) Karst. peaty forests in the Black Triangle region. *Dendrobiology*, 83, 1–19.
- Von Arx, G., Crivellaro, A., Prendin, A. L., Čufar, K., & Carrer, M. (2016). Quantitative wood anatomy—practical guidelines. *Frontiers in Plant Science*, 7(JUNE2016), 1–13.
- Wilson, R., Rao, R., Rydval, M., Wood, C., Larsson, L. Å., & Luckman, B. H. (2014). Blue Intensity for dendroclimatology: The BC blues: A case study from British Columbia, Canada. *Holocene*, 24(11), 1428–1438.

Expected date

2023/24 SS – FFWS – State Doctoral Examinations

The Dissertation Thesis Supervisor

Miloš Rydval, Ph.D.

Supervising department

Department of Forest Ecology

Electronic approval: 15. 3. 2024

prof. Ing. Miroslav Svoboda, Ph.D.

Head of department

Electronic approval: 18. 3. 2024

prof. RNDr. Tomáš Hlásny, PhD.

Chairperson of Field of Study Board

Electronic approval: 19. 3. 2024

prof. Ing. Róbert Marušák, PhD.

Dean

Prague on 20. 03. 2024

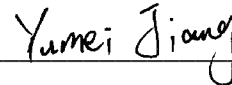
1906

DECLARATION OF INDEPENDENCE

I hereby declare that this Ph.D. Thesis, titled “Detecting the effect of non-climatic factors on climatic sensitivity of Norway Spruce in Central Europe via a multi-parameter approach”, was created independently and in an ethical manner. I declare all the information sources and literature have been indicated accordingly, and the Thesis was produced under direct supervision of my supervisor.

I agree with the disclosure of this Ph.D. Thesis in accordance with the Czech Law (Act No. 111/1998 Coll. Sb.) regardless of the Defense of Thesis results.

March 31st, 2024, Prague



Signature

SUMMARY

In dendroecology and dendroclimatological research, tree rings are used as a paleo-climate proxy. A wide range of research can be conducted using this proxy archive, such as tree growth or forest dynamics monitoring, forest disturbance (e.g., fire history, windstorm, bark beetle, etc.) and paleoclimate reconstructions of various climatic variables (e.g., temperature, precipitation, drought, etc.). However, tree growth and tree ring formation are determined by a complex combination of various climatic and non-climatic factors, making it necessary to distinguish and account for the impacts of climatic and non-climatic sources separately to achieve specific research objectives. By using tree-ring records from an extensive range of Central European forests, this thesis aims to disentangle the impacts of these climatic and non-climatic factors on the growth of Norway spruce trees with a particular focus on the impacts of non-climatic factors on the climatic sensitivity of different tree-ring parameters.

Firstly, I used a disturbance identification technique to detect disturbance signatures in datasets of multiple tree-ring parameters of Norway spruce (*Picea abies*) across the whole range of the Carpathian Mountains and evaluated to what extent natural disturbances influenced the temperature signals in those datasets (**Subsection 3.2/ 4.1/ 5.1**). Though the growth of forests in the studied region has experienced significant interference from various types of environmental events over the past centuries, the disturbance signatures in tree ring chronologies were more easily detectable in a smaller-scale scenario (i.e., at the site level) with reduced sample depth. Additionally, the detected disturbance signatures were mainly observed in tree-ring width chronologies during periods characterized by major growth releases. In contrast, Blue Intensity chronologies were generally less susceptible to disturbance impacts or not influenced at all. Blue Intensity chronologies also exhibited much stronger temperature signals compared to those in tree-ring width chronologies, and such signals were more stable over time.

Secondly, considering the recent pollution history of the Czech Republic and neighboring regions, I examined the impact of pollution on the temperature sensitivity of multiple tree-ring parameters by using the same statistical approach applied in relation to natural disturbances in the Carpathians (**Subsection 3.3/ 4.2/ 5.2**). As part of the research covered in this sub-topic, tree-ring parameters of one additional technique, quantitative wood anatomy, were also included. Pollution-related growth suppression trends were mainly detected in tree-ring width chronologies, especially at sites that experienced severe pollution levels. Growing season temperature signals were well-represented by both latewood Blue Intensity and cell wall

thickness chronologies. The climatic signals in those chronologies outperformed those of the tree-ring width chronologies and tended to remain more stable over time and, unlike tree-ring width, even retained a significant relationship with climatic variables during the period characterized by severe pollution levels.

Lastly, I investigated the impact of recent drought events on the drought resistance of several Central European tree species, considering the distinct drought conditions of the Czech Republic (**Subsection 3.4/ 4.3/ 5.3**). This study helped to contextualize the relative importance of climatic and non-climatic factors for tree growth dynamics in the region. Drought-induced growth reductions were found in all studied species but with different levels of magnitude. Norway spruce was found to be more susceptible to drought impacts compared to other species as it showed the largest growth reduction. The main drivers of drought resistance for different species were also explored. The findings of this research indicated that under the circumstance of climate change, drought-related impacts on forest systems will potentially threaten timber supply sustainability and other services. In addition, when comparing these drought-related impacts to the non-climatic impacts on tree growth, such climatic impacts were much more prominent, which indicated the significance of climate for tree growth.

The overall findings of this thesis revealed that the impacts of non-climatic factors on tree growth and climatic sensitivity are non-negligible, especially when using the tree-ring width parameter. In the context of dendroclimatology, measures need to be taken to better understand and reduce the influence of such impacts. For example, the Curve Intervention Detection method can be used for the identification of growth impacts, whereas the utilization of multiple tree ring parameters can assist with selection of more robust parameters for climate research. This work indicates that Blue Intensity and cell wall thickness have more stable climatic sensitivity characteristics and, in turn, would be more suitable for climate reconstruction purposes in either disturbed or historically polluted areas. This thesis represents a useful reference and inspiration for future studies with regards to alternative tree-ring parameters for specific research purposes or distinguishing and accounting for non-climatic impacts. These observations and recommendations are especially pertinent as forest disturbance events are expected to increase in response to global climate change.

Keywords:

Disturbance trend biases; Sulphur/nitrogen deposition; Drought resistance; Latewood blue intensity; Quantitative wood anatomy; Temperature signal; Curve intervention detection; Climatic extremes; Tree growth reduction

ACKNOWLEDGEMENTS

Time flies and, with the completion of this thesis, the several-year journey of my doctoral study is coming to an end. At this stage, I would like to express my sincere acknowledgement to everyone who has given me assistance along the way. Without your kind and generous help, I would not have been able to complete this journey on my own.

I would like to thank my supervisor Dr. Miloš Rydval, who has guided me from the beginning to the end in conducting the whole Ph.D. project, including initial thesis topic design, detailed methodology selection, field sampling, conducting experimental procedures, as well as statistical analysis and scientific manuscript writing, etc. Because of this support, I was able to get through many hard times during my study and continue the long-term journey till the end. I also very much appreciate the assistance from my colleague Dr. Krešimir Begović, from whom I have learned many experimental skills in generating and working with various tree-ring parameters. Additionally, he has also helped me a lot with analyzing data and scientific manuscript writing. I would also like to thank the whole REPLICATE project team, which I had the opportunity to be a part of and work with. This allowed me to learn from colleagues with diverse research backgrounds and learn to adapt to and work in various international research environments, and it also helped in improving my English language skills in scientific research as well.

I also would like to thank prof. Miroslav Svoboda who had accepted my Ph.D. application for becoming a doctoral student in the Department of Forest Ecology, which gave me the opportunity to continue my studies and the possibility to develop an academic career. I appreciate all the colleagues of the department, who had either helped me with my studies or in daily life. The international atmosphere of the whole department equipped me with a broader and international perspective for future work and life. I also acknowledge my faculty and university for any research funding support and an incentive system which helped me focus on the completion of the Ph.D. project. I would also like to thank colleagues of the two institutes, WSL in Switzerland and XTBG in China where I did my internships. It was a great pleasure to work with different research groups and communicate research ideas.

Last but not the least, I must thank my family and friends for any assistance in my life, my parents' understanding of my decision to continue my studies, the support of my friends during the pandemic period, and myself for persisting till the end and not running away halfway.

TABLE OF CONTENTS

SUMMARY	I
ACKNOWLEDGEMENTS	III
TABLE OF CONTENTS	V
LIST OF FIGURES	IX
LIST OF TABLES	XI
LIST OF ABBREVIATIONS	XIII
PREFACE	XV
1. INTRODUCTION	1
1.1 DISTURBANCE AND ITS IMPACT ON TREE GROWTH	2
1.2 POLLUTION AND ITS IMPACT ON TREE GROWTH.....	4
1.3 DROUGHT AND ITS IMPACT ON TREE GROWTH.....	7
1.4 AIMS AND OBJECTIVES	8
2. LITERATURE REVIEW	11
2.1 CLIMATE CHANGE AND FOREST DYNAMICS.....	11
2.2 TREE-RING BASED CLIMATE RECONSTRUCTION	13
2.3 NON-CLIMATIC FACTORS AND THEIR IMPACT ON TREE GROWTH.....	14
2.3.1 <i>Disturbance</i>	15
2.3.2 <i>Pollution</i>	17
2.3.3 <i>Reducing non-climatic impacts</i>	19
2.4 MULTIPLE TREE-RING PARAMETERS	20
2.4.1 <i>Tree-ring width</i>	21
2.4.2 <i>Blue Intensity</i>	22
2.4.3 <i>Quantitative wood anatomy</i>	23
3. METHODOLOGY	25
3.1 GENERAL INTRODUCTION OF THE METHODOLOGY	25
3.1.1 <i>Study area</i>	25
3.1.2 <i>Sample collection and preparation</i>	27
3.1.3 <i>Statistical analysis</i>	28

3.2 IMPACT OF DISTURBANCE SIGNATURES ON TREE-RING WIDTH AND BLUE INTENSITY CHRONOLOGY STRUCTURE AND CLIMATIC SIGNALS IN CARPATHIAN NORWAY SPRUCE	31
3.2.1 <i>Sampling sites</i>	31
3.2.2 <i>Sample collection and data generation</i>	32
3.2.3 <i>Disturbance detection and correction</i>	33
3.2.4 <i>RW chronology structure comparison</i>	33
3.2.5 <i>BI chronology development and structure comparison</i>	34
3.2.6 <i>Temperature sensitivity comparison</i>	36
3.3 IMPACT OF POLLUTION ON THE CLIMATIC SENSITIVITY OF MULTIPLE NORWAY SPRUCE TREE-RING PARAMETERS IN CENTRAL EUROPE	36
3.3.1 <i>Study sites</i>	36
3.3.2 <i>Sample collection and data generation</i>	38
3.3.3 <i>Tree-ring pollution signal and growth anomaly detection</i>	40
3.3.4 <i>Detection of pollution impacts on temperature signals in tree-ring width and latewood Blue Intensity</i>	40
3.3.5 <i>Detection of pollution impacts on QWA parameters</i>	41
3.3.6 <i>Dynamics of pollution and polluted forests</i>	42
3.4 DROUGHT RESISTANCE OF MAJOR TREE SPECIES IN THE CZECH REPUBLIC	42
3.4.1 <i>Study area and sample collection</i>	42
3.4.2 <i>Tree-ring sample processing</i>	44
3.4.3 <i>Climate data and identification of drought years</i>	45
3.4.4 <i>Statistical analyses</i>	46
4. RESULTS	49
4.1 IMPACT OF DISTURBANCE SIGNATURES ON TREE-RING WIDTH AND BLUE INTENSITY CHRONOLOGY STRUCTURE AND CLIMATIC SIGNALS IN CARPATHIAN NORWAY SPRUCE	49
4.1.1 <i>Disturbance trends in RW chronologies</i>	49
4.1.2 <i>Disturbance influence on RW and BI chronologies</i>	53
4.1.3 <i>Climatic sensitivity of RW and BI chronologies</i>	55
4.2 IMPACT OF POLLUTION ON THE CLIMATIC SENSITIVITY OF MULTIPLE NORWAY SPRUCE TREE-RING PARAMETERS IN CENTRAL EUROPE	60
4.2.1 <i>Historical pollution status and the detected pollution signals in tree rings</i>	60
4.2.2 <i>Tree growth trends revealed by different tree ring parameters</i>	62
4.2.3 <i>Temperature sensitivity of tree rings in different pollution periods</i>	63

4.2.4 <i>General growth trends, climate patterns, and forest dynamics in the context of pollution</i>	67
4.3 DROUGHT RESISTANCE OF MAJOR TREE SPECIES IN THE CZECH REPUBLIC	70
4.3.1 <i>Drought impacts on tree growth</i>	70
4.3.2 <i>Links between drought resistance, growth trend, and moisture availability</i>	72
4.3.3 <i>Drivers of drought resistance</i>	73
5. DISCUSSION	77
5.1 IMPACT OF DISTURBANCE SIGNATURES ON TREE-RING WIDTH AND BLUE INTENSITY CHRONOLOGY STRUCTURE AND CLIMATIC SIGNALS IN CARPATHIAN NORWAY SPRUCE.....	77
5.1.1 <i>Spatiotemporal disturbance characteristics of tree-ring chronologies</i>	77
5.1.2 <i>Temperature signals in the context of disturbance</i>	79
5.1.3 <i>Limitations of CID method</i>	81
5.1.4 <i>Subsection conclusion</i>	82
5.2 IMPACT OF POLLUTION ON THE CLIMATIC SENSITIVITY OF MULTIPLE NORWAY SPRUCE TREE-RING PARAMETERS IN CENTRAL EUROPE	83
5.2.1 <i>Degree of growth trend synchronization and pollution status</i>	83
5.2.2 <i>Stability of climatic signals in different tree ring parameters from polluted areas and their potential for climate reconstruction</i>	85
5.2.3 <i>Avoidance of pollution interference for dendroclimatic research in polluted areas</i>	87
5.2.4 <i>Subsection conclusion</i>	87
5.3 DROUGHT RESISTANCE OF MAJOR TREE SPECIES IN THE CZECH REPUBLIC	88
5.3.1 <i>Impacts of drought on tree growth</i>	88
5.3.2 <i>Differences in drought resistance among tree species</i>	89
5.3.3 <i>Elevational gradient in drought resistance</i>	90
5.3.4 <i>Effects of age, size, and drought intensity</i>	91
5.3.5 <i>Subsection conclusion</i>	91
5.4 COMPREHENSIVE DISCUSSION OF THE WHOLE THESIS	92
5.4.1 <i>Impacts of disturbance and pollution on tree-ring width, wood density and anatomy trends</i>	93
5.4.2 <i>Impact of non-climatic factors on the climatic signals in tree-rings</i>	95
5.4.3 <i>Tree growth in central European Forests within the context of climate change</i>	96
5.5 FUTURE RESEARCH PERSPECTIVES	98
6. CONCLUSION	99

REFERENCES.....	101
APPENDIX A.....	133
APPENDIX B.....	145
APPENDIX C.....	159

LIST OF FIGURES

Fig. 1. Map of sampled tree ring network with 34 sites distributed throughout four regions of disturbance study	32
Fig. 2. Map of sampled tree ring network in the Czech Republic and along the northern Slovakia-Poland border of pollution study.....	37
Fig. 3. Spatiotemporal variability in precipitation regimes and climatic conditions within the study area of drought study	43
Fig. 4. Regional level RW chronology structure comparison between disturbance-affected (RW_dis) and disturbance-corrected (RW_dis_CID) chronologies.	51
Fig. 5. Site level (Subset A) RW chronology structure comparison between disturbance-affected (RW_dis) and disturbance-corrected (RW_dis_CID) chronologies for five sites classified as ‘severely disturbed’	52
Fig. 6. Site level RW and blue intensity (BI) chronology structure comparison among three RW subgroups (RW_dis; RW_dis_CID; RW_undis) and two BI subgroups (BI_dis; BI_undis) comprising Subset C.....	54
Fig. 7. Site level temperature response assessment between RW and BI chronologies from five sites characterized as ‘severely disturbed’, and monthly / seasonal mean temperature for disturbed (dis) and undisturbed (undis) subsets for the 1901-2013 instrumental period.....	56
Fig. 8. Site level (31-year) running correlations between chronologies developed from RW and BI series, and seasonal mean temperature (June-July for RW, April-September for BI) of five selected sites with pronounced disturbance-related trends for the 1901-2013 instrumental period.	59
Fig. 9. Long term trends of tree growth represented by different tree ring parameters and pollution history of all studied sites.	61
Fig. 10. Tree-ring width (RW) chronologies before and after treatment using the Curve Intervention Detection (CID) method with both default (cid_def) and sensitive (cid_sen) detection thresholds.	62
Fig. 11. Growth climate correlations between different tree ring parameters (ring width and blue intensity) and CRU monthly / seasonal temperature for different pollution intensity periods.....	64
Fig. 12. 31-year running correlations between different tree ring parameter (ring width and blue intensity) chronologies and optimal seasonal temperatures for each parameter (selected according to seasonal correlation results in Fig. 11).	65
Fig. 13. Growth climate correlations between cell wall thickness (CWT) and CRU monthly / seasonal temperature for different pollution periods for sites CK and SLO.	66

Fig. 14. 31-year running correlations between cell wall thickness (CWT) of segments 8-10 and average April to September temperature for sites CK and SLO.	67
Fig. 15. Long-term trend comparison among ring width, blue intensity, and cell wall thickness (RW / BI / CWT) chronologies and seasonal CRU temperature after 1950.	68
Fig. 16. Normalized Difference Vegetation Index (NDVI) for the period 1981-2019 and instrumental defoliation history of the Giant Mountains in Krkonoše National Park (Czech-Poland border) for the four studied locations over the 1991-2016 period.	69
Fig. 17. Growth trajectories during the period 1950-2019 (A) and mean growth reductions between two periods (B).	71
Fig. 18. Impacts of the dry period (2015-2019) and extremely dry years (2003, 2015, 2018) on tree growth.....	72
Fig. 19. Links between drought resistance, tree sensitivity to variability in moisture availability and growth trends during the 1995-2019 period.	73
Fig. 20. Drivers of drought resistance based on RWI.....	74

Note: Only figures of the main text have been listed, supplementary figures can refer to the appendix.

LIST OF TABLES

Table 1. General information about the sampling sites of disturbance study.....	37
Table 2. Descriptive statistics for RW and BI chronologies of pollution study.	39
Table 3. Sampling information and environmental characteristics of drought study.....	44
Table 4. Descriptive statistics for regional chronologies composed of all series of disturbance study.....	50
Table 5. Information for subset A and B chronologies of disturbance study.	50
Table 6. Descriptive statistics and temperature response for subset C chronologies of disturbance study....	58
Table 7. Output from the GAMM final model based on RWI of drought study.....	75

Note: Only tables of the main text have been listed, supplementary tables can refer to the appendix.

LIST OF ABBREVIATIONS

- **ANOVA:** the least square regression analyses
- **aMXD:** anatomical maximum latewood density
- **BAI:** basal area increment
- **BI:** Blue Intensity
- **BI_dis:** latewood Blue Intensity series with disturbance impacts
- **BI_undis:** latewood Blue Intensity series with no disturbance impacts
- **CHMU:** the Czech Hydrometeorological Institute meteorological stations dataset
- **CID:** curve intervention detection method
- **CRU:** the Climate Research Unit dataset
- **CWA:** cell wall area
- **CWD:** Climatic Water Deficit
- **CWT:** cell wall thickness
- **CZ:** the Czech Republic
- **DBH:** diameter at breast height
- **DE:** Germany
- **GAM:** generalized additive models
- **GAMM:** generalized additive mixed model
- **LA:** lumen area
- **LWBI:** latewood Blue Intensity
- **ML:** the Maximum Likelihood approach
- **MXD:** maximum latewood density
- **NDVI:** the Normalized Difference Vegetation Index
- **PET:** the potential evapotranspiration
- **PL:** Poland
- **POL:** the high pollutant deposition period
- **post-POL:** period after the high pollutant deposition period
- **pre-POL:** periods before the high pollutant deposition period
- **REML:** the restricted Maximum Likelihood
- **REMOTE:** Research on Mountain Temperate Forest network
- **RW (RWI):** tree-ring width
- **RW_cid_def:** tree-ring width series treated by curve intervention method with default threshold (3.29 st.dev)
- **RW_cid_sen:** tree-ring width series treated by curve intervention method with sensitive threshold (2.81 st.dev)

- **RW_dis:** tree-ring width series prior to disturbance correction
- **RW_dis_CID:** tree-ring width series after disturbance correction
- **SPEI:** Standardized Precipitation Evapotranspiration Index
- **SPEI12:** the monthly Standardized Precipitation Evapotranspiration Index values with a 12-month time window
- **VPD:** Vapor Pressure Deficit

Note: All abbreviations are listed alphabetically.

PREFACE



Photo: by Yumei Jiang

I think that I shall never see
A poem lovely as a tree

A tree whose hungry mouth is prest
Against the earth's sweet flowing breast

A tree that looks at God all day
And lifts her leafy arms to pray

A tree that may in Summer wear
A nest of robins in her hair

Upon whose bosom snow has lain
Who intimately lives with rain

Poems are made by fools like me,
But only God can make a tree

By Joyce Kilmer, "Trees" from Poetry 2, no. 5 (August 1915): 153.

1. INTRODUCTION

Tree growth is influenced by various climatic and non-climatic factors. As represented by the conceptual linear aggregate model (Cook, 1985), the production of the annual growth increment is the aggregation of multiple components with total tree growth being the synthesis of factors including an age-related growth trend, climate trend, in some cases endogenous and exogenous disturbance, and variance due to random processes. It is necessary to take all these factors into consideration when conducting dendroclimatic research (Rydval et al., 2015), especially when assessing climatic sensitivity of tree growth and developing robust reconstructions of past climate, which requires accurate representation of climate-growth relationships at all timescales, including medium to low frequency trends in tree-ring data.

Non-climatic exogenous disturbance can affect growth trends in tree-ring width series and bias climatic information obtained from such records (Rydval et al., 2018). Different types of natural disturbances, such as fires, insect outbreaks and windthrows, are an integral part of forest ecosystem natural dynamics, and usually occur as relatively discrete events with varying frequencies, sizes, and severities at different spatial and temporal scales (Seidl et al., 2017). In Central Europe, reconstructions of disturbance histories have shown that most Carpathian forests are driven by frequent low-to-moderate severity disturbances, in which windstorms and subsequent bark beetle outbreaks are the main disturbance agents (Čada et al., 2013; Svoboda et al., 2014; Trotsiuk et al., 2014; Vacek et al., 2015; Zielonka et al., 2010). As a consequence of shifting climatic constraints on tree growth (e.g., intensifying droughts), trees can become predisposed to bark beetle outbreaks following large-scale windthrow events which in tandem with a warming climate enhance bark beetle phenology and trigger increases in mortality of physiologically weakened and/or mechanically damaged trees (Wermelinger, 2004; Marini et al., 2017).

In addition to disturbance, pollution is another source of non-climatic impacts which can influence tree growth and decrease the stability and strength of climate signals extracted from tree rings. Atmospheric pollution caused by heavy industrial deposition and other sources has profoundly influenced the functionality and development of natural ecosystems in many regions, with dramatic consequences in certain areas (Vacek et al., 2020; Modrzyński, 2003; Krejčí et al., 2013). During the second half of the twentieth century, levels of atmospheric pollution in parts of Central Europe were among the highest on the continent. Forest stands in previously severely polluted areas, including the northwest of the Czech Republic, have faced significant

growth declines and are, arguably, still facing consequences in the present (Neuhöferová, 2005). Moreover, weakened climate signals in tree ring records were found in some nearby regions (Wilson & Elling, 2004; Opala-Owczarek et al., 2019). The lingering effects of pollution trends highlight the need to account for important non-climatic elements when undertaking dendroclimatic research in polluted regions, especially involving the assessment of climatic sensitivity of trees (Rydval & Wilson, 2012).

Furthermore, heatwaves combined with severe drought are becoming a predominant climatic driver associated with the widespread synchronization of tree growth dynamics, either as the direct source of tree mortality (Allen, Breshears, & McDowell, 2015; Allen et al., 2010; Pederson et al., 2014), or by making large areas more susceptible to the effects of disturbances, such as bark beetle outbreaks in North America and Europe (Jarvis & Kulakowski, 2015; Marini et al., 2017; Seidl, Muller, et al., 2016). It has been reported that since the 1980s, drought-induced disturbances throughout Central European Mountain spruce forests have increased (Senf & Seidl, 2017), leading to an increase in the vulnerability of forests in this area. However, the increasing rate of large-scale disturbance due to drought remains unknown, and the possible impacts of drought, which will potentially also influence non-climatic impacts on tree growth, also need to be quantified.

1.1 DISTURBANCE AND ITS IMPACT ON TREE GROWTH

Tree growth is regulated by a range of internal biological processes and external environmental conditions. In a general sense, radial growth of trees can be viewed as a combination of several growth components, including climate variability, disturbance impacts, age and size status, and other random factors (Cook, 1985; Björklund et al., 2019). In recent decades, in-depth studies of the climatic impact on tree growth have drawn considerable attention of the scientific community to rapidly changing climatic conditions (Bošela et al., 2021; Gu et al., 2019; Jevšenak, 2019; Rydvalet al., 2017a; Schurman et al., 2019). The relationship between RW (RW) and the constraining climatic variables is traditionally considered to be linear (Fritts, 1976), but the primary climatic constraints are often temporally or spatially variable, leading to a high likelihood of more complex interactions of resource-limiting conditions and non-linear growth-climate responses (Breitenmoser et al., 2014; Bunn et al., 2018). Furthermore, non-climatic influences, such as disturbances (e.g., bark beetles outbreak, windstorms, etc.), represent one set of environmental factors which can modulate the relationship between growth and climate, thus complicating the extraction of climatic signals from tree rings (Cook and Kairiukstis, 1990; Pederson et al., 2013). Disturbance signatures can obscure climatic signals (Hughes, 2011; Fritts,

1963), leading to skewed interpretations of growth-climate relationships and systematic biases in RW-based dendroclimatic reconstructions (Nehrbass-Ahles et al., 2014; Rydval et al., 2015).

Removing disturbance trends from RW series is necessary to improve the presentation and extraction of climate signals from tree rings (Druckenbrod et al., 2013; Rydval et al., 2015). A range of methods have traditionally been used for detecting disturbances and developing disturbance reconstructions (Altman, 2020; Trotsiuk et al., 2018). However, such methods are generally unable to quantify the influence of disturbances on chronology structure. More recently, a method called ‘curve intervention detection’ (CID) was developed to characterize disturbance history and quantify the effects of disturbance trends on individual RW series and chronology structure (Druckenbrod, 2005; Druckenbrod et al., 2013; Rydval et al., 2015). Previous studies have demonstrated that the CID method can be used to successfully identify disturbance events (Trotsiuk et al., 2016), represent land use history (Druckenbrod et al. 2018), characterize associated chronology trends (Björklund et al., 2019), and isolate, remove and reduce the influence of disturbance trends on RW chronologies, leading to improved climate signal strength (Rydval et al., 2015, 2017b, 2018).

RW is an easy-to-measure and commonly used parameter in dendroclimatological studies (Fritts, 1976). However, the strength of the climate signal in RW is often relatively weak (Björklund et al., 2020; Fuentes et al., 2016; Heeter et al., 2019; Wilson et al., 2017), and the seasonal window is rather narrow (Björklund et al., 2017; Briffa et al., 2002) compared to other tree ring parameters, such as tree ring density and stable isotope ratios. In contrast, X-ray densitometric methods require costly equipment and are often complicated to develop robust datasets. The blue intensity (BI) tree-ring parameter emerged as a cheap surrogate to the traditional X-ray densitometric methods (Björklund et al., 2014, 2015; Rydval et al., 2014), measuring the values of reflected light in the blue wavelengths of the color spectrum that are directly related to tree ring density (Björklund et al., 2019; Campbell et al., 2007; Kaczka et al., 2018; McCarroll et al., 2002). Due to the high degree of similarity with density records, higher quality information on past climatic (especially summer temperature) conditions can be obtained from BI chronologies compared to RW chronologies (Heeter et al., 2019; Rydval et al., 2015, 2017a; Wang et al., 2020; Wilson et al., 2016). To our knowledge, however, apart from a few studies that have examined the ecological impacts on BI data in a limited context (e.g., Arbellay et al., 2018; Rydval et al., 2018), no study has yet systematically assessed the potential influence of disturbances on BI data.

The Carpathian Mountains harbor the largest assemblage of primary Norway spruce (*Picea abies* (L.) Karst) forests in Central-Eastern Europe (Mikoláš et al. 2019; Sabatini et al., 2018).

Extensive studies of Norway spruce growth-climate relationships have shown high sensitivity of Carpathian high-elevation spruce forests to growing season temperature (Bouriaud & Popa, 2009; Büntgen et al., 2007; Nagavciuc et al., 2019; Sedmáková et al., 2019; Svobodová et al., 2019). In addition to climatic drivers, natural disturbances have an important role in regulating forest structure, species composition, and developmental processes across spatial scales (Čada et al., 2020; Pavlin et al., 2021; Schurman et al., 2018; Turner 1987). Reconstructions of disturbance histories have shown that most Carpathian forests are driven by frequent low-to-moderate severity disturbances, with windstorms, and subsequent bark beetle outbreaks, as the main disturbance agents (Čada et al. 2013; Svoboda et al., 2014; Trotsiuk et al., 2014; Vacek et al. 2015; Zielonka et al., 2010). Large-scale windthrow events, in tandem with local weather conditions (e.g., droughts), promote bark beetle phenology and can trigger outbreaks through increases in mortality and reduced physiological health of weakened and damaged spruce trees (Wermelinger 2004, Marini et al. 2017). In closed-canopy forests, these types of disturbance events lead to abrupt and / or sustained increases in radial growth of surviving trees, in response to the associated changes in the surrounding canopy due to the neighboring tree die-off (Janda et al., 2017). Furthermore, future impacts of disturbances on forest ecosystems are expected to intensify under changing climatic conditions (Seidl et al., 2017). With evidence of spatially and temporally shifting rates of disturbance severity and frequency (Schurman et al., 2019; Seidl et al., 2017), the effects of such events on chronology structure, such as potential modification of the strength of growth-climate relationships, and possible consequences for extracting climate signals from dendrochronological records, remain unclear.

1.2 POLLUTION AND ITS IMPACT ON TREE GROWTH

Norway spruce is one of the most dominant and widespread tree species in Central European Mountains. However, due to the impact of air pollution which increased dramatically in many areas after the 1950s and culminated from the 1970s to the 1990s, large-scale spruce forest declines have been observed across biogeographic regions, especially in the so-called ‘Black Triangle’ area (Vacek et al., 2020). The Black Triangle is an area spanning parts of northern Bohemia (CZ), the southern part of Saxony (DE), and the southwestern part of Lower Silesia (PL) (Abraham et al., 2002), and it is a typical area which has experienced high sulphur deposition rates prior to the 1990s (above 5g m⁻² year⁻¹ in 1990; Grubler, 2002). For example, in the Czech Republic, the emissions of sulphur dioxide (SO₂) and nitrogen oxides (NO_x) were reported to increase sharply from 1950 until the 1980s (Dignon & Hameed, 1989; Smil, 1990, Kopáček & Veselý, 2005). Especially, the Jizerské Mts. of north Bohemia experienced the highest levels of atmospheric pollution in the 1970s and 1980s (Wilczyński, 2006), with more than a ten-fold increase in sulphur dioxide emissions within two decades, i.e., 45,000 and

500,000 tons of emissions in 1957 and 1980, respectively (Jirgle et al., 1983), originating from large thermal power plants around the town of Zittau in the territory of Germany and Poland (Matějka et al., 2010). Moreover, heavy pollution also impacted nearby regions, such as the Šumava Mts., which were reported to have been exposed to high levels of sulphur and nitrogen deposition during the last century (Santruckova et al., 2007). The Tatra Mts. likewise experienced the highest impact (6000 t / year) of various industrial emissions (e.g., SO₂, NO_x, Particulate matter) in 1995, though this represented a lower pollution intensity compared to the more severely affected areas (e.g., Ratanica, Czestochowa) (Grodzińska-Jurczak & Szarek-Łukaszewska, 1999). The pollution load started to decrease significantly in the early 1990s due to the desulfurization of power plants fuelled by lignite, and political and economic shifts (Kopáček & Veselý, 2005). As an example, SO₂ emissions thus fell by 88% and NO_x emissions by 62% in 2007 compared to a 1990 baseline in the Czech Republic (Helliwell et al., 2014).

Atmospheric pollution was a major environmental factor in the black triangle area and nearby regions, impacting tree growth during most of the second half of the 20th century (Moldan & Schnoor 1992). In the Czech Republic, large areas (21,000 ha) of high elevation (above 1,000 m a.s.l.) spruce forests were damaged (Vacek et al., 2020) during the period with the highest level of acid deposition (Hůnová et al., 2004; Borůvka et al., 2005). The Jizerské Mts. in the northern Czech Republic suffered the most severe growth decline and mortality events (Rydval & Wilson, 2012; Šrámek et al., 2008). The neighbouring area in Poland (i.e., the Sudetes Mountains) also faced similar substantial damage of forest stands (Slovik et al., 1995; Modrzyński, 2003). Moreover, substantial local damage to spruce stands even occurred in more distant areas such as the Šumava Mts. in southwest Bohemia (Vacek et al., 2019; Krejčí et al., 2013). Conversely, in the 1990s, forests were observed to recover, coinciding with the reduced pollution pressure of sulphur dioxide (Vacek et al., 2015; Putalová et al., 2019). In fact, forest growth was even shown to rapidly respond to changing pollution levels, co-varying with reduced growth under particularly severe pollution years and with increased growth under less severe pollution conditions (Rydval & Wilson, 2012).

Atmospheric pollution can impact tree growth both directly and indirectly. Direct impact is related to stomatal uptake of high concentrations of gaseous pollutants whereas indirect impact results from the deposition of pollutants due to the reaction between SO₂, NO_x and water, resulting in water and soil acidification (Bäck et al., 1995). This can cause disruption of biogeochemical cycling, which may subsequently lead to nutrient deficiencies and imbalances, ultimately resulting in a decline of tree vitality and growth (Sherman & Fahey 1994). However, the relative importance of direct (pollution in the air) and indirect impacts (deposition and soil acidification) on tree growth is still debatable (Hruška et al., 2023). In polluted areas, these

growth responses, which have been linked to high concentrations of pollutants, add additional complexity when attempting to disentangle environmental and climatic influences on growth within the context of climate change, potentially leading to biased representations of growth-climate relationships, especially in severely polluted regions. Though pollution-related growth suppression trends have been documented in various studies (Kolář et al., 2015; Sidor et al., 2021; Takahashi et al., 2020; Treml et al., 2022; S. Vacek et al., 2015; Z. Vacek et al., 2020), little attention has been given to uncovering their impacts on the climatic sensitivity of trees, which is vital in developing an optimal approach to extract and isolate climate signals in tree ring records from polluted areas. As an important non-climatic factor that can influence tree growth, the impact of environmental pollution should be considered when undertaking dendrochronological research in regions which have been historically subjected to atmospheric pollution and acid deposition. This is particularly important when attempting to develop robust dendroclimatic reconstructions in such locations.

While annual tree-ring width (RW) has been widely used in dendroecology and dendroclimatology, the performance and applicability of this parameter is often questioned (Fuentes et al., 2016; Heeter et al., 2019). Thus, a host of additional parameters have emerged to provide alternatives, for example, latewood Blue Intensity (LWBI) has proved to be a more climatically-sensitive variable compared with RW and it also appears to be less affected by natural disturbance, which represents a common non-climatic growth-influencing factor in many environments (Jiang et al., 2022; Rydval et al., 2018). Quantitative wood anatomy (QWA) provides another set of tree ring parameters based on cellular properties at a higher resolution and contains stronger and more stable climate signals compared to X-ray and Blue Intensity (BI) techniques (Björklund et al., 2020; Seftigen et al 2022; Lopes-Saez et al 2023). Moreover, climatic signals imprinted in QWA and BI datasets generally display a stronger co-variability between trees and sites compared to the signal in RW (Wilson et al., 2017). In view of the stronger climatic responses of both BI and QWA compared to RW, it is important to evaluate possible pollution impacts on these parameters to ascertain whether (and if so, then to what extent) they may also be affected by pollution-related biases. While it may be possible to reduce the influence of such biases in RW data using signal processing techniques to some extent, further research is required to evaluate whether other tree-ring parameters are more suitable for dendroclimatological research and the development of palaeoclimatological reconstructions. Such assessment of multi-parameter climatic sensitivity and paleoclimatic suitability of BI and QWA parameters has previously not been performed in the context of polluted regions.

1.3 DROUGHT AND ITS IMPACT ON TREE GROWTH

Rising greenhouse gas emissions have led to significant changes in weather and climate conditions, pushing the amplitude far beyond the ‘natural’ historic range of variation (Swanson et al., 2009; IPCC, 2021). Rises in surface temperatures observed over the last century do not align with changes in precipitation regimes (Twardosz et al., 2021). Consequently, extreme climate events, particularly ‘hotter droughts’, defined as simultaneous occurrence of heatwaves and droughts (Ionita et al., 2021; Markonis et al., 2021), become more frequent and severer. In Central Europe, the increased occurrence of hotter droughts has become the most important climatic driver (Markonis et al., 2021). Particularly, 2003 was exceptionally warm and dry (Rebetez et al., 2006), and 2014-2018 is considered as the driest five-year period since the 19th century (Moravec et al., 2021). These successive climate extremes have altered the structures and functioning of forest ecosystems with significant socio-economic impacts (Brás et al., 2021).

Forests have experienced severe impacts due to drought, with a notable increase in mortality rates of some economically important tree species, such as European beech (*Fagus sylvatica*) and Norway spruce (*Picea abies*) (Gazol & Camarero, 2022; Obladen et al., 2021). The 2018-2019 ‘megadrought’ resulted in a twofold increase in disturbed forest areas around Central Europe (Senf & Seidl, 2021). The megadrought not only cause the death of trees during or immediately after the drought event, but also reduced the growth of surviving trees (Rohner et al., 2021). Previous studies have reported that spring drought strongly impacts the radial growth of conifers such as larch and spruce, resulting in reduced growth trends (Vitasse et al., 2019). Similar warming-related growth reductions have also been observed in southern beech, although such growth responses appear to be more geographically variable (Serra-Maluquer et al., 2019). Another study indicated that tree growth under drought conditions is more strongly influenced by precipitation and climatic water balance rather than temperature (Bose et al., 2021). Therefore, reaching any general conclusions about how trees respond to drought conditions remains a challenging task.

Periods of extremely low growth act as disturbances in forests due to their episodic nature and the potential to induce major changes in forest structure (Lloret et al., 2011). The concept of resilience, defined as the capacity of an ecosystem, community or individual to recover after a disturbance and regain its pre-disturbance structure and function (Scheffer et al., 2001; Folke et al., 2004), provides a practical framework to quantify the cumulative effects of recurrent stressful episodes. Furthermore, the breakdown of this concept into several refined indices, such as resistance, recovery, resilience *per se* and relative resilience, enables the examination of

individual tree resilience based on tree ring growth (Lloret et al., 2011). Consequently, it becomes possible to distinguish between short-term impacts and long-lasting effects.

Short-term impacts, observed as growth anomalies during droughts, often vary depending on the tree developmental stages and environmental condition. These anomalies which are influenced by factors such as age and size (e.g., height), can help to provide a better understanding of trees' drought resistance. While such relationships have been investigated in various studies (Fernández de Uña et al., 2023; Lucas-Borja et al., 2021; Fajardo et al., 2019; Ding et al., 2017; Xu et al., 2018; Merlin et al., 2015), a comprehensive evaluation of their collective impact has yet to be conducted. This goal is complicated by various sources of uncertainty involving physiological interactions (i.e., within-species trait variation, trait covariation, and trait-environment covariation) and ecological complexity, which can confound predictions of mortality related to drought (Trugman et al., 2021). Moreover, regional climate variations and orographic gradients further influence drought resistance. For instance, trees growing at wetter sites can paradoxically show greater sensitivity to increased drought intensity, even though their higher water holding capacity typically buffers the impact of drought (Gazol et al., 2018; Thom et al., 2023a). This scenario is a consequence of trees' adaptations to differing local site conditions, such as better-developed root systems or reduced leaf area at drier sites, which enhance their resistance to drought (Cavin & Jump, 2017). Bose et al. (2020) also pointed out that the impacts of drought on growth depended on the type of site that trees grow on and their growth performance prior to the drought period. However, the extent to which tree-specific attributes modulate drought resistance remains uncertain. A better understanding of the most important factors which determine trees' resistance to drought will help to predict future forest development and ecosystem services more precisely (Pardos et al., 2021). Additionally, this knowledge can help guide foresters to adopt more appropriate management strategies for coping with extreme drought events in the long term.

1.4 AIMS AND OBJECTIVES

Because non-climatic factors are integral elements shaping the history of tree growth, discerning the importance and scope of these influences on tree ring development is crucial for understanding to what extent climate signals may be obscured due to their presence in tree ring datasets. This thesis aims to detect and assess the effects of non-climatic factors on climatic sensitivity in tree rings, considering the influences from both disturbance and pollution, by evaluating and comparing multiple tree-ring parameters (tree-ring width, Blue Intensity, and quantitative wood anatomy) using tree-ring samples from a wide range of Central European forests. Furthermore, in the thesis I also evaluate the extent to which these forests have been

affected by drought, focusing on several major tree species across the entire Czech Republic. Additionally, the findings of this thesis are expected to improve the development of climate reconstructions, especially in areas where large-scale disturbances or pollution have played a significant role in the past. This will provide more solid evidence to improve the reliability of tree ring chronologies by helping to better account for non-climatic factors such as those investigated here and will ultimately contribute to substantially improving the quality of historical climate reconstructions.

Specific objectives of the thesis are:

1) Detecting disturbance signatures in both tree-ring width and Blue Intensity chronologies on various spatial and temporal scales by applying a novel statistical method (Curve Intervention Detection), as well as exploring the extent to which temperature signals are affected by the detected disturbance signatures. To achieve this objective, we used two tree-ring parameters from a spatially extensive network of sites to assess how widespread and to what extent disturbance trends impact tree-ring chronologies within a dendroclimatic context. This objective was addressed by 1) assessing the presence of disturbance trends and their influence on RW chronology structure over different spatial (regional / site) scales and sampling subsets, 2) examining how the impact of disturbance events on the structure of tree ring chronologies differed between RW and BI parameters, and 3) investigating and comparing growth responses using RW and BI chronologies from multiple sites to establish the extent to which their respective climate signals were influenced by disturbance trends. More specifically, disturbance trends were identified and corrected by applying the CID method to all available Norway spruce RW series throughout the Carpathians. Chronology structure comparisons of RW chronologies concerning disturbance were conducted on both regional and local site scales, as well as on specific sampling subsets. For several key sites, subsets of series which displayed clear disturbance-related growth trends in RW chronologies and other subsets that were not affected in this way, were selected to assess the temperature sensitivity of RW and BI chronologies to this non-climatic influence.

2) Detecting pollution signatures in tree-ring width chronologies from historically heavily polluted areas and investigating their impact on the temperature signals of multiple tree-ring parameters (i.e., tree-ring width, Blue Intensity, quantitative wood anatomy) in different time periods with varying pollution intensity. This objective was to investigate the susceptibility of Norway spruce chronologies developed from various tree ring parameters (incl. RW, BI and QWA) to pollution (e.g., sulphur and nitrogen deposition) and evaluate the suitability of all investigated parameters for dendro / paleoclimatic applications. To achieve this, the study was conducted in several representative sites of the Czech Republic and nearby regions, with a

history of being subjected to different levels of pollutant deposition in the mid- to late 20th century. The impacts of pollution on the long-term growth trends of trees and climatic signals were explored in parallel for different tree ring parameters. In this way, we aimed to address the following questions: I . How chronologies of various tree ring parameters were affected by pollution on various spatiotemporal scales and how did these impacts differ among sites that experienced different timing and intensity of pollution? II . Did various tree ring parameters respond differently to pollution and, if so, which parameter was the least affected, and may therefore represent the most suitable option for dendroclimatological and palaeoclimatological research in historically polluted areas? III . How pollution has affected the climatic (i.e., temperature) signal in different tree ring parameters over time and is it possible to remove or minimize the pollution-related biases?

3) Investigating the impacts of several severe drought events and a drought period in the recent past on the growth of several major tree species in Central European forests, as well as examining the drivers of drought resistance of different species using a modeling approach. To achieve this objective, we used a dataset of ~ 1900 tree cores from managed forests in the Czech Republic to assess the impacts of recent major drought events on tree growth rates of five common and commercially valuable tree species which were widely distributed across Central Europe. The five species were European beech (*Fagus sylvatica*), Norway spruce (*Picea abies*), Scots pine (*Pinus sylvestris*), sessile oak (*Quercus petraea*) and pedunculate oak (*Quercus robur*). Firstly, we compared the mean growth rates of these species between two distinct periods, the 2015-2019 “dry period”, characterized by two exceptionally dry years in the studied region, and the 2005-2009 “reference period”, representing a period of average moisture conditions, to assess whether drought conditions induced varying impacts in different tree species. Secondly, we compared the relationships among drought resistance, growth trends and the sensitivity of trees to variations in moisture availability for each species during the 1995-2019 period to assess the sensitivity of individual trees to these three factors. Thirdly, we quantified the impacts of individual extreme drought years (specifically, 2003, 2015 and 2018) on tree growth and drought resistance, to determine whether any differences in impact intensity exist among different drought events. Lastly, we investigated the influences of environmental factors, individual tree attributes, and site characteristics on the tree growth responses to drought and examined the drivers of drought resistance.

2. LITERATURE REVIEW

2.1 CLIMATE CHANGE AND FOREST DYNAMICS

It has been reported that the increased greenhouse gas concentrations enhance the interannual (year-to-year) variability of summer climate in Europe (Seneviratne et al., 2006), increasing the possibility of frequent climate extremes, such as the unprecedented 2003 summer heatwave and drought (Schar et al. 2004; Luterbacher et al. 2004; Stott et al. 2004). The 2003 heatwave began in Europe in June and lasted until mid-August, and summer temperatures were 20-30% higher than the seasonal average throughout large areas of the continent, extending from northern Spain and Italy to the Czech Republic and Germany (De Bono et al., 2004). In fact, during recent decades, Europe experienced a series of heat extremes which have broken long-standing temperature records nearly everywhere (Barriopedro et al., 2011; King, 2017). In addition to 2003, the summer of 2018 was also exceptionally warm over most of Europe (Lorenz et al., 2019). Besides single extreme events, the average temperature in Europe in the 2005–2014 decade was also approximately 1.5 °C above the pre-industrial level (EEA 2014, 2015).

The European continent has already become one of the areas that experienced the most severe intensification of hot extremes since the 1950s (Donat et al., 2013; Fischer & Knutti, 2014; Lorenz et al., 2019). Furthermore, cool summers with heavy precipitation and devastating floods also occurred in 2002 (Christensen & Christensen, 2003; Pal et al., 2004) and 2005. There is no doubt that the increase in the frequency of climatic extremes will represent an important challenge to the future of European forestry. These extreme events are consistent with climate change projections as increasing greenhouse gas concentrations are expected to enhance the interannual variability of the European summer climate, both with regards to temperature and precipitation, with a higher associated risk of heatwaves (Schar et al., 2004; Meehl & Tebaldi 2004), droughts (Milly et al., 2005) and heavy precipitation events (Christensen & Christensen 2003; Frei et al., 2006).

According to the IPCC report (IPCC, 2014), forest ecosystems are likely to face substantial changes in structure and composition in the future as the climate becomes warmer and drier. Possible changes are linked to increases in carbon dioxide in the atmosphere due to increased industrial carbon emissions, solar radiation changes and a rise in global temperature variability caused by increased greenhouse gas concentrations with the largest increase in the northern boreal zones, which may potentially lead to the expansion of new forest areas. From the point of view of forests, they can either benefit (e.g., carbon fertilization) or suffer detrimental effects

(e.g., drought-induced mortality, more frequent forest fires and biotic outbreaks, major alterations to the distribution of certain species, etc.) as a consequence of these climate changes (Sohngen & Tian, 2016). Climate change has already influenced plant development and forest dynamics in Europe. For example, warming in early Spring (February-April) during the 1969-1998 period has led to an earlier beginning of the growing season by 8 days (Chmielewski & Rotzer, 2001). Climate change has also significantly influenced the geographical distributions of plant species (Dyderski et al., 2018) and phenology of trees (Kramer et al., 2000). Within the context of limited migration possibilities, in the future most of the species are likely to face a significant decrease in suitable habitat areas, with species whose distribution currently occupies the northernmost (and highest elevation) ranges subject to the highest threat level (Dyderski et al., 2018). Most of these changes are related to increasing temperatures and decreasing precipitation during the growing season (IPCC, 2013). The frequency of catastrophic winds, insect outbreaks, and forest fires also increases under warming climatic conditions (Seidl, Schelhaas, Rammer, & Verkerk, 2014). Consequently, tree survival rates may become (increasingly) negatively impacted by such changes (Saenz-Romero et al., 2017).

Trees must adapt to their environment while experiencing a multitude of natural and anthropogenic forms of stress, and therefore resilience and resistance to biotic and abiotic stresses is of great importance for long-lived tree species. They have to acclimate their growth and reproduction to constantly changing climatic conditions to survive for many decades or even centuries at the same location (Polle & Rennenberg, 2019). Different species may have different responses in reaction to climate change. Norway spruce is the most widespread and economically most important tree species in Europe (Brus et al., 2011). This widespread species dominates the Boreal forests in Northern Europe and the subalpine areas of the Alps and Carpathian Mountains. However, due to its shallow root system, it is particularly susceptible to heat and drought, and it is expected to become increasingly negatively affected in many areas as conditions become less favorable due to global warming (Eaton et al., 2016). Previous climate response research of primary Norway spruce forests in the Carpathian arc showed that climatic responses of different forest landscapes showed sensitivity to June and July temperatures (Björklund et al., 2019). This type of relationship has also been demonstrated in a multi-species tree-ring network including four conifer species (*Picea abies* (L.) Karst., *Larix decidua* Mill., *Abies alba* (L.) Karst., and *Pinus mugo* (L.)) in the Western Carpathians (Büntgen et al., 2007). Another investigation involving the latitudinal and elevational extent of Carpathian stands revealed a predominant increasing trend of tree growth with temperature (Schurman et al., 2019). Further research also revealed that climate-growth associations and climatic sensitivity seemed to additionally be modulated by elevation and tree age, respectively (Primicia et al., 2015), and

in an evaluation of species-specific climatic responses, Norway spruce showed a higher response to temperature than Scots pine and silver fir (Bouriaud & Popa, 2009).

2.2 TREE-RING BASED CLIMATE RECONSTRUCTION

Environmental conditions and events of the past that trees experienced during their growth can be evaluated by the scientific discipline called dendrochronology, which is based on the analysis of tree rings. This discipline has expanded worldwide and includes the important subfield of dendroclimatology, which aims to estimate climate back in time beyond the start of recorded meteorological measurements (Sheppard, 2010). The growth of trees responds to their surroundings, and they are subject to climatic stresses such as variations in temperature, rainfall, soil moisture, cloudiness, and wind stress. Climate therefore represents one of the main factors controlling tree-ring growth across all spatial and temporal scales and, therefore, the natural range of variation of the climate system can be reconstructed by the examination of the past through tree rings (Morgan et al. 1994). Dendroclimatology consists of several formal procedures, including site and tree selection, crossdating, measuring, data quality control, and tree ring chronology construction. Relationships between tree rings and climate are evaluated using statistical models for the period with meteorological records, and these relationships can then be used to reconstruct the climate of the past over the full length of the chronologies. Precipitation and temperature are the most commonly reconstructed climate parameters, from which the frequency of extreme years, mean condition variations, ranges of long-term variability, and changes in interannual variability can be analyzed (Sheppard, 2010; Speer 2010).

However, although the principle of climate reconstruction using tree rings is quite straightforward, considerable uncertainties in dendroclimatology exist. For example, tree ring datasets are subject to the influence of various non-climatic factors as well as noise. Furthermore, uncertainty and error of statistical models that attempt to represent the climate with tree ring datasets for a certain area is inevitable, since the model can never truly fully capture and accurately represent the climatic signal and it is worth noting that this really cannot even be achieved using measurements at multiple meteorological stations in the same area (Sheppard, 2010). Another related issue is the ‘divergence’ problem (D’Arrigo et al. 2008), which describes the diverging temporal trends between temperature records (increasing in the twentieth / twenty-first centuries) and tree growth in certain locations (decreasing after about 1960). This problem is especially evident in trees at some sites in the higher latitudes of the Northern Hemisphere which have been prominently used for the development of past temperature reconstructions (Grissino-Mayer, 2016). The ‘divergence’ phenomenon raises questions about the uniformitarianism principle, as relationships between tree growth and climate, which are

normally assumed to be consistent over time, may be unstable through time in certain cases. An investigation involving about 1965 dendroclimatological scientific articles shows that nearly 2/3 ($n = 1,269$) of all studies published from 1945 to 2015 did not test the stationarity of the relationship between climate and tree growth. In the remaining 1/3 of studies ($n = 696$), instances of non-stationarity, which represents a considerable shift in the climatic sensitivity of a tree-ring chronology over time, were reported in more than half (56%) of those cases. As for those studies that developed climate reconstructions, 37% were based on tested stationary relationships between climate and tree growth, but the remaining 63% could have potentially included some biases in their representation of past climate variability. Therefore, contrary to basic dendroclimatic principles and conventional assumptions, the general nature of the relationship between tree-growth parameters and climatic variables seems to be predominantly non-stationary (Wilmking et al., 2020).

In practice, the process of past climate reconstruction commonly assumes an approximate linear relationship between the tree-ring proxy (e.g., ring width, maximum latewood density, isotopic composition of the wood, or other properties) and the target environmental driver. This approach also presumes that non-linear processes cancel each other out (Cook and Peterson, 2011) and that all other confounding factors have been removed (Hughes, Kelly, Pilcher, & LaMarche, 1982). Such a presumed stable linear relationship is called the stationarity assumption (National Research Council, 2006). Though several approaches, such as high sample replication to average out noise, careful site and tree selection emphasizing high sensitivity to climate (Stine & Huybers, 2017), and statistical treatment of varying complexity (Fritts, 1976) are employed to maximize the explained climatic variability in an attempt to achieve a strong and representative regional climate signal as much as possible, it is ultimately impossible for any tree growth patterns to explain 100% of the variance of a target climate variable. In fact, the explained variance R^2 rarely exceeds 60%–70% and the common range is usually 30%–50% (Esper et al., 2016; St. George, 2014a; Wilmking et al., 2020). There is no doubt that dendroclimatology has played and will continue to play a significant role in the interdisciplinary research on climate change, however, every possible effort must be made to minimize or remove all these uncertainties to the extent that it is possible.

2.3 NON-CLIMATIC FACTORS AND THEIR IMPACT ON TREE GROWTH

Non-climatic factors (i.e., biological and microsite factors that regulate growth-climate relationships) can create challenges when attempting to extract climate signals from tree rings (Cook and Kairiukstis, 1990; Fang et al., 2014b; Fritts, 1976; Pederson et al., 2013; Wilmking

et al., 2005). Although it is usually assumed that the effects of internal disturbances and other sources of noise can be minimized by sampling larger numbers of trees over a larger area and avoiding trees visibly affected by localized disturbances, this may not always guarantee a disturbance-free chronology and external sources of disturbance can potentially introduce systematic biases in tree-ring based climate reconstructions in some cases (Nehrbass-Ahles et al., 2014). Thus, in addition to examining drought-related impacts on tree growth, this thesis focuses on the detection of the impacts caused by non-climatic factors on different tree-ring parameters, as well as potential influences that these can have on climatic (mainly temperature) signals. Considering the potential importance of non-climatic factors, in this thesis, natural (e.g., wind damage and bark beetle outbreaks) and anthropogenic (i.e., atmospheric pollution) sources of disturbance are the main non-climatic factors which have been investigated in detail.

2.3.1 Disturbance

Sources of forest disturbance include both abiotic (e.g., fire, drought, wind, as well as snow and ice) and biotic agents (e.g., insects and pathogens). Forests can be strongly influenced by these disturbances and understanding such impacts is important especially considering that the frequency and severity of natural disturbances, as well as drought events, are expected to increase due to climate change (Svobodová et al., 2019). It has been recognized that disturbances take the role of regulating forest structure, composition, and processes from small patches to large landscape scales (Pickett & White 1985; Turner 1987), influencing the structure, composition and function of an ecosystem, community, or population. They can also change the resource availability and the physical environment of forests (Pickett & White 1985). Disturbances are expected to be the most profound influence which climate change will have on forest ecosystems and understanding their effects is critical considering that the impacts of disturbances are likely to increase because of global warming (Seidl et al., 2017).

Disturbances affect virtually all forest ecosystems (Turner et al., 1998; Frelich, 2002) and are essential for many ecosystem processes, including nutrient cycling, carbon storage, and forest hydrology (Peterson & Pickett, 1995). In recent years, disturbance regimes have changed considerably (Seidl et al., 2011). In European primary forests, a large-scale reconstruction of disturbance history shows that decadal disturbance rates varied significantly through time and declined after 1920 (Schurman et al., 2018). Across the Ukrainian Carpathians, the influence of a mixed severity disturbance regime has been identified (Trotsiuk et al., 2014). In the Western Carpathians, at least three windthrow events of major and moderate severity occurred in the last 150 years on southern slopes of the Tatra Mountains, which may contribute to the coexistence of spruce and larch through differences in vulnerability and response to heavy windstorms

(Zielonka et al., 2010). A peak of canopy disturbance also occurred in the mid-19th century across the Western Carpathians, with the most important periods of disturbance in the 1820s and from the 1840s to the 1870s (Janda et al., 2017). Significant disturbances in spruce stands, which resulted from windstorms and bark beetle outbreaks, have also been identified (Čada et al., 2013; Vacek et al., 2015).

Disturbances and forest dynamics contribute to the demographic variation in tree growth rates, which confound estimates of tree growth responses to climate change. Growth rate fluctuations have been closely linked to known disturbances in Southern Romania (Schurman et al., 2018, 2019). Current stand size and age structure have also been strongly influenced by past disturbance activity (Janda et al., 2017). Disturbances shape forest structure and function (Attiwill, 1994) and changes in the factors driving disturbance patterns alter forest dynamics (Seidl et al., 2017; Turner, 2010). Disturbance history influences forest development, and consequently disturbance susceptibility (i.e., the susceptibility of trees to various disturbance agents) often depends on tree size and stem densities (Canham, Papaik, & Latty, 2001; Wermelinger, 2004). Disturbance-induced reductions in susceptibility can result in intervals of time in a stand's history where disturbance patterns are less responsive to climate variation (Swetnam & Betancourt, 1998). Disturbances also reduce canopy cover and the associated reduction in competition permits formerly suppressed trees to recruit into the canopy stratum.

In general, forest growth typically responds strongly and directly to changes in temperature and precipitation (Adams et al., 2004). Particularly the former is more important at high latitudes and elevations (Reichstein et al., 2007), though understanding the growth response at such locations can be complicated as the growth-climate relationship can change over time (e.g., due to climate change), for example by interactions between a lengthening growing season and increasing water stress or even the influence of drought conditions. However, because of morphological adaptations of individual trees, biotic and abiotic disturbance, and individual species' phenotypic plasticity, weak relationships marked by poor correlations between local climate and the tree ring record can occur (Arnan et al., 2012). At the single-tree level, the radial growth sequences of trees can be considered a combination of different growth components such as age and size limitations, disturbance events, impacts of climate variability and variance caused by unknown factors (Björklund et al., 2019). Tree growth is often climatically limited in natural environments, and ring widths have traditionally been hypothesized to have a linear relationship with the constraining climatic factor (Fritts, 1976). But in many cases, the primary climatic constraints are temporally or spatially variable, leading to a high likelihood of multiple resource limitation and non-linear growth climate responses (Breitenmoser et al., 2014; Bunn et al., 2018). Except size or age, disturbance and climate, there is also a more enigmatic variation

imprinted in the growth described as unique inter-annual variation of unidentified origin (Cook, 1985). The proportion of unique variation is inversely related to the general climate sensitivity of the trees, and especially to the ability to date tree rings (Stokes & Smiley, 1968). To better understand each of these factors, researchers have tried to decompose the variance induced from the various growth components of climate, disturbance, and undetermined sources in series of tree-ring measurements representing four different landscapes in three countries (including Slovakia, Ukraine, and Romania) across the Carpathian arc (Björklund et al., 2019). The results showed that disturbance variance certainly plays an important role in the aggregated growth in this region of Europe, though the climate-to-disturbance variance ratio (with a higher ratio representing a lower proportion of disturbance variability in relation to climate variability) increases from 2 (0.2 / 0.1) at the tree level to 6 (0.12/0.02) at the landscape level, disturbance is still detectable in larger spatial scales, this factor is even twice as prominent as in Northern Romania compared to the other landscapes.

2.3.2 Pollution

Due to the economic expansion after World War II, global emissions increased, and especially the increases in Sulphur dioxide (SO₂) and nitrogen oxides (NO_x), because of burning fossil fuels and particularly coal for energy purposes, were unprecedented (Grübler, 2002; Smith et al., 2011). In Europe, acidic air pollution became a serious concern across most of the continent in the second half of the 20th century (Stern, 2005). This was especially true in the area known as the “Black Triangle” region, where the emission loads were the highest (Grübler, 2002). The “Black Triangle” is an area along the Czech–Polish–German border (Grübler, 2002), and was designated as an “ecological disaster zone” by the United Nations Environment Programme (UNEP) because of the ecological impacts which resulted from the exploitation and utilization of large coal resources, the presence of numerous power plants and other heavy industrial facilities (Kopáček and Veselý, 2005), and topography that favored the occurrence of prolonged inversion events.

In the Czech Republic, air pollution had been the main environmental problem since around 1950 due to the extremely high SO₂ and particulate matter emissions from power plants and other industrial facilities (Moldan and Schnoor 1992). It was reported that the SO₂ and NO_x emissions in the Czech Republic increased sharply after approximately 1950 (Dignon and Hameed, 1989) and remained high until the late 1980s (Kopáček and Veselý, 2005). Furthermore, the SO₂ emissions were ranked as the most dangerous factor which negatively impacted the health status of forests in the entire Central European region (Ulrich, 1991), including the Czech Republic, between 1970 and 1990 (Materna 1999; Hůnová 2001). Even

after the 1990s, when air pollutant emissions (especially SO₂) were substantially reduced (Renner 2002; Hůnová et al. 2004), forests in some parts of the Czech Republic remained under threat of lasting damage linked to past emissions (Vacek et al., 2015). Similarly, Poland has also been recognized as one of the most polluted countries in Europe in late 20th century and Polish forests have been significantly damaged by pollution. Montane forests have been found to be the most affected, and coniferous species, which represent approximately 77.6% of the total forested area of Poland, were the most impacted (Grodzińska-Jurczak & Szarek-Łukaszewska, 1999).

Although the impacts on forest ecosystems have been traditionally treated separately for air pollution and climate change, the combined effects may significantly differ from a sum of separate effects, since many air pollutants and greenhouse gases have common sources, which affect the radiative balance, interact in the atmosphere, and affect ecosystems together in complex ways (Bytnerowicz et al., 2007). Atmospheric pollution impacts tree growth both directly and indirectly. Direct impact is related to stomatal uptake of high concentrations of gaseous pollutants. Indirect impact results from the deposition of pollutants due to the reaction between SO₂, NO_x and water (Bäck et al., 1995), which can cause disruption of biogeochemical cycling, and may further result in nutrient deficiency and imbalances, leading to a decline of tree vitality and growth (Sherman & Fahey, 1994). Generally, from the pernicious effects of atmospheric pollution (and more specifically SO₂) on plant and tree growth, it can be concluded that an increase in SO₂ concentrations in the atmosphere leads to a suppression of growth rates when these concentrations are very high, and when SO₂ concentrations decrease, a period of growth recovery follows (Rydval & Wilson, 2012).

Studies conducted along the boundary of the Czech Republic, Poland and Germany found that the lowest growth rates of Norway spruce coincided with the period of the highest atmospheric SO₂ concentrations in the Jizerské Mountains (Rydval & Wilson, 2012). In the same mountain area, tree ring analyses indicated a period of significant growth depression in 1979–1987 characterized by the highest SO₂ load. More recently, in the 2010–2015 period associated with considerably lower emissions, the SO₂ and NO_x concentrations were still found to influence foliation and diameter increment significantly in Norway spruce stands, with the maximum daily concentration of these pollutants being identified as the most negative growth-affecting factor (Vacek et al., 2020). In the Krkonoše Mountains, researchers documented that diameter increments of Norway spruce were strongly depressed in the 1979–1982 period, caused by the synergistic effects of climatic extremes and high SO₂ pollution in the 1980s and 1990s (Kolář et al., 2015). Similar results have also been observed at nearby sites along the Czech-Poland border (Vacek et al., 2015). In Polish forests, the extensive decline of forests throughout the Sudetes

Mountain range, and especially in the Black Triangle region, remains apparent (Vacek et al., 2020). A long-term decrease of Scots pine radial growth occurred after 1960 in the foothills of the Sudetes (southern Poland), which may have also been caused by non-climatic factors (i.e., industrial pollution; Wilczyński, 2006).

Although pollution-related growth suppression trends have been discovered in various studies, little attention has been directed towards investigating the pollution impact on the climatic sensitivity of trees, which is vital in improving the expression of climate signals in tree ring data from areas that have been impacted by pollution. It is also important to understand such relationships especially when attempting to develop dendroclimatic reconstructions using tree-ring data from polluted regions.

2.3.3 Reducing non-climatic impacts

To some extent, the signatures of non-climatic factors, such as disturbance trends, can be removed by some detrending methods, but these methods can, to a greater or lesser degree, affect the retention of long-term climate trends. Common ring width detrending methods, such as the negative exponential or linear functions, cannot model and remove shorter-term growth releases that are related to disturbance, which can lead to biases in the final chronologies. The cubic smoothing spline (Cook and Peters 1981) method can remove disturbance-related trends from tree-ring width series, but it also removes multi-decadal and long-term variability, which is a disadvantage for reconstructing past climate, as such trends may represent climatic variations. Disturbances bias the mid- to low-frequency components of a tree-ring width chronology, so it is necessary to address the disturbance trends when the tree-ring width data are intended for the development of dendroclimatic reconstructions. One methodological solution for this issue, called Combined Step and Trend intervention detection (CST) developed by Druckenbrod (2005) and Druckenbrod et al. (2013), has proved to be a robust procedure for detecting disturbances. This method can not only identify and assess the timing, duration, and magnitude of growth attributable to disturbance, but can also quantify the contribution of these events to ring width variation and remove their influence from the time series. Such types of time-series analysis with intervention detection (Box and Jenkins, 1970; Box & Tiao, 1975) represent a promising area for studying disturbance in ring width data (Druckenbrod, 2005).

Moreover, a modified version of the CST method, called curve intervention detection (CID), which includes an improved curve-based disturbance trend removal mechanism (Warren, 1980), has also been developed (Rydval et al., 2015). Curve Intervention Detection (CID) as a time-series-based method has been developed to characterize disturbance history and quantify the

effects of disturbance trends on individual ring width series and chronology structure (Druckenbrod, 2005; Druckenbrod et al., 2013). The CID method improves the two-step disturbance trend removal procedure used in the CST predecessor by correcting for the growth release in a single step using ring width index series. After correction, the time-series are re-expressed as raw (non-detrended) measurements after the original growth trends are added to the disturbance-corrected data. In this way, a range of detrending approaches can be applied to both the series not corrected for disturbance (i.e., prior to CID correction - pre-CID) and measurement series corrected for disturbance (post-CID) using commonly utilized detrending packages (e.g., ARSTAN; Cook & Holmes, 1986).

Based on the CID method, one study conducted in the Romanian Carpathians, in which the disturbance trends were identified and their effects on tree-ring width chronologies were reduced by applying the CID method, the time-series with disturbance trends included (pre-CID) and series with disturbance trends removed (post-CID) were compared (Rydval et al., 2018). The periods of growth release pulses associated with disturbance events were apparent both in highly-replicated mean chronologies as well as chronologies representing smaller subsets of samples. Moreover, notable differences between the corrected (post-CID) and uncorrected (pre-CID) versions of the mean chronologies were also apparent. In addition, changes in growth-climate correlations were found between the corrected (post-CID) chronologies and instrumental temperature which showed an overall improvement of the climate signals that they contained compared to those in the uncorrected (pre-CID) chronologies. In another study, the CID method was found to also improve the climate signal in chronologies of two regions in northern Britain, particularly in the more disturbance-affected area in the west of the Scottish Highlands (Rydval et al., 2015). The application of the CID method illustrates that it is possible to minimize the effects of disturbance in tree-ring width chronologies to enhance the climate signal. Since disturbance is a significant factor which can influence the response of trees to climate, then disturbance correction may represent an appropriate strategy to improve the calibration strength of dendroclimatic reconstructions and their overall quality.

2.4 MULTIPLE TREE-RING PARAMETERS

Trees are an important archive of environmental information. Records from tree rings provide high temporal resolution information of tree-species responses to global change, forest carbon and water dynamics, as well as past climate variability and extremes (Wilmking et al., 2020). More specifically, tree rings can help to gain a better understanding of past and contemporary forest carbon and water dynamics (Babst et al., 2014; Frank et al., 2015), responses of forest ecosystems and trees to global climate change (Charney et al., 2016), mortality events (Cailleret

et al., 2017; Park Williams et al., 2012), and late Holocene climate variability and its societal impacts (Büntgen et al., 2016), in addition to many other environmental aspects. There are various tree-ring properties and parameters which have been used in dendroclimatological research, such as tree-ring width, wood density with a particular focus on maximum latewood density (Schweingruber et al., 1978), stable isotopes (McCarroll & Loader, 2004), image-based Blue Intensity (Rydval et al., 2014), and parameters based on quantitative wood anatomy (Von Arx et al., 2016). In this thesis, I have mainly used the following three measurement techniques and associated parameters, including tree-ring width, Blue Intensity, and quantitative wood anatomy, to study the impacts of non-climatic factors on tree ring timeseries in addition to examining drought responses using extensive tree-ring width datasets.

2.4.1 Tree-ring width

Among the range of tree-ring parameters, tree-ring width (hereafter RW) is the most popular parameter which has been used in dendroecological/dendroclimatological research (in addition to other dendrochronological sub-disciplines such as dendroarchaeology, dendrogeomorphology) since in practice it is a parameter that is easy to measure (e.g., Grissino-Mayer, 1997). The beginning of scientific research of tree rings can be traced back to the early 1900s when the astronomer Andrew Ellicott Douglass noticed the similar variations in tree-ring width of multiple trees and later developed the techniques and principles which underlie dendrochronological methods used nowadays (Sheppard, 2010). However, the first quantitative climate reconstruction from tree rings was conducted in 1971 with RW data collected from 49 locations across western Canada and the United States (LaMarche and Fritts, 1971; St. George, 2014a), when Fritts et al. (1971) established the analytical framework to reconstruct climate from ring width records. Thereafter, there was a growing application of RW data in reconstructions of various climatic indicators and other relevant fields, such as, historical extension of water level fluctuations (Stockton and Fritts., 1973), river discharge reconstruction (Stockton and Jacoby, 1976), drought severity reconstruction (Stockton and Meko, 1975; Cook and Jacoby, 1977), paleotemperature estimation (LaMarche, 1974), and the pre-instrumental variability of moisture estimation (Blasing and Duvick, 1984), as well as the El Niño-Southern Oscillation (Lough and Fritts, 1985). Even now in the 21st century, RW still remains the most important source of data used to produce quantitative estimates of climate variabilities (St. George, 2014a). As of March 2013, the International Tree-Ring Data Bank (ITRDB) includes more than 3200 ring width records from all continents except Antarctica (St. George, 2014b).

However, the utilization of RW for dendroclimatic purposes is associated with a range of considerable complications inherent to its structure and properties, including non-climatic

information related to age and size trends (Cook & Kairiukstis, 1990; Weiner & Thomas, 2001), biological memory effects (Esper et al., 2015; Fritts, 1976), limitations in the accurate representation of climatic extremes (Rammig et al., 2014), internal and external disturbances (Rydval et al., 2018) or simply unexplained variability (Cook, 1985). In addition, in temperature-limited areas, an earlier onset of the growing season or increasing moisture limitation due to warming can contribute to non-linear growth responses in cell production (Rossi et al., 2013), and thus the growth-climate relationship based on RW is susceptible to distortion (Björklund et al., 2020). Furthermore, the period when temperature has the greatest influence on growth is also relatively short, often only one (Björklund et al., 2020, 2017; Briffa et al., 2002) or two months in RW which may be more susceptible to lower temporal stability of the climate signal. These limitations have promoted the development and application of other tree ring parameters.

2.4.2 Blue Intensity

Given the limitations of RW, the utilization of other parameters, which can provide a broader range of information about growth dynamics and climatic responses, has been explored. For example, high-quality information of past summer temperatures can be obtained from the Blue Intensity (hereafter BI) tree ring parameter (Rydval et al., 2014), which is generally considered to be a more climatically sensitive variable compared to RW (Rydval et al., 2018). It is also a more affordable technique which can provide similar results to X-ray density datasets (used for example to produce maximum latewood density chronologies), which are much more expensive to obtain (McCarroll et al., 2002). BI time-series have a very strong correlation with density chronologies and with climate variables. This means, to some extent, that BI has similar value for dendroclimatic studies as X-ray density (Björklund et al., 2014; Campbell et al., 2007; Rydval et al., 2014; Nagavciuc et al., 2019). Although various systems, such as WinDendro (WinDendro, 2023; Campbell et al., 2011; Guay et al., 1992), and LignoVision (Rinn, 2014) can be used to measure BI data, such measurements are most often generated with the program CooRecorder (Cybis, 2019), where the generation of BI values is based on the placement of points along scanned images of samples, which are used to calculate RW data. For example, to generate latewood Blue Intensity (hereafter LWBI) series, the equivalent of maximum latewood density, a window is placed around each point according to adjustable parameters that include width, offset, depth and % of latewood recognized as ‘dark’. Then the mean BI value of the ‘dark’ latewood is calculated and used as the LWBI value for a particular ring (Rydval et al., 2014).

An additional advantage of BI data is that usually, due to their strong high-frequency common signal, they can be used for dendroarchaeological purposes, and increased probability of

successfully cross-dating historical samples has been found when using BI data, which are also thought to be less impacted by site specific ecological influences (Wilson et al., 2017). Sensitivity of BI to summer climate variables is very similar to the response displayed by tree ring density records (Campbell et al., 2007). Many studies have found that BI shows stronger climatic signals than RW (Heeter et al., 2019; Fuentes et al., 2018; Rydval et al. 2017b), and when comparing the expression of high and low frequency signals, BI revealed better potential to represent temperature variability than RW (Fuentes et al., 2016). In another study from eastern Europe, though different tree-ring proxies captured different climate signals, the highest correlation coefficient was observed between the BI chronology from high elevation series and summer / autumn temperature in the Gheorgheni region of the eastern Carpathians (Romania; Popa et al., 2022). Although multiple studies have explored BI in the context of dendroclimatology and dendroarchaeology, the possible influence of ecological factors such as disturbances on climatic signals in BI datasets has not yet been explored. Therefore, exploration of the influence of non-climatic factors (e.g., disturbance and pollution) on the climatic sensitivities of BI parameters could be a promising direction moving forward.

2.4.3 Quantitative wood anatomy

Quantitative wood anatomy (hereafter QWA) is the numeric analysis of xylem anatomical traits of trees, shrubs, and herbaceous species and their relationship to plant functioning, growth, the environment, wood quality and species identification (von Arx et al., 2021). Nowadays, along with the improvements in computer performance and image analysis techniques, QWA has been increasingly applied to various dendrochronological research topics, such as climate-growth interactions (Carrer et al., 2018), stress responses, tree functioning (Castagneri et al., 2020), functional anatomical properties to identify tree provenances most resistant to climate change impacts (Rosner et al., 2016), and wood formation (Song et al., 2022) and production processes (Von Arx et al., 2016; Prendin et al., 2017). In dendroclimatological research, some commonly used dendro-anatomical parameters based on the QWA technique include, lumen area (LA), radial / tangential cell wall thickness (CWT), cell wall area (CWA), anatomical maximum latewood density (aMXD) (Björklund et al., 2020; Carrer et al., 2018), along with a range of other parameters. It has been shown that these parameters can contain much stronger climatic signals than RW and even other commonly used parameters, such as maximum latewood density (MXD), which usually exhibit strong climatic sensitivity. For example, Carrer et al. (2018) found that LA and especially CWT showed a stronger temperature response than RW, and CWT also showed the strongest correlation with temperature over the longest temporal period. In another study, summer temperature was found to be highly positively correlated with MXD and CWT chronologies of *Pinus cembra* in both earlywood and latewood, but not with RW in the

Carpathians (Știrbu et al., 2022). Maximum radial CWT, aMXD and latewood density have been reported to be the most promising parameters for temperature reconstruction, as the anatomical measurement technique offers a major advantage based on the very high resolution of sample images that provide an optimal level of detail (Björklund et al., 2020).

In addition to the considerable potential of containing stronger climatic signals, QWA also has the additional advantage of representing intra-annual variation which could offer more detailed climatic information that cannot be expressed by other parameters (Carrer et al., 2017; Castagneri et al., 2017). Although much has been done previously focusing on QWA in the context of ecological and climatological research, little attention has been paid to understanding the influence of non-climatic effects (particularly atmospheric and environmental pollution) on the series and chronologies of QWA parameters and more specifically whether this factor (pollution) can disrupt or in some way affect climatic signals contained in QWA parameter datasets. Since QWA parameters show clear advantages in capturing climatic (e.g., temperature) signals, it would be interesting to evaluate the susceptibility of QWA parameters to pollution and whether it is possible to avoid or minimize the interference from non-climatic factors on dendroclimatic records by utilizing QWA data in historically disturbed or polluted areas, where parameters such RW are strongly impacted.

3. METHODOLOGY

3.1 GENERAL INTRODUCTION OF THE METHODOLOGY

This subsection aims to provide a general description of the study area, sampling design, data collection and measurement, as well as the general data processing methodologies for each research objectives. More detailed information can be found in the following **subsections 3.2 - 3.4** of **Chapter 3** specifically in relation to each objective.

3.1.1 Study area

The research and implementation of individual sub-topics in this thesis was conducted using tree-ring data from a wide range of forests across Central and Eastern Europe. The specific sampling sites were selected based on either their climatic limitation (i.e., influenced by drought) or non-climatic impact (disturbed, polluted) background. To investigate the impact of disturbance, we considered the entirety of the Carpathian Mountains with four distinct sub-regions, incl. Slovakia (High and Low Tatras), north Romania (Călimani, hereafter Calimani; and Giumalău, hereafter Giumalau), south Romania (Făgăraș, hereafter Fagaras) and Ukraine (Gorgany). The Carpathian Mountains have experienced various disturbance events historically (**Subsection 2.3.1**) and, due to their widespread distribution in the region, high-elevation Norway spruce (*Picea abies* (L.) H. Karst.) primary forests were the focus of the work. This network is part of the “Research on Mountain Temperate (REMOTE) forest network”. The REMOTE dataset is a long-term international collaboration initiative based on a network of permanent sample plots in the forests of Central, Eastern, and Southeastern Europe. It aims to monitor selected parts of remaining primary forests using dendroecological approaches, that is, with analyses of past tree growth based on tree rings with a focus on various spatial scales including individual trees, stands, and landscape levels, which will contribute to the long-term scientific understanding of those unique remaining primary forests (more details about this network can be found online at <https://www.remoteforests.org>).

The climate of the Slovakian Tatras is continental, characterized by cool winters and relatively warm summers, with maximum precipitation occurring during the summer (Fleischer et al., 2005). Average annual precipitation is 864 mm, with maximum and minimum rates in June / July and October / February, respectively. The average temperature is 4.71 °C, with minimum and maximum temperatures occurring in January (-5.61 °C) and July (14.41 °C), respectively (Zielonka et al., 2010). In the Calimani and Giumalau Mountains, located in the eastern Carpathian arc of north Romania, mean temperature ranges from -6.5 °C in January to 13.3 °C

in July, and mean annual precipitation is 889 mm with a peak in the summer from June to July, based on the 1961–2012 period (Nagavciuc et al., 2020). The Fagaras Mountains (south Romania) are the highest part of the Romanian Carpathians (Chiroiu et al., 2015) with an annual average temperature of 2 °C (above 1800 m a.s.l.). The average amount of annual precipitation is 1254 mm (average for the 1979-2010 period; Stăncescu & Milian, 1988). The Gorgany Mountains (Ivano-Frankivsk region, Ukraine) represent one of the largest primeval spruce forest preserves in Central Europe, and both locations (Grofa and Syvulya), selected from this area for our research purposes, represent this forest type with the long-term continuous presence of Norway spruce as the dominant species. Monthly mean temperature in this area is between 16.4 °C in July and -7.6 °C in January, and annual precipitation ranges between 853 mm and 1007 mm, with a peak during June and July (Zemanová et al., 2017).

Considering the prominent pollution history in the Black Triangle region (**Subsection 2.3.2**), the area could be seen as ideal to study the impact of pollution on tree growth. Thus, six high-elevation Norway spruce sites were sampled in the Czech Republic and along the border of northern Slovakia and Poland to better understand the impact of pollution on a range of tree-ring parameters. These sites are distributed in the Jizerské Mountains of northern Bohemia, Klínovec in western Bohemia, the Šumava Mountains in south-western Bohemia, and the Tatra Mountains along the Slovakia-Poland border. These sites occupy environments with a range of climatic conditions. In the northern Czech Republic, average annual temperatures at the Jizerka meteorological station are around 3.8 °C, with temperatures ranging from about -5.0 °C in January to around 13.1 °C in July, on average. The total annual sum of precipitation at the Jizerka ombrometric station reaches around 1,300 mm (Tolasz et al., 2007). The Šumava Mountains, representing a forested montane area in southern Bohemia, experience on average 1,091 mm of annual precipitation and the mean annual temperature is 4.2°C (S. Vacek et al., 2006). Along the Slovakia-Poland border, the mean annual temperature at Babia Góra ranges from 0.4 °C at the summit to 6.4 °C at the foothills of the massif (Obreńska-Starkel, 2004). The warmest and most humid month is July with a mean temperature of 12.7 °C and an average precipitation sum of 220 mm in the subalpine forest (Buras et al., 2018).

As drought can profoundly impact forest stands directly and could also exacerbate the impact of non-climatic factors on tree growth (Orbán et al., 2023), considering the occurrence of several drought extremes in Europe in recent decades, research plots have been established along the entire territory of the Czech Republic to identify the extent to which trees were affected by recent drought events. The whole study area encompasses a broad climatic gradient, with the mean annual temperature between 5.16 and 10.29 °C and total annual precipitation ranging from 494 to 1074 mm (1990-2019 averages; Abatzoglou et al., 2018). The elevation varies between 209

and 1016 m a.s.l., with mountainous formations along the Czech border, and lowlands follow the Elbe River and the Morava River. The humidity gradient generally follows the elevational gradient, with lowland areas displaying the lowest precipitation inputs.

3.1.2 Sample collection and preparation

For the detection of disturbance and pollution impacts, only tree ring cores of Norway spruce (*Picea abies*) were collected from each site using a Haglöf increment borer (5 mm) at breast height. As for investigating the impact of drought, several species were cored to gain a holistic understanding of the effects of drought on forests containing different species. The sampled tree species included European beech (*Fagus sylvatica*), Norway spruce (*Picea abies*), Scots pine (*Pinus sylvestris*), sessile oak (*Quercus petraea*) and pedunculate oak (*Quercus robur*). Overall, nearly 15000 tree cores were used for disturbance impact detection throughout the Carpathian Mountains, 236 cores for pollution impact detection in the Czech Republic and along the Slovakia-Poland border, and 1908 cores for drought impact identification within the Czech Republic. Collected cores of inadequate quality (e.g., suffering from rot or containing other major defects) were excluded.

All cores were extracted perpendicularly to the slope direction and then prepared with standard dendrochronological procedures (Fritts, 1976; Stokes & Smiley 1968). After being air-dried, mounted on wooden mounts, glued, and sanded with fine-grit sanding paper, RW was measured using a LintabTM traversing measuring stage and TSAP-WinTM computer software (Rinntech, Heidelberg, Germany) for all cores. Subsets of samples were selected based on relevant study purposes to generate BI and QWA data. To generate BI data, selected cores were first scanned using an Epson Expression 10 000 XL scanner combined with SilverFast Ai scanning software, and then measured using the CooRecorder / CDendro software (Cybis, 2019). Within the scope of this thesis, though several different BI parameters were generated, further analysis was only conducted for LWBI, thus only results of LWBI are presented in **Chapter 4**.

To generate QWA data, paraffin-embedded thin sections were prepared following standard QWA laboratory working procedures (Von Arx et al., 2016) and then imaged using a slide scanner (ZEISS Axio Scan.Z1) with microscope imaging software. Thereafter, numerous anatomical parameters were measured using the software ROXAS v3.0 (von Arx & Carrer, 2014). Several QWA parameters (e.g., CWT, LA) known to contain climatic information (**Subsection 2.4.3**) were developed and used for further analysis.

3.1.3 Statistical analysis

3.1.3.1 Detecting disturbance signatures in multiple tree-ring parameters on different spatiotemporal scales and evaluating their impact on temperature signals

The Curve Intervention Detection (CID) method was applied to all RW series to detect disturbance trends in RW data. Generally, this method is designed to correct or remove disturbance trends in RW series using a statistical approach before applying a traditional detrending procedure, and a detailed description of this method can be found in Rydval et al. (2016, 2018). After applying the CID method, two sets of RW chronologies were developed, with one set composed of series prior to disturbance correction (RW_dis) and the other composed of series in which the disturbance trends are removed (RW_dis_CID). In addition to identifying disturbance-affected (i.e., “disturbed”) and unaffected (i.e., “undisturbed”) series, the disturbed series can also be separated based on the type of detected disturbance trend (i.e., growth release or growth suppression).

Next, the impact of disturbance signatures on RW chronologies was assessed by comparing the chronology structure of the two sets of series - untreated (RW_dis) and treated using CID (RW_dis_CID) - in different spatial and temporal scenarios, that is, from a single site to a regional level and from full-length chronologies to specific time windows containing clusters of disturbance. By performing these comparisons, it was possible to identify chronologies that were considerably affected by disturbance (i.e., “severely disturbed sites”). From the severely disturbed sites, subsets of samples were selected for re-surfacing and scanning to generate LWBI data. As the CID method was only designed for RW data, it is not applicable to LWBI data. Therefore, an attempt to detect disturbance signatures in LWBI chronologies was performed by comparing the chronology structure of two sets of LWBI series which were categorized as either disturbed (BI_dis) or undisturbed (BI_undis) based on the categorization of their RW counterparts as either disturbed or undisturbed. Possible impacts of disturbance on the temperature signals in RW and LWBI chronologies were identified and compared by using the Pearson correlation coefficient (r) to compare different types of RW and LWBI chronologies with CRU TS4.03 (0.5°) gridded monthly temperature datasets. The stability of seasonal temperature signals in the tree-ring chronologies was tested by evaluating 31-year running correlations between the chronologies and the primary limiting climate variable identified by Pearson's correlation analysis. The influence of disturbance on different frequencies (i.e., interannual variability and decadal-scale trends) was also evaluated by comparing chronologies

developed using different detrending approaches that retain lower frequency trends or only high-frequency components.

3.1.3.2 Detecting pollution signatures in tree-ring width chronologies and their impact on the temperature signals of various tree-ring parameters

The CID method was also used to detect pollution signatures, as pollution-related impacts can appear as suppression trends in RW chronologies. Furthermore, three different settings with varying detection sensitivity of the CID method were applied to test how it might affect the detection of pollution signatures. Visualization of the pollution signatures was performed by comparing the structure of different types of RW chronologies (including untreated RW series, RW corrected with standard CID settings, and series corrected using CID with higher sensitivity), and then cross checking with historical atmospheric pollution data (i.e., sulphur and nitrogen deposition) for each site. Defoliation and vegetation dynamics revealed by the monthly Normalized Difference Vegetation Index (NDVI) of the studied sites were also investigated to gain a better understanding of the impacts of pollution. In addition to RW chronologies, LWBI chronologies were also developed and their structure compared with RW chronologies to explore how the impact of pollution on different tree-ring parameters differs. QWA data (e.g., lumen area, LA; cell wall thickness, CWT; etc.) were used to explore the pollution impact from an anatomical perspective with high resolution, which made it possible to perform intra-annual assessments and also helped provide physiological explanations for the impacts observed in the other parameters.

To develop a clearer idea about how pollution can influence the temperature signals in tree ring data, including different tree-ring parameters, growth-climate relationships were compared using the Pearson correlation coefficient (r). Such comparisons were conducted for different temporal windows with varying pollution influence (i.e., before, during and after the high pollutant deposition period) using different tree-ring parameters (RW, LWBI, QWA) and different types of chronologies (incl. CID-treated and untreated). Additionally, 31-year running correlations were used to test the stability of the detected temperature signals for the full period of overlap between the tree ring and instrumental datasets. Pointer year analysis was applied to detect the negative / positive years with growth anomalies which might be related to pollution, and was conducted with the 'bsgc' function in the dendROLAB package in R.

3.1.3.3 Identifying extreme droughts and their impact on the growth of major tree species, as well as the drivers of drought resistance

To investigate the impact of drought, several extreme droughts were first identified based on the Terraclimate database (Abatzoglou et al., 2018) for the period 1958-2019. Using this dataset, the potential evapotranspiration (PET) and the monthly Standardized Precipitation Evapotranspiration Index values with a 12-month time window (SPEI12) were calculated. Extreme drought years were identified by a median SPEI12 value < -1.5 and a median CWD and VPD above the 90th percentile of the median value over the 1958-2020 period. Three drought years (i.e., 2003, 2015 and 2018) were identified and the drought period 2015-2019, with 2005-2009 as the reference period, was also considered in the drought impact evaluation.

General growth trends of five tree species during the period 1950-2019 were investigated by developing RW and basal area increment (BAI) chronologies. Growth differences during the 2015- 2019 dry period and the 2005-2009 reference period were then compared. Thereafter, ‘drought resistance’ for the dry period as well as the single drought extremes was calculated and compared with a focus on species, elevation, and extreme years. Resistance is defined as the reversal of the reduction in ecological performance during disturbance and is estimated as the ratio between the performance during and before the disturbance. In the case of drought, it refers to the ratio between the growth during the drought period and the growth during the respective pre-drought period (Lloret et al., 2011; Kaufman, 1982, MacGillvray et al. 1995). The relationships among growth trends, drought resistance and sensitivity of trees to variability in moisture availability were also investigated. The Generalized Additive Mixed Model (GAMM) was used to assess the dominant drivers of drought resistance by including various variables (i.e., species, year, SPEI12, tree size, age, and altitude) in the model and evaluating their importance. GAMMs are a type of statistical model that combines the flexibility of generalized additive models (GAMs) with the ability to account for random effects in mixed-effect models. Like GAMs, GAMMs allow for non-linear relationships between predictors and the response variable by fitting smooth functions to each predictor. Moreover, GAMMs also allow for the inclusion of random effects, which capture the variability of observations within groups or clusters (Pedersen et al., 2019; Ravindra et al., 2019; Wood et al., 2015).

3.2 IMPACT OF DISTURBANCE SIGNATURES ON TREE-RING WIDTH AND BLUE INTENSITY CHRONOLOGY STRUCTURE AND CLIMATIC SIGNALS IN CARPATHIAN NORWAY SPRUCE

3.2.1 Sampling sites

Samples for this study were collected in the Carpathian Mountains focusing on high-elevation Norway spruce (*Picea abies* (L.) H. Karst.) primary forests. These forests have developed under natural disturbance regimes with little to no evidence of past human impact but are not necessarily in an old-growth stage of development (Svoboda et al., 2014). Site selection was based on a complex field survey, historical evidence from local experts, and literature and historical maps (Janda et al., 2017; Svoboda et al., 2014; Trotsiuk et al., 2014). Sampling plots at each site were established using a stratified random design involving a 100 x 100 m or 141.4 x 141.4 m grid cell overlaid for each site using GIS. Circular sample plots were established within each grid cell at a restricted random position (the inner 0.49 ha core in each 2-ha cell) using GPS (further details can be found in Svoboda et al., 2014). Permanent study plots (PSP) were established by delineating a circular area of 1000 m² (500 m² in two instances), depending on the stand structure. In total, 34 sites distributed throughout four distinct regions across Central-Eastern Europe were examined (Fig. 1, Table A1), including the High and Low Tatras in Slovakia (SLO), Calimani and Giumalau in northern Romania (ROM_N), Făgăraș in southern Romania (ROM_S), and Gorgany in Ukraine (UKR). This collection of sites is part of the Research on Mountain Temperate Primary Forests (REMOTE) network (<https://www.remoteforests.org>) and the selected sampling sites were located within a high-elevation range of 1298 to 1629 m a.s.l (Table A1).

Climatically, the coldest (warmest) months are January (July) for the whole study area, with a monthly mean temperature range of -8.3 to -4.4°C in January and 14.3 to 17.7 °C in July for different parts of the Carpathians (Fig. A1b). The southern Carpathians (ROM_S) is the warmest region compared with the western (SLO) and eastern Carpathians (UKR and ROM_N), with a monthly mean temperature of -4.4°C in January and 17.7°C in July. The western Carpathians (SLO) is the wettest region with average monthly precipitation of 85.4 mm. On the contrary, the southern Carpathians (ROM_S) is the driest region with average monthly precipitation of only 63.9 mm (Fig. A1a).

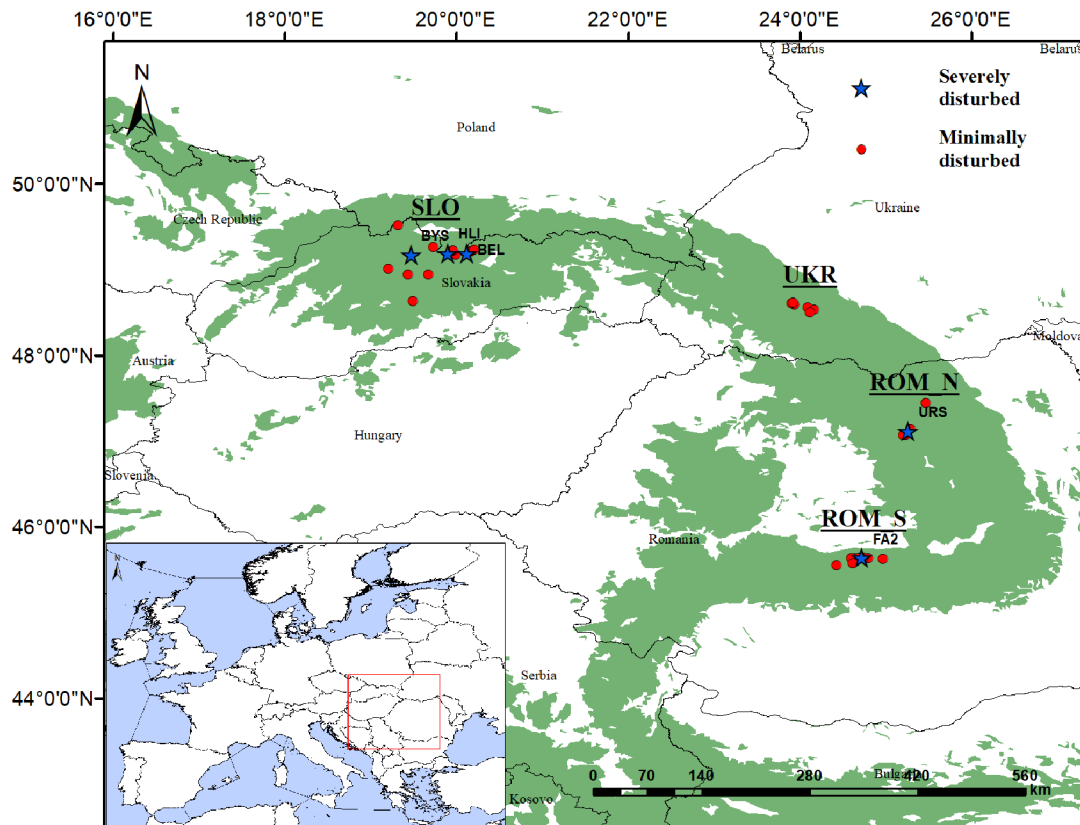


Fig. 1. Map of sampled tree ring network with 34 sites distributed throughout four regions. The sites grouped by four geographic regions include Slovakia (SLO), Ukraine (UKR), North Romania (ROM_N), and South Romania (ROM_S). Sites characterized as ‘Severely disturbed’ were selected for RW / BI chronology comparison. BEL, BYS, HLI, FA2, URS refer to the sites Bielovodska Dolina, Bystra, Hlina, Ucisoara and Ursul, respectively.

3.2.2 Sample collection and data generation

The collection of 25 (or 15 for 500 m² plots) randomly selected, non-suppressed trees (i.e., with at least half of the projected crown under open canopy conditions) with a diameter at breast height (DBH) > 10 cm were cored in each plot at the height of 1 m above the ground using a 5 mm Haglöf increment borer. One core per tree was extracted perpendicularly to the slope direction and prepared with standard dendrochronological procedures (Čada et al., 2020; Schurman et al., 2019). In total, a set of nearly 15000 Norway spruce tree ring cores were collected with a temporal span ranging from 1566 to 2015, covering almost 450 years. (Table. A1). All cores were air-dried, mounted on wooden mounts, glued, and sanded with fine-grit sanding paper. RW was measured to an accuracy of 0.01 mm using a LintabTM traversing measuring stage and TSAP-WinTM computer software (Rinntech, Heidelberg, Germany). All measured RW series were cross-dated following standard dendrochronological approaches (Stokes and Smiley, 1996), and the cross-dating was checked with CDendro 8.1 (Larsson, 2016).

3.2.3 Disturbance detection and correction

The curve intervention detection (CID) method was used to assess the timing and magnitude of disturbance trends in individual RW series (Druckenbrod, 2005; Druckenbrod et al., 2013; Rydval et al., 2015, 2018). It should be noted that the CID method was developed to detect (and correct) trends associated with disturbance events that produce a sudden and protracted growth release or suppression response. As such, its application in this study was suitable for detecting release trends linked to known disturbance agents throughout the Carpathians. The specific implementation of this method followed the procedure described in Rydval et al. (2018). Generally, a constant of 1 mm was added to all measurements before applying the CID procedure to avoid producing zero growth or illogical negative RW measurement values in parts of the corrected series in some instances (Rydval et al., 2015). After that, all RW series were power transformed to account for heteroscedasticity and stabilize series variance (Cook & Peters, 1997) and detrended using negative exponential or linear functions. Disturbance trends were identified as outliers from 9 to 30-year running mean distributions based on the residual series of each detrended RW series and autoregressive model estimates. The identified release / suppression trend was removed by subtracting a curve (Warren, 1980) fitted to the series from the point where the initiation of the disturbance-related trend was identified. This procedure was repeated until no additional outliers were detected. The disturbance-corrected series were then converted to the original (non-detrended) measurement format to provide flexibility for performing subsequent chronology standardization. The entire procedure was conducted in MATLAB (R2017a) using CID version 1.05. Although possible suppression trends were also identified and removed from RW series during the CID procedure, this study primarily focused on growth release trends which are typically associated with the disturbance response of trees in the studied region, and suppressions were therefore not explicitly considered.

3.2.4 RW chronology structure comparison

Two groups of RW chronologies for each site / region were developed in ARSTAN after the application of CID (Cook and Krusic, 2005). The first group of chronologies was composed of disturbance-affected series containing disturbance trends (RW_dis), whereas the second group was composed of series corrected for disturbance trends using the CID procedure (RW_dis_CID). To develop the chronologies, all RW series were first power-transformed and then detrended by subtracting fitted negative exponential or negatively sloping linear functions. The mean chronology index was calculated using Tukey's robust biweight mean to reduce the influence of outlier values (Cook & Kairiukstis, 1990), and variance stabilization of the mean chronology was performed according to the procedure described in Osborn et al. (1997).

Chronology structure comparisons were conducted for the two groups of RW chronologies (RW_dis / RW_dis_CID) at regional and site scales. Considering that not all series contained signatures of disturbance events, an additional subset of chronology pairs (subset A), composed only of series with at least one detected release event, was developed and compared at the site scale. Series without any identified disturbance event were excluded from this subset, representing a hypothetical 'worst case' subset where all collected samples contain disturbance signatures, simulating the most extensive potential influence of disturbance on RW chronologies at a particular site. When comparing chronology structure differences, indices of RW_dis higher than those of RW_dis_CID chronologies represented releases. Conversely, indices of RW_dis lower than those of RW_dis_CID chronologies represented suppressions. Only sections of chronologies with at least 10 series were considered for assessing disturbance-related trends.

Comparison of subset A chronology pairs was used to identify sites that were classified either as 'severely disturbed' or 'minimally disturbed'. Severely disturbed sites were characterized by one or multiple periods with major differences in the structure of the RW_dis and RW_dis_CID chronologies, reflecting a larger proportion of disturbance-affected series with more temporally synchronous disturbance trends. In contrast, 'minimally disturbed' sites exhibited only minor differences between RW_dis and RW_dis_CID, reflecting a smaller proportion of disturbance-affected series with a more random temporal distribution. For those sites identified as severely disturbed, another subset of series (subset B) was selected to represent series with temporally constrained detected release trends. Subset B chronologies were therefore composed of series with release events that only occurred within the 'severe disturbance' period which was defined on the basis of the subset A chronology structure comparison. The 'severe disturbance' period was defined as the period with the highest sum of absolute residuals of the RW_dis / RW_dis_CID paired chronologies over a 100-year period (Fig. A2). The temporal range of 100 years was used to ensure adequate series replication for subset B chronologies. The influence of disturbance trends on the structure of subset B chronologies was assessed in the same way as described above. The general sample selection procedure for all subsets was conceptually illustrated in supplementary Fig. A3.

3.2.5 BI chronology development and structure comparison

For each of the severely disturbed sites identified by RW chronology structure comparison, two groups composed of 30 samples per group were selected, representing a disturbed (dis) and undisturbed (undis) group of series. These 30-series group pairs for the selected sites represent subset C (Fig. A3). The disturbed (dis) group consisted of series with at least one release event detected by the CID method, whereas the undisturbed (undis) group was composed of series

without any detected disturbance event from the CID assessment of RW series. For each site, the original tree ring samples of the two groups were subsequently used to generate BI series from suitable samples and develop corresponding BI chronologies.

Since there were no discolorations or apparent visual color differences between the heartwood and sapwood of Norway spruce in our study sites, chemical treatments to remove resins and other extractable compounds were not performed (Rydval et al., 2018). Samples in poor condition (e.g., showing signs of substantial damage or suffering from fungal decay) were excluded in order to avoid potentially biased light reflectance measurements. Samples selected for BI analysis were re-surfaced with finer sanding paper up to 1200 grit grade to prepare a smoother surface and remove any previous surface staining artifacts or markings, which could affect the accuracy of BI measurement. The samples were then scanned at a resolution of 2400 dpi using an Epson Expression 10 000 XL scanner combined with SilverFast Ai (v.6.6 - Laser Soft Imaging AG, Kiel, Germany) scanning software. The scanner was color-calibrated with the SilverFast IT8 calibration procedure using a Fujicolor Crystal Archive IT8.7 / 2 calibration target before scanning (Rydval et al., 2014). BI values were measured from scanned images with CooRecorder measurement software and crossdating was checked with CDendro v.8.1 (Larsson, 2016). As latewood BI has been shown to be temperature-sensitive in temperature-limited environments in the northern hemisphere, we only focused on the latewood BI parameter in this study (Andreu-Hayles et al., 2018; Björklund et al., 2020; Dolgova, 2016; Harley et al., 2021; Rydval et al., 2017a; Wilson et al., 2017). Individual raw BI series were inverted to ensure a positive relationship with RW and instrumental data (Rydval et al., 2014). All BI series were detrended and standardized similarly to RW series with the exception that BI series were not power transformed and were detrended only using negative-sloping linear functions. For each ‘severely disturbed’ site, BI chronologies for disturbed (BI_dis) and undisturbed (BI_undis) groups were developed.

As CID was developed to treat RW data only (Druckenbrod et al., 2013), this technique was not applied to BI series. To assess the potential influence of disturbance on the structure of BI chronologies, a chronology comparison was performed between BI disturbed (BI_dis) and undisturbed (BI_undis) groups. These BI chronologies were compared with their RW chronology counterparts (RW_dis, RW_undis) as well as the disturbance-corrected RW chronology (RW_dis_CID) to assess how disturbances influence the structure of chronologies developed from these two parameters. Structure differences between disturbed (RW_dis) and undisturbed (RW_undis) chronologies provided additional corroboration for the comparison of disturbance-affected (RW_dis) and disturbance-corrected (RW_dis_CID) chronologies and so helped evaluate the performance of the CID method. In addition to unfiltered chronologies, inter-

annual (first difference) versions of RW and BI chronologies were also developed and compared to assess any possible influence of disturbance on their high-frequency structures.

3.2.6 Temperature sensitivity comparison

To assess the impact of disturbance signatures on the climatic signal, the temperature sensitivity of both RW and BI chronologies developed from disturbed (dis) and undisturbed (undis) groups, as well as disturbance-corrected (dis_CID) RW chronologies, was compared. For each site included in the temperature sensitivity analysis, the relevant 0.5° CRU TS 4.03 gridded monthly mean temperature dataset covering 1901-2013 corresponding to the location of each respective site was used for this assessment (Harris et al., 2014). Responses of RW and BI chronologies to temperature were assessed using the Pearson correlation coefficient. Correlations between tree ring indices and climate variables were calculated for individual months (from previous August to current September) and specific response seasons. 31-year running correlations between chronologies and the primary limiting climate variable identified by Pearson's correlation were calculated to assess changes in growth-climate relationships and any potential influence of disturbance trends over time. Tree-ring indices and climate variables converted to z-scores (Steiger, 1980) were also compared to examine the coupling between tree growth and climate visually.

3.3 IMPACT OF POLLUTION ON THE CLIMATIC SENSITIVITY OF MULTIPLE NORWAY SPRUCE TREE-RING PARAMETERS IN CENTRAL EUROPE

3.3.1 Study sites

This research was conducted at six high-elevation Norway spruce sites in the Czech Republic and the border of northern Slovakia / Poland, representing four pollution-affected locations (Fig. 2; Table 1). Multiple mountain ranges were involved, incl. the Jizerské Mts. of northern Bohemia, Klínovec in western Bohemia, Šumava Mts. in south-western Bohemia, and the Tatra Mts. along the Slovakia-Poland border. These sites occupy environments with a range of climatic conditions. According to the Climate Research Unit dataset (CRU TS 4.07; Harris et al., 2020; Table 1), in the northern Bohemia forests of the Czech Republic (NBH), the annual temperature ranges from 5.6 to 10 °C, and the total annual sum of precipitation ranges from 489 to 891 mm. In western Bohemia (WBH), the climate conditions are similar, with the annual temperature ranging from 5.4 to 9.5 °C, and the total annual sum of precipitation ranging from 457 to 889 mm. Climate conditions in south-western Czechia (SWC) and the northern Slovakia-

Poland border (SP) are colder and wetter, with an average annual temperature of 6.7 °C and total annual precipitation sum of 844 mm for SWC, and an average annual temperature of 6.9 °C and the total annual precipitation sum of 1067 mm for SP. Climate conditions indicated by the spatially-interpolated meteorological stations dataset of the Czech Hydrometeorological Institute (CHMU) show similar temperature patterns (Fig. B2A), though on average with lower values. The gridded dataset may underestimate precipitation conditions, especially considering that higher values are recorded for sites NB (1395 mm) and SLO (1750 mm) compared to the CRU dataset (Table 1).

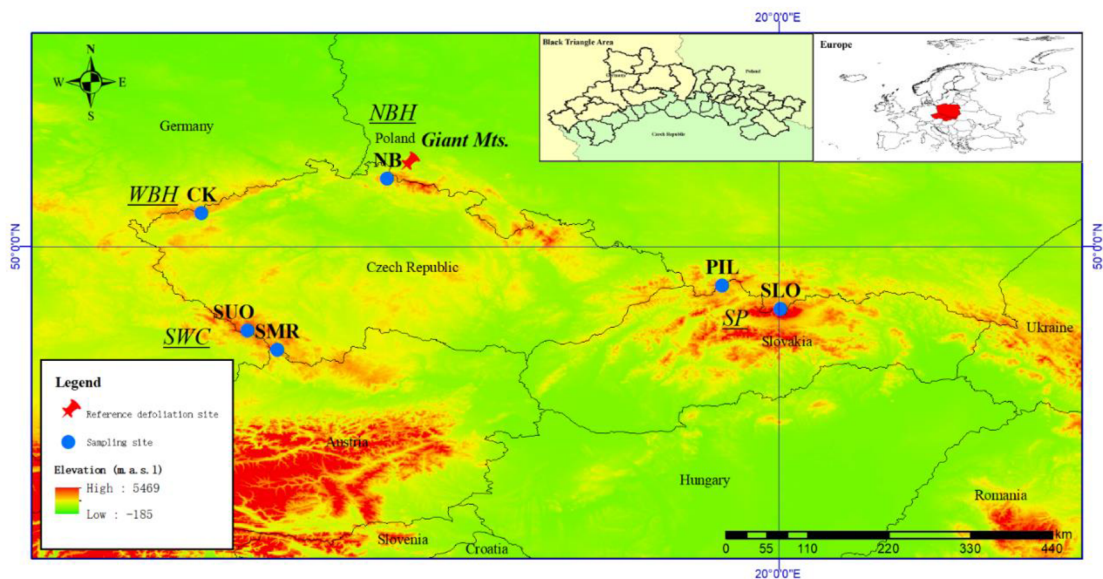


Fig. 2. Map of sampled tree ring network in the Czech Republic and along the northern Slovakia-Poland border. The studied sites (blue points) are NB, CK, SUO, SMR, PIL, SLO. These locations also represent the grid points for which the pollution data (sulfur / nitrogen deposition) were extracted. The underscored codes in italics represent the four general locations to which the sampled sites belong, with NBH and WBH referring to forests in North Bohemia and West Bohemia, SWC refers to South-West Czechia, SP refers to the Slovakia and Poland border. For these four locations, Normalized Difference Vegetation Index (NDVI) datasets were extracted for the period 1981-2019. The red thumbtack marks the site with a reference defoliation record.

Table 1. General information about the sampling sites. ‘N. tree’ represents the number of trees which were used to analyze RW, BI and QWA datasets. ‘t_CRU’ and ‘p_CRU’ are CRU climate datasets with min-max ranges in brackets for the 1901-2020 period. ‘t_CHMU’ and ‘p_CHMU’ are spatially interpolated Czech Hydrometeorological Institute (CHMU) meteorological station datasets with min-max ranges in brackets for the 1961-2012 period. ‘Sulfur’ and ‘Nitrogen’ are the maximum deposition volume for each site during the period 1900-2020. Years of maximum deposition are 1979 and 1980 for sulfur and nitrogen, respectively. ‘Sulfur (EMEP MSC-W model)’ represents sulfur deposition values extracted from the 1900-2050 EMEP MSC-W model.

Location	NBH	WBH	SWC		SP	
Site	Jizerské Mts.	Klinovec	Šumava-Ostrý	Šumava-Hochficht	Pilsko	Dubrawiska
Site (short name)	NB	CK	SUO	SMR	PIL	SLO
Longitude (°)	15.25	13.00	13.56	13.92	19.32	20.03
Latitude (°)	50.82	50.40	48.98	48.74	49.52	49.24
Elevation (m.a.s.l)	930	1050	1210	1320	1384	1650
N. Tree (RW/BI)	79	20	40	20	30	12
N. Tree (QWA)	/	8	/	/	/	8
t_CRU (°C)	7.70 (5.6-10)	7.31 (5.4-9.5)	6.74 (4.8-8.8)		6.86 (4.5-9)	
p_CRU (mm)	663 (489-891)	667 (457-889)	844 (620-1111)		1067 (809-1467)	
t_CHMU (°C)	5.15 (-3.81-14.23)	4.53 (-0.60-13.50)	3.78 (-4.55-12.74)	3.67 (-4.61-12.65)	/	/
p_CHMU (mm)	1395	981	1265	1119	950	1750
Sulfur (EMEP MSC-W model) (mg/m ² /year)	6256	6502	4930		6751	
Sulfur (kg/ha/year)	30.72	19.8	10.75	10.29	20.72	20.86
Nitrogen (kg/ha/year)	20.77	19.52	17.8	16.9	17.9	15.68

3.3.2 Sample collection and data generation

Norway spruce trees that appeared generally healthy were chosen and cored at each site using a Haglöf increment borer (5 mm) at breast height. All cores were air-dried, mounted on wooden sample mounts, glued, and sanded. Samples with no apparent discoloration issues were scanned at a resolution of 2400 dpi using an Epson Expression 10000 XL scanner combined with SilverFast Ai (v.6.6 - Laser Soft Imaging AG, Kiel, Germany) scanning software. Thereafter, both RW and BI (note that hereafter BI refers to latewood Blue Intensity) data were measured from the scanned images using the CooRecorder / CDendro software (Cybis, 2019). Several detrending methods for tree ring index calculation were compared before selecting a suitable approach for each parameter. Details of the comparison are provided in the supplementary information section (Fig. B3). All RW series were power transformed to stabilize series variance (Cook & Peters, 1997) and detrended by applying a modified negative exponential curve and indices computed as residuals via subtraction in the R package *dplR* (Bunn et al., 2015). BI series were inverted to express a positive relationship with wood density in order to facilitate a direct comparison with climatic variables (Rydval et al., 2014), and a linear curve (approximated in *dplR* by a smoothing spline with a 50% frequency response of 500-yr) was used in the subsequent detrending procedure. All RW and BI chronologies were truncated to the period with

replication of ten or more series to ensure chronology robustness for analysis (Table 2).

Table 2. Descriptive statistics for RW and BI chronologies. ‘N. series’ represents the total number of series which have been used for RW, BI and QWA analysis. ‘AC1’, and ‘Rbar’ represent first-order autocorrelation and inter-series correlation, respectively. ‘Rep.>=10’ refers to the period when replication reaches ten or more series and represents the temporal range of truncated chronologies. ‘MSL’ indicates the mean segment length, ‘AGR’ is the average growth rate, ‘Stdev’ is the standard deviation.

Type	Site	N. series	First year	Last year	Length	MSL	AGR	Stdev	AC1	Rbar	Rep.>=10
RW	NB	79	1905	2019	115	76	3.38	1.16	0.76	0.61	1928-2019
	CK	20	1831	2016	186	155	2.32	0.66	0.81	0.60	1857-2014
	SMR	20	1755	2020	266	172	2.38	0.71	0.85	0.71	1842-2019
	SUO	40	1689	2018	330	177	2.14	0.55	0.83	0.50	1838-2018
	PIL	30	1572	2012	441	246	2.24	0.64	0.81	0.49	1719-2012
	SLO	12	1788	2008	221	118	2.04	0.38	0.71	0.56	1917-2008
BI	NB	79	1906	2019	114	76	1.81	0.16	0.45	0.43	1928-2019
	CK	20	1831	2016	186	154	1.86	0.17	0.46	0.46	1857-2014
	SMR	20	1755	2020	266	172	1.81	0.13	0.54	0.57	1842-2019
	SUO	40	1689	2018	330	177	1.88	0.16	0.61	0.44	1838-2018
	PIL	30	1572	2012	441	246	1.92	0.17	0.59	0.36	1719-2012
	SLO	12	1788	2008	221	118	1.87	0.11	0.31	0.66	1917-2008

A subset totalling 16 samples from two sites (CK and SLO, 8 from each site) were selected for QWA sample preparation and wood anatomical parameter generation. These two sites represented locations with some of the most (CK) and least (SLO) pronounced tree growth suppression trends, as indicated by RW, around the period of highest pollution loading, which was considered to reflect relatively strong and weak pollution impact, respectively. Geographically, CK is located in a severely polluted area within the range of the Black Triangle, whereas SLO is located in an area that was comparatively less affected by pollution because of the blocking of wind-transported pollutants by the Tatra Mts. (Fig. 2; Chropeňová et al., 2016; Sekula et al., 2021). The selected cores were first cut into small pieces (length ~ 2 cm) and then refluxed with ethanol (99.5%) using a Soxhlet apparatus for 12 h to remove extractives (resins). Then, samples were individually processed using a mix of alcohol and xylol, followed by paraffin embedding in cassettes, and then cut into thin sections of 12 µm thickness using a sledge or rotary microtome with Feather N35 histological blades (Gärtner et al., 2015; Von Arx et al., 2016). Sections were then stained with a mixture of safranin and astra blue to increase contrast, and permanently fixed on glass slides with Canada balsam (Björklund et al., 2020; Von Arx et al., 2016). Permanent slides were dried in an oven at 60 °C for 12 h and then imaged using a slide scanner (ZEISS Axio Scan.Z1) with associated image processing software (ZEISS ZEN 3.4, blue edition). The program ROXAS v3.0 (von Arx & Carrer, 2014) was used to detect

anatomical structures of tracheid cells and annual ring borders semi-automatically. Moreover, we also applied an updated version of ROXAS (ROXAS AI; Katzenmaier et al., 2023) equipped with a deep learning algorithm for higher-quality image segmentation and compared the resulting data quality with the traditionally used manual post-processing approach. After comparison, the ROXAS AI output was chosen for its superior properties. A wide range of anatomical parameters was produced, and a subset of the most ‘relevant’ parameters was selected for subsequent analysis.

3.3.3 Tree-ring pollution signal and growth anomaly detection

To identify the pollution impact on tree-ring width series, the Curve Intervention Detection (CID) method was applied to all RW series before detrending to detect the timing and magnitude of pollution-related suppression trends (Druckenbrod et al., 2013; Rydval et al., 2018). The CID method is capable of capturing disturbance-related trends and reduce their effects on RW chronologies (Druckenbrod, 2005; Druckenbrod et al., 2013; Rydval et al., 2015, 2018; Jiang et al., 2022), which can improve the climate signal in tree ring datasets (Rydval et al., 2015). The implementation of this method was explored because pollution-related impacts can manifest as suppression trends in tree ring chronologies. Two sets of CID-treated RW chronologies were generated, with one set using the standard (default) setting (3.29 st.dev., *cid_def*) for disturbance detection, whereas the other set of chronologies employed a more sensitive (2.81 st.dev., *cid_sen*) setting which can potentially detect and remove less pronounced disturbance trends that would otherwise not be identified with the standard option (though this increased sensitivity may also increase the risk of false positives). Although an even more sensitive setting (2.58 st.dev.) was also tested, it was not evaluated further since the results were very similar compared to the 2.81 st.dev. sensitivity setting. Pointer year analysis was also explored to detect years with negative / positive growth anomalies (Fig. B4). While both positive and negative anomalies were identified, only potential relationships between negative anomalies and the impact of pollution were investigated. This analysis was conducted with the *dendRolAB* package in R using the ‘*bsgc*’ function, which represents the bias-adjusted standardized growth change method, a novel approach allowing the identification of pointer years following years of successive growth decline (Buras et al., 2020, 2022).

3.3.4 Detection of pollution impacts on temperature signals in tree-ring width and latewood Blue Intensity

To assess the potential impact of pollution on climate signals in different tree ring parameters, responses of RW and BI chronologies to climate variables were assessed using the Pearson correlation coefficient (r) with the package *treeclim* in R (Zang & Biondi, 2015). Growth-climate

response was assessed for the common FULL period (1930-2008), as well as in three distinct periods representing varying exposure to pollution. These three 30-yr periods were defined as pre-POL (1930-1959), POL (1960-1989) and post-POL (1990-2008) (Table 2), approximately corresponding to the periods before, during and after the temporal span associated with high rates of pollutant deposition based on sulphur / nitrogen deposition datasets (Fig. 9E, F; Fig. B1) and literature records (Dignon and Hameed, 1989; Smil, 1990, Kopáček and Veselý, 2005). To reduce uncertainty regarding the impact of varying time divisions on the responses, we additionally evaluated growth-climate relationships over an extended pollution period spanning 40 years. This period was subdivided into four intervals: 1902-2012, 1911-1950, 1951-1990, and 1991 to the end year (limited according to a sample size of ten or more series), representing the FULL, pre-POL, POL, and post-POL periods, respectively. Temporal stability of the climatic signal was quantified using a 31-yr running correlation between RW / BI chronologies and key seasonal temperature variables identified by monthly / seasonal growth-climate responses. In addition to examining the impact of pollution on medium frequency (decadal) trends, the strength of the high frequency (interannual) signals was also investigated as a possible response to pollution in terms of both climatic response and the common growth signal as represented by the inter-series correlation ($Rbar$).

Climatic timeseries were extracted from the CRU TS 4.07 (0.5°) gridded monthly dataset (Harris et al., 2020) covering the period 1901-2020. The climatic response of CID-treated RW chronologies (RW_cid_def / RW_cid_sen) was also assessed over the last century (1902-2012). As the 0.5° gridded CRU temperature dataset is coarser in terms of its spatial resolution and so might be less precise compared to some other datasets, a monthly meteorological climate dataset was also extracted from a 1x1 km grid based on spatial interpolation of Czech Hydrometeorological Institute (CHMU) meteorological stations covering the 1961-2012 period (Tumajer et al., 2023). This dataset was used to evaluate the sensitivity of the growth-climate responses to changes in the target instrumental dataset used as a reference. This evaluation was only performed for four sites (NB, CK, SUO, SMR), since the two Slovakia-Poland border sites (SLO, PIL) were located farther away from the nearest Czech grid with available instrumental data.

3.3.5 Detection of pollution impacts on QWA parameters

Timeseries of QWA parameter datasets were produced by averaging eight series for each site based on each parameter. Mean cell wall thickness (CWT) and lumen area (LA) were selected for the identification of pollution impacts on QWA. Each ring was divided into ten segments/sectors of equal width along the radial direction from earlywood to latewood (S1 to

S10; Fig. B5), thus we developed ten CWT and LA inter-annual time series for two different sites which represented successive time windows within the growing season (*sensu* Carrer et al., 2018). Long-term growth trends of CWT and LA for the ten segments were compared over the past century, where segments with prominent growth deviations were identified and compared with the periods of varying pollution intensity. We also evaluated the growth-climate sensitivities for the CWT and LA sector ensembles during the four pollution periods similarly to what was conducted for RW and BI. However, the temporal stability of the detected climatic signal was only assessed for the most climatically sensitive segment. For LA, we assessed responses to moisture availability through correlations with SPEI (Standardized Precipitation Evapotranspiration Index; Vicente-Serrano et al., 2010) extracted from the CRU datasets with a resolution of 0.5 degrees and aggregated over three months.

3.3.6 Dynamics of pollution and polluted forests

To examine the potential impact of pollution on tree growth and forest health, tree ring chronologies were compared in relation to historical atmospheric pollution data. We compared two types of pollution datasets. The first dataset represents the total annual sulphur deposition which was extracted from the 1900-2050 EMEP MSC-W model for the four locations (NBH, WBH, SWC, SP), covering all study sites (Fig. B1; Engardt et al., 2017). The second dataset contained both sulphur and nitrogen deposition records for the period 1950-2013 and was estimated by the method introduced in Oulehle et al (2016). Furthermore, we extracted the satellite-derived index of photosynthetic activity, i.e., the monthly Normalized Difference Vegetation Index (NDVI), from the 0.1° 'NOAA/NCEI CDR NDVI database' (Vermote, Eric, NOAA CDR Program. 2019) for the period 1981-2020 to check the vegetation dynamics following the period of heavy pollutant deposition. Finally, we compared the other data to a defoliation record from the nearby Krkonoše National Park in the Giant Mts. (along the Czech-Poland border) covering the 1911-2016 period. The degree of defoliation was transformed to percentages of defoliation, which represent the average value of a given defoliation degree (Vacek et al., 2020).

3.4 DROUGHT RESISTANCE OF MAJOR TREE SPECIES IN THE CZECH REPUBLIC

3.4.1 Study area and sample collection

The study sites were distributed within the territory of the Czech Republic, encompassing a broad environmental and altitudinal gradient, spanning an elevational range from 209 to 1016

m a.s.l, with mean annual temperatures ranging from 5.16 to 10.29 °C and total annual precipitation ranging from 494 to 1074 mm (1990-2019 averages; Fig. 3A, B). Within the research area, forests have been extensively managed for centuries. Norway spruce was the most widely planted tree species (Mansfeld, 2011), representing approximately 42% of the total forested area in the Czech Republic (Cienciala et al., 2016). Other commercially important tree species include Scots pine (16.1%), European beech (9.0%), pedunculate and sessile oak (7.5%) (eAGRI, 2021). We strategically selected 74 plots from a broader network of existing managed forest plots located throughout the entire country and collected samples in 2019. Within each plot, a random selection of 20-30 dominant and codominant trees per species, with a diameter at breast height (DBH) greater than 10 cm, was randomly sampled. One core per tree was extracted for dendrochronological analysis. A total of 1908 trees were cored of which 1810 cores met the quality criteria for further analysis. Cores exhibiting poor quality (e.g., rot or poor structural integrity) were excluded. The sampled plots generally represented relatively young stands, with tree age ranging from 23 to 284 years (Table 3), and DBH ranging from 113 to 940 mm with most trees within the 200-400 mm range (Table 3; Fig. C1). As all samples were collected at the end of the growing season, tree rings for the year of sampling were fully formed.

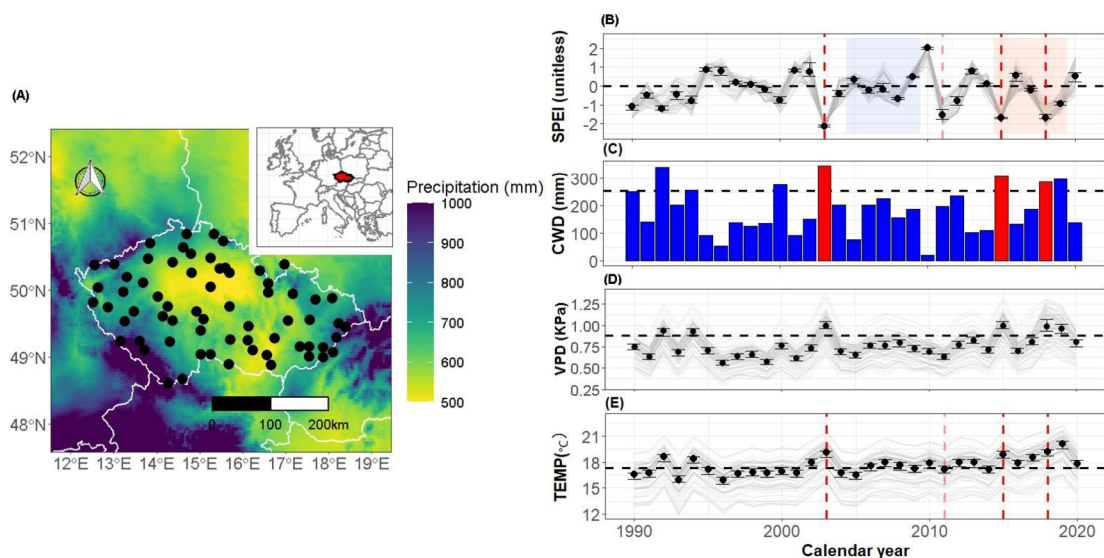


Fig. 3. Spatiotemporal variability in precipitation regimes and climatic conditions within the study area. (A) Average annual precipitation over 1981-2010 (black dots show the location of the study plots), (B) Temporal variability of SPEI12 - Standardized Precipitation Evapotranspiration Index (SPEI) was computed for the hydrological year from October to September. Gray lines are site-specific time series; black dots represent the median values for each calendar year with gray shading showing 95% confidence intervals. Vertical red dashed lines denote years with median SPEI values below -1.5 indicative of extremely dry years (e.g., 2003, 2015, 2018). The black dashed line indicates a SPEI value of zero, i.e., average moisture conditions. Red shading highlights the recent period, characterized by two dry extremes in 2015 and 2018. The blue shaded area highlights the five-year “reference” period in terms of moisture conditions with median SPEI values above -1 and below 1. (C) Climatic Water Deficit (CWD) based on

the hydrological year. The dashed horizontal line corresponds to the 90th percentile of the median CWD chronology from 1958-2020. (D) Summer (June-August) Vapor Pressure Deficit (VPD). (E) Mean summer (June-August) temperature with black dots and error bars representing the median and 95% confidence intervals, respectively. Vertical red dashed lines denote drought years indicated by SPEI for comparison. Light gray lines are site-specific time series and the horizontal dashed line represents the 90th percentile between 1958 and 2020. Note that, in (B), the year 2011 is represented by a lighter red dashed line as it has been omitted from the analysis of extreme drought years because although the median SPEI for that year is below the threshold of -1.5, neither CWD nor VPD was exceptionally high (see panels C-D).

Species	No. plots	Elevation (m a.s.l.)	Temperature (°C)	Precipitation (mm)	No. trees	DBH (mm)	Age (years)
<i>Fagus sylvatica</i>	18	576 (269-946)	7.89 (5.16- 9.08)	708 (554 - 963)	471 (421)	362 (113-940)	87 (28 - 284)
<i>Picea abies</i>	21	694 (342-1016)	7.23 (5.30 – 8.81)	771 (558 - 1074)	539 (510)	383 (157-736)	84 (23 - 174)
<i>Pinus sylvestris</i>	19	445 (218-634)	8.47 (7.27 - 9.71)	667 (494 - 1019)	497 (483)	329 (115-570)	98 (46 - 148)
<i>Quercus petraea</i>	10	351 (250-537)	9.11 (8.41 - 10.29)	632 (503 - 783)	251 (250)	347 (141-789)	102 (46 - 174)
<i>Quercus robur</i>	6	320 (209-465)	9.28 (8.57 - 10.22)	535 (511- 556)	150 (146)	341 (145-845)	91 (43 - 153)

Table 3. Sampling information and environmental characteristics. For each species, both the mean values and ranges (min – max, in parentheses, italic) are shown for parameters, including elevation, average temperature and annual precipitation sums for 1990-2019, diameter at breast height (DBH) and tree age. For the number of trees (No. trees), the numbers in parentheses (italic) represent the effective number of samples included in the analyses.

3.4.2 Tree-ring sample processing

All cores were air-dried and mounted on wooden boards, then progressively surfaced with sandpaper of increasingly finer grain (400 -1500 grit) until the ring boundaries were clearly visible. Ring widths were measured under a binocular microscope using a Lintab measuring

device coupled with TSAPWin software with a precision of 0.01 mm. The ring-width series were then visually cross-dated and validated using CDendro software (Larsson, 2016). A modified negative exponential curve was fitted to each ring-width series to remove ontogenetic trends, and the detrended series of ring-width indices (RWI) were calculated as residuals by subtraction using the R package *dplR* (Bunn, 2008). As basal area increment (BAI) is known to be less affected by biological trends compared to raw or detrended ring-width series (Biondi & Qeadan, 2008; Sullivan et al., 2016; Labrecque-Foy et al., 2023), we calculated BAI for each series using the *'bai.out'* function of the R package *dplR*. We then evaluated the relationship between drought resistances calculated based on RWI and BAI using correlation analysis. As both versions of resistance indices demonstrated high correlations with each other (Pearson's $r \geq 0.90$, Fig. C2), we considered both types of growth indices (RWI and BAI) to be appropriate for drought impacts quantification. For the purposes of this study, we opted to perform all subsequent analyses using RWI and included the BAI version of the results in the supplementary materials for reference.

3.4.3 Climate data and identification of drought years

Climate data (minimum and maximum temperature, precipitation, and climatic water deficit) were extracted from the Terraclimate database (Abatzoglou et al., 2018) for the period 1958-2019. Terraclimate provides monthly gridded climate data at a spatial resolution of approximately 4 km for the Czech Republic. From this dataset, we first calculated the potential evapotranspiration (PET) using Hargreave's equation and then calculated the values of the monthly standardized precipitation evapotranspiration index using a 12-month time window (SPEI12), specifically representing the period from October of the previous year to September of the current year. Both PET and SPEI12 were calculated using the *SPEI* package in R (Vicente-Serrano et al., 2017). The drought years were identified based on the median annual SPEI12 values, with a SPEI12 below -1.5 considered indicative of severe drought (Potop et al., 2014). Nonetheless, as SPEI is a normalized index and cannot be used as an indicator of absolute dryness of a site (Zang et al., 2020), we additionally validated potential drought years using the Climatic Water Deficit (CWD) metric, defined as the difference between potential and actual evapotranspiration and the summer Vapor Pressure Deficit (VPD), indicative of atmospheric dryness. Moreover, as tree mortality can occur as a result of the combined effects of drought and high temperatures (Brodribb et al. 2020), we also examined the summer temperatures for the study areas, which showed similar trends to VPD (Fig. 3E). Finally, we selected years with a median SPEI12 value < -1.5 and a median CWD and VPD above the 90th percentile of the median value over the 1958-2020 period (i.e., > 240 mm and 0.88 kPa, respectively). Using this

methodology, three drought years (i.e., 2003, 2015 and 2018) were retained and considered for further analysis.

3.4.4 Statistical analyses

We first assessed the impact of the recent dry period on tree growth by calculating the ratio between the mean RWI for the 2015-2019 “dry period”, which includes two severe drought (2015 and 2018), and the average RWI for 2005-2009, considered as the “reference period” in terms of moisture conditions (i.e., $0.99 > \text{SPEI}_{12} > -0.99$; Fig. 3B). This ratio, referred to as “drought resistance”, represents the direct impact of the dry period on tree growth rates, and acts as an analogue for the resistance index of Lloret et al. (2011). To assess differences in drought resistance among species, we utilized a linear mixed-effects model with logarithmic transformation of drought resistance as the response variable and species identity as the only explanatory variable. The modelling was performed at the tree level, with plot included as the random factor. Subsequently, we calculated the least square means for each species and evaluated the differences between them through pairwise comparisons, applying a Bonferroni correction for multiple comparisons (Lenth et al., 2018). We conducted a similar assessment involving differences in drought sensitivity across elevation gradients (defined as “high elevation” above 650 m a.s.l., and “low elevation” at or below 650 m a.s.l.) and drought years. The 650 m gradient threshold was an approximate middle value of the two species’ elevation ranges (Table 2; *Picea abies* and *Fagus sylvatica*).

Next, we evaluated the resistance of trees to individual drought events following the same procedure as for the entire 2015-2019 period. However, in this case, drought resistance was calculated as the ratio between the growth rate during a particular drought year and the mean growth rate of the two years immediately preceding the dry event, following the approach of Lloret et al. (2011). As our dataset extended only up to 2019 (i.e., only one year after the 2018 drought), we did not perform an analysis of the recovery or resilience of trees to drought. We then estimated recent trends in growth rates of individual trees by computing Sen’s slope (a method used to identify trends in univariate time series; Sen 1968) for individual RWI series over the 1995-2019 period. Subsequently, we evaluated the sensitivity of individual trees to interannual variability in moisture availability (i.e., sensitivity to SPEI, based on the Spearman’s rank coefficient between RWI and SPEI₁₂), drought resistance, and growth trends (based on Sen’s slope of RWI) over the same period (1995-2019) and compared them across species.

Third, we fitted a Generalized Additive Mixed Model (GAMM) using the R-package *mgcv* (Wood, 2011) to assess the dominant drivers of drought resistance, accounting for potential

autocorrelation in the model's residuals. An AIC-based goodness of fit assessment of interaction terms was performed using the Maximum Likelihood ('ML') approach; then the final model (Equation. C1) was fitted using restricted Maximum Likelihood ('REML').

4. RESULTS

4.1 IMPACT OF DISTURBANCE SIGNATURES ON TREE-RING WIDTH AND BLUE INTENSITY CHRONOLOGY STRUCTURE AND CLIMATIC SIGNALS IN CARPATHIAN NORWAY SPRUCE

4.1.1 Disturbance trends in RW chronologies

On a regional scale, the CID method was applied to 13 287 series after excluding short series < 30 years and series that could not be reliably cross-dated, with replication ranging from 2364 to 4886 series among regions (Table 4). Overall, a considerable proportion (34.6%) of the investigated Norway spruce trees throughout the Carpathians exhibited at least one release event in their lifetime (Table A1), although the timing and severity of release events varied among sites (Fig. A4). When comparing the RW_dis and RW_dis_CID chronologies based on large regional scale aggregation of series for the four regions, apparent differences between the paired RW chronologies were minimal (Fig. 4) and virtually no disturbance trends were detected within the well-replicated period after 1850 for all regions. Minor differences between the paired chronologies appeared only for Slovakia (SLO) in the less replicated early period between 1710 and 1830. On this scale, release events, whose temporal distribution was mostly asynchronous, generally did not leave a clear disturbance trend imprint on the chronologies. When assessed at the site scale (subset A) where chronologies consisted of 123-441 series (Table 5), with the exception of five sites (incl. BEL, HLI, BYS, FA2 and URS), most of the sites still showed no apparent disturbance trends even when undisturbed series were excluded (Fig. 5; Fig. A5). Large disturbance trends were found in three site chronologies (BEL, BYS, URS), particularly in early periods with weaker replication, whereas disturbance trends of HLI and FA2 were less pronounced (Fig. 5). Major disturbance trends appeared immediately after or coincided with synchronized (i.e., temporally concentrated) release events, especially in chronologies from BEL and BYS.

Region	No. of series	Chronology extent	Period with rep. ≥ 10	No. of released series	No. of release events	AGR (+/- SD)	AC 1	Rbar	Release events per series
SLO	4886	1566-2014	1635-2013	1776	3092	2.53 (+/-0.61)	0.78	0.39	1.74
UKR	2364	1607-2012	1653-2011	889	1581	2.16(+/-0.53)	0.74	0.30	1.74
ROM_N	2956	1631-2015	1693-2010	1270	2213	2.56(+/-0.73)	0.81	0.42	1.69
ROM_S	3081	1602-2013	1655-2012	1230	2081	2.5(+/-0.74)	0.81	0.44	1.78

Table 4. Descriptive statistics for regional chronologies composed of all series. The four regions include Slovakia (SLO), Ukraine (UKR), North Romania (ROM_N), and South Romania (ROM_S). AGR (+/- SD), AC1, and Rbar represent average growth rate (+/- standard deviation), first-order autocorrelation, and inter-series correlation, respectively. ‘Rep.’ refers to ‘series replication’. ‘No. of series’ represents the number of RW series for each region. ‘No. of released series’ refers to the number of released samples in each region, and ‘No. of release events’ refers to the number of release events detected for each region calculated from all released samples.

Site	Subset	No. of released series	Chronology extent	Period with rep. ≥ 10	Severe disturbance (100-yr)	No. of release events	Release events per series
BEL	Subset A	162	1591-2013	1709-2013	1714-1813	351	2.17
	Subset B	45	1591-2013	1718-2013	-	155	3.44
HLI	Subset A	125	1685-2012	1761-2012	1761-1860	190	1.52
	Subset B	57	1685-2012	1769-2012	-	105	1.84
BYS	Subset A	132	1683-2012	1764-2012	1767-1866	194	1.47
	Subset B	39	1708-2012	1784-2012	-	73	1.87
FA2	Subset A	123	1670-2012	1770-2012	1882-1981	220	1.79
	Subset B	93	1670-2012	1804-2012	-	180	1.94
URS	Subset A	441	1700-2010	1734-2010	1744-1843	794	1.80
	Subset B	67	1713-2010	1757-2010	-	167	2.49

Table 5. Information for subset A and B chronologies. Subset A only contains series with at least one detected release event whereas subset B only contains series with the disturbance event identified within the 100-year ‘severe disturbance’ period displayed in Fig. 5. ‘Rep.’ refers to ‘series replication’. ‘Rep.’ refers to ‘series replication’. ‘No. of released series’ refers to the number of series of all released samples in each site. ‘No. of release events’ refers to the number of release events detected for each site calculated from all released samples.

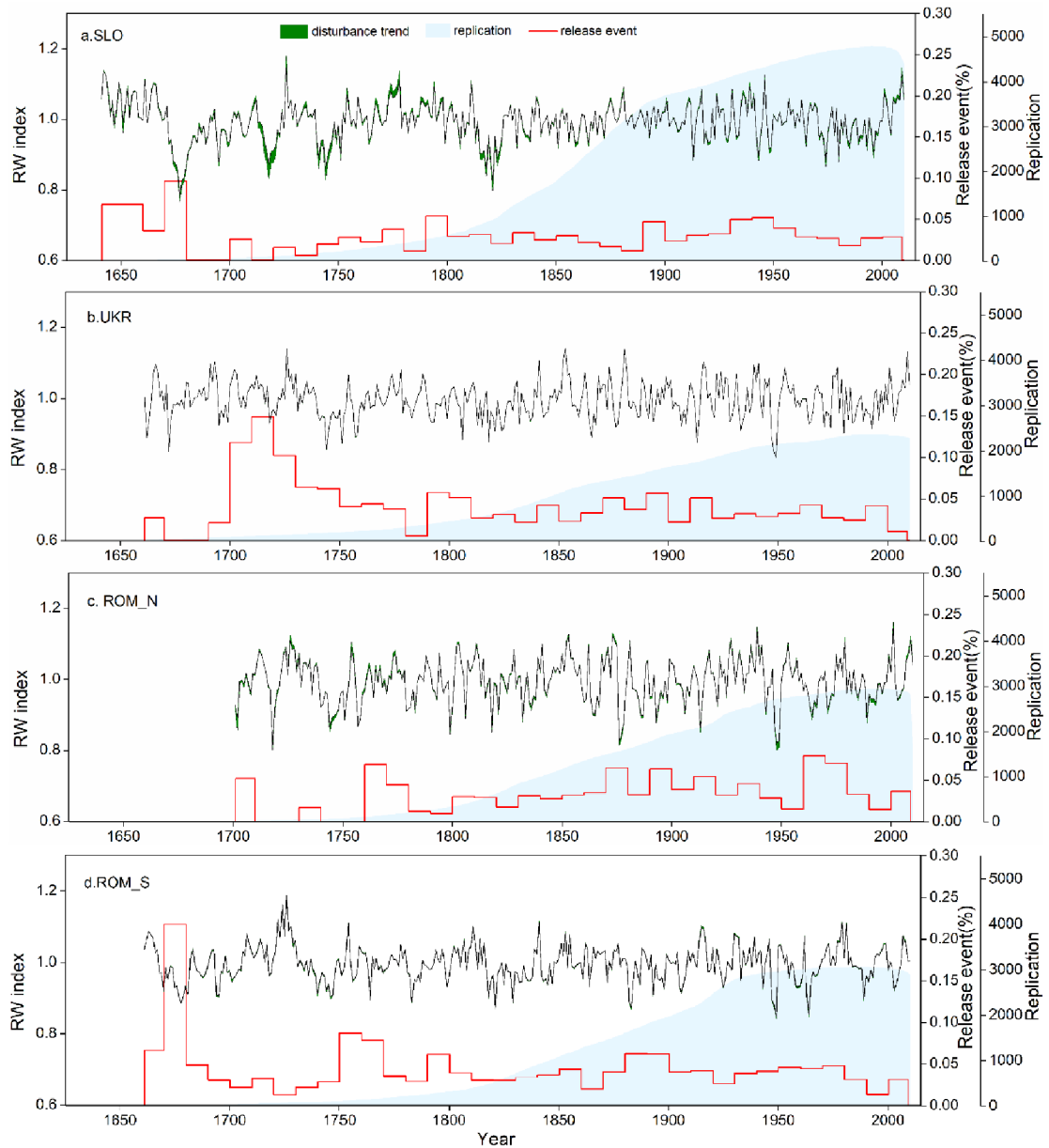


Fig. 4. Regional level RW chronology structure comparison between disturbance-affected (RW_dis) and disturbance-corrected (RW_dis_CID) chronologies. Green shading indicates disturbance trends identified by the CID method and represents the difference between the RW_dis and RW_dis_CID chronologies. The shaded area above (below) the solid black curve shows release (suppression) trends. Regional-level chronologies were developed from all available series within each region. The ‘release event’ disturbance history (red line) was calculated based on the CID method and disturbance events were grouped according to the decade in which the disturbances were initiated. Release event (%) was calculated using the decadal number of release events and replication [release event (%) = decadal number of release events / decadal average replication]. Blue shading represents series replication. All chronologies were truncated to the period with replication ≥ 10 series.

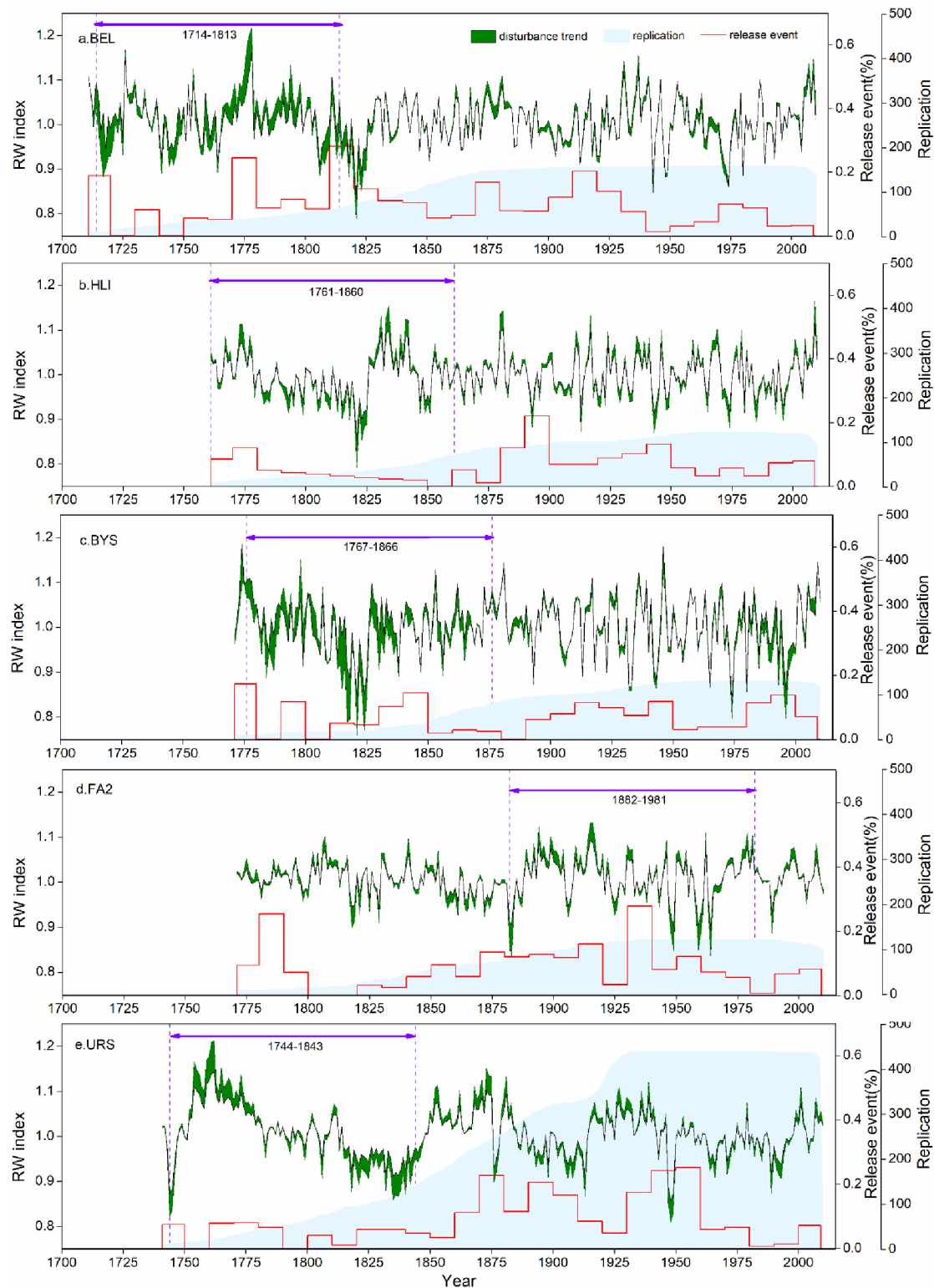


Fig. 5. Site level (Subset A) RW chronology structure comparison between disturbance-affected (RW_dis) and disturbance-corrected (RW_dis_CID) chronologies for five sites classified as ‘severely disturbed’, highlighting the presence of disturbance trends. Green shading indicates disturbance trends identified by the CID method and represents the difference between the RW_dis and RW_dis_CID chronologies. Purple line with arrows marks the 100-year ‘severe disturbance’ period identified based on residual calculation results of RW_dis and RW_dis_CID chronologies (Fig. A2). Release event (%) (red line) was

calculated using the decadal number of release events and replication [release event (%) = decadal number of release events / decadal average replication]. Blue shading represents series replication. All chronologies were developed using only released series from each site and were truncated to the period with replication ≥ 10 series.

For the five sites identified as severely disturbed, periods of ‘severe disturbance’ were identified using subset B series as 1714-1813, 1761-1860, 1767-1866, 1882-1981, 1744-1843 for BEL, HLI, BYS, FA2 and URS, respectively (Fig. 5; Table 5; Fig. A2). Generally, disturbance trends in subset B chronologies were similar to those displayed by subset A (Fig. 5; Fig. A6). However, with the temporally constrained growth release period and reduced replication (39-93 series; Table 5), these features were more pronounced, most notably in the case of BEL, BYS, and URS. Subset B chronologies of URS showed the most apparent association between release events and major disturbance trends.

4.1.2 Disturbance influence on RW and BI chronologies

The impact of disturbance events on the structure of BI chronologies (as well as relevant RW chronologies) was examined in more detail in subset C (Fig. 6). Disturbance influences on RW chronologies, displayed either as disturbance trends identified by CID in the RW_dis / RW_dis_CID comparison (Fig. 6A) or as structure differences between the disturbed (RW_dis) and undisturbed (RW_undis) chronologies (Fig. 6B), tended to occur around the same period for each site, and most notably in the case of BEL (around 1770-1800) and URS (around 1850-1880) (Fig. 6A, B). The detected disturbance trends based on the RW_dis / RW_dis_CID comparison were also coupled with the temporal distribution of growth release events for each subset, becoming more apparent with the reduction of scale and series replication (Figs. 4-6, Figs. A6-7), especially for sites BEL and URS. The comparison of BI_dis and BI_undis showed that BI chronologies generally contain less decadal and lower-frequency variance than RW chronologies (Fig. 6C). Furthermore, ‘structure differences’ between the BI_dis and BI_undis chronologies were much less pronounced compared to their RW counterparts for the identified periods of ‘severe disturbance’. No obvious differences were observed in high frequency paired chronologies for either RW or BI (Fig. A8).

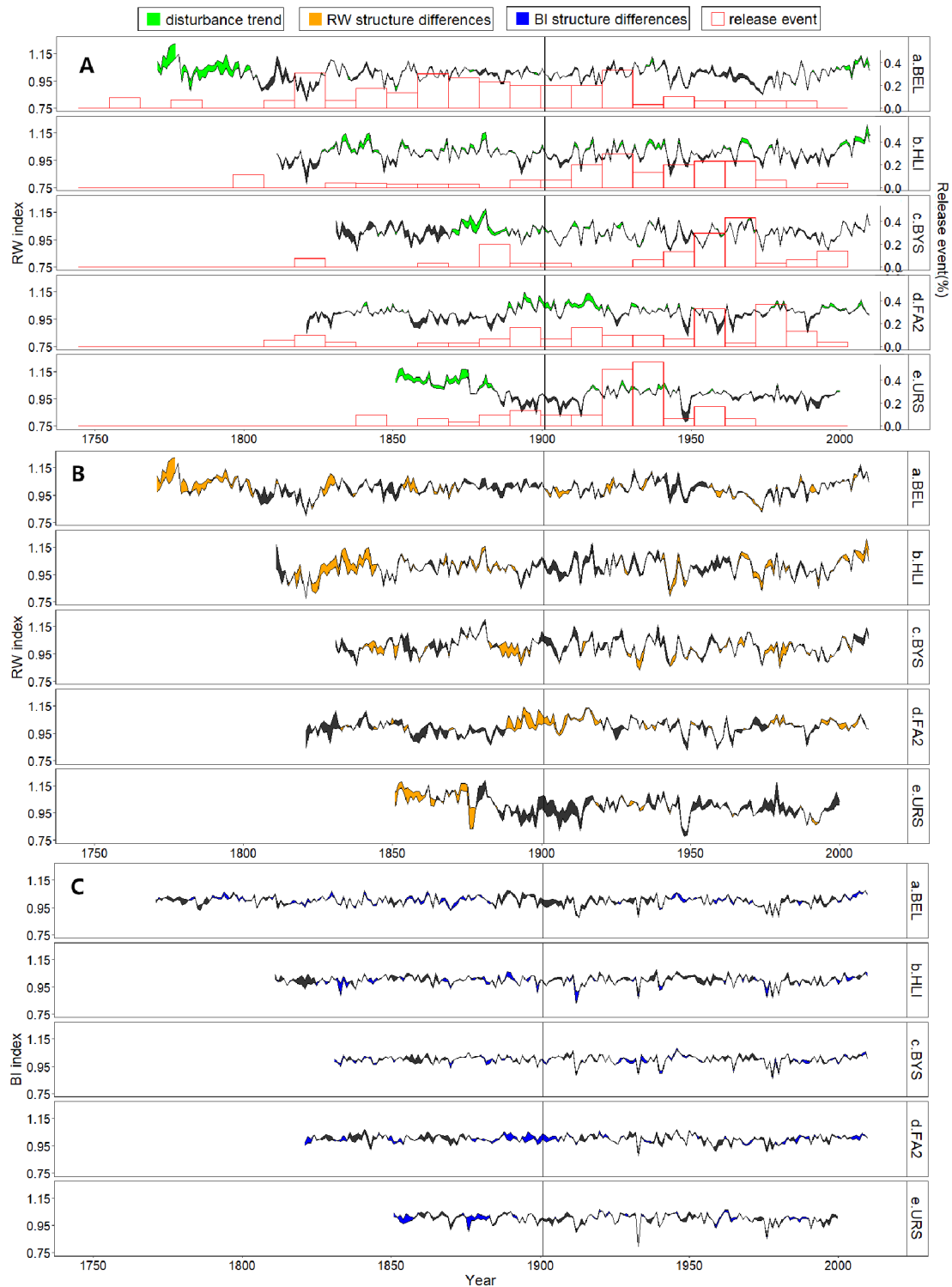


Fig. 6. Site level RW and blue intensity (BI) chronology structure comparison among three RW subgroups (RW_dis; RW_dis_CID; RW_undis) and two BI subgroups (BI_dis; BI_undis) comprising Subset C. Panels A, B, C refer to the chronology comparison between RW_dis / RW_dis_CID, RW_dis / RW_undis, and BI_dis / BI_undis, respectively. The proportion of release events (red bars in panel A) was calculated from the decadal number of release events and replication [release event (%) = decadal number of release events / average decadal replication]. Green shading indicates disturbance trends identified by CID by representing the difference between disturbance-affected (RW_dis) and disturbance-corrected

(RW_dis_CID) chronologies. Similarly, orange (blue) shading represents structure differences between disturbed and undisturbed RW (BI) chronologies. Periods with black shading represent detected suppression trends ($RW_dis < RW_dis_CID$) or structure differences ($RW_dis < RW_undis$; $BI_dis < BI_undis$). All chronologies were truncated to the period with replication ≥ 10 series. The period after 1901 represents the temporal range for the growth-climate response assessment of all five sites.

4.1.3 Climatic sensitivity of RW and BI chronologies

RW chronologies of three sites (BEL, HLI, URS) showed significant ($p < 0.01$) positive correlations with June and July monthly mean temperature (Fig. 7). A significant positive correlation with previous October temperature was displayed by HLI, BYS and URS. RW chronologies of FA2 also showed a weak, though significant, negative correlation with previous August and September temperatures (Fig. 7d). In general, there were no significant differences in temperature response among the three types of RW chronologies (RW_dis, RW_dis_CID, RW_undis). BI chronologies of all five sites consistently showed significant positive correlations with temperature from April to September, except for a few individual months for some sites (e.g., June for HLI and BYS; May-June for FA2, July for URS) (Fig. 7, Fig. A9). Furthermore, BI_dis chronologies showed higher correlations than BI_undis for four of the five sites (i.e., BEL, HLI, BYS and FA2) investigated in more detail. However, this difference was found not to be statistically significant ($p = 0.234$) and a further assessment of high-frequency versions of the chronologies also did not reveal any significant differences (Fig. A10). Finally, the BI chronologies exhibited significantly higher correlation values than RW chronologies in most months throughout the growing season. Seasonal correlations demonstrated similar relationships to the individual monthly comparisons (Fig. 7, Table 6), with a much stronger response of BI chronologies to April-September temperature ($r = 0.56-0.75$) compared to RW ($r = 0.30-0.60$). The seasonality of the RW chronologies was shorter than that of BI, with the optimal seasonal response centered on June-July, except for FA2 which did not exhibit any significant summer temperature response (Fig. 7, Table 6).

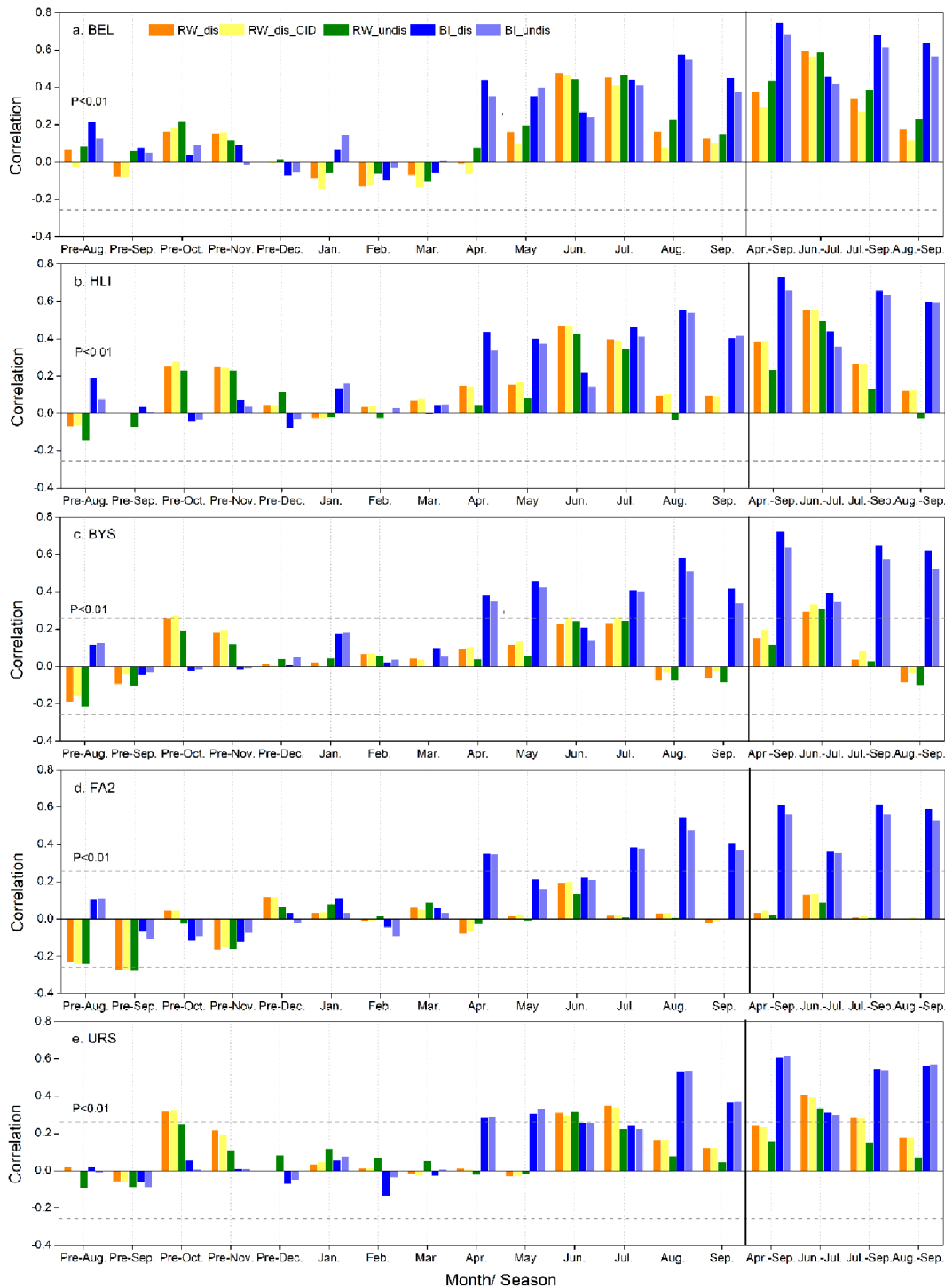


Fig. 7. Site level temperature response assessment between RW and BI chronologies from five sites characterized as ‘severely disturbed’, and monthly / seasonal mean temperature for disturbed (dis) and undisturbed (undis) subsets for the 1901-2013 instrumental period. RW chronologies are composed of disturbance-affected (RW_dis), disturbance-corrected (RW_dis_CID) and undisturbed (RW_undis) series. This temperature response assessment was based on the Subset C chronologies described in Table 3. Note that BI chronologies represent BI series divided into the disturbed (BI_dis) and undisturbed (BI_undis) groups according to the CID disturbance assessment of RW series.

Running correlations displayed a temporally stronger and more robust relationship between BI chronologies and seasonal temperature than RW chronologies (Fig. 8). The response of BI_dis chronologies was consistently stronger over the 20th century compared to BI_undis for HLI, BYS and FA2, whereas the response for BEL and URS was more mixed. A distinct decrease in correlation was observed in RW chronologies of the FA2 site in the second half of the 20th century, reaching negative values around the 1960-1980 period (Fig. 8d). Though less severe, a similar reduction was visible in both BI chronologies over the same period. Similarly, a sharp decline in the running correlation was observed for the URS site, although this decline was not as pronounced as in FA2 and only appeared in the RW_undis chronology (Fig. 6B, 8e). In general, no consistent differences in the pattern of running correlations were identified between the three types of RW chronologies.

Site	Group	No. of series	No. of release events	Chronology extent	First year with rep. ≥ 10	First year with EPS ≥ 0.85	AC1	Rbar	Correlation with Apr-Sep temperature	Correlation with Jun-Jul temperature
BEL	RW_dis	30	112	1591-2013	1720	1795	0.85	0.78	0.38	0.60
	RW_undis	30		1678-2013	1759	1905	0.77	0.61	0.44	0.59
	RW_dis_CID	30		1591-2013	1720	1795	0.74	0.62	0.30	0.57
	BI_dis	23	112	1591-2013	1721	1795	0.65	0.37	0.75	0.46
	BI_undis	24		1678-2013	1765	1905	0.71	0.32	0.68	0.42
HLI	RW_dis	30	67	1685-2012	1769	1885	0.86	0.52	0.39	0.56
	RW_undis	30		1684-2012	1775	1900	0.83	0.44	0.23	0.50
	RW_dis_CID	30		1685-2012	1769	1885	0.85	0.52	0.39	0.55
	BI_dis	23	67	1685-2012	1810	1885	0.60	0.30	0.74	0.44
	BI_undis	27		1680-2012	1798	1870	0.57	0.26	0.66	0.36
BYS	RW_dis	30	56	1708-2012	1826	1905	0.80	0.60	0.15	0.30
	RW_undis	30		1627-2012	1779	1915	0.67	0.55	0.11	0.31
	RW_dis_CID	30		1708-2012	1826	1890	0.69	0.36	0.20	0.33
	BI_dis	27	56	1748-2012	1830	1885	0.61	0.11	0.73	0.40
	BI_undis	26		1627-2012	1794	1870	0.66	0.44	0.64	0.35
FA2	RW_dis	30	58	1670-2012	1795	1920	0.88	0.64	0.03	0.13
	RW_undis	30		1692-2012	1811	1925	0.82	0.51	0.03	0.09
	RW_dis_CID	30		1670-2012	1795	1920	0.85	0.63	0.05	0.14
	BI_dis	29	58	1670-2012	1795	1920	0.70	0.31	0.61	0.37
	BI_undis	27		1692-2012	1813	1925	0.78	0.38	0.56	0.35
URS	RW_dis	30	87	1713-2010	1777	1825	0.90	0.82	0.24	0.40
	RW_undis	30		1674-2010	1842	1860	0.78	0.62	0.16	0.33
	RW_dis_CID	30		1713-2-10	1777	1825	0.88	0.82	0.24	0.39
	BI_dis	30	87	1714-2009	1778	1870	0.64	0.29	0.61	0.31
	BI_undis	23		1678-2009	1847	1875	0.64	0.23	0.62	0.30

Table 6. Descriptive statistics and temperature response for subset C chronologies in Fig. 7, comprising three RW (disturbance-affected, disturbance-corrected, undisturbed) and two BI (disturbed, undisturbed) chronologies for each site. Note that BI series were classified as either ‘disturbed’ or ‘undisturbed’ based on the CID disturbance detection assessment of their RW counterparts. The number of BI series was lower than that of RW for some sites / groups due to the exclusion of several samples to avoid sample quality or discoloration issues which could affect the BI chronologies. AC1, and Rbar represent first-order autocorrelation and inter-series correlation, respectively. ‘Rep.’ refers to ‘series replication’, ‘EPS’ represents Expressed Population Signal, and ‘No. of series’ refers to the number of RW / BI series for each site. ‘No. of release events’ refers to the number of release events detected in each site / group calculated from all released cores.

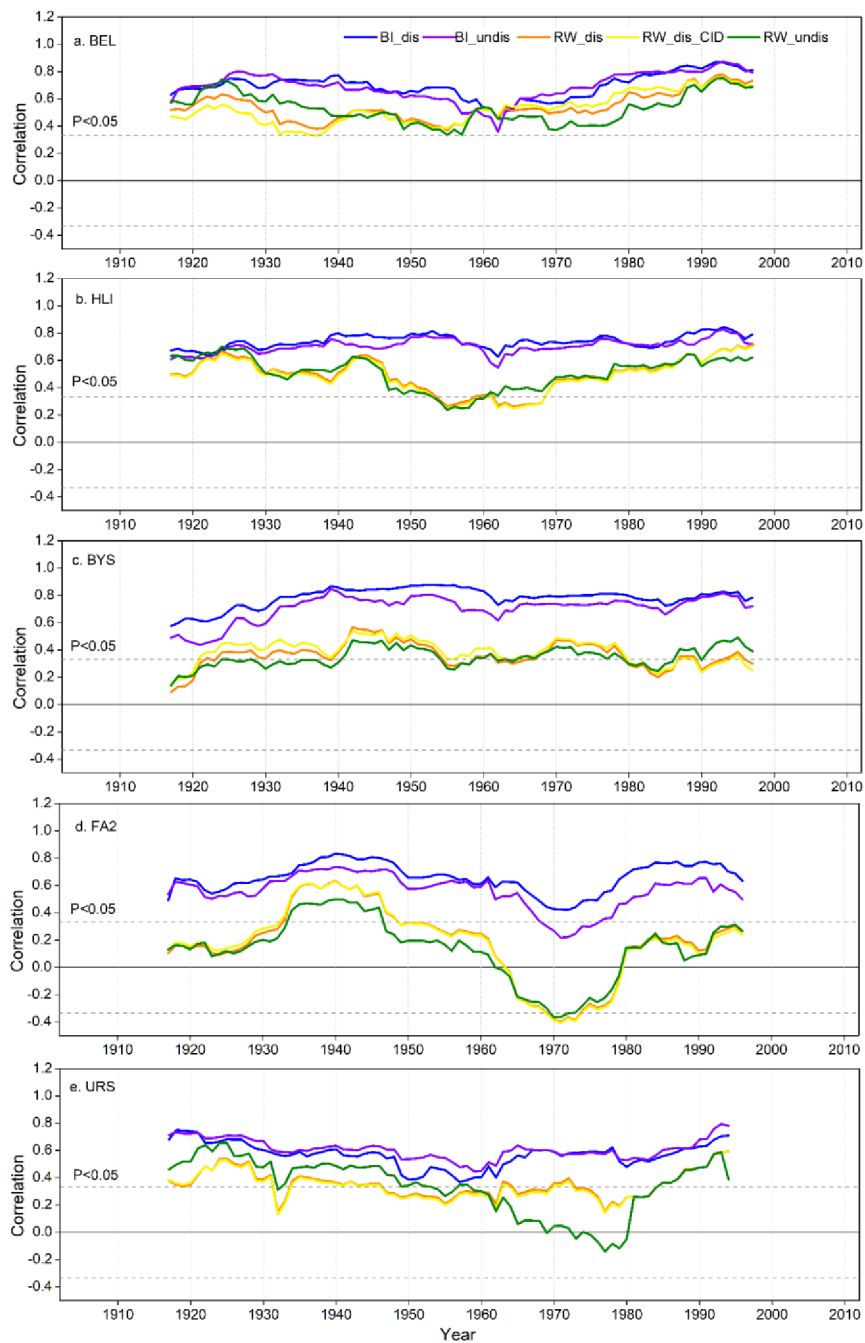


Fig. 8. Site level (31-year) running correlations between chronologies developed from RW and BI series, and seasonal mean temperature (June-July for RW, April-September for BI) of five selected sites with pronounced disturbance-related trends for the 1901-2013 instrumental period.

4.2 IMPACT OF POLLUTION ON THE CLIMATIC SENSITIVITY OF MULTIPLE NORWAY SPRUCE TREE-RING PARAMETERS IN CENTRAL EUROPE

4.2.1 Historical pollution status and the detected pollution signals in tree rings

Both pollution datasets revealed that our study sites were heavily exposed to sulfur and nitrogen deposition during the 1960-1990s, with the peak centered around the year 1980, and a gradual decline thereafter (Fig. 9E, F; Fig. B1; Fig. B12 E, F). The pollution intensity varied somewhat among sites, with NB located in northern Bohemia exhibiting the heaviest loading (30.72 mg ha⁻¹ year⁻¹ of sulfur and 20.77 mg ha⁻¹ year⁻¹ of nitrogen). SMR and SUO in South-western Czechia were exposed to the lowest sulfur deposition intensities in relative terms (10.75 and 10.29 mg ha⁻¹ year⁻¹ in SUO and SMR, respectively; Table 1). The effectiveness of applying the CID method for pollution signal detection and correction in RW chronologies varied among sites and detection sensitivity settings, with the most prominent suppression trends being corrected in NB and CK during the 1970s to 1980s, especially by the sensitive CID setting (cid_sen; Fig. 10). In contrast, marginal differences in chronology structure were observed for the two north Slovakia-Poland border sites (PIL and SLO) when comparing the growth trends before and after CID processing.

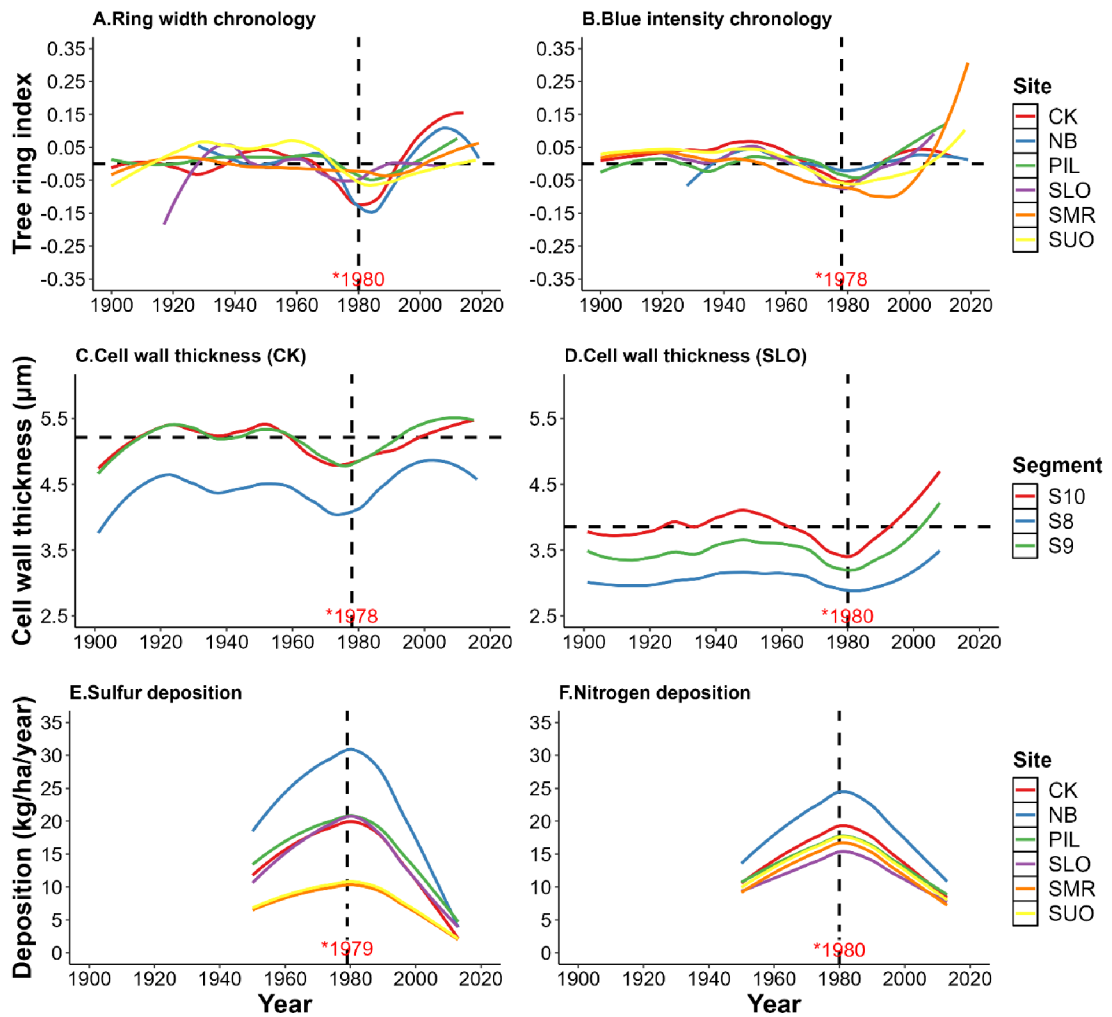


Fig. 9. Long term trends of tree growth represented by different tree ring parameters and pollution history of all studied sites. (A) and (B) display the RW and BI chronologies. (C) and (D) display the cell wall thickness (CWT) of segments 8-10 for sites CK and SLO. (E) and (F) display the sulfur and nitrogen deposition for the period 1950 to 2013. RW and BI chronologies are truncated before the year 1900 and the replication of all sites over the period 1900-2013 exceeds 10 series, except for the start year for CK and SLO are 1928 and 1917, respectively. Vertical dashed lines mark years with the highest average pollution levels (E, F) and the lowest average growth values of different parameters (A-D). Horizontal dashed lines in C and D represent the average CWT of segment 10 for site CK (for the 1900-2016 period) and SLO (for the 1900-2008 period), respectively. Solid curves represent smoothed values using the ‘loess’ method (with the following parameter settings: $n = 80$, $span = 0.4$) in the R package ‘ggplot2’.



Fig. 10. Tree-ring width (RW) chronologies before and after treatment using the Curve Intervention Detection (CID) method with both default (cid_def) and sensitive (cid_sen) detection thresholds. Vertical dashed lines mark the year 1980 in which most sites exhibit the lowest chronology index value. All chronologies are truncated before 1900 and replication over the full period reaches or exceeds 10 series.

4.2.2 Tree growth trends revealed by different tree ring parameters

RW chronologies of all sites revealed varying but concurrent growth declines during similar periods (i.e., 1970s to 1980s), especially for sites NB, CK, with the lowest site level averaged index values occurring in 1980 (Fig. 9A; Fig. B12A). Similar growth declines were also captured by BI chronologies, albeit with a lesser magnitude and occurring earlier (the lowest site averaged growth occurred in 1978) compared to RW chronologies (Fig. 9B; Fig. B12B). Furthermore, the most prominent and longest lasting BI chronology decline was found in SMR, with the lowest growth occurring around 1995-1996. Accordingly, extreme years with negative growth were identified in RW chronologies around 1980 by the bias-adjusted standardized growth change pointer year analysis approach, especially in the case of NB and CK (Fig. B4A; Table B1A). Other common extreme negative growth years (e.g., 1995 and 1996) occurred in the 1990s for the two sites in south-western Czechia (SUO and SMR). The negative extreme year 1978 was detected in BI chronologies from all sites (Fig. B4B; Table B1B).

Growth trends revealed by various QWA parameters for the range of tree ring segments were quite diverse, with growth reductions in CWT at both sites during the 1970s to 1980s. The growth reductions were more prominent in the latter segments, especially from S8 to S10 (Fig. 9C, D; Fig. B5A, B). SLO exhibited more severe growth reductions compared to CK. For example, the CWT in segment S10 declined by 34% in 1980 at SLO, compared to 30% in 1978 at CK. Considering the three segments (S8-10) for CK and SLO, the years 1978 and 1980 showed the lowest growth, respectively (Fig. 9C, D; Fig. B12 C, D). Slight reductions in LA in segments S1 to S8 were found in CK, but such reductions were considerably less prominent than those observed in CWT. In general, LA index values were stable over time for SLO (Fig. B5).

4.2.3 Temperature sensitivity of tree rings in different pollution periods

The growth-climate relationships varied among different pollution periods and sites; such variations were particularly obvious in RW chronologies (Fig. 11; Fig. B6). In the FULL period, ring width was significantly correlated with June-July temperature for sites SMR, PIL, SLO, whereas April-August temperature was significantly correlated with the NB and CK site chronologies. Furthermore, these RW temperature signals decayed alongside heavier pollution, with widespread weakening or even absence of these signals in periods POL and post-POL (Fig. 11A; Fig. B6A). Temperature signals captured using LWBI over the FULL period were generally more representative for the full warm season as well as stronger compared to those of RW. April-September temperature was often found significantly correlated with LWBI (Fig. 11B; Fig. B6B), but in the south Czech sites July-September appeared more influential (Fig. B6B). In addition, the BI temperature signal was fairly stable across all pollution intensity periods for most sites. The effects of CID correction on the temperature signals in RW chronologies were mixed, ranging from improved correlations for SUO / PIL / SLO to weakened correlations for NB / CK (Fig. B7). When evaluating the temperature signals in relation to the alternative temperature dataset from the CHMU meteorological stations, the April-September temperature signal remained the most relevant for BI and a similar summer temperature signal as with the CRU dataset was also observed for RW (Fig. B8).

From a long-term perspective, the detected RW temperature signals (June-July for sites SMR, SUO, SLO and PIL; April-August for sites NB and CK) were variable as the signal strength of most sites weakened and became non-significant ($p < 0.01$) roughly around the 1970s and 1980s (Fig. 12). Although the CID method had some influence on the RW temperature signals, the outcome was mixed with no obvious net effect (Fig. B9). Compared to the temperature signal in RW, the detected BI temperature signals (Apr.-Sep. for site NB, CK, SLO and PIL; Jul.-Sep. for site SUO and SMR) were more stable and significantly correlated throughout the last century

(with only minor or no weakening) even in periods with strong pollution loading (1960-1990s), except for the site NB during the 1950s to 1960s when the correlation was not significant ($p < 0.01$; red curve in Fig. 12a).

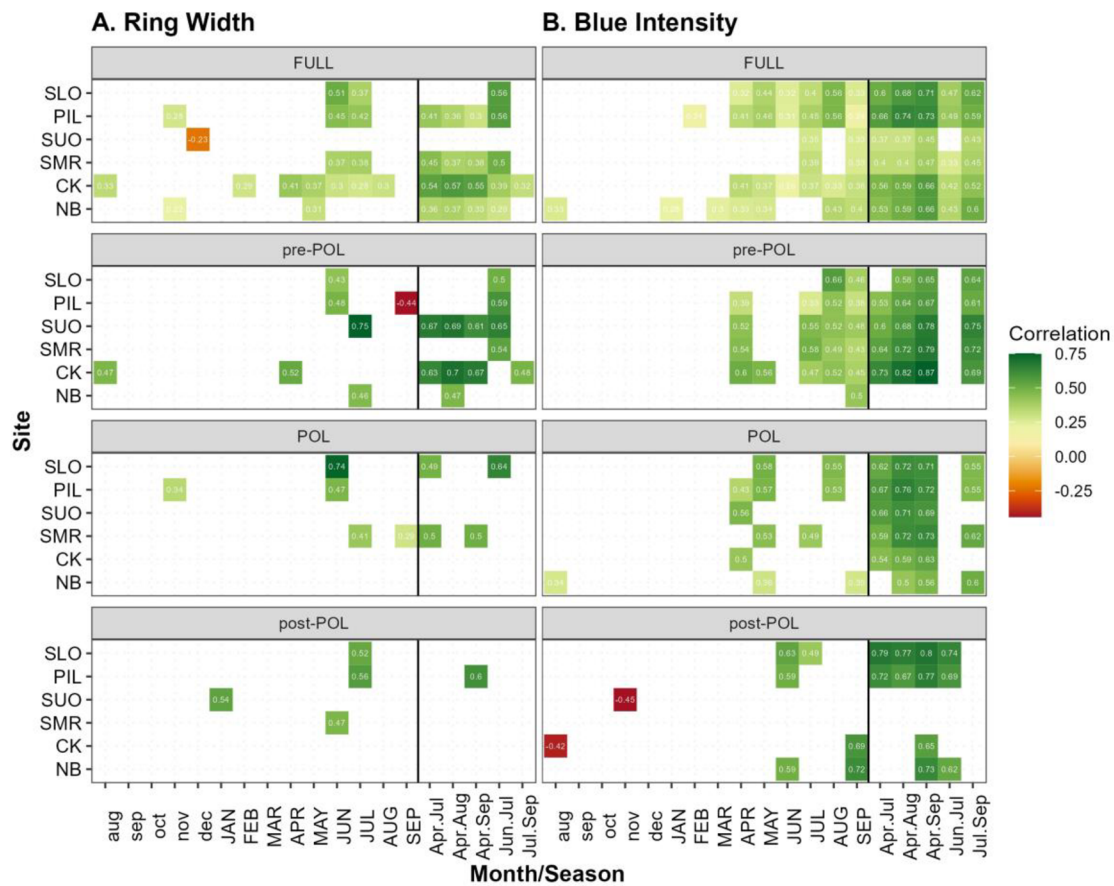


Fig. 11. Growth climate correlations between different tree ring parameters (ring width and blue intensity) and CRU monthly / seasonal temperature for different pollution intensity periods. The FULL period represents the common period for all sites from 1930-2008. Pre-POL, POL and post-POL represent the three segmented periods based on pollution history, including the pre-pollution period (1930-1959), heavily polluted period (1960-1989) and post-pollution period (1990-2008), respectively. Only significant correlations are displayed with a significance level of 0.01. Lowercase letters along the x-axis indicate months of the previous year relative to the growth year.

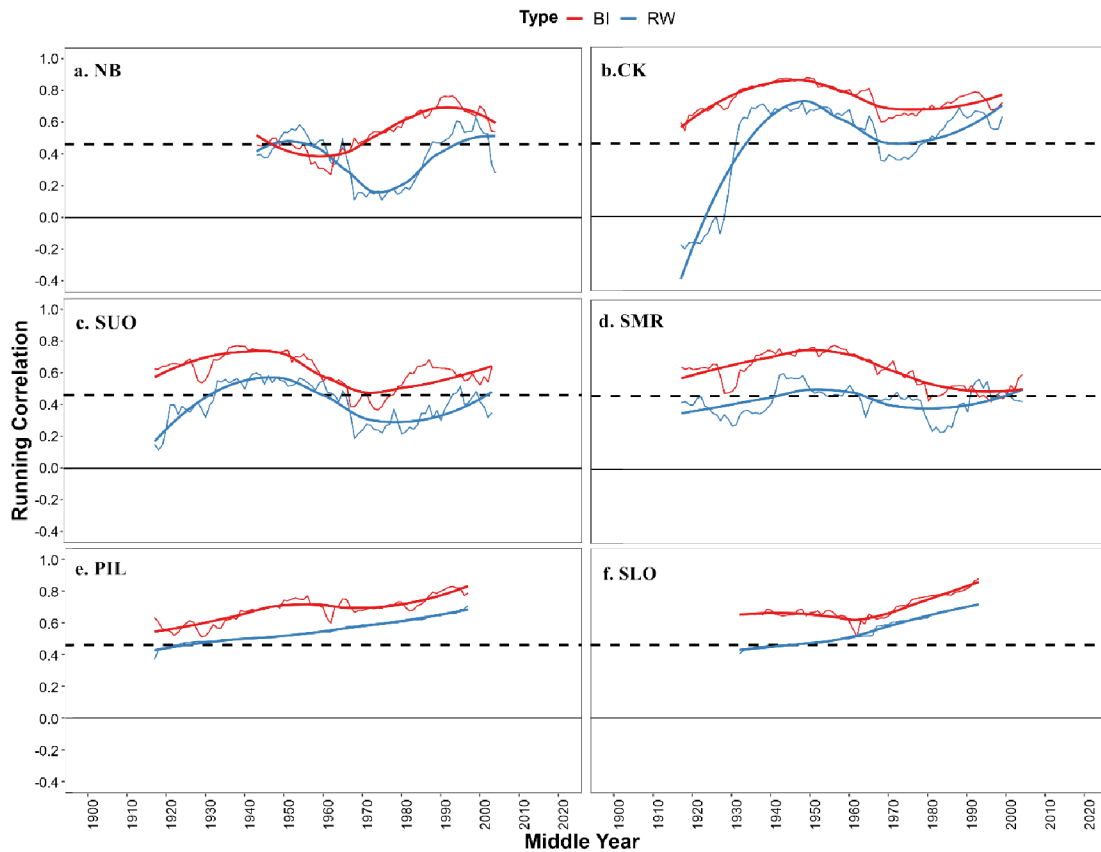


Fig. 12. 31-year running correlations between different tree ring parameter (ring width and blue intensity) chronologies and optimal seasonal temperatures for each parameter (selected according to seasonal correlation results in Fig. 11). The correlation periods are truncated in 1902, with replication for all sites over the entire period reaching or exceeding ten series. RW chronologies are correlated with Jun.-Jul. (for sites SMR, SUO, SLO and PIL), and Apr.-Aug. (for sites NB and CK) seasonal CRU temperatures. BI chronologies are correlated with Apr.-Sep. (for sites NB, CK, SLO and PIL), and Jul.-Sep. (for sites SUO and SMR) seasonal CRU temperatures. Horizontal bold dashed lines represent the 0.01 significance level. Thick lines represent smoothed values using the ‘loess’ method (with the following parameter settings: $n = 80$, $span = 0.4$) in the R package ‘ggplot2’.

Considering the QWA data, growing season temperature signals (Apr.-Sep.) were present in CWT chronologies from both sites, mainly have been found in segments S8-10 (FULL period; Fig. 13). The detected CWT temperature signal was strongest and most stable in segment S10 regardless of the pollution period considered, except for CK during the heavily polluted period ‘POL’ which contained the strongest signal in S8-9 (POL period; Fig. 13A). In the temporal growth-climate response comparison, apparent weakening in the Apr.-Sep. temperature signal occurred during the 1960s-1990s in segment S10 of both sites. The weaker period for SLO was earlier and shorter compared to CK, however, the relationship with temperature remained significant for both sites (Fig. 14). No convincing temperature signal or moisture availability

signal (SPEI) was found in the LA parameter, although the month of June showed significant correlations with LA for SLO (Fig. B10, B11).

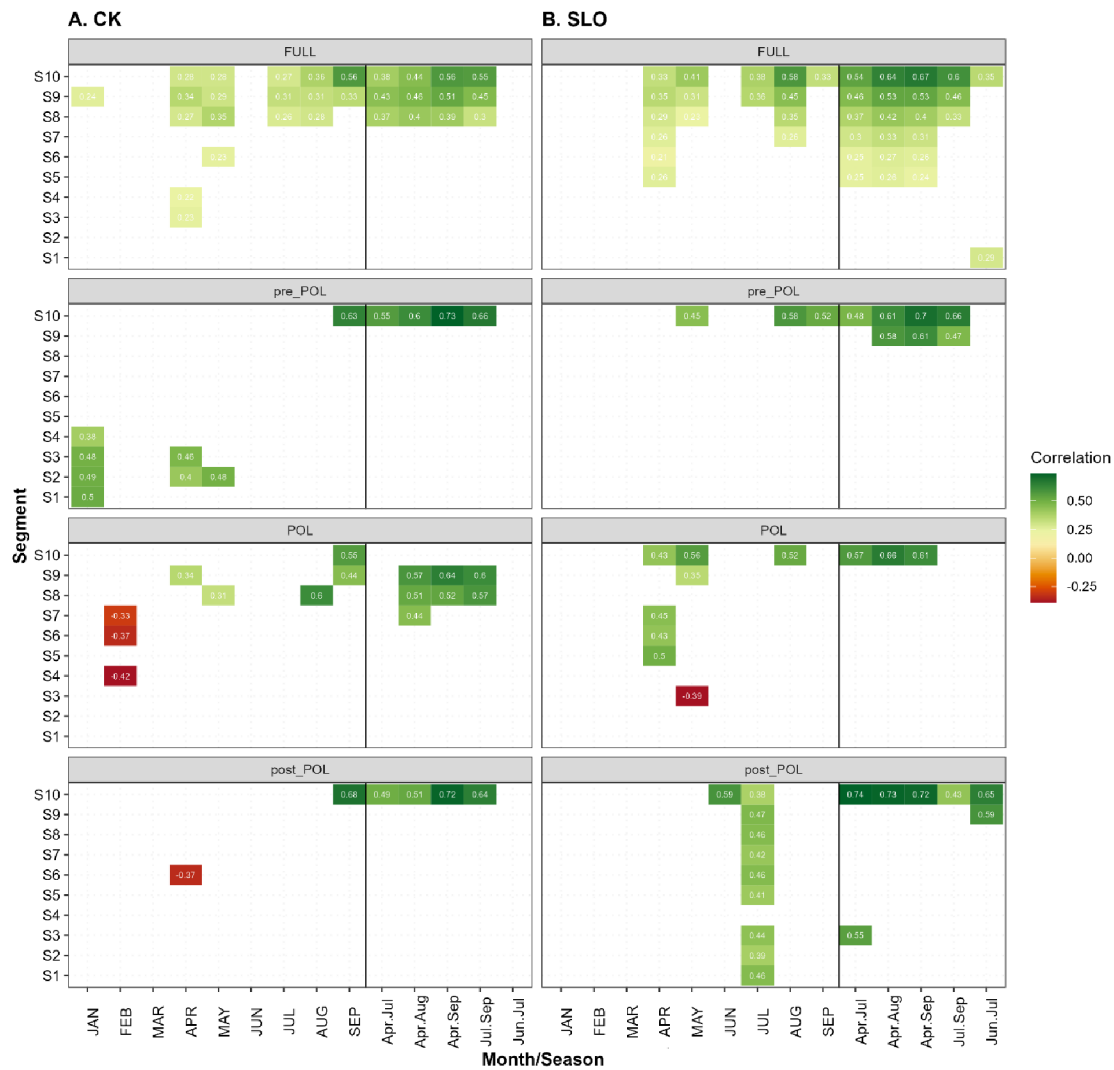


Fig. 13. Growth climate correlations between cell wall thickness (CWT) and CRU monthly / seasonal temperature for different pollution periods for sites CK and SLO. The temporal range of the four periods (FULL, pre-POL, POL, post-POL) are 1901-2016, 1930-1959, 1960-1989, 1990-2016 for CK, and 1901-2008, 1930-1959, 1960-1989, 1990-2008 for SLO. Pre-POL, POL and post-POL represent the three segmented periods based on pollution history, including the pre-pollution period, heavily polluted period and post-pollution period, respectively. Only significant correlations are displayed with a significance level of 0.01.

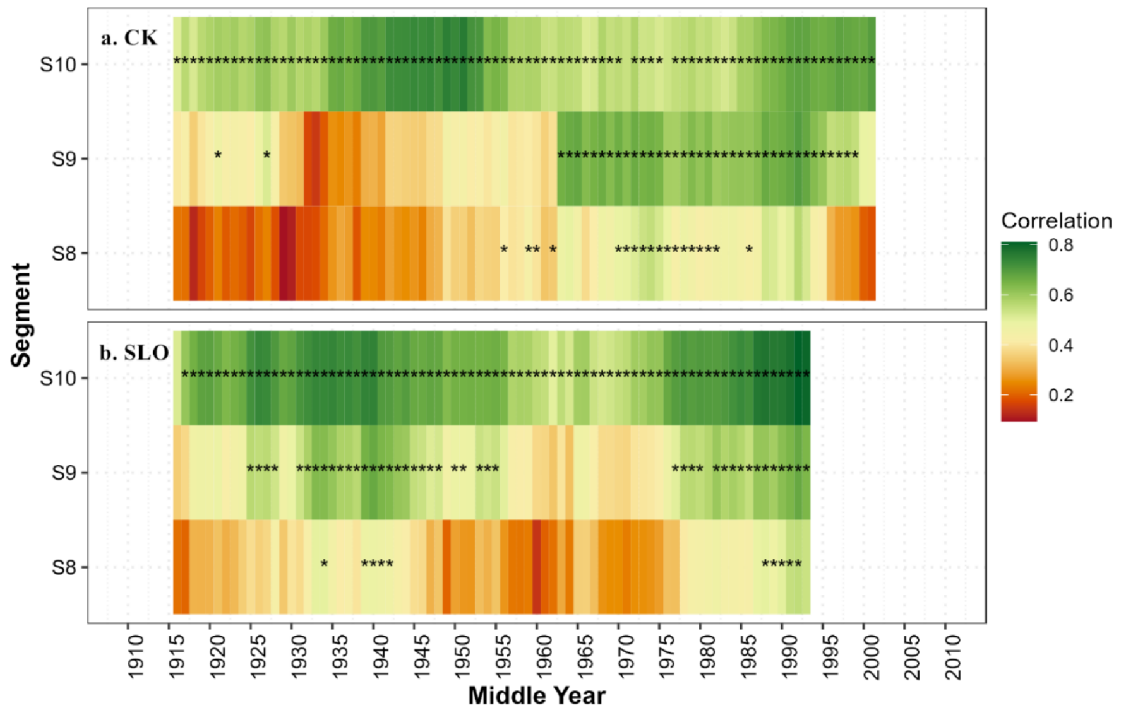


Fig. 14. 31-year running correlations between cell wall thickness (CWT) of segments 8-10 and average April to September temperature for sites CK and SLO. The correlation periods are 1901-2016 and 1901-2008 for CK and SLO, respectively. The correlations are plotted using the center year. The asterisks '*' represent the 0.01 significance level.

4.2.4 General growth trends, climate patterns, and forest dynamics in the context of pollution

When comparing the tree ring chronologies and temperature timeseries, two specific periods associated with notable growth reductions were apparent. During the period around 1980, large departures of RW chronologies from the temperature series can be observed in NB, CK, SUO and PIL (Fig. 15A), however, this pattern was not found for the BI chronologies (Fig. 15B). Moreover, during the period around 1996, the RW chronologies also displayed some considerable deviations from the temperature series for sites SUO and SMR. While the BI chronologies displayed lower index values particularly in the late 1970s, they maintained a high degree of agreement with their respective temperature series which exhibited lower temperatures around the same time. The CWT chronologies behaved in a similar manner as BI, with a high degree of agreement between the CWT chronologies and temperature signal series during the two low growth periods (Fig. 15C). The NDVI dataset showed an increasing trend in the most recent decades following the heavy pollution period (i.e., 1981-2012) across all four locations covering the studied sites, with the summer season (i.e., Jun.-Jul.) exhibiting the highest values (Fig. 16A). Furthermore, observational data of defoliation showed a declining trend over the period of available instrumental data during 1991-2016 (Fig. 16B).

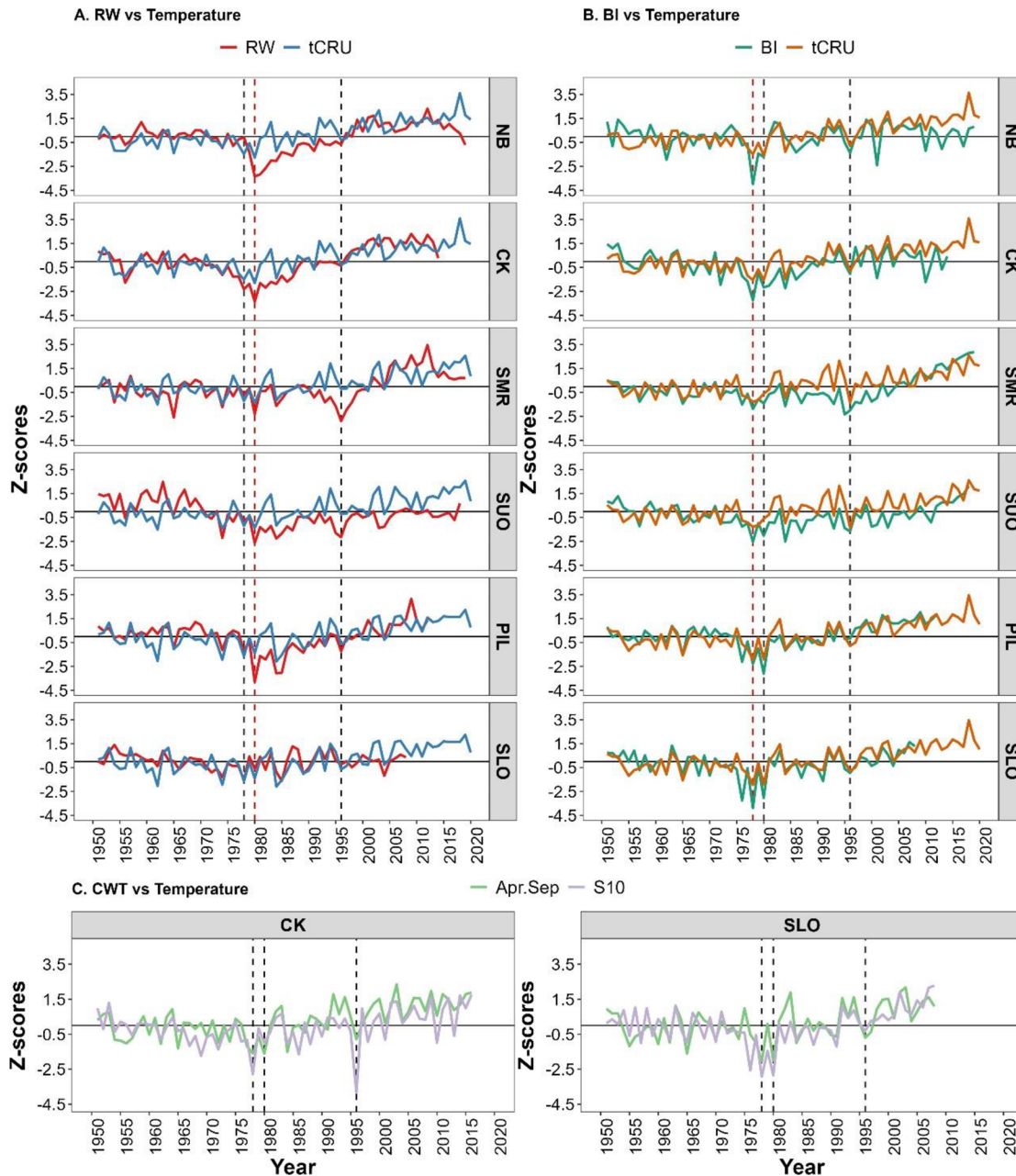
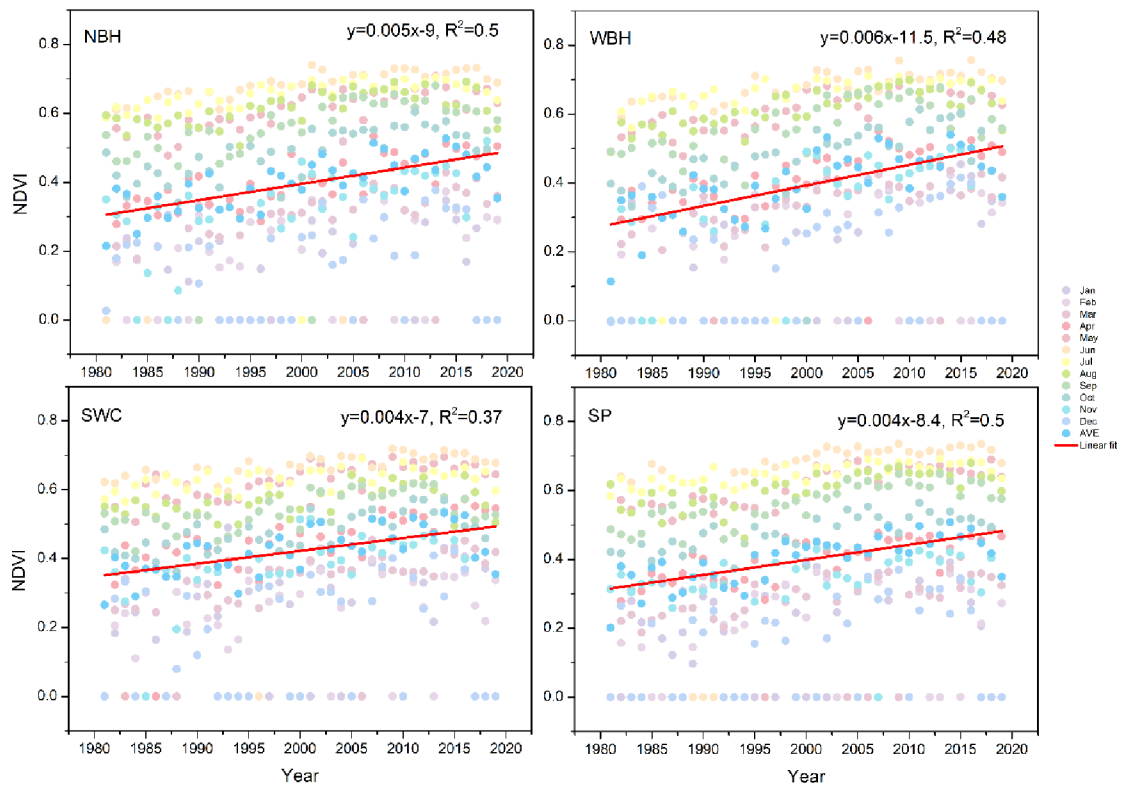


Fig. 15. Long-term trend comparison among ring width, blue intensity, and cell wall thickness (RW / BI / CWT) chronologies and seasonal CRU temperature after 1950. The optimal temperature signal seasons (tCRU) for RW / BI chronologies and temperature datasets were determined according to the monthly / seasonal growth climate correlations with CRU temperatures in Fig.11, and include: Jun.-Jul. (for sites SMR, SUO, SLO and PIL), Apr.-Aug. (for sites NB and CK) for RW chronologies; Apr.-Sep. (for sites NB, CK, SLO and PIL), Jul.-Sep. (for sites SUO and SMR) for BI chronologies. Optimal seasonal temperature signals for CWT of the two (CK and SLO) sites are from April to September as displayed in Fig.14. In panel C, only segment 10 is displayed for the two sites. The vertical dashed lines mark years exhibiting lowest growth years revealed by different parameters, they are 1978,1980,1996 from the left to right. Red vertical dashed lines represent the lowest growth year for RW and BI, respectively.

A. Normalized Difference Vegetation Index (NDVI)



B. Instrumental Defoliation history of Giant Mountains

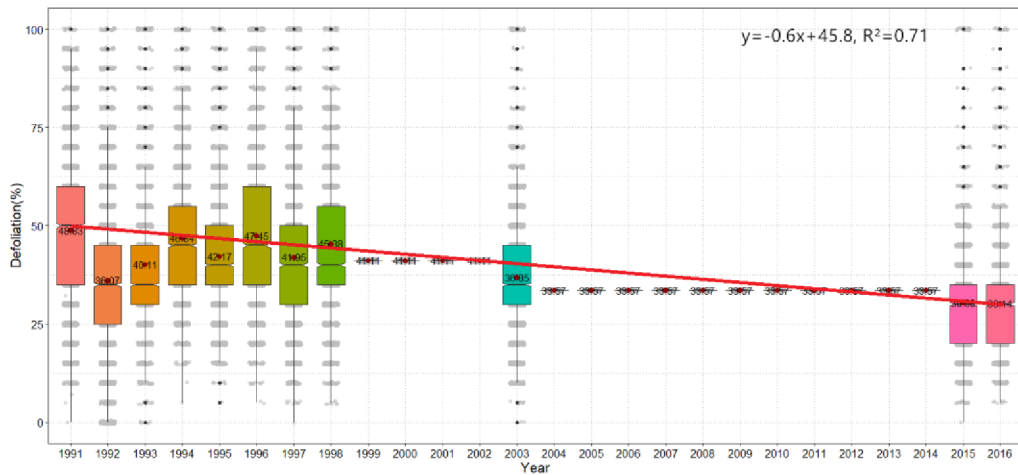


Fig. 16. Normalized Difference Vegetation Index (NDVI) (A) for the period 1981-2019 and instrumental defoliation history of the Giant Mountains in Krkonoše National Park (Czech-Poland border) for the four studied locations over the 1991-2016 period (B). Years with missing data were filled using mean values of adjacent years in panel B.

4.3 DROUGHT RESISTANCE OF MAJOR TREE SPECIES IN THE CZECH REPUBLIC

4.3.1 Drought impacts on tree growth

The growth rates of all species decreased during the dry period of 2015-2019. The decrease in the median RWI chronologies was most pronounced for Norway spruce (Fig. 17A). Compared to the average growth conditions of 2005-2009, RWI in 2015-2019 decreased by 30 % in Norway spruce, 13 % in Scots pine, 24 % in European beech, 22 % in sessile oak, and 24 % in pedunculate oak (Fig. 17B). BAI indicated very similar decreasing trends, with Scots pine showing the lowest growth reduction (-18% in BAI) (Fig. C3). These results were supported by least square regression analyses (ANOVA) comparing individual dry years and the 5-yr mean dry period with the reference period. In particular, the analyses revealed that all species experienced distinct growth reductions, with Norway spruce being the least resistant species ($\hat{\mu} = 0.69 \pm 0.06$) and Scots pine being the most resistant species ($\hat{\mu} = 0.86 \pm 0.08$). No significant differences were observed among angiosperms (Fig. 18A). A clear elevational pattern in drought resistance was only found for European beech, which exhibited a lower drought resistance ($\hat{\mu} = 0.72 \pm 0.04$) at low elevations (Figs. 18B, C4). Impacts of the dry period or dry years on tree growth evaluated with BAI showed identical results (see Fig. C5).

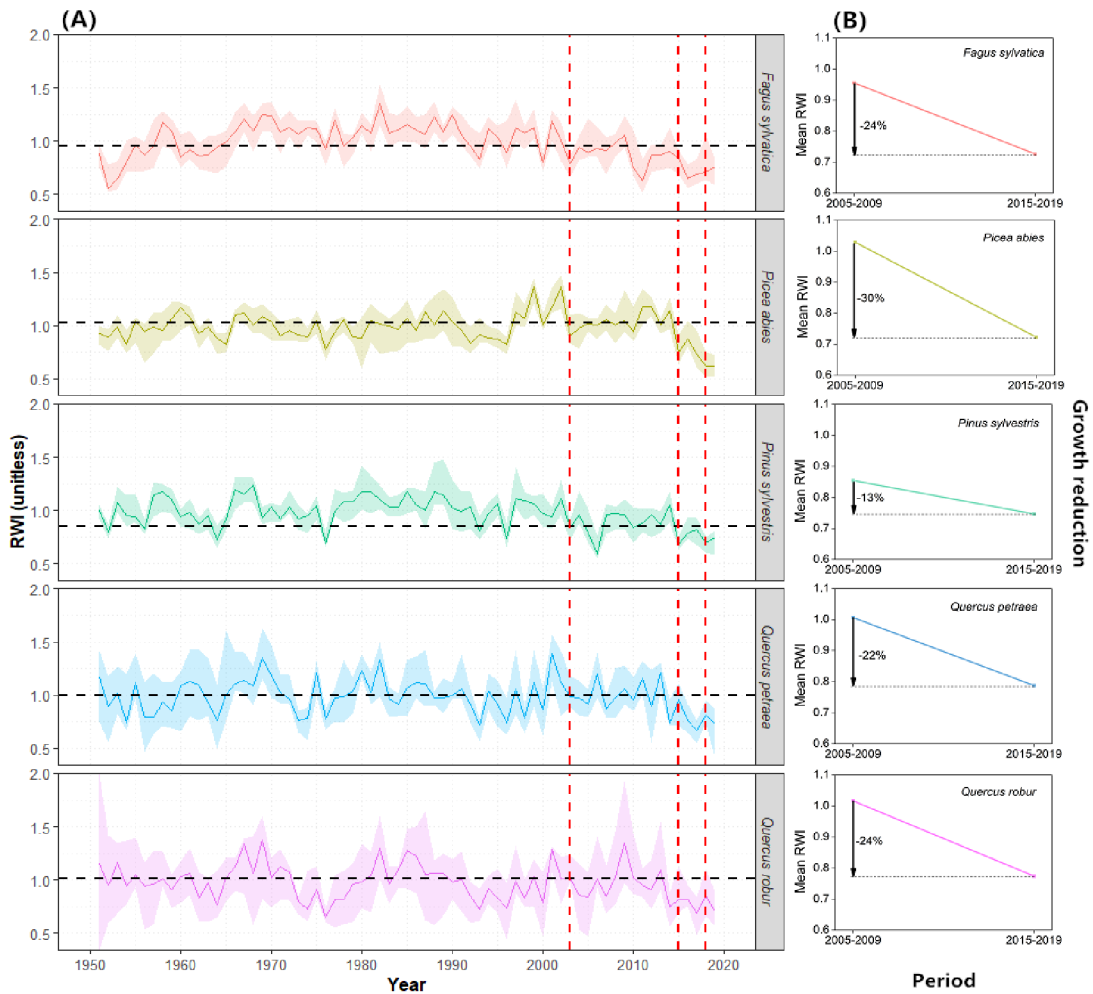


Fig. 17. Growth trajectories during the period 1950-2019 (A) and mean growth reductions between two periods (B). In (A), the median values (solid lines) and 95% confidence intervals of RWI are displayed for individual species. Vertical red dashed lines denote extremely dry years (2003, 2015, 2018). Horizontal black dashed lines represent the mean RWI of the “reference” period (2005-2009). In (B), the medians of the mean RWI for the specified periods are displayed. Vertical black arrows and colored diagonal lines indicate relative growth reductions from the reference period (2005-2009) to the dry period (2015-2019).

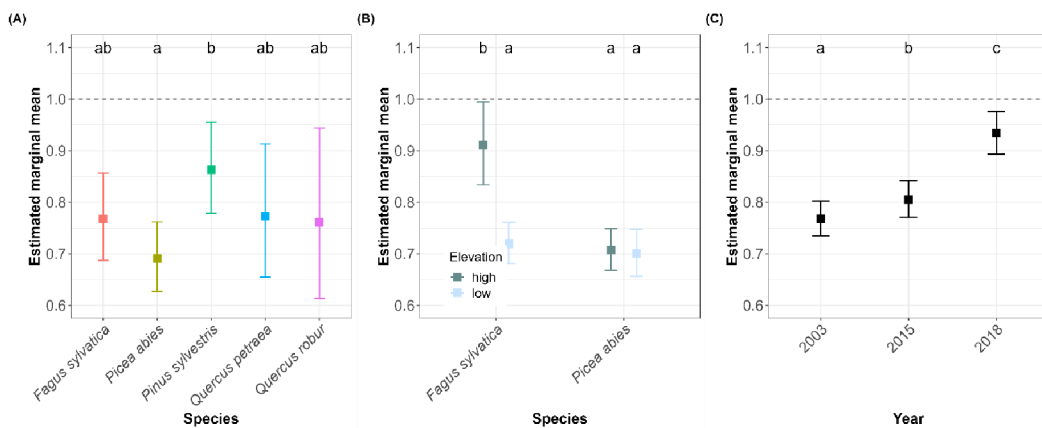


Fig. 18. Impacts of the dry period (2015-2019) and extremely dry years (2003, 2015, 2018) on tree growth. Panels A and B represent linear modeled logarithmic transformed least-square means of the ratio (drought resistance) between the average RWI of the 2015-2019 and 2005-2009 periods (plain squares, back transformed to the original scale) and 95% confidence intervals. Results are shown (A) by species, and (B) by elevation classes, for beech and spruce (i.e., the only two species distributed across the entire elevation gradient). In (B), elevations higher than 650 m a.s.l were classified as “high elevation”, and those at or below 650 m a.s.l. as “low elevation”. (C) Displays the logarithmic transformation least squares models of the ratio between the growth rate during the individual drought year and the mean growth rates for the two years immediately preceding the dry event. Different letters at the top of each panel indicate significant differences in mean values ($p < 0.05$). Black dashed lines denote a ratio of 1, representing the RWI during the reference period.

4.3.2 Links between drought resistance, growth trend, and moisture availability

Tree species that were less affected by drought (i.e., those with high drought resistance) exhibited significantly higher RWI during the 1995-2019 dry period (Fig. 19A). The relationship was similar for all species, as well as for low/high elevation populations (Fig. C6). Furthermore, drought resistance and growth trends decreased linearly with increasing tree sensitivity to variability of moisture levels (i.e., sensitivity to SPEI), indicating a higher probability of growth suppression due to drought (Fig. 19B-C). Similar relationships of these three dimensions were also evident in the analysis of BAI (Fig. C7).

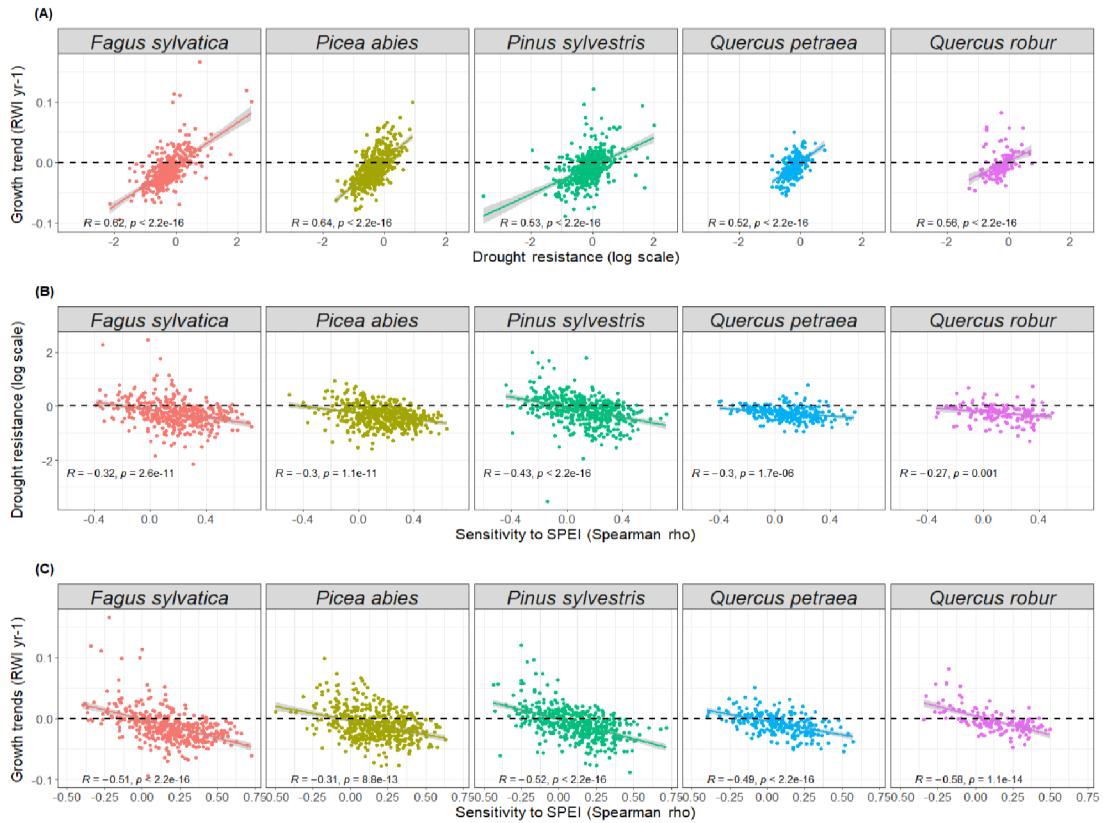


Fig. 19. Links between drought resistance, tree sensitivity to variability in moisture availability (i.e., sensitivity to SPEI, based on Spearman's rank coefficient between RWI and SPEI12) and growth trends (based on Sen's slope of RWI) during the 1995-2019 period. Dots represent observed values and shading indicates 95% confidence intervals. Spearman rho (r) and p-values are also presented.

4.3.3 Drivers of drought resistance

The impact of individual drought events on drought resistance differed significantly among species and drought years (Table 7; Fig. 20; Fig. C7). The GAMM model indicated that the growth of all species decreased significantly ($p < 0.05$) in 2003 with Norway spruce and European beech being the most affected species by drought (Fig. 20A). However, when comparing the responses between the extreme years of 2003 and 2018, the two coniferous species exhibited the largest drought resistance declines. In contrast, the three broadleaved species displayed a reversed pattern with the highest drought resistances in 2018 (Fig. 20A). The impacts of individual drought events were strongly related to the intensity of drought (Fig. 20B), but this relationship also varied among species. Specifically, the drought resistance of the two coniferous species and sessile oak declined almost linearly with increased drought intensity (i.e., more negative SPEI12 values). However, drought resistance of European beech and pedunculate oak exhibited a U-shaped relationship with SPEI, especially in the case of pedunculate oak, for which a SPEI12 threshold of approximately -1.5 was identified. Beyond this threshold, the

response of drought resistance to SPEI reversed (Fig. 20B). Model predictions based on BAI showed similar results (Fig. C8; Table C2).

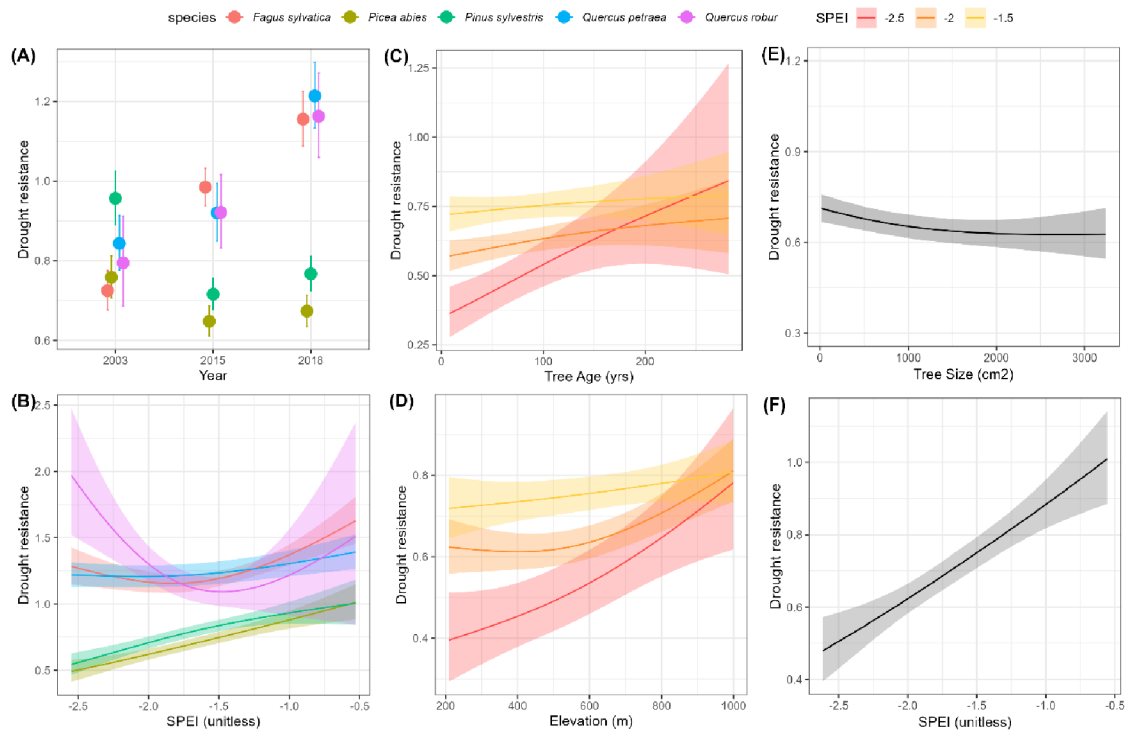


Fig. 20. Drivers of drought resistance based on RWI, displaying predicted mean values (dots) and their 95% confidence intervals (lines) in A. Functions (lines) and confidence bounds (shadings) presented in B – F indicate resistance of trees to extreme dry years. The relationships involving drought resistance are shown for (A) SPEI, year and species, and the functions are shown for SPEI and (B) species, (C) tree age, (D) elevation, (E) tree size, and (F) SPEI for single species. Each panel represents relationships with explanatory variables, fixed to their mean values except for the variable of interest. In panels B-F, results are based on the year 2018, and in panels C-F, results are based on the tree species Norway spruce.

(A) Parametric terms					
Variable	Estimate	Std. Error	t value	p-value	Signif .
(Intercept)	0.88	0.01	65.38	0.0000	***
Species <i>Picea abies</i> (vs <i>Fagus sylvatica</i>)	0.00	0.02	0.09	0.9255	NS
Species <i>Pinus sylvestris</i> (vs <i>Fagus sylvatica</i>)	0.10	0.02	5.43	0.0000	***
Species <i>Quercus petraea</i> (vs <i>Fagus sylvatica</i>)	0.05	0.02	2.33	0.0197	*
Species <i>Quercus robur</i> (vs <i>Fagus sylvatica</i>)	0.06	0.03	2.03	0.0428	*
Year 2015 (vs 2003)	0.14	0.01	9.97	0.0000	***
Year 2018 (vs 2003)	0.22	0.02	12.07	0.0000	***
Species <i>Picea abies</i> : year 2015	-0.21	0.02	-9.82	0.0000	***
Species <i>Pinus sylvestris</i> : year 2015	-0.27	0.02	-11.76	0.0000	***
Species <i>Quercus petraea</i> : year 2015	-0.10	0.02	-4.92	0.0000	***
Species <i>Quercus robur</i> : year 2015	-0.07	0.03	-2.30	0.0216	*
Species <i>Picea abies</i> : year 2018	-0.27	0.02	-11.65	0.0000	***
Species <i>Pinus sylvestris</i> : year 2018	-0.33	0.02	-13.13	0.0000	***
Species <i>Quercus petraea</i> : year 2018	-0.04	0.02	-1.70	0.0892	NS
Species <i>Quercus robur</i> : year 2018	-0.04	0.03	-1.10	0.2705	NS
(B) Smooth terms					
Variable	edf	Ref.df	F	p-value	Signif .
s(SPEI): Species <i>Fagus sylvatica</i>	1.80	2.00	5.33	0.0024	**
s(SPEI): Species <i>Picea abies</i>	1.69	2.00	19.75	0.0000	***
s(SPEI): Species <i>Pinus sylvestris</i>	1.77	2.00	19.19	0.0000	***
s(SPEI): Species <i>Quercus petraea</i>	0.00	2.00	0.00	0.7066	NS
s(SPEI): Species <i>Quercus robur</i>	1.69	2.00	9.81	0.0000	***
s(Elevation)	1.45	2.00	7.12	0.0001	***
s(Age)	1.17	2.00	4.56	0.0016	**
s(Size)	1.62	2.00	10.38	0.0000	***
ti(SPEI, Elevation)	3.46	4.00	8.44	0.0000	***
ti(SPEI, Age)	2.03	4.00	2.84	0.0015	**

Table 7. Output from the GAMM final model based on RWI, showing estimated coefficients, standard errors, and t-values for parametric terms, estimated degree of freedom (edf), reference degree of freedom (Ref. df), F-value (F) for smooth terms. Significance levels (Signif.) are as follows: NS = non-significant; * = p-value < 0.05, ** = p-value < 0.01, *** = p-value < 0.001. Non-significant variables have been removed from the final model based on AIC scores. The outputs of the full model (equation 1) are shown in Table S1.

Age, size, and elevation played significant roles in determining drought resistance (Fig. 20). Overall, older trees at higher elevations exhibited higher drought resistance, although drought intensity significantly modulated this relationship (Fig. 20C-D). During low (SPEI= -1.5) and moderate (SPEI= -2) intensity of droughts, the differences in drought resistance between young and old trees were moderate. However, under high intensity of droughts (SPEI = -2.5), the increase in drought resistance with age was prominent (Fig. 20C). Drought resistance also increased with elevation (Fig. 20D) and this relationship was positively associated with SPEI12, implying that the buffering effect of elevation against droughts was more pronounced when droughts were more intense. Finally, larger trees exhibited lower drought resistance compared to smaller trees, although this trend was quite moderate (Fig. 20E).

5. DISCUSSION

5.1 IMPACT OF DISTURBANCE SIGNATURES ON TREE-RING WIDTH AND BLUE INTENSITY CHRONOLOGY STRUCTURE AND CLIMATIC SIGNALS IN CARPATHIAN NORWAY SPRUCE

5.1.1 Spatiotemporal disturbance characteristics of tree-ring chronologies

Overall, the results indicate a varying degree of disturbance impact (in terms of magnitude and timing) on RW chronologies across a range of sites, spatial scales, and sampling scenarios. Whereas no apparent disturbance trends were found at the regional level (Fig. 4), the disturbance trends were more apparent in RW chronologies on the site-level and subset scales (Figs. 5, 6, A6), although only for a minority of sites (Fig. A5). The presence of disturbance signatures in chronologies at each scale mainly was related to differences in series replication. Higher replication results typically in the strengthening of the common climatic signal and the dilution of more localized effects of disturbance in the mean chronology (Hughes, 2011). In contrast, the presence of disturbance trends may become more apparent in chronologies with weaker replication where the disturbance effects are superimposed over common climatic drivers. Series replication can therefore determine whether a disturbance event of a given magnitude / severity and spatial extent translates to an appreciable impact on chronology structure as this influence is related to the proportion of investigated trees that record a particular event. Since replication varied considerably (from dozens to thousands of series) at various scales and sampling subsets, this interaction of replication with disturbance severity and spatial extent determined whether disturbance events affected chronology structure. Chronologies developed from a larger number of series sampled over larger areas were less likely to capture smaller-scale, more localized events. In line with these concepts and our observations, Björklund et al. (2019) demonstrated that enhanced disturbance activity or radial growth response to disturbances at sites in northern Romania had no dampening effect on the climate response at the large-scale ‘landscape’ level.

As the majority of Carpathian forests (except for Făgăraș) are generally driven by low-to-moderate disturbance severity (Čada et al. 2020), the “dilution” phenomenon observed in this study can be attributed to the absence of major large-scale and high-severity disturbance events which could synchronize disturbance responses throughout an entire landscape and temporarily overshadow macroclimatic variability as the primary growth-determining driver. Therefore,

although the magnitude and extent of disturbance events in the Carpathians may have been sufficient to affect chronologies at some sites in specific periods, such events were unable to affect chronologies at the landscape scale. Furthermore, the presence of disturbance trends may not be eliminated even when ensuring that chronologies exceed the commonly applied EPS (> 0.85) threshold generally considered an indicator of chronology representativeness (Wigley et al., 1984), as disturbance trends typically affect decadal to multi-decadal trends without significantly affecting interannual variance (Rydval et al., 2015, 2018). Nonetheless, our findings indicate that while disturbances do affect trends in RW chronologies from some Carpathian sites, their impact on chronology structure for most high-elevation Norway spruce sites throughout the Carpathian Mountains is negligible when chronologies are highly replicated.

In addition to the spatial-scale and replication-related controls on the modification of chronology structure by disturbance trends, distinct temporal patterns were also identified. The timing and magnitude of disturbance trends in RW chronologies, represented by the difference between disturbance-affected (RW_dis) and disturbance-corrected (RW_dis_CID) chronologies, was generally consistent with the disturbance history (represented by the percentage of series with a release in a particular period), although these two datasets were not entirely synchronized. The disturbance impact on tree growth can persist for years (Jacquet & Altermatt, 2020; Thom et al., 2017; Trotsiuk et al., 2016) due to the longer-term changes in resource availability and competitive changes, which can offset the recorded timing of the disturbance event (i.e., release year) and the actual growth release trend in the series or chronology. Furthermore, differences in the magnitude of disturbance trends varied among sites, with BEL, BYS and URS displaying more considerable differences in chronology structure compared to HLI and FA2 (Figs. 5, 6). This observation reflects variations in the timing and proportion of trees that experienced disturbance events at each location, which is most likely linked to the severity and spatial extent of those events. In addition to the higher temporal concentration of disturbance events, such differences could also partly be explained by a higher incidence of a disturbance at specific sites (e.g., BEL and URS) which have a higher ratio of release events per series compared to other sites (Table 5).

It should be noted that differences in the comparison between disturbed and undisturbed chronologies (Fig. 6B, C) represent differences in chronology structure rather than purely expressing disturbance trends, as these chronologies were composed of two groups of series rather than the same series corrected for disturbance trends. Therefore, some differences between these chronology versions could be attributed not only to disturbance, but to some extent also potential differences in the structure of individual series that make up those chronologies. Nevertheless, the high degree of overlapped agreement in the timing of identified

disturbance trends with CID (Fig. 6A) and differences in the disturbance-affected vs. undisturbed chronologies (Fig. 6B) suggests that these differences in structure also express disturbance-related variations, and such comparisons may represent an alternative way of identifying disturbance trends. This agreement further demonstrates that CID treatment of disturbance-affected series can effectively identify and correct disturbance trends, resulting in chronologies that are more similar to those developed from undisturbed series.

One particularly important finding of this study was that no clear differences were found when comparing trends of the disturbed and undisturbed BI chronologies in the periods when their RW chronology counterparts contained release trends associated with disturbances (Fig. 6). The results from this extensive network of sites agree with initial small-scale findings of Rydval et al. (2018) from a single site in Romania and provide further evidence that the BI parameter is insensitive to disturbance events. However, while BI series / chronologies appear insensitive to disturbance events associated with a protracted increase in radial growth, Arbella et al. (2018) found that BI responded to insect defoliation events similarly to RW with reduced BI values. These differences in RW and BI sensitivity to different types of events point to the potential future utilization of multiple tree ring parameters to help identify specific disturbance agents and their effects on tree growth, and so establish a better and more detailed understanding of past ecological events overall. Further research is clearly still required to fully understand the various ecological influences on BI and tree ring density.

5.1.2 Temperature signals in the context of disturbance

The considerable spatial and temporal variability among sites in the strength of the RW temperature signal (restricted to the June-July season), and its absence from the FA2 site chronology (Fig. 7), was consistent with other regional studies (e.g., Schurman et al. 2019). In contrast, the temperature signal of BI chronologies, which represented a wider (April-September) seasonal window, was much stronger, more spatially consistent, and more temporally stable compared to RW across all sites throughout the Carpathians, including FA2. These response characteristics suggest that it should be possible to obtain strong regional temperature signals using BI even when such signals are weak or absent in RW chronologies. Unlike latewood density (and by extension BI), which mainly depends on photosynthate accumulation during the growing season of the ring formation year, RW often also depends on photosynthates from previous years (Wang et al., 2020). Therefore, the weaker sensitivity of RW to summer temperature in the year of ring formation may possibly also be related to the stronger biological persistence of RW data (Table 6).

When examining the climate response of the three types of RW chronologies (RW_dis, RW_dis_CID and RW_undis) from sites with clear disturbance trends, it appeared that the detected disturbance trends did not have an apparent influence on the temperature signals in RW data as differences in the strength of the optimal season temperature response of these RW chronologies were mostly minor and mixed (Figs. 7, 8). These minimal differences in climate sensitivity are likely related to the temporal misalignment of the detected disturbance periods and available instrumental data, as most of the major disturbance trends were identified prior to the 20th century (Fig. 6). Thus, any potential improvement of the climate signal by removing disturbance trends was challenging to assess as the changes in chronology structure could not be reflected in the climate response analysis. This finding is noteworthy as it suggests that even when disturbance trends do not affect the correlation in the instrumental period and may therefore be undetectable with climate response analysis, trends caused by disturbance can still exist in the pre-instrumental period.

Unlike the weaker temperature response of RW_undis compared to RW_dis at URS between 1960 and 1980, which was likely related to differences in chronology composition, the decreased correlation between all RW and BI chronologies at FA2 with summer temperature in the second half of the 20th century (Fig. 8) may have been related to deposition of atmospheric pollutants in that area during that period. Atmospheric pollution affected large areas of central and eastern Europe in the second half of the 20th century (particularly the 1970s and 1980s) due to fossil fuel burning associated with heavy industry and power generation (Grubler 2002; Mikulenska et al., 2020). Whereas the period of greatest exposure to very high concentrations of atmospheric pollutants has been reported to coincide with protracted periods of tree growth decline in severely polluted areas (Rydval & Wilson, 2012; Sidor et al., 2021), weakening climatic sensitivity of Norway spruce in response to lower levels of background pollution (instead of a clear decline in tree ring index values) has also been documented (Wilson & Elling, 2004). In any case, considering the timing, type of response, and the proximity of the Făgăraș Mountains to large urban areas and industrial facilities as well as other local point-sources of pollution within the context of high regional background levels of atmospheric pollution around the 1970s, this could represent a plausible cause (Akinyemi et al., 2013; Mylona, 1996). If this observation was in fact responsible for the weakened response of both parameters around that period, it would raise questions about the potential susceptibility of BI to environmental pollution.

The higher correlations between BI_dis and April-September temperature compared with BI_undis chronologies in most of the examined BI sites (Fig. 7, 8; Table 6) raises an interesting point about climate sensitivity of undisturbed trees compared to disturbance-affected trees as it would suggest that BI chronologies from trees affected by past disturbance may exhibit a higher

sensitivity to temperature. Although this difference did not reach the threshold of statistical significance considering the limited number of BI datasets explored in this study, a possible explanatory mechanism may nonetheless exist. In higher-density closed-canopy forests, trees experience higher competition from neighboring individuals, but are also less exposed to ambient conditions and may therefore be buffered from temperature extremes (Saulnier et al., 2020). However, mortality of neighboring trees as a consequence of disturbance opens up the canopy, potentially reducing competition as well as increasing exposure to ambient temperatures. Greater exposure to ambient conditions could thus lead to higher temperature sensitivity in disturbance-affected trees, as previously reported in Primicia et al. (2015). This observation may therefore warrant further investigation to examine more extensive collections of BI chronologies.

As a temperature-sensitive proxy, the BI parameter has drawn considerable attention in recent years and our findings further support the growing body of literature indicating that there is considerable potential for BI data in paleoclimatic applications. In addition to several clear advantages over RW (incl., seasonally broader, spatially and temporally stronger and more robust temperature signal), the insensitivity of BI to disturbances that result in growth release trends in the RW series represents a further asset. Nevertheless, RW still managed to detect decent summer temperature (June-July) signals, especially considering sites BEL and HLI. This is in line with the work of Tuovinen et al. (2009) in Fennoscandia, which proposed that RW-based paleoclimate reconstructions should be restricted to temperature of midsummer (July), whereas MXD (and by extension BI) is typically more suitable for reconstructing the temperature of a broader seasonal window (June to August), as these two tree ring parameters provide different but complementary paleoclimatic signals (Björklund et al., 2020; Tuovinen et al., 2009). Utilization of both BI and RW in paleoclimate reconstructions could therefore allow the exploration of different seasonal signals.

5.1.3 Limitations of CID method

Although the CID procedure generally improves the climate response in RW chronologies, particularly when they are affected by major disturbance trends, this treatment can also lead to over-correction in some cases, which can then lead to minor reductions in climate response correlations (Rydval et al., 2015, 2018). The mixed temperature response results of the disturbance-corrected (RW_dis_CID) chronologies concerning the disturbance-affected (RW_dis) versions could therefore partly be related to the effectiveness of CID correction over the instrumental period. More specifically, this mixed performance was probably related to the fairly small proportion of series with disturbance trends in a given period and their relatively even dispersion over the 20th century in combination with some degree of over-correction in

certain instances. It is also worth mentioning that the CID method is not capable of detecting very brief responses to disturbances (ca. < 10 years) or any other short-term non-climatic impacts that might affect individual series and potentially even chronologies as discussed by Björklund et al. (2019). They also pointed out that the potential positive effects of disturbance detection and removal on climate reconstructions might mainly affect the multi-decadal rather than inter-annual periods.

5.1.4 Subsection conclusion

Our findings indicate that chronologies developed from subsets composed of a relatively small number of samples are most susceptible to the effects of disturbance. In contrast, highly replicated, spatially extensive RW datasets are unlikely (or less likely) to be affected by disturbance. This observation represents a critical finding with potential consequences for long RW-based chronologies and climate reconstructions which often tend to be relatively weakly replicated back in time. In addition, the apparent relative insensitivity of BI to disturbance in periods when RW data are affected by pronounced growth release trends could be used to better understand climatic and ecological influences on growth by examining both parameters in tandem. The strong and spatiotemporally more stable representation of temperature signals in BI chronologies indicates considerable potential for widespread application of the blue intensity parameter in dendroclimatological research without considering ecological signals.

Limitations of this research include the CID method itself which, as an imperfect tool, may in some instances falsely identify trends not related to disturbance or fail to capture small magnitude or short duration responses to disturbance. Also, due to the limited temporal availability of instrumental data, investigating of the influence of disturbance on growth-climate responses was temporally limited to the post-1900 period. Despite efforts to ensure adequate sample replication and only examine chronologies representative of the larger population, comparison between disturbance-affected and undisturbed chronologies could be influenced by additional factors (e.g., sample composition) which may complicate the interpretation of the results. In addition, samples for this study were only collected from high-elevation primary forests, which limits the generality of the results across the species' broader natural distribution range (e.g., Central-European low-elevation spruce forests).

In future research, the influence of other non-climatic factors (e.g., pollution) on tree radial growth could also be examined. Though not explicitly considered here, an evaluation of suppression trends, which were also present in some site chronologies, could be conducted. Moreover, investigating the climatic sensitivity of different BI parameters (e.g., earlywood RW

and BI, latewood RW, and delta-BI) to other climatic variables (e.g., precipitation or moisture availability) in connection with potential influences of disturbance may also be worthwhile. In general, investigations using multiple tree ring parameters can help evaluate and better understand non-climatic impacts such as disturbance on tree ring chronologies, which should ultimately benefit the utilization of those chronologies in dendroclimatic studies and further improve the overall reliability of reconstructions of past climatic conditions.

5.2 IMPACT OF POLLUTION ON THE CLIMATIC SENSITIVITY OF MULTIPLE NORWAY SPRUCE TREE-RING PARAMETERS IN CENTRAL EUROPE

5.2.1 Degree of growth trend synchronization and pollution status

Our results revealed high synchronization of growth trends and pollution loads, especially in the case of RW chronologies. Prominent growth declines occurred in RW during the heavily polluted period (1970s-1980s) and at heavily polluted sites (NB and CK), indicating the negative impacts of pollution on tree growth, as well as the characteristic of RW as the most susceptible parameter to pollution. Pollution-induced growth declines involving RW and tree mortality are well-documented phenomena (Kandler & Innes, 1995; Kharuk et al., 2023; Mathias & Thomas, 2018; Sidor et al., 2021; S. Vacek et al., 2015; Z. Vacek et al., 2020). A variety of plant physiological processes acting jointly lead to such an outcome. High levels of pollutants can lead to a reduction in growth and productivity by causing injury to foliage and disrupting physiological processes, such as enzyme activity or production, stomatal closure and carbon allocation (Chappelka & Freer-Smith, 1995; Grill et al., 2005; Savard, 2010). Leaves exposed to pollutants (e.g., SO₂, NO_x), are subject to faster water loss and increased transpiration rates because of the accelerated cuticular loss or disruption of the leaf epidermis. These conditions ultimately lead to stomatal closure to prevent water loss (Wright et al., 1987). While reduced stomatal conductance may result in an increased water-use efficiency (Thomas et al., 2013), achieving high growth rates is not possible in the presence of high SO₂ concentrations (Kwak et al., 2016). Pollutants can also induce changes in photo-assimilate allocation, such as higher allocation to shoots for defence and repair, which inevitably lead to reductions in root growth and biomass production (Spence et al., 1990; Friend & Tomlinson, 1992; Chappelka & Chevone, 1992). Moreover, the increased soil acidification due to increasing acid deposition can result in subsequent leaching of base cations from the soil-rooting zone, which manifests as the depletion of the ion-exchange soil complex and the suppression of litter decomposition (Kolář et al., 2015), which represents an obstacle for soil nutrient acquisition and assimilation for tree growth as well.

Although moderate chronology declines were also observed in BI chronologies, neither the sites (SLO and SMR) that experienced the most severe decline nor the timing of the decline (1978 and 1995-1996) seem to correspond with the degree and spatiotemporal patterns of pollution impact which affected RW (Fig. 9B). It is worth considering that additional factors may exist, which could have induced the declines observed in the BI chronologies within the context of high background pollution levels. For example, cold temperatures in specific years could help explain the lower index values while maintaining high consistency between the BI chronologies and the temperature series (compared to RW), especially displayed by the site SLO in the period around 1980, and SMR in the period around 1996 (Fig. 15), as both periods were marked by years with low temperatures (Fig. B2A). Historically, an extremely cold and harsh winter with a sudden drop in temperature (~ 25 °C in 24 h) was recorded on New Year's Eve of 1978 / 1979 in the Czech Republic (Rein & Štekl, 1981). Furthermore, another extreme winter in 1995 / 1996 marked by a sudden temperature decrease in November 1995 was also observed and was followed by heavy frosts and long-term inversion conditions (Samusevich et al., 2017). The pointer year analysis conducted in the study by Cejkova et al (2009) also showed a severe winter in 1995 and cold summer in 1996 in the Šumava Mts., which is consistent with our findings for the SMR site (Fig. B4B; Table B1B). Harsh winter conditions were shown to create environments more conducive to effective air pollutant accumulation (Lomský et al., 2013), with freezing temperatures and high SO₂ concentrations acting in tandem leading to forest decline (Sheppard & Pfanz, 2001). Extreme climatic stress (e.g., drought, temperature changes) within the context of high air pollutant concentrations (e.g., SO₂, NO_x, and O₃) has also been linked with more severe damage of conifer species (e.g., Norway spruce, Scots pine) (Vacek et al., 2015, 2017). Moreover, as BI is an excellent surrogate for X-ray density (Björklund et al., 2013; Campbell et al., 2007; McCarroll et al., 2002; Rydval et al., 2014), variations in BI mostly reflect density changes in tree rings. Though less attention has been paid to the impact of pollution on density in recently years, decreased maximum density and latewood proportions in tree ring datasets from locations affected by pollution have been reported (Kim & Fukazawa, 1997; Sander et al., 1995; S. Ohta, 1978).

In the case of QWA, latewood CWT of CK did not exhibit any pronounced growth reductions, although a period of lower values occurred in SLO during the 1970s-1980s, coinciding with the heavily polluted period. Although the sulphur deposition levels of both sites were similar, the more pronounced CWT decline in S10 observed for SLO indicates that this location may have faced an extra stress factor other than pollution, and the lower temperature at SLO compared to CK around the late 1970s is likely responsible (Fig. 15C). This may also be related to the higher temperature sensitivity of CWT, which is discussed further in the following subsection.

5.2.2 Stability of climatic signals in different tree ring parameters from polluted areas and their potential for climate reconstruction

Growing season temperature signals were captured by most of the tree ring parameters (except for LA). However, the optimal seasonal length and signal intensity differed among different sites and parameters, with stronger and longer seasonal temperature signals (Apr.-Sep.) captured by BI and CWT from most sites, which revealed the higher climatic (i.e., temperature) sensitivities of these parameters. Previous studies have also found that the growing season temperature (Apr.-Sep.) is a key climatic variable for the growth of high elevation conifer tree species in large parts of Central and Eastern Europe (Björklund et al., 2019; Büntgen & Di Cosmo, 2016; Horodnic & Roibu, 2020; Jiang et al., 2022; Putalová et al., 2019; Schurman et al., 2019). Furthermore, the temperature signal in ring width chronologies appeared to be more temporally restricted (i.e., Jun.-Jul.), whereas the signal in blue intensity is stronger and extends over a longer season (e.g., Apr.-Sep.) (Rydval et al., 2018; Seftigen et al., 2020).

However, one of the more noteworthy findings of this research was that the temperature signals appeared to be temporally unstable (i.e., signal weakening) under severe pollution stress, especially during the period with the most severe rates of pollutant deposition (Fig. 11; Fig. 12; Fig. 13; Fig. 14). Such signal weakening was mainly revealed by the RW chronologies, which indicates the increased susceptibility of this parameter to pollution, with the temperature signal substantially reduced or even absent (i.e., non-significant) during ('POL') and after ('post-POL') the high pollutant deposition period. In contrast, the temperature signals contained in BI and CWT were more stable and appeared to be less affected by pollution. However, some caution may still be required when applying BI or CWT in a dendroclimatic context to ensure climate signal consistency over time in areas impacted by pollution. For certain sites, the temperature signal in BI and also the most climatically-sensitive segment (S10) of CWT did show some signs of weakening, particularly during the severe pollution (POL) period. The latter finding supports previous observations that the impact of pollution can extend to the wood anatomical level, as reported by other researches (Lexa, 2021; Mulenga et al., 2022; Samusevich et al., 2017). Despite some signs of minor weakening during the most severe pollution period, this did not appear to impact the significance and signal strength considerably. This suggests that both the BI and CWT parameters may represent suitable options as climatic proxies, which are minimally affected or unaffected by pollution, for dendroclimatological research or historical climate reconstruction purposes in polluted areas.

Historically, reduced temperature sensitivity of trees growing in certain high-elevation and high-latitude areas around the Northern Hemisphere was identified (Briffa et al., 1998). Whereas tree growth showed a consistent decline after 1940, reaching the lowest level in the late 1970s and 1980s, temperatures continued to increase in the latter part of the 20th century, leading to divergence between tree growth and mean summer temperatures, becoming clearly recognisable after 1960, especially in areas close to Central Europe. Although a single clear cause of such an apparent and widespread phenomenon has not been identified, considering the overlap in timing and location, there is a possibility that pollution may have represented at least a contributing factor to some extent, which would align with the findings of our study and such a connection has also been suggested previously (e.g., Rydval & Wilson 2012). However, it is also worth noting that we observed a clear (though temporary) trend divergence only in RW at certain locations. In contrast, the phenomenon identified by Briffa et al. (1998) also affected the trends in density chronologies. Nonetheless, it should, however, also be pointed out that climate signal weakening, another hallmark of the divergence phenomenon, was also detected in BI and CWT chronologies in addition to RW in our study. In another study, Franceschini et al. (2013) reported that neither large sets of climatic predictors nor accounting for their non-linearities resolved the divergence (declining relationship) in latewood density response of Norway spruce to temperature during 1970 to 2000 in north-eastern France. In that study, the authors suggested testing for pollution-driven growth impacts and avoidance of using relationships based only on a single parameter for temperature reconstruction.

Additionally, lower correlations between ring width and temperature for sites located on slopes with more effective acid fog deposition were previously reported, and greater distance from the pollution source was associated with an increase in climatic sensitivity (Opala-Owczarek et al., 2019). As mentioned above, exposure to pollutants can induce leaf stomata closure and eventually affect productivity and growth, whereas elevated temperature tends to stimulate stomatal opening (Driesen et al., 2020; Feller, 2006; Gommers, 2020) to ensure adequate gas exchange, thus trees need to find a balance between increasing photosynthesis or reducing water loss. It is possible that pollution stress (displayed as water stress) may overtake growing season temperature and act as the main limiting factor determining tree growth when this impact is sufficiently severe. Apart from the impact of pollution on the stability of temperature signals, other climatic signals could also be influenced by pollution. For example, the precipitation signal in silver fir (*Abies alba Mill*) was reported to have suffered from a weakening in the 1960s during a period of heavy SO₂ emissions in the Lower Bavarian Forest region in southern Germany (Wilson & Elling, 2004). Altogether, this evidence strongly indicates the existence of pollution impacts on the climate sensitivity of tree ring datasets, which should be carefully considered in research conducted in potentially affected locations.

5.2.3 Avoidance of pollution interference for dendroclimatic research in polluted areas

With the development of human society, industrial pollution became a worldwide concern which has heavily influenced the health and development of forest ecosystems (Taylor et al., 1994). These complications extend beyond Europe (Kandler et al., 1995; Katzensteiner et al., 1992) to forests, for example in north American (Johnson & Taylor, 1989; McLaughlin, 1998) and east Asia (Izuta, 2017; Takahashi et al., 2020). These findings highlight the importance of considering the impact of pollution in dendroclimatological research, particularly in areas that have experienced such impacts more recently or still experience high levels of pollution at the present time. Furthermore, efforts to reduce or eliminate such impacts are crucial. The Curve Intervention Detection method we adopted in this study represents a practical approach in detecting pollution-related growth anomalies which can help to correct decadal climate signal trends in tree ring width (Jiang et al., 2023; Rydval et al., 2015). Though not examined in this study, other statistical methods, such as principal component analysis (PCA; Abdi, 2013) may also be useful in assessing the homogeneity of inter-site chronologies and more effectively extracting climatic signals when major differences associated with non-climatic (i.e., pollution) influences exist among various sites. Moreover, it would be helpful to adopt the use of different tree ring parameters, such as latewood blue intensity and cell wall thickness, which appear to be more resilient and better able to resist pollution impacts as demonstrated by this study. Finally, in the context of climate reconstruction, the parameter and period used for calibration should be carefully chosen, taking into account the possible instability of the climate signal (especially in tree ring width) in relation to variable pollution levels over time (Fig. 11, 12), in order to minimize non-climatic impacts and retain reliable signals.

5.2.4 Subsection conclusion

Overall, our study revealed that the apparent growth declines observed in Norway spruce around the 1970s-1980s in the Czech Republic and neighbouring regions were closely linked to the widespread impact of pollution in Central Europe during the 1960s-1990s. We observed a strong link in the long-term patterns between these growth declines and the pollution levels. The prominence of this type of relationship (i.e., pollution impact on tree growth) differed considerably among tree ring parameters, which indicated the varying degree of resilience of these parameters to pollution. Ring width (RW) was generally more susceptible to pollution impact, which manifested as either trend divergence or climate signal weakening. The CID method can help mitigate these issues to some extent, particularly for more severely polluted sites. The latewood blue intensity (BI) parameter was less impacted by pollution and retained a stronger and temporally more stable (Apr.-Sep.) temperature signal, and thus appears to

represent a more suitable parameter for paleoclimatic reconstruction in areas affected by pollution. Considering the quantitative wood anatomy (QWA) parameters, cell wall thickness (CWT) of the outer section of latewood (especially the last segment - S10) contained strong, significant, and temporally stable climate signals similar to BI. Apart from pollution, cold temperatures were likely responsible for the moderate growth declines observed in BI and CWT, considering the generally high degree of agreement between these parameters and the target climatic variable. Nonetheless, the moderate temperature signal weakening observed for some sites even in BI and CWT is notable and worthy of further examination. In practice, our study suggests that it would be prudent to take pollution impacts on tree ring datasets into account when conducting dendroclimatological research in historically polluted areas, especially when considering the utilization of the more traditional ring width parameter. Whenever possible, it is worth adopting a more diverse range of tree ring parameters, such as latewood blue intensity and cell wall thickness, to capture the stronger and more stable growing season temperature signals more effectively. Furthermore, the adoption of certain statistical approaches, such as CID, could be applied for sites with more severe pollution impacts and help to reduce protracted growth suppression trends.

5.3 DROUGHT RESISTANCE OF MAJOR TREE SPECIES IN THE CZECH REPUBLIC

5.3.1 Impacts of drought on tree growth

Our results show that all major Central European tree species were negatively affected by the extremely dry period 2015-2019, leading to pronounced tree growth reductions in the Czech Republic compared to the previous decade (Fig. 17; Fig. C3). In fact, our observations might underestimate the actual extent of the drought-related impacts, considering that only living trees were sampled for our study and thus drought-induced mortality was not evaluated. Previous research has demonstrated that declining growth in trees can represent an early-warning signal which may indicate impending mortality (Gentilesca et al., 2017), and drought induced growth declines have been widely reported among various tree species around the world in recent decades (Sánchez-Salguero et al., 2012; Gentilesca et al., 2017; Venegas-González et al., 2018; Jing et al., 2022). For example, studies have noted significant growth reductions of European beech during the 2018 extreme drought year compared to average growth over the preceding 2010-2017 period (Rohner et al., 2021), while montane conifers also displayed reduced growth corresponding to more intense drought (Bohner & Diez, 2021). Our study contributes to the current body of knowledge on this topic by identifying recent drought impacts on the growth of several tree species based on the quantitative assessment of tree ring data from the Czech

Republic, which provides critical insights into the drought risks faced by Central European forests (Hlásny et al., 2014).

5.3.2 Differences in drought resistance among tree species

Although drought-induced growth reductions were identified for all studied species, the severity of the impacts varied considerably among them. Scots pine displayed the least susceptibility, whereas Norway spruce appeared to be the most susceptible species to drought stress, indicating species-specific differences in drought resistance. One study from an area close to the Czech Republic in Bavaria, Germany, identified Norway spruce as the most drought-susceptible among species commonly found in the region (Thom et al., 2023a). Additionally, Norway spruce has also been found to be the least drought-tolerant compared to species such as silver fir (*Abies alba*) and Douglas fir (*Pseudotsuga menziesii*) (Vitali et al., 2017). As a species adapted to colder climates, Norway spruce has a naturally dominant presence in mountain forests. However, in recent centuries, Norway spruce has been extensively planted outside of its natural distribution areas in the Czech Republic. Historical estimates suggest that its past natural coverage represented approximately 12% of the forested area, contrasting with its current coverage of 42% (Cienciala et al., 2016). While past growth conditions were more favorable in many ways in the areas where it was introduced than in its natural habitats (e.g., warmer temperatures, deeper and more fertile soils). Due to ongoing climate changes, these areas are becoming increasingly dry and therefore less suitable for Norway spruce, which is already demonstrating signs of constrained growth due to limited moisture availability.

In contrast, the natural distribution of Scots pine covers a substantial proportion of the Czech Republic (Durrant et al., 2016). Evolutionary selection has equipped Scots pine with specific functional traits that enhance its adaptability to drier environmental conditions. These traits include precise stomatal control, which limits transpiration when the soil moisture deficit exceeds a certain threshold. This control mechanism, known as isohydric behavior, allows Scots pine to close stomata earlier than other species and can help prevent excessive water loss (Poyatos et al., 2008; Martínez-Vilalta et al., 2009; Martínez-Sancho et al., 2017). Thus, Scots pine might be less impacted by recent global warming compared to Norway spruce, which is characterized by weaker isohydric behavior. Differing site conditions might also contribute to these variations, for instance, Thom et al (2023a) identified Scots pine as a less drought tolerant species in Bavaria, Germany, whereas a different performance of this species was identified in our study. The higher overall productivity exhibited by the investigated sites in that study compared to sites in the Czech Republic might potentially reflect a preference for carbon

allocation patterns that prioritize growth over investment in the reserve pool (Rezaie et al., 2023; Merganičová et al., 2019).

Compared to the two coniferous species, the three broad-leaved species were comparably less impacted by the two most recent droughts (2015, 2018; Fig. 20A). The species-specific drought resistance results from a trade-off between hydraulic integrity and carbon acquisition, constrained by species- and population-specific functional traits (Serra-Maluquer et al., 2022). Some species, such as European beech, can respond to scarce water supplies by shedding leaves (Leuschner 2020). Such morphological and physiological adjustments restrict atmospheric carbon uptake, limiting resource availability for primary and secondary growth (Forner et al., 2018; Manzoni, 2014). The trees less affected by drought were those that were not limited by moisture availability, as indicated by the negative correlation between growth trends (drought resistance) and SPEI (Fig. 19). The increase of functional trait diversity (e.g., budburst date, radial growth onset, carbon allocation patterns, optimal photosynthesis temperature, etc.) in broad-leaved and coniferous species can lead to complementary effects in mixed forest stands compared to monospecific stands, which may help reduce drought stress, for example via belowground partitioning and spatiotemporal niche separation, and the utilization of water resources in different soil layers (Pardos et al., 2021).

5.3.3 Elevational gradient in drought resistance

Our results suggest that locations where trees are currently temperature-limited, such as montane and subalpine forests, may act as climate refugia amid climate change. While Norway spruce populations were similarly affected by drought at high and low elevations, high-elevation populations of European beech were less impacted by droughts compared to their low-elevation counterparts (Fig. 18B). Our findings are also supported by other studies as drought effects usually tend to be less pronounced at high elevations where trees experience cooler temperatures and high precipitation conditions (Viviroli et al., 2007; Fig. 3A). Historically, lower temperature conditions have limited tree growth in high-elevation environments. However, as a consequence of climate change, these limitations have been diminishing and this effect is expected to continue in the future, potentially leading to increased tree growth (Doxa et al., 2022; Tumajer et al., 2017). Other studies have also identified significant drought-induced growth reductions for European beech at low elevations (Dulamsuren et al., 2017; Obladen et al., 2021). Conversely, high-elevation conditions may buffer the impacts of drought on tree growth due to increased cloud cover and higher air humidity, which can help maintain stable growth or even increase growth rates as climatic conditions continue to change (Leuschner, 2020; Rozas et al., 2015).

However, it is important to note that the elevational gradient of our study was limited to a range of 209 to 1016 m a.s.l. and we were only able to test the influence of elevation for two species due to data limitations. A more extensive elevational range covering multiple species could help to improve the predictions of drought impact in relation to varying elevation. Additionally, previous studies have reported the existence of genetic variations among *Pinus hartwegii* populations along elevational gradients in relation to drought-induced cavitation resistance (Sáenz-Romero et al., 2013). This indicates the potential importance of genetic differentiation among populations along distinct elevations and implies the need to consider such genotypes-environment relationships to better understand and more precisely quantify elevational drought resistance in future studies.

5.3.4 Effects of age, size, and drought intensity

Our findings highlight the potential for changes in drought resistance in relation to the developmental state of the studied tree species, particularly during period of high-intensity drought. Despite previous research suggesting that younger trees exhibit higher drought resistance than older trees (Ding et al., 2017; Lloret et al., 2011), our study challenges those findings by demonstrating that older trees are less impacted by high intensity droughts relative to younger individuals. Greater vulnerability of younger trees to severe droughts compared to older trees of similar size may be linked to less developed root systems that limits access to deeper water resources when moisture in the upper soil layers is depleted (Bolte et al., 2016). Our results also showed that, in general, smaller trees were more resistant to drought. Smaller trees of the same age follow a slow growth strategy with trees investing more carbon into their reserve pool and improving structural adaptations, such as osmolyte accumulation in leaves, denser wood, and narrower conduits (Polle et al., 2019; Zhou et al., 2012). Favorable microclimate conditions might also play a role, smaller trees can benefit from the protection of larger trees through shading, which facilitates higher transpiration rates, increased latent heat fluxes and reduced vapor pressure deficit (Thom et al., 2023b). The extent of drought resistance among species is also influenced by varying drought intensity. For the two conifers, the relationship between drought resistance and drought intensity was nearly linear, indicating that higher drought intensity (low SPEI) resulted in lower drought resistance (Fig. 20B). Thus, Norway spruce and Scots pine were more severely impacted by extreme droughts than by milder water shortages, especially in the two most recent drought years (Fig. 20A-B).

5.3.5 Subsection conclusion

Our findings revealed significant growth reductions in five major Central European tree species in the Czech Republic during the 2015-2019 drought period, as evident from both RWI and BAI

records. However, the extent and magnitude of the drought impact varied among species when considering either single extreme drought years or extended (5-yr) dry periods. Of the species examined, Scots pine and Norway spruce were identified as the least and most affected species, respectively. The drought resistance of the three broad-leaved species to the two most recent extreme droughts was considerably higher than that of coniferous species. These differences in drought resistance could be related to varying site conditions and species-specific functional traits. Whereas the impact of age on drought resistance was regulated by drought intensity, influence of size was more moderate compared to age. While we also observed an elevational gradient in drought resistance of European beech, further research that would also consider genetic variation is required to validate this finding.

Our study provides valuable insights into the responses of Central European tree species to drought. In light of our findings and given the expected trajectory of future climatic conditions in Central Europe, it appears improbable that Norway spruce could remain a viable option for timber production in the lowlands of the Czech Republic, while other major European tree species might have better adaptation potential. While sandy soils in lowland regions are particularly associated with limited options for selecting suitable tree species, our study suggests Scots pine may be one of the most resilient choices of species to safeguard against the impacts of future drier conditions. Increasing species diversity could help reduce overall disturbance risks and may also foster niche complimentary, supporting the survival of trees. Proactive adaptive measures, including increasing species diversity, structural complexity, and promoting genetic exchange, as recommended by previous research (Thom et al., 2023) will help to safeguard the future supply of ecosystem services under intensified drought regimes.

5.4 COMPREHENSIVE DISCUSSION OF THE WHOLE THESIS

This thesis aimed to develop a better understanding of climatic and non-climatic influences on tree growth and their interplay. This included exploring the impact of climatic extremes on the growth of different Central European tree species. A particular focus of this work was on quantifying the impacts of non-climatic factors, such as disturbance and pollution, on tree growth and climatic signals, with the goal of identifying whether some parameters are less impacted by such factors and may thus be more suitable for dendroclimatological research and paleoclimatic reconstruction in disturbance- / pollution-affected regions. Specifically, the impacts of the investigated non-climatic factors on tree growth were detected and evaluated by applying a novel statistical approach (CID) to ring width series, whereas the strength of climatic

signals was compared by conducting growth-climate response analysis for chronologies of different tree-ring parameters. In the following subsections, I further evaluate and provide a synthesis of the presented results, considering the specific impacts of different factors. Moreover, considering the findings of this thesis, potential new topics and direction of future research related to this work are discussed.

5.4.1 Impacts of disturbance and pollution on tree-ring width, wood density and anatomy trends

The impacts of non-climatic factors were most prominent and detectable in RW chronologies. The impacts of disturbances on RW chronologies varied considerably across sites, spatial scales, and sampling scenarios, and were linked with series replication differences and the spatiotemporal differences in disturbance histories distinct for individual sites. Differences in the magnitude of disturbance trends varied among sites, reflecting variations in the timing and proportion of trees experiencing disturbances. Disturbance-induced canopy removal in natural forests can lead to an abrupt and/or sustained increase in radial growth of neighboring surviving trees (i.e., growth release; Lorimer and Frelich, 1989), whereas small-scale changes in horizontal and vertical forest structure (i.e., gap dynamics) favor competition between neighboring trees, which often lead to decreased radial growth when growing conditions are unfavorable (i.e., suppression; Canham 1985). These growth dynamics are captured as variations of RW. However, in the context of RW chronologies, the extent to which chronology trends were affected by these growth dynamics patterns was influenced considerably by sample depth, with disturbances leaving a profound impact on RW chronology structure when replication was limited, and large-scale highly-replicated chronologies demonstrating lower susceptibility to the effects of smaller-scale disturbance events. Higher replication strengthens the common climatic signal and dilutes localized disturbance effects in mean chronologies, whereas weaker replication makes disturbance trends more apparent in individual site chronologies, superimposing them over common climatic drivers. While disturbance magnitude and extent in the Carpathians clearly affects site-specific RW chronologies, their impact at the landscape scale was negligible when chronologies were highly replicated. This “dilution” phenomenon observed throughout the Carpathian forests can be attributed to low-to-moderate disturbance severity events which, in the absence of major large-scale disturbances that could synchronize responses throughout the landscape, drive tree growth dynamics. (Fig. 4; Fig. 5).

In Central Europe, growth was highly synchronized with pollution trends, particularly in RW chronologies. Strong RW declines during heavily polluted periods indicate a strong negative impact of pollution on tree growth and emphasize the susceptibility of RW to pollution-induced

decline which can further lead to mortality. The effects of pollutants on physiological processes, foliage damage, and disruptions in enzymatic activity, likely contributed to the RW reductions. Although the prevalence of pollution-induced suppression trends has not been explored for scenarios with different sample depth, apparent declining trends were detected at the studied Central European sites with sample sizes comparable to those selected for disturbance trend detection (Fig. 9; Fig. 10). Pollution impacts on RW were mirrored by changes in anatomical properties, specifically latewood cell wall thickness (CWT; Fig.9; Fig. B5). However, the degree of CWT reductions in latewood during the heavy pollution period was obscured due to climatic (e.g., low temperature) influences around the same time, making it more difficult to distinguish which of the factors played a more prominent role on the cellular level (Chappelka & Freer-Smith, 1995).

Overall, LWBI was less impacted (pollution) and non-significantly influenced (disturbance) by non-climatic factors and although there were minor variations in the LWBI chronology structure, this was minimal compared to those observed in RW chronologies (Fig. 6). No clear differences between disturbed and undisturbed LWBI chronologies were found during periods matching the disturbance-related trends in RW chronologies. This aligns strongly with previous findings suggesting that LWBI is insensitive to disturbance events associated with radial growth increases (Rydval et al., 2018). However, differences in sensitivity between RW and LWBI to different types of events suggests the potential utility of adopting a multiparameter approach for identifying specific disturbance agents and understanding past ecological events. LWBI chronologies did show moderate declines during the highest peak of pollution (1970s), but these variations did not correspond with the spatiotemporal patterns of pollution impacts observed in RW chronologies. Additional factors, such as extreme cold temperatures, likely contributed to the observed LWBI patterns, highlighting the complexity of investigating pollution-related impacts (Fig. 9). Moreover, compared to other parameters, LWBI showed a higher coherence and stability during historical periods marked by high levels of disturbance or pollution.

Overall, this research has shown distinct capabilities of different tree-ring parameters in capturing non-climatic impacts and how these factors influence the short and long-term chronology properties. RW was found to be the most susceptible parameter showing the most prominent growth variations during periods affected by non-climatic factors, with the degree of the influence determined by either the sampling scale or the intensity of non-climatic influences. LWBI and quantitative wood anatomy parameters appeared to be considerably less sensitive to non-climatic factors compared to ring width, based on our studied sites. Therefore, it is necessary to adopt different parameters for different research purposes based on their characteristics and consider their applicability in practice. For instance, ring width could possibly be used as an

indicator of pollution stress or disturbance impact in Norway Spruce forests (Tereza et al., 2019; Rydval et al., 2018). In contrast, LWBI and cell wall thickness are more suitable for capturing stable temperature signals (Fuentes et al., 2018; Heeter et al., 2019; Bjorklund et al., 2020).

Finally, one of the findings revealed by assessing various tree ring parameters and non-climatic factors includes the advantages of using the CID method to detect and isolate non-climatic trends in RW series, which proved to be a useful tool for identifying and correcting abnormal trends in RW chronologies from disturbed or polluted sites. However, its usefulness varies and may possibly be influenced by the extent and intensity of non-climatic impacts, with either over-correction or under-correction of the trends occurring in some instances (Rydval et al., 2015, 2018). This limitation could be tested and to some extent minimized by adjusting the detection threshold (i.e., sensitivity) of the CID method as was done here in the context of pollution trend detection in **Subsection 4.2**.

5.4.2 Impact of non-climatic factors on the climatic signals in tree-rings

Tree rings are one of the main proxies used in paleoclimatic research. However, as demonstrated by the results presented in the previous subsections, the impacts of non-climatic factors on the climatic sensitivity of tree rings can be substantial, although such impacts differed among various tree ring parameters when considering different non-climatic factors (**Subsection 4.1, 4.2**).

The temperature signal in RW chronologies was influenced the most of all the examined parameters, with weakening caused by either disturbance (Fig. 7) or pollution (Fig. 11), considering also that RW chronologies exhibited the most pronounced growth variations associated with non-climatic factors. The most heavily polluted sites displayed the greatest continuous drop in the temperature signal (Fig. 12), and the pollution-induced signal declines in RW chronologies were considerably more apparent than those induced by disturbance, especially at site FA2 (Fig. 8), which was located within a historically polluted region. During the most severely polluted period (i.e., the ‘POL’ period), the climatic signals were observed to reduce substantially or even become absent in RW chronologies (Fig. 11). In addition, the assessment of the impact of disturbance on the climatic signals in RW was also influenced by the temporal misalignment between the detected disturbance periods and available instrumental data, which can lead to an underestimation of this impact. From a long-term perspective, the instabilities of RW climatic signals displayed in the studied sites examined in this thesis, revealed the impacts of traditionally less considered non-climatic factors on RW climatic signals, indicating that a more considerate sampling or statistical approach is necessary in future studies.

Unlike RW, LWBI performed quite well in capturing growing season temperature signals in both disturbed and polluted areas, which highlights its advantages for conducting dendroclimatological studies in these types of environments. The much stronger and more stable temperature signals contained in LWBI chronologies that represent a broader growing season, combined with its characteristic of being minimally impacted by non-climatic factors, strengthens its utility as an efficient temperature-sensitive proxy parameter, as also indicated by other studies (e.g., Wilson et al., 2016; Rydval et al., 2015, 2017a; Heeter et al., 2019; Wang et al., 2020). Moreover, despite the non-climatic impacts on RW series, the difficulties of attempting to extract climatic signals using this parameter can be avoided by developing LWBI chronologies (Fig. 11). Latewood cell wall thickness appeared to display similar temperature signals as those found in LWBI. Despite minor reductions in signal strength, the significance of the detected signals for both LWBI and cell wall thickness was not influenced by either disturbance (Fig. 8) or pollution (Fig. 14). With highly significant and temporally stable temperature signals, cell wall thickness can also be considered a promising tree ring parameter for temperature reconstruction in areas affected by non-climatic influences.

From the perspective of climate reconstruction, the temporally more stable temperature signals contained in LWBI, as well as in latewood cell wall thickness, are crucial regarding the stationarity assumption for climate reconstruction, as a stable linear relationship between the tree-ring proxy and the target environmental driver is necessary. The unstable climatic signals detected in RW chronologies due to various non-climatic factors (Fig. 8; Fig. 12) can undoubtedly lead to reduced accuracy or reliability of reconstructions of certain climatic variables (e.g., temperature), and potentially represent a contributing factor to the ‘divergence’ problem. The usefulness of the curve intervention detection method in improving the climatic signals which may be influenced by non-climatic factors is mixed. In addition to being susceptible to false positives/negatives to some extent, a further limitation of this method is that it is not capable of detecting very short-term disturbance pulses (Björklund et al., 2019). While it is clear that non-climatic factors can impact climatic signals in tree ring datasets, the varying degree of such impacts on the climatic signals of different tree-ring parameters could prove useful in either informing the selection of suitable parameters for dendroclimatological purposes or guiding efforts to reduce unfavorable non-climatic impacts on dendrochronological datasets.

5.4.3 Tree growth in central European Forests within the context of climate change

Within the context of global warming, increases in extreme climate events such as drought, along with an increased frequency of forest disturbances (e.g., wind, insect outbreaks, and forest

fires, etc.), combined with historical environmental issues (e.g., pollution), trees and forests are facing enormous developmental pressures (Seidl et al., 2014; King, 2017). In light of the global impact of climate change, tree growth in Central European forests is inevitably influenced both by climatic and non-climatic factors, which is supported by the findings of this thesis. In particular, climatic factors (i.e., drought) appeared to play a prominent role in impacting tree growth in the five studied species (Fig. 17), and the observed drought-induced growth reductions have a profound impact on forest productivity in the studied region as demonstrated in Matula et al. (2023) using dendrometer records. The increasing risk of drought faced by Central European forests (Hlásny et al., 2014), requires more attention. Species-specific drought resistance provides valuable insights for increasing functional trait diversity in mixed forest stands, which can help to strengthen the effectiveness of anti-drought measures (Pardos et al., 2021). Additionally, afforestation initiatives should take into account the environmental conditions of native habitats, for common species, such as for Norway spruce (Cienciala et al., 2016), to ensure better adaptation of these species to new environments.

Though only a single species (Norway spruce) was investigated in relation to the impacts of non-climatic factors, it provides a sufficient representation of the impacts of disturbance and pollution on tree growth more generally. The findings indicate that Norway spruce will likely become more vulnerable as a consequence of climate change. Due to its high ecological plasticity and economic versatility (Schmidt-Vogt, 1977), Norway spruce is one of the most important tree species in Central and Northern Europe. Its distribution has been significantly expanded by the widespread cultivation of the species outside its natural range (Spiecker, 2003), which has had both positive and negative effects (Spiecker, 2000), although secondary spruce forests are especially vulnerable to changing climatic conditions (Hlásny et al., 2017). Both forest managers and regional stakeholders should pay more attention to these considerations and should try to reduce possible forest damage caused by either climatic or non-climatic factors in order to stabilize forest production.

Furthermore, the elevational drought resistance results reveal the varying capacities of different species to respond to climate change, and that even within the same species, the responses can vary between high and low elevations (Fig. 18). As the analysis focused on evaluating the impact of non-climatic factors only on high-elevation Norway spruce in relation to temperature sensitivity, considerable uncertainties remain regarding the impacts on a broader range of species over more extensive elevational gradients. Further investigations are therefore required to explore these uncertainties, considering additional internal and/or external factors. Finally, while the dynamics of tree growth impacted by various climatic and non-climatic factors were mainly reflected in RW data, other tree-ring parameters, including Blue Intensity and

quantitative wood anatomy parameters, were less affected. This indicates that the selection of specific tree-ring parameters should reflect specific research objectives. For example, RW may be more useful for monitoring tree growth dynamics, whereas Blue Intensity may be preferable when attempting to capture temperature signals.

5.5 FUTURE RESEARCH PERSPECTIVES

The findings of this thesis indicated that both growth trends and climatic signals in tree rings were influenced by non-climatic factors, with different tree ring parameters responding differently to these impacts, and that the growth of trees in Central European forests is facing challenges from both climatic extremes and non-climatic factors within the context of climate change. There is a range of potential directions for future research related to the findings of this thesis. This could involve further exploration to deepen the understanding of the current results or expanding the research into broader areas. Firstly, considering that only a single species has been investigated in the context of non-climatic impacts, it would be useful to extend the research to include more species, since the responses of different species to the same non-climatic factors could be either similar or differ considerably, as was observed in relation to climatic factors by the differing reactions of various species to drought. Furthermore, as the reaction of tree species with different phenological types is also unknown, whether broadleaves and conifers respond similarly or differently to non-climatic factors could also be explored. Secondly, variations of the investigated effects along different elevations could be investigated considering the different micro-environmental conditions along an elevational gradient. Thirdly, the effects of other non-climatic factors (e.g., soil type) could also be explored, especially for the extension of the study on pollution impacts, since increased sulphur and nitrogen deposition will accelerate soil acidification and affect soil chemistry, for example by depleting the ion-exchange capacity of the soil complex and suppressing litter decomposition, ultimately impacting tree radial growth (Kolář et al., 2015; Oulehle et al., 2012). Furthermore, tree ring parameters based on other techniques, such as wood density and especially wood anatomy, should receive more attention. In the long run, the research presented in this thesis serves as a valuable initial step in exploring the impacts of non-climatic factors on tree growth and the climatic sensitivity of tree rings, which offers a solid foundation to improve future studies involving climate reconstruction.

6. CONCLUSION

In this thesis, I conducted extensive dendrochronological research involving Central and Eastern European forests, covering a large geographical range including mountain areas across the entire range of the Carpathian Mountains, as well as high and low elevation locations throughout the Czech Republic. By exploring multiple tree-ring parameters and applying novel statistical approaches, this work aimed to uncover the impacts of climatic and especially several non-climatic factors on tree growth and tree-ring climatic sensitivity in an effort to examine forest dynamics under climate change and explore options to improve the calibration of climate reconstructions in areas affected by distinct non-climatic influences.

While the impacts of disturbance varied on different spatial and temporal scales, the disturbance signature was particularly apparent in RW chronologies developed from smaller subsets of series with lower replication, whereas this influence was diluted in large-scale regional chronologies with abundant series replication. The susceptibility of different tree-ring parameters to disturbance was also found to be quite variable, with LWBI representing the least influenced parameter which contained stronger and more stable temperature signals. These characteristics strongly indicate its greater suitability for dendroclimatic and climate reconstruction purposes in areas affected by disturbance. In practice, either substantially increasing the sample depth and the represented study area or adopting tree-ring parameters more resistant to the effects of disturbance (such as LWBI) will help increase the utility of disturbance-impacted tree-ring samples. Although some improvement could be achieved by applying the Curve Intervention Detection method, its utility proved to be limited. Nonetheless, this thesis shows that it is possible to use this method to detect pollution impacts, as distinct growth suppression trends were identified for heavily polluted sites and periods. Such impacts were mainly observed in RW chronologies in the forests of northern Bohemia within the range of the Black Triangle area. Despite observing some limited improvements in RW chronologies after applying CID, the stronger temperature signal and consistently better performance of LWBI with only minor pollution impact once again demonstrated the advantages of utilizing this parameter in affected areas. In addition, one of the quantitative wood anatomical parameters, i.e., cell wall thickness, also showed higher resistance to pollution, indicating the dendroclimatic potential of QWA in areas affected by pollution.

The primary climatic driver influencing both LWBI and CWT chronologies of high-elevation Norway spruce within the studied area was found to be temperature over an extended growing season (April to September) and these temperature signals appeared to be less affected by either

disturbance or pollution. Although ring width chronologies were also able to retain a shorter (i.e., June to July) seasonal temperature signal, the temporal instability of this signal limited its utility, particularly with the additional stressful influence of disturbance or pollution. Climatic factors were undoubtedly the main environmental variables controlling tree growth. My detailed evaluation of recent drought events on the growth of several major tree species throughout the Czech Republic revealed widespread drought-related impacts. While all investigated species suffered from severe growth reductions in response to extreme drought, the drought resistance of different species was found to be variable, with Norway spruce being the most drought-sensitive species, exhibiting higher vulnerability to the changing climate.

This thesis highlights the importance of considering the impacts of non-climatic factors on the climatic sensitivity of tree ring datasets, especially the negative impacts of disturbance and pollution on the widely used RW parameter. These findings are not only relevant for the studied region, but also applicable throughout a broad geographical range where non-climatic factors play a significant role. The varying sensitivity of different parameters to non-climatic impacts and capability to represent robust climate signals can offer valuable guidance in selecting the most suitable parameters for particular research purposes, especially for climate reconstruction efforts. As Norway spruce is an ecologically and economically important tree species in Central Europe, it is important to emphasize its vulnerability and relative inability to resist the impacts of both non-climatic and climatic factors amid ongoing climate change. As a continuation of the work presented in this thesis, further studies could explore either expanding the detection of non-climatic impacts to additional species and consider other geographical or physiological factors. Such efforts will contribute to further improving our understanding of the interplay between climatic and non-climatic factors on the growth and climatic sensitivity of trees.

REFERENCES

- Abatzoglou, J. T., Dobrowski, S. Z., Parks, S. A., & Hegewisch, K. C. (2018). *TerraClimate, a high-resolution global dataset of monthly climate and climatic water balance from 1958-2015*. Scientific Data. <https://doi.org/10.1038/sdata.2017.191>
- Abdi, H., Williams, L. J., & Valentin, D. (2013). Multiple factor analysis: principal component analysis for multitable and multiblock data sets. *Wiley Interdisciplinary reviews: computational statistics*, 5(2), 149-179.
- Abraham, J., Berger, F., Ciechanowicz-Kusztal, R., Jodłowska-Opyd, G., Kallweit, D., Keder, J., Kulaszka, W., Novák, J. (2002). Common report on air quality in the black triangle region 2002. <https://www.wroclaw.wios.gov.pl/pliki/miedzynarodowe/raport2002.pdf>
- Adams B, White A, Lenton TM. (2004). An analysis of some diverse approaches to modelling terrestrial net primary productivity. *Ecological Modelling*, 177, 353–391.
- Akinyemi, F. O., Hutchinson, S. M., Mîndrescu, M., & Rothwell, J. J. (2013). Lake sediment records of atmospheric pollution in the Romanian Carpathians. *Quaternary International*, 293, 105-113.
- Allen, C. D., Breshears, D. D., & McDowell, N. G. (2015). On underestimation of global vulnerability to tree mortality and forest die-off from hotter drought in the Anthropocene. *Ecosphere*, 6, 1–55.
- Allen, C. D., Macalady, A. K., Chenchouni, H., Bachelet, D., McDowell, N., Vennetier, M., ... Gonzalez, P. (2010). A global overview of drought and heat-induced tree mortality reveals emerging climate change risks for forests. *Forest Ecology and Management*, 259, 660–684.
- Altman, J. (2020). Tree-ring-based disturbance reconstruction in interdisciplinary research: Current state and future directions. *Dendrochronologia*, 63(June), 125733. <https://doi.org/10.1016/j.dendro.2020.125733>
- Andreu-Hayles, L., D'Arrigo, R., Oelkers, R., Anchukaitis, K. J., Gaglioti, B., Wilson, R., Wiles, G. C., Frank, D., & Davi, N. K. (2018). Temperature Variability from Blue Intensity (BI) and Maximum Latewood Density (MXD) tree-ring chronologies from the North American Boreal Forests. *Agufm*, 2018, PP43C-1949.
- Arbellay, E., Jarvis, I., Chavardès, R. D., Daniels, L. D., & Stoffel, M. (2018). Tree-ring proxies of larch bud moth defoliation: Latewood width and blue intensity are more precise than RW. *Tree Physiology*, 38(8), 1237–1245. <https://doi.org/10.1093/treephys/tpy057>

- Arnan X, Lopez BC, Mart inez-Vilalta J, Estorach M, Poytatos R (2012) The age of monumental olive trees (*Olea europaea*) in northeastern Spain. *Dendrochronologia*, 30, 11–14.
- Attiwill, P. M. (1994). The disturbance of forest ecosystems: The ecological basis for conservative management. *Forest Ecology and Management*, 63, 247–300.
- Babst, F., Alexander, M. R., Szejner, P., Bouriaud, O., Klesse, S., Roden, J., ... Trouet, V. (2014). A tree-ring perspective on the terrestrial carbon cycle. *Oecologia*, 176(2), 307–322.
- Bäck, J., Huttunen, S., Turunen, M., & Lamppu, J. (1995). Effects of acid rain on growth and nutrient concentrations in Scots pine and Norway spruce seedlings grown in a nutrient-rich soil. *Environmental Pollution*, 89(2), 177–187.
- Barriopedro, D., Fischer, E. M., Luterbacher, J., Trigo, R. M., & García-Herrera, R. (2011). The hot summer of 2010: Redrawing the temperature record map of Europe. *Science* (New York, N.Y.), 332(6026), 220–4.
- Biondi, F., & Qeadan, F. (2008). A theory-driven approach to tree-ring standardization: defining the biological trend from expected basal area increment. *Tree-Ring Research*, 64(2), 81–96.
- Björklund, J. A., Gunnarson, B. E., & Seftigen, K. (2013). Is blue intensity ready to replace maximum latewood density as a strong temperature proxy? A tree-ring case study on Scots pine from northern Sweden. *Climate of the Past Discussions*, 9(5), 5227–5261. <https://doi.org/10.5194/cpd-9-5227-2013>
- Björklund, J. A., Gunnarson, B. E., Seftigen, K., Esper, J., & Linderholm, H. W. (2014). Blue intensity and density from northern fennoscandian tree rings, exploring the potential to improve summer temperature reconstructions with earlywood information. *Climate of the Past*, 10(2), 877–885. <https://doi.org/10.5194/cp-10-877-2014>
- Björklund, J., Gunnarson, B. E., Seftigen, K., Zhang, P., & Linderholm, H. W. (2015). Using adjusted Blue Intensity data to attain high-quality summer temperature information: A case study from Central Scandinavia. *Holocene*, 25(3), 547–556. <https://doi.org/10.1177/0959683614562434>
- Björklund, J., Rydval, M., Schurman, J. S., Seftigen, K., Trotsiuk, V., Janda, P., Mikoláš, M., Dušátko, M., Čada, V., Bače, R., & Svoboda, M. (2019). Disentangling the multi-faceted growth patterns of primary *Picea abies* forests in the Carpathian arc. *Agricultural and Forest Meteorology*, 271(October 2018), 214–224. <https://doi.org/10.1016/j.agrformet.2019.03.002>
- Björklund, J., Seftigen, K., Fonti, P., Nievergelt, D., & von Arx, G. (2020). Dendroclimatic potential of dendroanatomy in temperature-sensitive *Pinus sylvestris*.

- Dendrochronologia*, 60(February), 125673.
<https://doi.org/10.1016/j.dendro.2020.125673>
- Björklund, J., Seftigen, K., Schweingruber, F., Fonti, P., von Arx, G., Bryukhanova, M. V., Cuny, H. E., Carrer, M., Castagneri, D., & Frank, D. C. (2017). Cell size and wall dimensions drive distinct variability of earlywood and latewood density in Northern Hemisphere conifers. *New Phytologist*. <https://doi.org/10.1111/nph.14639>
- Blasing, T. T., & Duvick, D. (1984). Reconstruction of precipitation history in North American corn belt using tree rings. *Nature*, 307(5947), 143-145.
- Boakye, E. A., Bergeron, Y., Girardin, M. P., & Drobyshev, I. (2021). Contrasting growth response of jack pine and trembling aspen to climate warming in Quebec mixedwoods forests of eastern Canada since the early twentieth century. *Journal of Geophysical Research: Biogeosciences*, 126(5), e2020JG005873.
- Bohner, T., & Diez, J. (2021). Tree resistance and recovery from drought mediated by multiple abiotic and biotic processes across a large geographic gradient. *Science of the Total Environment*, 789. <https://doi.org/10.1016/j.scitotenv.2021.147744>
- Bolte, A., Czajkowski, T., Coccozza, C., Tognetti, R., De Miguel, M., Pšidová, E., ... & Müller, J. (2016). Desiccation and mortality dynamics in seedlings of different European beech (*Fagus sylvatica* L.) populations under extreme drought conditions. *Frontiers in plant science*, 7, 751.
- Bono, D. (2004). Impacts on summer 2003 heat wave in Europe. *UNEP/DEWA/GRID Eur. Environ. Alert Bull.*, 2, 1.
- Borůvka, L., Podrázský, V., Mládková, L., Kuneš, I., & Drábek, O. (2005). Some approaches to the research of forest soils affected by acidification in the Czech Republic. *Soil Science & Plant Nutrition*, 51(5), 745-749.
- Bose, A. K., Gessler, A., Bolte, A., Bottero, A., Buras, A., Cailleret, M., ... & Rigling, A. (2020). Growth and resilience responses of Scots pine to extreme droughts across Europe depend on predrought growth conditions. *Global Change Biology*, 26(8), 4521-4537.
- Bose, A. K., Scherrer, D., Camarero, J. J., Ziche, D., Babst, F., Bigler, C., ... & Rigling, A. (2021). Climate sensitivity and drought seasonality determine post-drought growth recovery of *Quercus petraea* and *Quercus robur* in Europe. *Science of the Total Environment*, 784, 147222.
- Bosela, M., Tumajer, J., Cienciala, E., Dobor, L., Kulla, L., Marčiš, P., Popa, I., Sedmák, R., Sedmáková, D., Sitko, R., Šebeň, V., Štěpánek, P., & Büntgen, U. (2021). Climate warming induced synchronous growth decline in Norway spruce populations across biogeographical gradients since 2000. *Science of the Total Environment*, 752(August 2020). <https://doi.org/10.1016/j.scitotenv.2020.141794>

- Bouriaud, O., & Popa, I. (2009). Comparative dendroclimatic study of Scots pine, Norway spruce, and silver fir in the Vrancea Range, Eastern Carpathian Mountains. *Trees - Structure and Function*, 23(1), 95–106. <https://doi.org/10.1007/s00468-008-0258-z>
- Box, G. E., & Tiao, G. C. (1975). Intervention analysis with applications to economic and environmental problems. *Journal of the American Statistical Association*, 70(349), 70-79.
- Box, G. E., Jenkins, G. M., Reinsel, G. C., & Ljung, G. M. (2015). *Time series analysis: forecasting and control*. John Wiley & Sons.
- Brás, T. A., Seixas, J., Carvalhais, N., & Jagermeyr, J. (2021). Severity of drought and heatwave crop losses tripled over the last five decades in Europe. *Environmental Research Letters*, 16(6). <https://doi.org/10.1088/1748-9326/abf004>
- Breitenmoser, P., Brönnimann, S., Frank, D. (2014). Forward modelling of RW and comparison with a global network of tree-ring chronologies. *Clim. Past*. 10, 437–449.
- Briffa, K. R., Schweingruber, F. H., Jones, P. D., Osborn, T. J., Shiyatov, S. G., & Vaganov, E. A. (1998). Reduced sensitivity of recent tree-growth to temperature at high northern latitudes. *Nature*, 391(6668), 678–682. <https://doi.org/10.1038/35596>
- Briffa, K.R., Osborn, T.J., Schweingruber, F.H., Jones, P.D., Shiyatov, S.G., Vaganov, E.A. (2002). RW and density data around the Northern Hemisphere: part 1, local and regional climate signals. *Holocene*. 12 (6), 737–757.
- Brodribb, T. J., Powers, J., Cochard, H., & Choat, B. (2020). Hanging by a thread? Forests and drought. *Science*, 368(6488), 261-266.
- Brus DJ, Hengeveld GM, Walvoort DJJ, Goedhart PW, Heidema AH, Nabuurs GJ, Gunia K (2011) Statistical mapping of tree species over Europe. *Eur J For Res* 131(1):145–157
- Bunn, A. G., Salzer, M. W., Anchukaitis, K. J., Bruening, J. M., & Hughes, M. K. (2018). Spatiotemporal variability in the climate growth response of high elevation bristlecone pine in the White Mountains of California. *Geophysical Research Letters*, 45(24), 13-312.
- Bunn, A., Korpela, M., Biondi, F., Campelo, F., Mérian, P., Qeadan, F., ... & Klesse, S. (2015). Package ‘dplR’. *Dendrochronology Program Library in R, Version*, 1(3).
- Bunn, A.G., 2008. A dendrochronology program library in R (dplR), *Dendrochronologia*, 26,115-124.
- Bunn, A.G., Salzer, M.W., Anchukaitis, K.J., Bruening, J.M., Hughes, M.K. (2018). Spatiotemporal variability in the climate growth response of high elevation bristlecone pine in the White Mountains of California. *Geophys. Res. Lett.*
- Büntgen, U., & Di Cosmo, N. (2016). Climatic and environmental aspects of the Mongol withdrawal from Hungary in 1242 CE. *Scientific Reports*, 6(February), 1–9. <https://doi.org/10.1038/srep25606>

- Büntgen, U., Frank, D. C., Kaczka, R. J., Verstege, A., Zwijacz-Kozica, T., & Esper, J. (2007). Growth responses to climate in a multi-species tree-ring network in the Western Carpathian Tatra Mountains, Poland and Slovakia. *Tree Physiology*, 27(5), 689–702. <https://doi.org/10.1093/treephys/27.5.689>
- Büntgen, U., Myglan, V. S., Ljungqvist, F. C., McCormick, M., Di Cosmo, N., Sigl, M., ... Kirilyanov, A. V. (2016). Cooling and societal change during the Late Antique Little Ice Age from 536 to around 660 AD. *Nature Geoscience*, 9, 231–236.
- Buras, A., Ovenden, T., Rammig, A., & Zang, C. S. (2022). Refining the standardized growth change method for pointer year detection: Accounting for statistical bias and estimating the deflection period. *Dendrochronologia*, 74(September 2021), 125964. <https://doi.org/10.1016/j.dendro.2022.125964>
- Buras, A., Rammig, A., & Zang, C. S. (2020). A novel approach for the identification of pointer years. *Dendrochronologia*, 63(March), 125746. <https://doi.org/10.1016/j.dendro.2020.125746>
- Buras, A., Spyt, B., Janecka, K., & Kaczka, R. (2018). Divergent growth of Norway spruce on Babia Góra Mountain in the western Carpathians. *Dendrochronologia*, 50, 33-43.
- Bytnerowicz, A., Omasa, K., & Paoletti, E. (2007). Integrated effects of air pollution and climate change on forests: A northern hemisphere perspective. *Environmental Pollution*, 147(3), 438-445.
- Čada, V., Svoboda, M., & Janda, P. (2013). Dendrochronological reconstruction of the disturbance history and past development of the mountain Norway spruce in the Bohemian Forest, central Europe. *Forest Ecology and Management*, 295, 59-68.
- Čada, V., Trotsiuk, V., Janda, P., Mikoláš, M., Bače, R., Nagel, T. A., Morrissey, R. C., Tepley, A. J., Vostarek, O., Begović, K., Chaskovskyy, O., Dušátko, M., Kameniar, O., Kozák, D., Lábusová, J., Málek, J., Meyer, P., Pettit, J. L., Schurman, J. S., ... Svoboda, M. (2020). Quantifying natural disturbances using a large-scale dendrochronological reconstruction to guide forest management. *Ecological Applications*, 30(8), 1–13. <https://doi.org/10.1002/eap.2189>
- Cailleret, M., Jansen, S., Robert, E. M. R., Desoto, L., Aakala, T., Antos, J. A., ... Martínez-Vilalta, J. (2017). A synthesis of radial growth patterns preceding tree mortality. *Global Change Biology*, 23(4), 1675–1690.
- Campbell, R., McCarroll, D., Loader, N. J., Grudd, H., Robertson, I., & Jalkanen, R. (2007). Blue intensity in *Pinus sylvestris* tree-rings: Developing a new palaeoclimate proxy. *Holocene*, 17(6), 821–828. <https://doi.org/10.1177/0959683607080523>
- Campbell, R., McCarroll, D., Robertson, I., Loader, N. J., Grudd, H., & Gunnarson, B. (2011). Blue intensity in *Pinus sylvestris* tree rings: a manual for a new palaeoclimate proxy. *Tree-Ring Research*, 67(2), 127-134.

- Canham, C. D. (1985). Suppression and release during canopy recruitment in *Acer saccharum*. *Bulletin of the Torrey Botanical Club*, 134-145.
- Canham, C. D., Papaik, M. J., & Latty, E. F. (2001). Interspecific variation in susceptibility to windthrow as a function of tree size and storm severity for northern temperate tree species. *Canadian Journal of Forest Research*, 31, 1–10.
- Carrer, M., Castagneri, D., Prendin, A. L., Petit, G., & von Arx, G. (2017). Retrospective analysis of wood anatomical traits reveals a recent extension in tree cambial activity in two high-elevation conifers. *Frontiers in Plant Science*, 8, 737.
- Carrer, M., Unterholzner, L., & Castagneri, D. (2018). Wood anatomical traits highlight complex temperature influence on *Pinus cembra* at high elevation in the Eastern Alps. *International Journal of Biometeorology*, 62(9), 1745–1753.
<https://doi.org/10.1007/s00484-018-1577-4>
- Castagneri, D., Fonti, P., von Arx, G., & Carrer, M. (2017). How does climate influence xylem morphogenesis over the growing season? Insights from long-term intra-ring anatomy in *Picea abies*. *Annals of botany*, 119(6), 1011-1020.
- Castagneri, D., Prendin, A. L., Peters, R. L., Carrer, M., von Arx, G., & Fonti, P. (2020). Long-term impacts of defoliator outbreaks on larch xylem structure and tree-ring biomass. *Frontiers in plant science*, 11, 1078.
- Cavin, L., & Jump, A. S. (2017). Highest drought sensitivity and lowest resistance to growth suppression are found in the range core of the tree *Fagus sylvatica* L. not the equatorial range edge. *Global Change Biology*, 23(1), 362–379. <https://doi.org/10.1111/gcb.13366>
- Čejková, A., Čejková, A., & Kolář, T. (2009). Extreme Radial Growth Reaction of Norway Spruce Along An Altitudinal Gradient in the Šumava Mountains. *Geochronometria*, 33(1), 41–47. <https://doi.org/10.2478/v10003-009-0012-6>
- Chappelka, A. H. (1992). Tree responses to ozone. *Surface level ozone exposures and their effects on vegetation*, 271-324.
- Chappelka, A. H., & Freer-Smith, P. H. (1995). Predisposition of trees by air pollutants to low temperatures and moisture stress. *Environmental Pollution*, 87(1), 105–117.
[https://doi.org/10.1016/S0269-7491\(99\)80013-X](https://doi.org/10.1016/S0269-7491(99)80013-X)
- Charles, D. (1985). Suppression and release during canopy recruitment in *Acer saccharum*.
- Chiroiu, P., Stoffel, M., Onaca, A., & Urdea, P. (2015). Testing dendrogeomorphic approaches and thresholds to reconstruct snow avalanche activity in the Făgăraș Mountains (Romanian Carpathians). *Quaternary Geochronology*, 27, 1-10.
- Chmielewski, F. M., & Rotzer, T. (2001). Response of tree phenology to climate change across Europe. *Agricultural and Forest Meteorology*, 108(2), 101–112.
- Chouldechova, A., & Hastie, T. (2015). Generalized additive model selection. arXiv preprint arXiv:1506.03850.

- Christensen, J. H. & Christensen, O. B. (2003). Severe summertime flooding in Europe. *Nature*, 421, 805–806.
- Chropeňová, M., Gregušková, E. K., Karásková, P., Příbylová, P., Kukučka, P., Baráková, D., & Čupr, P. (2016). Pine needles and pollen grains of *Pinus mugo* Turra—A biomonitoring tool in high mountain habitats identifying environmental contamination. *Ecological Indicators*, 66, 132-142.
- Cienciala, E., Russ, R., Šantrůčková, H., Altman, J., Kopáček, J., Hůnová, I., Štěpánek, P., Oulehle, F., Tumajer, J., & Stáhl, G. (2016). Discerning environmental factors affecting current tree growth in Central Europe. In *Science of the Total Environment* (Vol. 573, pp. 541–554). <https://doi.org/10.1016/j.scitotenv.2016.08.115>
- Cook E R and Kairiukstis L (ed). (1990). *Methods of Dendrochronology: Applications in the Environmental Sciences* (Dordrecht: Kluwer) p 394.
- Cook, E. R., & Jacoby Jr, G. C. (1977). Tree-ring-drought relationships in the Hudson Valley, New York. *Science*, 198(4315), 399-401.
- Cook, E. R., & Pederson, N. (2011). Uncertainty, emergence, and statistics in dendrochronology. *Dendroclimatology: progress and prospects*, 77-112.
- Cook, E. R., & Peters, K. (1997). Calculating unbiased tree-ring indices for the study of climatic and environmental change. *The Holocene*, 7(3), 361-370.
- Cook, E.R. (1985). A time series analysis approach to tree ring standardization. Ph. D. thesis, University of Arizona, Tucson, Arizona.
- Cook, E.R. and Holmes, R.L. 1986. Users manual for program ARSTAN. In: Holmes, R.L., Adams, R.K., and Fritts, H.C. Tree-ring chronologies of western North America: California, eastern Oregon and northern Great Basin. Chronology Series 6. Tucson: Laboratory of Tree-Ring Research, University of Arizona: 50–56.
- Cook, E.R., and Peters, K. (1981). The smoothing spline: a new approach to standardizing forest interior RW series for dendroclimatic studies. *Tree-Ring Bull.* 41: 45–53.
- Cook, E.R., Kairiukstis, L.A. (1990) . *Methods of Dendrochronology: Applications in the Environmental Sciences*. Dordrecht: Kluwer Academic Publishers, 394 pp.
- Cook, E.R., Krusic, P.J.(2005). Program ARSTAN: A Tree-Ring Standardization Program Based on Detrending and Autoregressive Time Series Modeling, With Interactive Graphics. Tree-Ring Laboratory Lamont Doherty Earth Observatory of Columbia University, Palisades, NY.
- Cui, M., Chen, Y., Zheng, M., Li, J., Tang, J., Han, Y., ... & Zhang, G. (2018). Emissions and characteristics of particulate matter from rainforest burning in the Southeast Asia. *Atmospheric Environment*, 191, 194-204.
- Cybis (2019) CooRecorder basics.
<http://www.cybis.se/forfun/dendro/helpcoorecorder7/index.htm>.

- D'Arrigo, R., Wilson, R., Liepert, B., & Cherubini, P. (2008). On the 'divergence problem' in northern forests: a review of the tree-ring evidence and possible causes. *Global and planetary change*, 60(3-4), 289-305.
- De Micco, V., Carrer, M., Rathgeber, C. B., Camarero, J. J., Voltas, J., Cherubini, P., & Battipaglia, G. (2019). From xylogenesis to tree rings: wood traits to investigate tree response to environmental changes. *IWA journal*, 40(2), 155-182.
- Dignon, J., & Hameed, S. (1989). Global emissions of nitrogen and sulphur oxides from 1860 to 1980. *Japca*, 39(2), 180-186.
- Ding, H., Pretzsch, H., Schütze, G., & Rötzer, T. (2017). Size-dependence of tree growth response to drought for Norway spruce and European beech individuals in monospecific and mixed-species stands. *Plant Biology*, 19(5), 709–719.
<https://doi.org/10.1111/plb.12596>
- Dolgova, E. (2016). June-September temperature reconstruction in the Northern Caucasus based on blue intensity data. *Dendrochronologia*, 39, 17–23.
<https://doi.org/10.1016/j.dendro.2016.03.002>
- Donat, M. G., Alexander, L. V., Yang, H., Durre, I., Vose, R., Dunn, R. J. H., et al. (2013). Updated analyses of temperature and precipitation extreme indices since the beginning of the twentieth century: The HadEX2 dataset. *Journal of Geophysical Research: Atmospheres*, 118, 2098–2118.
- Doxa, A., Kamarianakis, Y., & Mazaris, A. D. (2022). Spatial heterogeneity and temporal stability characterize future climatic refugia in Mediterranean Europe. *Global Change Biology*, 28(7), 2413-2424.
- Driesen, E., Van den Ende, W., De Proft, M., & Saeys, W. (2020). Influence of environmental factors light, CO₂, temperature, and relative humidity on stomatal opening and development: A review. *Agronomy*, 10(12). <https://doi.org/10.3390/agronomy10121975>
- Druckenbrod, D. L. (2005). Dendroecological reconstructions of forest disturbance history using time-series analysis with intervention detection. *Canadian Journal of Forest Research*, 35(4), 868–876. <https://doi.org/10.1139/x05-020>
- Druckenbrod, D. L., Pederson, N., Rentch, J., & Cook, E. R. (2013). A comparison of times series approaches for dendroecological reconstructions of past canopy disturbance events. *Forest Ecology and Management*, 302, 23–33.
<https://doi.org/10.1016/j.foreco.2013.03.040>
- Druckenbrod, D.L., Neiman, F.D., Richardson, D.L. and Wheeler, D. (2018). Land-use legacies in forests at Jefferson's Monticello plantation. *Journal of Vegetation Science*, 29(2), pp.307-316.
- Dulamsuren, C., Hauck, M., Kopp, G., Ruff, M., & Leuschner, C. (2017). European beech responds to climate change with growth decline at lower, and growth increase at higher

- elevations in the center of its distribution range (SW Germany). *Trees - Structure and Function*, 31(2), 673–686. <https://doi.org/10.1007/s00468-016-1499-x>
- Durrant, T. H., De Rigo, D., & Caudullo, G. (2016). *Pinus sylvestris* in Europe: distribution, habitat, usage and threats. *European atlas of forest tree species*, 14, 845-846.
- Dyderski, M. K., Paż, S., Frelich, L. E., & Jagodziński, A. M. (2018). How much does climate change threaten European forest tree species distributions? *Global Change Biology*, 24(3), 1150–1163.
- eAGRI. (2021). INFORMATION ON FORESTS AND FORESTRY IN THE CZECH REPUBLIC 2020, *Ministry of Agriculture of the Czech Republic (eAGRI) and The Forest Management Institute (FMI)*, p9. https://www.uhul.cz/wp-content/uploads/Zprava_o_stavu_lesa_2020_aj_web.pdf
- Eaton, E. G. S. D. J., Caudullo, G., Oliveira, S., & De Rigo, D. (2016). *Quercus robur* and *Quercus petraea* in Europe: distribution, habitat, usage and threats. *European atlas of forest tree species*, 160-163.
- Engardt, M., Simpson, D., Schwikowski, M., & Granat, L. (2017). Deposition of sulphur and nitrogen in Europe 1900–2050. Model calculations and comparison to historical observations. *Tellus, Series B: Chemical and Physical Meteorology*, 69(1), 1–20. <https://doi.org/10.1080/16000889.2017.1328945>
- Esper, J., Carnelli, A. L., Kamenik, C., Filot, M., Leuenberger, M., & Treydte, K. (2017). Spruce tree-ring proxy signals during cold and warm periods. *Dendrobiology*, (77), 3-18.
- Esper, J., Krusic, P. J., Ljungqvist, F. C., Luterbacher, J., Carrer, M., Cook, E., ... & Büntgen, U. (2016). Ranking of tree-ring based temperature reconstructions of the past millennium. *Quaternary Science Reviews*, 145, 134-151.
- Esper, J., Schneider, L., Smerdon, J.E., Schöne, B.R., Büntgen, U. (2015). Signals and memory in RW and density data. *Dendrochronologia*. 35, 62–70.
- European Environment Agency 2014, 2015. <http://www.eea.europa.eu/>.
- Fajardo, A., McIntire, E. J., & Olson, M. E. (2019). When short stature is an asset in trees. *Trends in ecology & evolution*, 34(3), 193-199.
- Fang, K., Wilmking, M., Davi, N., Zhou, F., Liu, C. (2014). An ensemble weighting approach for dendroclimatology: drought reconstructions for the northeastern Tibetan Plateau. *PLoS ONE* 9 (1), e86689.
- Feller, U. (2006). Stomatal opening at elevated temperature: an underestimated regulatory mechanism. *General and Applied Plant Physiology, Special Issue, January 2006*, 19–31. http://obzor.bio21.bas.bg/ipp/gapbfiles/pisa-06/06_pisa_19-31.pdf
- Fernández-de-Uña, L., Martínez-Vilalta, J., Poyatos, R., Mencuccini, M., & McDowell, N. G. (2023). The role of height-driven constraints and compensations on tree vulnerability to drought. *New Phytologist*, 239(6), 2083-2098.

- Fischer, E. M., & Knutti, R. (2014). Detection of spatially aggregated changes in temperature and precipitation extremes. *Geophysical Research Letters*, 41, 547–554.
- Fleischer, P., Godzik, B., Bicarova, S., & Bytnerowicz, A. (2005). Effects of air pollution and climate change on forests of the Tatra Mountains, Central Europe. In *Plant responses to air pollution and global change* (pp. 111-121). Springer Japan.
- Folke, C., Carpenter, S., Walker, B., Scheffer, M., Elmqvist, T., Gunderson, L., & Holling, C. S. (2004). Regime shifts, resilience, and biodiversity in ecosystem management. *Annu. Rev. Ecol. Evol. Syst.*, 35, 557-581.
- Forner, A., Valladares, F., & Aranda, I. (2018). Mediterranean trees coping with severe drought: Avoidance might not be safe. *Environmental and Experimental Botany*, 155, 529–540. <https://doi.org/10.1016/j.envexpbot.2018.08.006>
- Franceschini, T., Bontemps, J. D., Perez, V., & Leban, J. M. (2013). Divergence in latewood density response of Norway spruce to temperature is not resolved by enlarged sets of climatic predictors and their non-linearities. *Agricultural and Forest Meteorology*, 180, 132–141. <https://doi.org/10.1016/j.agrformet.2013.05.011>
- Frank, D. C., Poulter, B., Saurer, M., Esper, J., Huntingford, C., Helle, G., ... Weigl, M. (2015). Water-use efficiency and transpiration across European forests during the Anthropocene. *Nature Climate Change*, 5, 579–583.
- Frei, C., Scho'll, R., Fukutome, S., Schmidli, J. & Vidale, P. L. (2006). Future change of precipitation extremes in Europe: An intercomparison of scenarios from regional climate models. *J. Geophys. Res.* 111, D06105.
- Frelich, L. E. (2002). *Forest dynamics and disturbance regimes: studies from temperate evergreen-deciduous forests*. Cambridge University Press.
- Friend, A. L., & Tomlinson, P. T. (1992). Mild ozone exposure alters 14C dynamics in foliage of *Pinus taeda* L. *Tree Physiology*, 11(3), 215-227.
- Fritts, H. (1976). *Tree rings and climate*. London, UK; New York, NY; San Francisco, CA: Blackburn Press, 567 pp.
- Fritts, H. C. (1971). Dendroclimatology and dendroecology. *Quaternary Research*, 1(4), 419-449.
- Fritts, H.C. (1963). Computer programs for tree-ring research. *Tree-ring Bulletin*. 25 (3/4): 2-7.
- Fuentes, M., Björklund, J., Seftigen, K., Salo, R., Gunnarson, B. E., Linderholm, H. W., & Aravena, J. C. (2016). A comparison between RW and Blue Intensity high and low frequency signals from *Pinus sylvestris* L. from the Central and Northern Scandinavian Mountains. *TRACE - Tree Rings in Archeology, Climatology and Ecology*, 14, 38–43. <https://doi.org/10.2312/GFZ.b103-16042.A>

- Fuentes, M., Salo, R., Björklund, J., Seftigen, K., Zhang, P., Gunnarson, B., ... & Linderholm, H. W. (2018). A 970-year-long summer temperature reconstruction from Rogen, west-central Sweden, based on blue intensity from tree rings. *The Holocene*, 28(2), 254-266.
- Gärtner, H., Lucchinetti, S., & Schweingruber, F. H. (2015). A new sledge microtome to combine wood anatomy and tree-ring ecology. *IAWA journal*, 36(4), 452-459.
- Gazol, A., & Camarero, J. J. (2022). Compound climate events increase tree drought mortality across European forests. In *Science of the Total Environment* (Vol. 816). <https://doi.org/10.1016/j.scitotenv.2021.151604>
- Gazol, A., Camarero, J. J., Vicente-Serrano, S. M., Sánchez-Salguero, R., Gutiérrez, E., de Luis, M., Sangüesa-Barreda, G., Novak, K., Rozas, V., Tíscar, P. A., Linares, J. C., Martín-Hernández, N., Martínez del Castillo, E., Ribas, M., García-González, I., Silla, F., Camisón, A., Génova, M., Olano, J. M., ... Galván, J. D. (2018). Forest resilience to drought varies across biomes. *Global Change Biology*, 24(5), 2143–2158. <https://doi.org/10.1111/gcb.14082>
- Gentilesca, T., Camarero, J. J., Colangelo, M., Nole, A., & Ripullone, F. (2017). Drought-induced oak decline in the western Mediterranean region: an overview on current evidences, mechanisms and management options to improve forest resilience. *iForest-Biogeosciences and Forestry*, 10(5), 796.
- George, S. S. (2014a). An overview of RW records across the Northern Hemisphere. *Quaternary Science Reviews*, 95, 132-150.
- George, S. S. (2014b). The global network of RWs and its applications to paleoclimatology. *ANNUAL RECORDERS OF THE PAST*, 16.
- Gommers, C. (2020). Keep Cool and Open Up: Temperature-Induced Stomatal Opening. *Plant Physiology*, 182(3), 1188–1189. <https://doi.org/10.1104/PP.20.00158>
- Grill, D., Pfan, H., Lomsky, B., Bytnerowicz, A., Grulke, N. E., & Tausz, M. (2005). Physiological responses of trees to air pollutants at high elevation sites. *Plant Responses to Air Pollution and Global Change*, 37–44. https://doi.org/10.1007/4-431-31014-2_5
- Grissino-Mayer, H. D. (2016). Dendroclimatology. *International Encyclopedia of Geography: People, the Earth, Environment and Technology: People, the Earth, Environment and Technology*, 1-6.
- Grissino-Mayer, H.D. (1997). Computer assisted, independent observer verification of tree ring measurements. *Tree-ring Bulletin*.
- Grodzińska-Jurczak, M., & Szarek-Łukaszewska, G. (1999). Evaluation of SO₂ and NO₂-related degradation of coniferous forest stands in Poland. *Science of the Total Environment*, 241(1–3), 1–15. [https://doi.org/10.1016/S0048-9697\(99\)00305-8](https://doi.org/10.1016/S0048-9697(99)00305-8)
- Grubler, A. (2002). Trends in Global Emissions: Carbon, Sulphur, and Nitrogen. *Encyclopedia of Global Environmental Change*, 3(May), 35–53.

- Gu, H., Wang, J., Ma, L., Shang, Z., & Zhang, Q. (2019). Insights into the BRT (boosted regression trees) method in the study of the climate-growth relationship of Masson pine in subtropical China. *Forests*, *10*(3), 1–20. <https://doi.org/10.3390/f10030228>
- Guay, R., Gagnon, R., & Morin, H. (1992). A new automatic and interactive tree ring measurement system based on a line scan camera. *The Forestry Chronicle*, *68*(1), 138–141.
- Harley, G. L., Heeter, K. J., Maxwell, J. T., Rayback, S. A., Maxwell, R. S., Reinemann, T. E. P., & H. Taylor, A. (2021). Towards broad-scale temperature reconstructions for Eastern North America using blue light intensity from tree rings. *International Journal of Climatology*, *41*(S1), E3142–E3159. <https://doi.org/10.1002/joc.6910>
- Harris, I., Jones, P. D., Osborn, T. J., & Lister, D. H. (2014). Updated high-resolution grids of monthly climatic observations - the CRU TS3.10 Dataset. *International Journal of Climatology*, *34*(3), 623–642. <https://doi.org/10.1002/joc.3711>
- Harris, I., Osborn, T. J., Jones, P., & Lister, D. (2020). Version 4 of the CRU TS monthly high-resolution gridded multivariate climate dataset. *Scientific data*, *7*(1), 109.
- Heeter, K. J., Harley, G. L., Van De Gevel, S. L., & White, P. B. (2019). Blue intensity as a temperature proxy in the eastern United States: A pilot study from a southern disjunct population of *Picea rubens* (Sarg.). *Dendrochronologia*, *55*(April), 105–109. <https://doi.org/10.1016/j.dendro.2019.04.010>
- Helliwell, R. C., Wright, R. F., Jackson-Blake, L. A., Ferrier, R. C., Aherne, J., Cosby, B. J., ... & Schöpp, W. (2014). Assessing recovery from acidification of European surface waters in the year 2010: evaluation of projections made with the MAGIC model in 1995. *Environmental science & technology*, *48*(22), 13280–13288.
- Hlásny, T., Barka, I., Roessiger, J., Kulla, L., Trombik, J., Sarvašová, Z., ... & Čihák, T. (2017). Conversion of Norway spruce forests in the face of climate change: a case study in Central Europe. *European Journal of Forest Research*, *136*, 1013–1028.
- Hlásny, T., Mátyás, C., Seidl, R., Kulla, L., Merganičová, K., Trombik, J., ... & Konôpka, B. (2014). Climate change increases the drought risk in Central European forests: What are the options for adaptation? *Central European Forestry Journal*, *60*(1), 5–18.
- Horodnic, S. A., & Roibu, C. C. (2020). Collective growth patterns reveal the high growing potential of older silver fir trees in a primeval forest in Romania's Southern Carpathians. *Notulae Botanicae Horti Agrobotanici Cluj-Napoca*, *48*(2), 1085–1099. <https://doi.org/10.15835/nbha48211949>
- Hruška, J., Oulehle, F., Chuman, T., Kolář, T., Rybníček, M., Trnka, M., & McDowell, W. H. (2023). Forest growth responds more to air pollution than soil acidification. *PLoS ONE*, *18*(3 March), 1–21. <https://doi.org/10.1371/journal.pone.0256976>
- https://regentinstruments.com/assets/windendro_about.html. (accessed 07.02.2024).

- Hughes, M. K. (2011). *Dendroclimatology in High-Resolution Paleoclimatology*. 17–34.
https://doi.org/10.1007/978-1-4020-5725-0_2
- Hughes, M. K., Kelly, P. M., Pilcher, J. R., & LaMarche, V. C. (1982). *Climate from tree rings*. New York, NY: *Cambridge University Press*.
- Hunova, I. (2001). Spatial interpretation of ambient air quality for the territory of the Czech Republic. *Environmental Pollution*, 112(2), 107-119.
- Hůnová, I., Šantroch, J., & Ostatnická, J. (2004). Ambient air quality and deposition trends at rural stations in the Czech Republic during 1993–2001. *Atmospheric Environment*, 38(6), 887-898.
- Ionita, M., Dima, M., Nagavciuc, V., Scholz, P., & Lohmann, G. (2021). Past megadroughts in central Europe were longer, more severe and less warm than modern droughts. *Communications Earth and Environment*, 2(1). <https://doi.org/10.1038/s43247-021-00130-w>
- IPCC, (2014). *Climate Change 2014: Impacts, Adaptation, and Vulnerability. Part A: Global and Sectoral Aspects*. In: Field, C.B., Barros, V.R., Dokken, D.J., Mach, K.J., Mastrandrea, M.D., Bilir, T.E., Chatterjee, M., Ebi, K.L., Estrada, Y.O., Genova, R.C., Girma, B., Kissel, E.S., Levy, A.N., MacCracken, S., Mastrandrea, P.R., White, L.L. (Eds.), *Contribution of Working Group II to the Fifth Assessment Report of the Intergovernmental Panel on Climate Change*. Cambridge University Press, Cambridge, United Kingdom and New York, NY, USA (1132 pp.)
- IPCC. (2021). *Climate change 2021: The physical science basis*. In V. Masson- Delmotte, P. Zhai, A. Pirani, S. L. Connors, C. Péan, S. Berger, N. Caud, Y. Chen, L. Goldfarb, M. I. Gomis, M. Huang, K. Leitzell, E. Lonnoy, J. B. R. Matthews, T. K. Maycock, T. Waterfield, O. Yelekçi, R. Yu, & B. Zhou (Eds.), *Contribution of working group I to the sixth assessment report of the Intergovernmental Panel on Climate Change*. *Cambridge University Press*.
- Izuta, T. (Ed.). (2017). *Air pollution impacts on plants in East Asia*. Springer.
- Jacquet, C., & Altermatt, F. (2020). The ghost of disturbance past: Long-term effects of pulse disturbances on community biomass and composition: Ghost of disturbance past. *Proceedings of the Royal Society B: Biological Sciences*, 287(1930).
<https://doi.org/10.1098/rspb.2020.0678>
- Janda, P., Trotsiuk, V., Mikoláš, M., Bače, R., Nagel, T. A., Seidl, R., ... & Svoboda, M. (2017). The historical disturbance regime of mountain Norway spruce forests in the Western Carpathians and its influence on current forest structure and composition. *Forest Ecology and Management*, 388, 67-78.
- Jarvis, D. S., & Kulakowski, D. (2015). Long-term history and synchrony of mountain pine beetle outbreaks in lodgepole pine forests. *Journal of Biogeography*, 42, 1029–1039.

- Jevšenak, J. (2019). Daily climate data reveal stronger climate-growth relationships for an extended European tree-ring network. *Quaternary Science Reviews*, 221. <https://doi.org/10.1016/j.quascirev.2019.105868>
- Jiang, Y., Begović, K., Nogueira, J., Schurman, J. S., Svoboda, M., & Rydval, M. (2022). Impact of disturbance signatures on RW and blue intensity chronology structure and climatic signals in Carpathian Norway spruce. *Agricultural and Forest Meteorology*, 327(March). <https://doi.org/10.1016/j.agrformet.2022.109236>
- Jing, M., Zhu, L., Liu, S., Cao, Y., Zhu, Y., & Yan, W. (2022). Warming-induced drought leads to tree growth decline in subtropics: Evidence from tree rings in central China. *Frontiers in Plant Science*, 13, 964400.
- Jirgla J, Kučera J, Tichý J & Materna J. (1983). Poškození lesů v Jizerských horách imisemi. *Zprávy lesnického výzkumu* 28: 16–24.
- Johnson, D. W., & Taylor, G. E. (1989). Role of air pollution in forest decline in eastern North America. *Water, Air, and Soil Pollution*, 48, 21-43.
- Kaczka, R. J., Spyt, B., Janecka, K., Beil, I., Büntgen, U., Scharnweber, T., Nievergelt, D., & Wilmking, M. (2018). Different maximum latewood density and blue intensity measurements techniques reveal similar results. *Dendrochronologia*, 49(March 2017), 94–101. <https://doi.org/10.1016/j.dendro.2018.03.005>
- Kandler, O., & Innes, J. L. (1995). Air pollution and forest decline in Central Europe. *Environmental Pollution*, 90(2), 171–180. [https://doi.org/10.1016/0269-7491\(95\)00006-D](https://doi.org/10.1016/0269-7491(95)00006-D)
- Katzenmaier, M., Garnot, V. S. F., Björklund, J., Schneider, L., Wegner, J. D., & von Arx, G. (2023). Towards ROXAS AI: Deep learning for faster and more accurate conifer cell analysis. *Dendrochronologia*, 81, 126126.
- Katzensteiner, K., Glatzel, G., Kazda, M., & Sterba, H. (1992). Effects of air pollutants on mineral nutrition of Norway spruce and revitalization of declining stands in Austria. *Water, Air, and Soil Pollution*, 61, 309-322.
- Kaufman, L. H. (1982). Stream aufwuchs accumulation: disturbance frequency and stress resistance and resilience. *Oecologia*, 52, 57-63.
- Kharuk, V. I., Petrov, I. A., Im, S. T., Golyukov, A. S., Dvinskaya, M. L., & Shushpanov, A. S. (2023). Pollution and Climatic Influence on Trees in the Siberian Arctic Wetlands. *Water*, 15(2), 215. <https://doi.org/10.3390/w15020215>
- Kim, J. K., & Fukazawa, K. (1997). Changes in RW and density of *Pinus thunbergii* growing in the vicinity of industrial complex in Korea. *Journal of Forest Research*, 2(2), 109–113. <https://doi.org/10.1007/BF02348478>

- King, A. D. (2017). Attributing changing rates of temperature record breaking to anthropogenic influences. *Earth's Future*, 5, 1156–1168.
<https://doi.org/10.1002/2017EF000611>
- Kolář, T., Čermák, P., Oulehle, F., Trnka, M., Štěpánek, P., Cudlín, P., Hruška, J., Büntgen, U., & Rybníček, M. (2015). Pollution control enhanced spruce growth in the “Black Triangle” near the Czech-Polish border. *Science of the Total Environment*, 538, 703–711.
<https://doi.org/10.1016/j.scitotenv.2015.08.105>
- Kopáček, J., & Veselý, J. (2005). Sulphur and nitrogen emissions in the Czech Republic and Slovakia from 1850 till 2000. *Atmospheric environment*, 39(12), 2179–2188.
- Kramer, K., Leinonen, I., & Loustau, D. (2000). The importance of phenology for the evaluation of impact of climate change on growth of boreal, temperate and Mediterranean forests ecosystems: An overview. *International Journal of Biometeorology*, 44(2), 67–75.
- Krejčí, F., Vacek, S., Bílek, L., Mikeska, M., Hejčmanová, P., & Vacek, Z. (2013). The effects of climatic conditions and forest site types on disintegration rates in *Picea abies* occurring at the Modrava Peat Bogs in the Šumava National Park. *Dendrobiology*, (70).
- Kwak, J. H., Lim, S. S., Lee, K. S., Viet, H. D., Matsushima, M., Lee, K. H., Jung, K., Kim, H. Y., Lee, S. M., Chang, S. X., & Choi, W. J. (2016). Temperature and air pollution affected tree ring $\delta^{13}\text{C}$ and water-use efficiency of pine and oak trees under rising CO₂ in a humid temperate forest. *Chemical Geology*, 420, 127–138.
<https://doi.org/10.1016/j.chemgeo.2015.11.015>
- Labrecque-Foy, J. P., Angers-Blondin, S., Ropars, P., Simard, M., & Boudreau, S. (2023). The Use of Basal Area Increment to Preserve the Multi-Decadal Climatic Signal in Shrub Growth Ring Chronologies: A Case Study of *Betula glandulosa* in a Rapidly Warming Environment. *Atmosphere*, 14(2), 319.
- LaMarche Jr, V. C. (1974). Paleoclimatic Inferences from Long Tree-Ring Records: Intersite comparison shows climatic anomalies that may be linked to features of the general circulation. *Science*, 183(4129), 1043–1048.
- LaMarche Jr, V. C., & Fritts, H. C. (1971). Anomaly patterns of climate over the western United States, 1700–1930, derived from principal component analysis of tree-ring data. *Monthly Weather Review*, 99(2), 138–142.
- Larsson, L. (2016). CDendro & Coorecorder program package for tree ring measurements and 601 crossdating of the data, version 8.1.1. <http://www.cybis.se/forfun/dendro>.
- Lenth, R., Love, J., & Herve, M. (2018). Package “emmeans.” In *The R Journal* (pp. 1–57).
- Leuschner, C. (2020). Drought response of European beech (*Fagus sylvatica* L.)—A review. *Perspectives in Plant Ecology, Evolution and Systematics*, 47(April), 125576.
<https://doi.org/10.1016/j.ppees.2020.125576>

- Lexa, M. (2021). Effect of imission to xylem anatomy of Norway Spruce. *Wood Research*, 66(4), 528–543.
- Liu, H. (2008). Generalized additive model. Department of Mathematics and Statistics University of Minnesota Duluth: Duluth, MN, USA, 55812.
- Lloret, F., Keeling, E. G., & Sala, A. (2011). Components of tree resilience: Effects of successive low-growth episodes in old ponderosa pine forests. *Oikos*, 120(12), 1909–1920. <https://doi.org/10.1111/j.1600-0706.2011.19372.x>
- Lomský, B., Šrámek, V., & Novotný, R. (2013). The health and nutritional status of Norway spruce stands in the Krušné hory Mountains 15 years subsequent to the extreme winter of 1995/96. *Journal of Forest Science*, 59(9), 359-369.
- Lorenz, R., Stalhandske, Z., & Fischer, E. M. (2019). Detection of a climate change signal in extreme heat, heat stress, and cold in Europe from observations. *Geophysical Research Letters*, 46(14), 8363-8374.
- Lorimer, C. G., & Frelich, L. E. (1989). A methodology for estimating canopy disturbance frequency and intensity in dense temperate forests. *Canadian Journal of Forest Research*, 19(5), 651-663.
- Lough, J. M., & Fritts, H. C. (1985). The Southern Oscillation and tree rings: 1600–1961. *Journal of Applied Meteorology and Climatology*, 24(9), 952-966.
- Lucas-Borja, M. E., Andivia, E., Candel-Pérez, D., Linares, J. C., & Camarero, J. J. (2021). Long term forest management drives drought resilience in Mediterranean black pine forest. *Trees - Structure and Function*, 35(5), 1651–1662. <https://doi.org/10.1007/s00468-021-02143-6>
- Luterbacher, J., Dietrich, D., Xoplaki, E., Grosjean, M., & Wanner, H. (2004). European seasonal and annual temperature variability, trends, and extremes since 1500. *Science*, 303(5663), 1499-1503.
- MacGillivray, C. W., Grime, J. P., & The Integrated Screening Programme (ISP) Team. (1995). Testing predictions of the resistance and resilience of vegetation subjected to extreme events. *Functional Ecology*, 640-649.
- Mansfeld, V. (2011). Norway spruce in forest ecosystems of the Czech Republic in relation to different forest site conditions. *Journal of Forest Science*, 57(11), 514-522.
- Manzoni, S. (2014). Integrating plant hydraulics and gas exchange along the drought-response trait spectrum. In *Tree Physiology* (Vol. 34, Issue 10, pp. 1031–1034). <https://doi.org/10.1093/treephys/tpu088>
- Marini, L., Økland, B., Jøonsson, A. M., Bentz, B., Carroll, A., Forster, B., ... Schroeder, M. (2017). Climate drivers of bark beetle outbreak dynamics in Norway spruce forests. *Ecography*, 40, 1426–1435.

- Markonis, Y., Kumar, R., Hanel, M., Rakovec, O., Máca, P., & Kouchak, A. A. (2021). The rise of compound warm-season droughts in Europe. *Science Advances*, 7(6).
<https://doi.org/10.1126/sciadv.abb9668>
- Martínez-Sancho, E., Dorado-Liñán, I., Hacke, U. G., Seidel, H., & Menzel, A. (2017). Contrasting hydraulic architectures of scots pine and sessile oak at their southernmost distribution limits. *Frontiers in Plant Science*, 8, 598.
- Martínez-Vilalta J, Cochard H, Mencuccini M et al. (2009) Hydraulic adjustment of Scots pine across Europe. *New Phytol* 184:353–364.
- Matějka K, Vacek S & Podrázský V. (2010). Development of forest soils in the Krkonoše Mountains in the period 1980–2009. *Journal of Forest Science* 56: 485–504.
- Materna, J. (1999). Development and causes of forest damage in the Ore Mountains[Czech Republic]. *Journal of Forest Science-UZPI (Czech Republic)*, 45(4).
- Mathias, J. M., & Thomas, R. B. (2018). Disentangling the effects of acidic air pollution, atmospheric CO₂, and climate change on recent growth of red spruce trees in the Central Appalachian Mountains. *Global Change Biology*, 24(9), 3938–3953.
<https://doi.org/10.1111/gcb.14273>
- Matula, R., Knířová, S., Vitámvas, J., Šrámek, M., Kníř, T., Ulbrichová, I., ... & Plichta, R. (2023). Shifts in intra-annual growth dynamics drive a decline in productivity of temperate trees in Central European forest under warmer climate. *Science of The Total Environment*, 905, 166906.
- McCarroll, D., Pettigrew, E., Luckman, A., Guibal, F., & Edouard, J. L. (2002). Blue reflectance provides a surrogate for latewood density of high-latitude pine tree rings. *Arctic, Antarctic, and Alpine Research*, 34(4), 450–453. <https://doi.org/10.2307/1552203>
- McCarroll, D., & Loader, N. J. (2004). Stable isotopes in tree rings. *Quaternary Science Reviews*, 23(7-8), 771-801.
- McLaughlin, D. (1998). A decade of forest tree monitoring in Canada: evidence of air pollution effects. *Environmental Reviews*, 6(3-4), 151-171.
- Meehl, G. A. & Tebaldi, C. (2004). More intense, more frequent, and longer lasting heat waves in the 21st century. *Science*, 305, 994–997.
- Merganičová, K., Merganič, J., Lehtonen, A., Vacchiano, G., Sever, M. Z. O., Augustynczyk, A. L., ... & Reyer, C. P. (2019). Forest carbon allocation modelling under climate change. *Tree Physiology*, 39(12), 1937-1960.
- Merlin, M., Perot, T., Perret, S., Korboulewsky, N., & Vallet, P. (2015). Effects of stand composition and tree size on resistance and resilience to drought in sessile oak and Scots pine. *Forest Ecology and Management*, 339, 22–33.
<https://doi.org/10.1016/j.foreco.2014.11.032>

- Mikoláš, M., Ujházy, K., Jasík, M., Wiezik, M., Gallay, I., Polák, P., ... & Keeton, W. S. (2019). Primary forest distribution and representation in a Central European landscape: Results of a large-scale field-based census. *Forest Ecology and Management*, 449, 117466.
- Mikulenka, P., Prokūpková, A., Vacek, Z., Vacek, S., Bulušek, D., Simon, J., Šimůnek, V., & Hájek, V. (2020). Effect of climate and air pollution on radial growth of mixed forests: *Abies alba* Mill. vs. *Picea abies* (L.) Karst. *Central European Forestry Journal*, 66(1), 23–36. <https://doi.org/10.2478/forj-2019-0026>
- Milly, P. C. D., Dunne, K. A. & Vecchia, A. V. (2005). Global pattern of trends in streamflow and water availability in a changing climate. *Nature*, 438, 347–350.
- Modrzyński, J. (2003). Defoliation of older Norway spruce (*Picea abies*/L./Karst.) stands in the Polish Sudety and Carpathian mountains. *Forest Ecology and Management*, 181(3), 289-299.
- Moldan, B., & Schnoor, J. L. (1992). Czechoslovakia: examining a critically ill environment. *Environmental science & technology*, 26(1), 14-21.
- Moravec, V., Markonis, Y., Rakovec, O., Svoboda, M., Trnka, M., Kumar, R., & Hanel, M. (2021). Europe under multi-year droughts: How severe was the 2014–2018 drought period? *Environmental Research Letters*, 16(3). <https://doi.org/10.1088/1748-9326/abe828>
- Morgan, P., Aplet, G. H., Haufler, J. B., Humphries, H. C., Moore, M. M., & Wilson, W. D. (2018). Historical range of variability: a useful tool for evaluating ecosystem change. In *Assessing forest ecosystem health in the inland west* (pp. 87-111). Routledge.
- Mulenga, C., Clarke, C., & Meincken, M. (2022). Effect of copper mining pollution-induced heavy metal toxicities on *B. longifolia* Benth wood cell characteristics. *European Journal of Forest Research*, 0123456789. <https://doi.org/10.1007/s10342-022-01524-x>
- Mylona, S. (1997). Sulphur dioxide emissions in Europe 1880-1991 and their effect on sulphur concentrations and depositions. *Tellus B*, 49, pp.447-448.
- Nagavciuc, V., Kern, Z., Ionita, M., Hartl, C., Konter, O., Esper, J., & Popa, I. (2020). Climate signals in carbon and oxygen isotope ratios of *Pinus cembra* tree-ring cellulose from the Călimani Mountains, Romania. *International Journal of Climatology*, 40(5), 2539-2556.
- Nagavciuc, V., Roibu, C. C., Ionita, M., Mursa, A., Cotos, M. G., & Popa, I. (2019). Different climate response of three tree ring proxies of *Pinus sylvestris* from the Eastern Carpathians, Romania. *Dendrochronologia*, 54(February), 56–63. <https://doi.org/10.1016/j.dendro.2019.02.007>
- National Research Council. (2006). Surface temperature reconstructions for the last 2,000 years. Washington, DC: *The National Academies Press*.

- Nehrbass-Ahles, C., Babst, F., Klesse, S., Nötzli, M., Bouriaud, O., Neukom, R., Dobbertin, M., & Frank, D. (2014). The influence of sampling design on tree-ring-based quantification of forest growth. *Global Change Biology*, 20(9), 2867–2885. <https://doi.org/10.1111/gcb.12599>
- Neuhöferová, P. (Ed.) (2005). Restoration of forest ecosystems of the Jizerské hory Mountains, Proceedings of Extended Summaries, 26 September, 2005, Kostelec nad Černými lesy, CUA FFE Prague, Department of Silviculture and FGMRI Jiloviště-Strnady, RS Opočno.
- Obladen, N., Dechering, P., Skiadaresis, G., Tegel, W., Keßler, J., Höllerl, S., Kaps, S., Hertel, M., Dulamsuren, C., Seifert, T., Hirsch, M., & Seim, A. (2021). Tree mortality of European beech and Norway spruce induced by 2018-2019 hot droughts in central Germany. *Agricultural and Forest Meteorology*, 307. <https://doi.org/10.1016/j.agrformet.2021.108482>
- Obrębska-Starkel, B. (2004). Climate of the Babia Góra massif. *Babiogórski National Park: Nature Monograph, Krakow: Publishing House and Printing House of the Society of Slovaks in Poland*, 137-151.
- Ohta, S. (1978). Observation of tree ring structure by soft x-ray densitometry. I. The effects of air pollution on annual ring structure. *Mokuzai Gakkaishi;(Japan)*, 24(7).
- Opala-Owczarek, M., Błaś, M., Owczarek, P., Sobik, M., & Godek, M. (2019). A dendroclimatological study of east- and west-facing slopes in mountainous areas subjected to strong air pollution (the Sudetes, Central Europe). *Physical Geography*, 40(2), 186–208. <https://doi.org/10.1080/02723646.2018.1547872>
- Orbán, I., Ónodi, G., & Kröel-Dulay, G. (2023). The role of drought, disturbance, and seed dispersal in dominance shifts in a temperate grassland. *Journal of Vegetation Science*, 34(4), e13199.
- Osborn TJ, Briffa KR and Jones PD. (1997). Adjusting variance for sample-size in tree ring chronologies and other regional mean time-series. *Dendrochronologia* 15(89): 89-99.
- Oulehle, F., Cosby, B. J., Wright, R. F., Hruška, J., Kopáček, J., Krám, P., ... & Moldan, F. (2012). Modelling soil nitrogen: the MAGIC model with nitrogen retention linked to carbon turnover using decomposer dynamics. *Environmental Pollution*, 165, 158-166.
- Oulehle, F., Kopáček, J., Chuman, T., Černohous, V., Hůňová, I., Hruška, J., Krám, P., Lachmanová, Z., Navrátil, T., Štěpánek, P., Tesař, M., & Evans, C. D. (2016). Predicting sulphur and nitrogen deposition using a simple statistical method. *Atmospheric Environment*, 140, 456–468. <https://doi.org/10.1016/j.atmosenv.2016.06.028>
- Pal, J. S., Giorgi, F., & Bi, X. (2004). Consistency of recent European summer precipitation trends and extremes with future regional climate projections. *Geophysical Research Letters*, 31(13).

- Pardos, M., del Río, M., Pretzsch, H., Jactel, H., Bielak, K., Bravo, F., Brazaitis, G., Defosse, E., Engel, M., Godvod, K., Jacobs, K., Jansone, L., Jansons, A., Morin, X., Nothdurft, A., Oreti, L., Ponette, Q., Pach, M., Riofrío, J., ... Calama, R. (2021). The greater resilience of mixed forests to drought mainly depends on their composition: Analysis along a climate gradient across Europe. *Forest Ecology and Management*, 481. <https://doi.org/10.1016/j.foreco.2020.118687>
- Park Williams, A., Allen, C. D., Macalady, A. K., Griffin, D., Woodhouse, C. A., Meko, D. M., ... McDowell, N. G. (2012). Temperature as a potent driver of regional forest drought stress and tree mortality. *Nature Climate Change*, 3, 292–297.
- Pavlin, J., Nagel, T. A., Svitok, M., Pettit, J. L., Begović, K., Mikac, S., Dikku, A., Toromani, E., Panayotov, M., Zlatanov, T., Haruta, O., Dorog, S., Chaskovskyy, O., Mikoláš, M., Janda, P., Frankovič, M., Rodrigo, R., Vostarek, O., Synek, M., ... Svoboda, M. (2021). Disturbance history is a key driver of tree lifespan in temperate primary forests. In *Journal of Vegetation Science*. <https://doi.org/10.1111/jvs.13069>
- Pedersen, E. J., Miller, D. L., Simpson, G. L., & Ross, N. (2019). Hierarchical generalized additive models in ecology: an introduction with mgcv. *PeerJ*, 7, e6876.
- Pederson, N., Bell, A. R., Cook, E. R., Lall, U., Devineni, N., Seager, R., ... & Vranes, K. P. (2013). Is an epic pluvial masking the water insecurity of the greater New York City region?. *Journal of Climate*, 26(4), 1339-1354.
- Pederson, N., Dyer, J. M., McEwan, R. W., Hessler, A. E., Mock, C. J., Orwig, D. A., ... Cook, B. I. (2014). The legacy of episodic climatic events in shaping temperate broadleaf forests. *Ecological Monographs*, 84, 599–620.
- Peterson, C.J., and Pickett, S.T.A. (1995). Forest reorganization: A case study in an old-growth forest catastrophic blowdown. *Ecology*, 76 (3): 763–774.
- Pickett, S.T.A. & White, P.S. (1985) Patch dynamics: a synthesis. *The Ecology of Natural Disturbance and Patch Dynamics* (eds S.T.A. Pickett & P.S. White), pp. 371–384. Academic Press, Inc., San Diego.
- Polle, A., & Rennenberg, H. (2019). Physiological responses to abiotic and biotic stress in forest trees. *Forests*, 10(9), 2–5.
- Polle, A., Chen, S. L., Eckert, C., & Harfouche, A. (2019). Engineering drought resistance in forest trees. In *Frontiers in Plant Science* (Vol. 9, Issue January). <https://doi.org/10.3389/fpls.2018.01875>
- Popa, A., Popa, I., Roibu, C. C., & Badea, O. N. (2022). Do Different Tree-Ring Proxies Contain Different Temperature Signals? A Case Study of Norway Spruce (*Picea abies* (L.) Karst) in the Eastern Carpathians. *Plants*, 11(18), 2428.
- Potop, V., Boroneanț, C., Možný, M., Štěpánek, P., & Skalák, P. (2014). Observed spatiotemporal characteristics of drought on various time scales over the Czech Republic.

- Theoretical and Applied Climatology*, 115(3–4), 563–581.
<https://doi.org/10.1007/s00704-013-0908-y>
- Poyatos, R., Llorens, P., Piñol, J., & Rubio, C. (2008). Response of Scots pine (*Pinus sylvestris* L.) and pubescent oak (*Quercus pubescens* Willd.) to soil and atmospheric water deficits under Mediterranean mountain climate. *Annals of Forest Science*, 65(3), 1.
- Prendin, A. L., Petit, G., Carrer, M., Fonti, P., Björklund, J., & von Arx, G. (2017). New research perspectives from a novel approach to quantify tracheid wall thickness. *Tree physiology*, 37(7), 976-983.
- Primicia, I., Camarero, J. J., Janda, P., Čada, V., Morrissey, R. C., Trotsiuk, V., Bače, R., Teodosiu, M., & Svoboda, M. (2015). Age, competition, disturbance and elevation effects on tree and stand growth response of primary *Picea abies* forest to climate. *Forest Ecology and Management*, 354, 77–86. <https://doi.org/10.1016/j.foreco.2015.06.034>
- Putalová, T., Vacek, Z., Vacek, S., Štefančík, I., Bulušek, D., & Král, J. (2019). RWs as an indicator of air pollution stress and climate conditions in different Norway spruce forest stands in the Krkonoše Mountains *Central European Forestry Journal*, 65(1), 21–33. <https://doi.org/10.2478/forj-2019-0004>
- Rammig, A., Wiedermann, M., Donges, J. F., Babst, F., von Bloh, W., Frank, D., ... & Mahecha, M. D. (2014). Tree-ring responses to extreme climate events as benchmarks for terrestrial dynamic vegetation models. *Biogeosciences Discussions*, 11(2).
- Ravindra, K., Rattan, P., Mor, S., & Aggarwal, A. N. (2019). Generalized additive models: Building evidence of air pollution, climate change and human health. *Environment international*, 132, 104987.
- Rebetez, M., Mayer, H., Dupont, O., Schindler, D., Gartner, K., Kropp, J. P., & Menzel, A. (2006). Heat and drought 2003 in Europe: A climate synthesis. In *Annals of Forest Science* (Vol. 63, Issue 6, pp. 569–577). <https://doi.org/10.1051/forest:2006043>
- Reichstein, M., Papale, D., Valentini, R., Aubinet, M., Bernhofer, C., Knohl, A., ... & Seufert, G. (2007). Determinants of terrestrial ecosystem carbon balance inferred from European eddy covariance flux sites. *Geophysical Research Letters*, 34(1).
- Rein, F., & Štekl, J. (1981). The extremeness of the cold front of Dec. 31, 1978 over the CSR. *Travaux géophysiques*, 29, 379-404.
- Renner, E. (2002). The black triangle area—fit for Europe?. *AMBIO: A Journal of the Human Environment*, 31(3), 231-235.
- Rezaie, N., D'Andrea, E., Scartazza, A., Gričar, J., Prislán, P., Calfapietra, C., ... & Matteucci, G. (2023). Upside down and the game of C allocation. *Tree Physiology*, tpad034.
- Rinn (2014): LignoVisionTM.
<http://www.rinntech.de/content/view/18/49/lang,english/index.html>. (accessed 07.02.2024).

- Rohner, B., Kumar, S., Liechti, K., Gessler, A., & Ferretti, M. (2021). Tree vitality indicators revealed a rapid response of beech forests to the 2018 drought. *Ecological Indicators*, *120*. <https://doi.org/10.1016/j.ecolind.2020.106903>
- Rosner, S., Světlík, J., Andreassen, K., Borja, I., Dalsgaard, L., Evans, R., ... & Solberg, S. (2016). Novel hydraulic vulnerability proxies for a boreal conifer species reveal that opportunists may have lower survival prospects under extreme climatic events. *Frontiers in Plant Science*, *7*, 831.
- Rossi, S., Anfodillo, T., Čufar, K., Cuny, H. E., Deslauriers, A., Fonti, P., ... & Rathgeber, C. B. (2013). A meta-analysis of cambium phenology and growth: linear and non-linear patterns in conifers of the northern hemisphere. *Annals of botany*, *112*(9), 1911-1920.
- Rozas, V., Camarero, J. J., Sangüesa-Barreda, G., Souto, M., & García-González, I. (2015). Summer drought and ENSO-related cloudiness distinctly drive *Fagus sylvatica* growth near the species rear-edge in northern Spain. *Agricultural and Forest Meteorology*, *201*, 153–164. <https://doi.org/10.1016/j.agrformet.2014.11.012>
- Rydval, M., & Wilson, R. (2012). The impact of industrial SO₂ pollution on north Bohemia conifers. *Water, Air, & Soil Pollution*, *223*(9), 5727-5744.
- Rydval, M., Druckenbrod, D. L., Svoboda, M., Trotsiuk, V., Janda, P., Mikoláš, M., Čada, V., Bače, R., Teodosiu, M., & Wilson, R. (2018). Influence of sampling and disturbance history on climatic sensitivity of temperature-limited conifers. *Holocene*, *28*(10), 1574–1587. <https://doi.org/10.1177/0959683618782605>
- Rydval, M., Druckenbrod, D., Anchukaitis, K. J., & Wilson, R. (2015). Detection and removal of disturbance trends in tree-ring series for dendroclimatology. *Canadian Journal of Forest Research*, *46*(3), 387–401. <https://doi.org/10.1139/cjfr-2015-0366>
- Rydval, M., Gunnarson, B. E., Loader, N. J., Cook, E. R., Druckenbrod, D. L., & Wilson, R. (2017a). Spatial reconstruction of Scottish summer temperatures from tree rings. *International Journal of Climatology*, *37*(3), 1540–1556. <https://doi.org/10.1002/joc.4796>
- Rydval, M., Larsson, L. Å., McGlynn, L., Gunnarson, B. E., Loader, N. J., Young, G. H. F., & Wilson, R. (2014). Blue intensity for dendroclimatology: Should we have the blues? Experiments from Scotland. *Dendrochronologia*, *32*(3), 191–204. <https://doi.org/10.1016/j.dendro.2014.04.003>
- Rydval, M., Loader, N. J., Gunnarson, B. E., Druckenbrod, D. L., Linderholm, H. W., Moreton, S. G., Wood, C. V., & Wilson, R. (2017b). Reconstructing 800 years of summer temperatures in Scotland from tree rings. *Climate Dynamics*, *49*(9–10), 2951–2974. <https://doi.org/10.1007/s00382-016-3478-8>

- Sabatini, F. M., Burrascano, S., Keeton, W. S., Levers, C., Lindner, M., Pötzschner, F., ... Kuemmerle, T. (2018). Where are Europe's last primary forests? Diversity and Distributions, 24, 1426–1439. <https://doi.org/10.1111/ddi.12778>
- Sáenz-Romero, C., Lamy, J. B., Loya-Rebollar, E., Plaza-Aguilar, A., Burrett, R., Lobit, P., & Delzon, S. (2013). Genetic variation of drought-induced cavitation resistance among *Pinus hartwegii* populations from an altitudinal gradient. *Acta Physiologiae Plantarum*, 35, 2905-2913.
- Sánchez-Salguero, R., Navarro-Cerrillo, R. M., Camarero, J. J., & Fernández-Cancio, Á. (2012). Selective drought-induced decline of pine species in southeastern Spain. *Climatic Change*, 113, 767-785.
- Saenz-Romero, C., Lamy, J.-B., Ducouso, A., Musch, B., Ehrenmann, F., Delzon, S., ... Kremer, A. (2017). Adaptive and plastic responses of *Quercus petraea* populations to climate across Europe. *Global Change Biology*, 23, 2831–2847.
- Samusevich, A., Zeidler, A., & Vejpusťková, M. (2017). Influence of air pollution and extreme frost on wood cell parameters at Mountain Spruce Stands (*Picea abies* (L.) Karst.) in the Ore Mountains. *Wood Research*, 62(1), 79–90.
- Sander, C., Eckstein, D., Kyncl, J., & Dobrý, J. (1995). The growth of spruce (*Picea abies* (L.) Karst) in the Krkonoše-(Giant) Mountains as indicated by ring width and wood density. *Annales Des Sciences Forestieres*, 52(5), 401–410. [https://doi.org/10.1016/0003-4312\(96\)89710-4](https://doi.org/10.1016/0003-4312(96)89710-4)
- Šantrůčková, H., Šantrůček, J., Šetlik, J., Svoboda, M., & Kopáček, J. (2007). Carbon isotopes in tree rings of Norway spruce exposed to atmospheric pollution. *Environmental science & technology*, 41(16), 5778-5782.
- Saulnier, M., Schurman, J., Vostarek, O., Rydval, M., Pettit, J., Trotsiuk, V., Janda, P., Bače, R., Björklund, J., & Svoboda, M. (2020). Climatic drivers of *Picea* growth differ during recruitment and interact with disturbance severity to influence rates of canopy replacement. *Agricultural and Forest Meteorology*, 287(February). <https://doi.org/10.1016/j.agrformet.2020.107981>
- Savard, M. M. (2010). Tree-ring stable isotopes and historical perspectives on pollution - An overview. *Environmental Pollution*, 158(6), 2007–2013. <https://doi.org/10.1016/j.envpol.2009.11.031>
- Schär, C., & Jendritzky, G. (2004). Hot news from summer 2003. *Nature*, 432(7017), 559-560.
- Scheffer, M., Carpenter, S., Foley, J. A., Folke, C., & Walker, B. (2001). Catastrophic shifts in ecosystems. *Nature*, 413(6856), 591-596.
- Schmidt-Vogt, H., Jahn, G., Kral, F., & Vogellehner, D. (1977). Die Fichte 1. Taxonomie, Verbreitung, Morphologie, Ökologie, Waldgesellschaften. *Verlag Paul Parey, Hamburg and Berlin*.

- Schurman, J. S., Babst, F., Björklund, J., Rydval, M., Bače, R., Čada, V., Janda, P., Mikolas, M., Saulnier, M., Trotsiuk, V., & Svoboda, M. (2019). The climatic drivers of primary Picea forest growth along the Carpathian arc are changing under rising temperatures. *Global Change Biology*, 25(9), 3136–3150. <https://doi.org/10.1111/gcb.14721>
- Schurman, J. S., Trotsiuk, V., Bače, R., Čada, V., Fraver, S., Janda, P., Kulakowski, D., Labusova, J., Mikoláš, M., Nagel, T. A., Seidl, R., Synek, M., Svobodová, K., Chaskovskyy, O., Teodosiu, M., & Svoboda, M. (2018). Large-scale disturbance legacies and the climate sensitivity of primary Picea abies forests. *Global Change Biology*, 24(5), 2169–2181. <https://doi.org/10.1111/gcb.14041>
- Schweingruber, F. H., Fritts, H. C., Bräker, O. U., Drew, L. G., & Schär, E. (1978). The X-ray technique as applied to dendroclimatology.
- Sedmáková, D., Sedmák, R., Bosela, M., Ježík, M., Blaženec, M., Hlásny, T., & Marušák, R. (2019). Growth-climate responses indicate shifts in the competitive ability of European beech and Norway spruce under recent climate warming in East-Central Europe. *Dendrochronologia*, 54(February), 37–48. <https://doi.org/10.1016/j.dendro.2019.02.001>
- Seftigen, K., Fuentes, M., Ljungqvist, F. C., & Björklund, J. (2020). Using Blue Intensity from drought-sensitive Pinus sylvestris in Fennoscandia to improve reconstruction of past hydroclimate variability. *Climate Dynamics*, 55(3–4), 579–594. <https://doi.org/10.1007/s00382-020-05287-2>
- Seidl, R., Muller, J., Hothorn, T., B€assler, C., Heurich, M., & Kautz, M. (2016). Small beetle, large-scale drivers: How regional and landscape factors affect outbreaks of the European spruce bark beetle. *Journal of Applied Ecology*, 53, 530–540.
- Seidl, R., SCHELHAAS, M. J., & Lexer, M. J. (2011). Unraveling the drivers of intensifying forest disturbance regimes in Europe. *Global Change Biology*, 17(9), 2842–2852.
- Seidl, R., Schelhaas, M.-J., Rammer, W., & Verkerk, P. J. (2014). Increasing forest disturbances in Europe and their impact on carbon storage. *Nature Climate Change*, 4, 806–810.
- Seidl, R., Thom, D., Kautz, M., Martin-Benito, D., Peltoniemi, M., Vacchiano, G., Wild, J., Ascoli, D., Petr, M., Honkaniemi, J., Lexer, M. J., Trotsiuk, V., Mairota, P., Svoboda, M., Fabrika, M., Nagel, T. A., & Reyer, C. P. O. (2017). Forest disturbances under climate change. *Nature Climate Change*, 7(6), 395–402. <https://doi.org/10.1038/nclimate3303>
- Sekula, P., Bokwa, A., Bartyzel, J., Bochenek, B., Chmura, Ł., Galkowski, M., & Zimnoch, M. (2021). Measurement report: Effect of wind shear on PM 10 concentration vertical structure in the urban boundary layer in a complex terrain. *Atmospheric Chemistry and Physics*, 21(15), 12113–12139.

- Sen, P. K. (1968). Estimates of the regression coefficient based on Kendall's tau. *Journal of the American statistical association*, 63(324), 1379-1389.
- Seneviratne, S. I., Lüthi, D., Litschi, M., & Schär, C. (2006). Land-atmosphere coupling and climate change in Europe. *Nature*, 443(7108), 205–209.
- Senf, C., & Seidl, R. (2017). Natural disturbances are spatially diverse but temporally synchronized across temperate forest landscapes in Europe. *Global Change Biology*, 1–11.
- Senf, C., & Seidl, R. (2021). Mapping the forest disturbance regimes of Europe. *Nature Sustainability*, 4(1), 63–70. <https://doi.org/10.1038/s41893-020-00609-y>
- Serra-Maluquer, X., Gazol, A., Anderegg, W. R. L., Martínez-Vilalta, J., Mencuccini, M., & Camarero, J. J. (2022). Wood density and hydraulic traits influence species' growth response to drought across biomes. *Global Change Biology*, 28(12), 3871–3882. <https://doi.org/10.1111/gcb.16123>
- Serra-Maluquer, X., Gazol, A., Sangüesa-Barreda, G., Sánchez-Salguero, R., Rozas, V., Colangelo, M., ... & Camarero, J. J. (2019). Geographically structured growth decline of rear-edge Iberian *Fagus sylvatica* forests after the 1980s shift toward a warmer climate. *Ecosystems*, 22, 1325-1337.
- Sheppard, L., & Pfanz, H. (2001). *Impacts of air pollutants on cold hardiness* (pp. 335-366). Springer Netherlands.
- Sheppard, P. R. (2010). Dendroclimatology: extracting climate from trees. *Wiley Interdisciplinary Reviews: Climate Change*, 1(3), 343-352.
- Sherman, R. E., & Fahey, T. J. (1994). The effects of acid deposition on the biogeochemical cycles of major nutrients in mature red spruce ecosystems. *Biogeochemistry*, 24, 85–114.
- Sidor, C. G., Vlad, R., Popa, I., Semeniuc, A., Apostol, E., & Badea, O. (2021). Impact of industrial pollution on radial growth of conifers in a former mining area in the eastern carpathians (Northern Romania). *Forests*, 12(5). <https://doi.org/10.3390/f12050640>
- Slovik, S., Siegmund, A., Kindermann, G., Riebeling, R., & Balázs, Á. (1995). Stomatal SO₂ uptake and sulfate accumulation in needles of Norway spruce stands (*Picea abies*) in Central Europe. *Plant and Soil*, 168, 405-419.
- Smil, V. (1990). Nitrogen and phosphorus. In: Turner, B.L., et al. (Eds.), *The Earth as Transformed by Human Action*. Cambridge University Press, New York, pp. 423–436.
- Smith, S. J., van Aardenne, J., Klimont, Z., Andres, R. J., Volke, A., & Delgado Arias, S. (2011). Anthropogenic sulphur dioxide emissions: 1850–2005. *Atmospheric Chemistry and Physics*, 11(3), 1101-1116.
- Sohngen, B., & Tian, X. (2016). Global climate change impacts on forests and markets. *Forest Policy and Economics*, 72, 18-26.

- Song, W., Zhao, B., Mu, C., Ballikaya, P., Cherubini, P., & Wang, X. (2022). Moisture availability influences the formation and characteristics of earlywood of *Pinus tabuliformis* more than latewood in northern China. *Agricultural and Forest Meteorology*, 327, 109219.
- Speer, J. H. (2010). *Fundamentals of tree-ring research*. University of Arizona Press.
- Spence, R. D., Rykiel Jr, E. J., & Sharpe, P. J. (1990). Ozone alters carbon allocation in loblolly pine: assessment with carbon-11 labeling. *Environmental Pollution*, 64(2), 93-106.
- Spiecker, H. (2000). Growth of Norway spruce (*Picea abies* [L.] Karst.) under changing environmental conditions in Europe. In *EFI Proceedings* (Vol. 33, pp. 11-26). Finland European Forest Institute, Joensuu.
- Spiecker, H. (2003). Silvicultural management in maintaining biodiversity and resistance of forests in Europe—temperate zone. *Journal of environmental Management*, 67(1), 55-65.
- Šrámek, V., Slodičák, M., Lomský, B., Balcar, V., Kulhavý, J., Hadaš, P., ... & Sloup, M. (2008). The Ore Mountains: Will successive recovery of forests from lethal disease be successful. *Mountain Research and Development*, 28(3), 216-221.
- Stancescu, M., & Milian, N. (2012). HEAVY PRECIPITATION IN THE FAGARAS MOUNTAINS, 1-4 JUNE, 1988. *Aerul si Apa. Componente ale Mediului*, 265.
- Steiger, J.H. (1980). Tests for comparing elements of a correlation matrix. *Psychol. Bull.* 87, 245–251.
- Stern, D. I. (2005). Global sulphur emissions from 1850 to 2000. *Chemosphere*, 58(2), 163-175.
- Stine, A. R., & Huybers, P. (2017). Implications of Liebig's law of the minimum for tree-ring reconstructions of climate. *Environmental Research Letters*, 12(11), 114018.
- Știrbu, M. I., Roibu, C. C., Carrer, M., Mursa, A., Unterholzner, L., & Prendin, A. L. (2022). Contrasting climate sensitivity of *Pinus cembra* tree-ring traits in the Carpathians. *Frontiers in Plant Science*, 13, 855003.
- Stockton, C. W., & Fritts, H. C. (1973). LONG-TERM RECONSTRUCTION OF WATER LEVEL CHANGES FOR LAKE ATHABASCA BY ANALYSIS OF TREE RINGS 1. *JAWRA Journal of the American Water Resources Association*, 9(5), 1006-1027.
- Stockton, C. W., & Jacoby, G. (1976). Long-term surface-water supply and streamflow trends in the Upper Colorado River Basin. Available from the National Technical Information Service, Springfield VA 22161 as PB-264 533, Price codes: A 05 in paper copy, A 01 in microfiche. *Lake Powell Research Project Bulletin*, (18).
- Stockton, C. W., & Meko, D. M. (1975). A long-term history of drought occurrence in western United States as inferred from tree rings. *Weatherwise*, 28(6), 244-249.

- Stokes, M. A., & Smiley, T. L. (1996). An introduction to tree-ring dating. Tucson, AZ: *University of Arizona Press*.
- Stokes, M.A., Smiley, T.L. (1968). An Introduction to Tree-Ring Dating. University of Chicago Press, Chicago, Illinois.
- Stott, P. A., Stone, D. A. & Allen, M. R. (2004). Human contribution to the European heatwave of 2003. *Nature*, 432, 610–614.
- Sullivan, P. F., Pattison, R. R., Brownlee, A. H., Cahoon, S. M., & Hollingsworth, T. N. (2016). Effect of tree-ring detrending method on apparent growth trends of black and white spruce in interior Alaska. *Environmental Research Letters*, 11(11), 114007.
- Svoboda, M., Janda, P., Bače, R., Fraver, S., Nagel, T. A., Rejzek, J., ... & Lehejček, J. (2014). Landscape-level variability in historical disturbance in primary *Picea abies* mountain forests of the Eastern Carpathians, Romania. *Journal of Vegetation Science*, 25(2), 386–401.
- Svobodova, K., Langbehn, T., Bjorklund, J., Rydval, M., Trotsiuk, V., Morrissey, R. C., ... Svoboda, M. (2019). Increased sensitivity to drought across successional stages in natural Norway spruce (*Picea abies* (L.) Karst.) forests of the Calimani Mountains, Romania. *Trees-Structure and Function*, 33(5), 1345–1359.
- Swanson, K. L., Sugihara, G., & Tsonis, A. A. (2009). Long-term natural variability and 20th century climate change. *Proceedings of the National Academy of Sciences of the United States of America*, 106(38), 16120–16123. <https://doi.org/10.1073/pnas.0908699106>
- Swetnam, T. W., & Betancourt, J. L. (1998). Mesoscale disturbance and ecological response to decadal climatic variability in the American Southwest. *Journal of Climate*, 11, 3128–3147.
- Takahashi, M., Feng, Z., Mikhailova, T. A., Kalugina, O. V., Shergina, O. V., Afanasieva, L. V., Heng, R. K. J., Majid, N. M. A., & Sase, H. (2020). Air pollution monitoring and tree and forest decline in East Asia: A review. *Science of the Total Environment*, 742, 140288. <https://doi.org/10.1016/j.scitotenv.2020.140288>
- Taylor, G. E., Johnson, D. W., & Andersen, C. P. (1994). Air pollution and forest ecosystems: a regional to global perspective. *Ecological Applications*, 4(4), 662–689.
- Thom, D. (2023). Natural disturbances as drivers of tipping points in forest ecosystems under climate change—implications for adaptive management. *Forestry*, 96(3), 305–315.
- Thom, D., Ammer, C., Annighöfer, P., Aszalós, R., Dittrich, S., Hagge, J., ... & Seidl, R. (2023b). Regeneration in European beech forests after drought: the effects of microclimate, deadwood and browsing. *European Journal of Forest Research*, 142(2), 259–273.

- Thom, D., Buras, A., Heym, M., Klemmt, H. J., & Wauer, A. (2023a). Varying growth response of Central European tree species to the extraordinary drought period of 2018–2020. *Agricultural and Forest Meteorology*, *338*, 109506.
- Thom, D., Rammer, W., & Seidl, R. (2017). Disturbances catalyze the adaptation of forest ecosystems to changing climate conditions. *Global Change Biology*, *23*(1), 269–282. <https://doi.org/10.1111/gcb.13506>
- Thomas, R. B., Spal, S. E., Smith, K. R., & Nippert, J. B. (2013). Evidence of recovery of *Juniperus virginiana* trees from sulphur pollution after the Clean Air Act. *Proceedings of the National Academy of Sciences of the United States of America*, *110*(38), 15319–15324. <https://doi.org/10.1073/pnas.1308115110>
- Tolasz, R., Míková, T., Valeriánová, A., & Voženílek, V. (2007). Climate atlas of Czechia. *Czech Hydrometeorological Institute, Prague*, 256.
- Treml, V., Mašek, J., Tumajer, J., Rydval, M., Čada, V., Ledvinka, O., & Svoboda, M. (2022). Trends in climatically driven extreme growth reductions of *Picea abies* and *Pinus sylvestris* in Central Europe. *Global Change Biology*, *28*(2), 557–570. <https://doi.org/10.1111/gcb.15922>
- Trotsiuk, V., Pederson, N., Druckenbrod, D. L., Orwig, D. A., Bishop, D. A., Barker-Plotkin, A., Fraver, S., & Martin-Benito, D. (2018). Testing the efficacy of tree-ring methods for detecting past disturbances. *Forest Ecology and Management*, *425*(October), 59–67. <https://doi.org/10.1016/j.foreco.2018.05.045>
- Trotsiuk, V., Svoboda, M., Janda, P., Mikolas, M., Bace, R., Rejzek, J., ... & Myklush, S. (2014). A mixed severity disturbance regime in the primary *Picea abies* (L.) Karst. forests of the Ukrainian Carpathians. *Forest ecology and management*, *334*, 144-153.
- Trotsiuk, V., Svoboda, M., Weber, P., Pederson, N., Klesse, S., Janda, P., Martin-Benito, D., Mikolas, M., Seedre, M., Bace, R., Mateju, L., & Frank, D. (2016). The legacy of disturbance on individual tree and stand-level aboveground biomass accumulation and stocks in primary mountain *Picea abies* forests. *Forest Ecology and Management*, *373*, 108–115. <https://doi.org/10.1016/j.foreco.2016.04.038>
- Trugman, A. T., Anderegg, L. D., Anderegg, W. R., Das, A. J., & Stephenson, N. L. (2021). Why is tree drought mortality so hard to predict?. *Trends in Ecology & Evolution*, *36*(6), 520-532.
- Tumajer, J., Altman, J., Štěpánek, P., Treml, V., Doležal, J., & Cienciala, E. (2017). Increasing moisture limitation of Norway spruce in Central Europe revealed by forward modelling of tree growth in tree-ring network. *Agricultural and Forest Meteorology*, *247*, 56-64.
- Tumajer, J., Begović, K., Čada, V., Jeníček, M., Lange, J., Mašek, J., Kaczka, R. J., Rydval, M., Svoboda, M., Vlček, L., & Treml, V. (2023). Ecological and methodological drivers

- of non-stationarity in tree growth response to climate. *Global Change Biology*, 29(2), 462–476. <https://doi.org/10.1111/gcb.16470>
- Tuovinen, M., McCarroll, D., Los, S., Grudd, H., & Jalkanen, R. (2009). Spatial and temporal stability of the climatic signal in northern Fennoscandian pine RW and maximum density. *Boreas*, 38(1), 1–12. <https://doi.org/10.1111/j.1502-3885.2008.00046.x>
- Turner, M. G. (2010). Disturbance and landscape dynamics in a changing world. *Ecology*, 91, 2833–2849.
- Turner, M. G. (Ed.). (1987). *Landscape heterogeneity and disturbance*. New York: Springer-Verlag.
- Turner, M. G., Baker, W. L., Peterson, C. J., & Peet, R. K. (1998). Factors influencing succession: lessons from large, infrequent natural disturbances. *Ecosystems*, 1, 511-523.
- Twardosz, R., Walanus, A., & Guzik, I. (2021). Warming in Europe: Recent Trends in Annual and Seasonal temperatures. In *Pure and Applied Geophysics* (Vol. 178, Issue 10, pp. 4021–4032). <https://doi.org/10.1007/s00024-021-02860-6>
- Ulrich, B. (1991). Conclusions from 10 years of research into forest ecosystems and damage to forest. *For Holz*, 46(21), 3-12.
- Vacek, S., Hůnová, I., Vacek, Z., Hejčmanová, P., Podrázský, V., Král, J., Putalová, T., & Moser, W. K. (2015). Effects of air pollution and climatic factors on Norway spruce forests in the Orlické hory Mountains (Czech Republic), 1979–2014. *European Journal of Forest Research*, 134(6), 1127–1142. <https://doi.org/10.1007/s10342-015-0915-x>
- Vacek, S., Podrázský, V., Hejčman, M., & Remeš, J. (2006). Effect of Mg fertilization on yellowing disease of Norway spruce at higher elevations of the Šumava Mts., Czech Republic. *Journal of Forest Science*, 52(10), 474-481.
- Vacek, S., Vacek, Z., Remeš, J., Bílek, L., Hůnová, I., Bulušek, D., Putalová, T., Král, J., & Simon, J. (2017). Sensitivity of unmanaged relict pine forest in the Czech Republic to climate change and air pollution. *Trees - Structure and Function*, 31(5), 1599–1617. <https://doi.org/10.1007/s00468-017-1572-0>
- Vacek, S., Vacek, Z., Ulbrichová, I., Remeš, J., Podrázský, V., Vach, M., ... & Putalová, T. (2019). The effects of fertilization on the health status, nutrition and growth of Norway spruce forests with yellowing symptoms. *Scandinavian Journal of Forest Research*, 34(4), 267-281.
- Vacek, Z., Vacek, S., Prokůpková, A., Bulušek, D., Podrázský, V., Hůnová, I., Putalová, T., & Král, J. (2020). Long-term effect of climate and air pollution on health status and growth of *Picea abies* (L.) Karst. peaty forests in the Black Triangle region. *Dendrobiology*, 83, 1–19. <https://doi.org/10.12657/denbio.083.001>
- Venegas-González, A., Juñent, F. R., Gutiérrez, A. G., & Tomazello Filho, M. (2018). Recent radial growth decline in response to increased drought conditions in the northernmost

- Nothofagus populations from South America. *Forest Ecology and Management*, 409, 94–104.
- Vermote, Eric; NOAA CDR Program. (2019): NOAA Climate Data Record (CDR) of AVHRR Normalized Difference Vegetation Index (NDVI), Version 5. [indicate subset used]. NOAA National Centers for Environmental Information. <https://doi.org/10.7289/V5ZG6QH9>. Accessed [date].
- Vicente-Serrano, S. M., Beguería, S., & López-Moreno, J. I. (2010). A multiscale drought index sensitive to global warming: The standardized precipitation evapotranspiration index. *Journal of Climate*, 23(7), 1696–1718. <https://doi.org/10.1175/2009JCLI2909.1>
- Vicente-Serrano, S. M., Tomas-Burguera, M., Beguería, S., Reig, F., Latorre, B., Peña-Gallardo, M., Luna, M. Y., Morata, A., & González-Hidalgo, J. C. (2017). A high resolution dataset of drought indices for Spain. *Data*, 2(3). <https://doi.org/10.3390/data2030022>
- Vitali, V., Büntgen, U., & Bauhus, J. (2017). Silver fir and Douglas fir are more tolerant to extreme droughts than Norway spruce in south-western Germany. *Global Change Biology*, 23(12), 5108–5119. <https://doi.org/10.1111/gcb.13774>
- Vitasse, Y., Bottero, A., Cailleret, M., Bigler, C., Fonti, P., Gessler, A., ... & Wohlgemuth, T. (2019). Contrasting resistance and resilience to extreme drought and late spring frost in five major European tree species. *Global Change Biology*, 25(11), 3781–3792.
- Viviroli, D., Dürr, H. H., Messerli, B., Meybeck, M., & Weingartner, R. (2007). Mountains of the world, water towers for humanity: Typology, mapping, and global significance. *Water resources research*, 43(7).
- von Arx, G., & Carrer, M. (2014). Roxas -A new tool to build centuries-long tracheid-lumen chronologies in conifers. *Dendrochronologia*, 32(3), 290–293. <https://doi.org/10.1016/j.dendro.2013.12.001>
- von Arx, G., Carrer, M., Crivellaro, A., De Micco, V., Fonti, P., Lens, F., ... & Sass-Klaassen, U. (2021). Q-NET—a new scholarly network on quantitative wood anatomy. *Dendrochronologia*, 70, 125890.
- Von Arx, G., Crivellaro, A., Prendin, A. L., Čufar, K., & Carrer, M. (2016). Quantitative wood anatomy—practical guidelines. *Frontiers in Plant Science*, 7(JUNE2016), 1–13. <https://doi.org/10.3389/fpls.2016.00781>
- Wang, F., Arseneault, D., Boucher, É., Galipaud Gloaguen, G., Deharte, A., Yu, S., & Trouchechout, N. (2020). Temperature sensitivity of blue intensity, maximum latewood density, and ring width data of living black spruce trees in the eastern Canadian taiga. *Dendrochronologia*, 64(October). <https://doi.org/10.1016/j.dendro.2020.125771>
- Warren, W.G. (1980). On removing the growth trend from dendrochronological data. *Tree-ring Bull.* 40: 35–44.

- Weiner, J., Thomas, S.C. (2001). The nature of tree growth and the “age-related decline in forest productivity”. *Oikos*, 94 (2), 374–376.
- Wermelinger, B. (2004). Ecology and management of the spruce bark beetle *Ips typographus*—a review of recent research. *Forest ecology and management*, 202(1-3), 67-82.
- Wigley, T. M., Briffa, K. R., & Jones, P. D. (1984). On the average value of correlated time series, with applications in dendroclimatology and hydrometeorology. *Journal of Applied Meteorology and Climatology*, 23(2), 201-213.
- Wilczyński, S. (2006). The variation of RWs of Scots pine (*Pinus sylvestris* L.) affected by air pollution. *European Journal of Forest Research*, 125(3), 213–219.
<https://doi.org/10.1007/s10342-005-0106-2>
- Wilmking, M., D'arrigo, R., Jacoby, G. C., & Juday, G. P. (2005). Increased temperature sensitivity and divergent growth trends in circumpolar boreal forests. *Geophysical Research Letters*, 32(15).
- Wilmking, M., van der Maaten-Theunissen, M., van der Maaten, E., Scharnweber, T., Buras, A., Biermann, C., ... & Trouillier, M. (2020). Global assessment of relationships between climate and tree growth. *Global Change Biology*, 26(6), 3212-3220.
- Wilson, R., & Elling, W. (2004). Temporal instability in tree-growth/climate response in the Lower Bavarian Forest region: Implications for dendroclimatic reconstruction. *Trees - Structure and Function*, 18(1), 19–28. <https://doi.org/10.1007/s00468-003-0273-z>
- Wilson, R., Anchukaitis, K., Briffa, K. R., Büntgen, U., Cook, E., D'Arrigo, R., Davi, N., Esper, J., Frank, D., Gunnarson, B., Hegerl, G., Helama, S., Klesse, S., Krusic, P. J., Linderholm, H. W., Myglan, V., Osborn, T. J., Rydval, M., Schneider, L., ... Zorita, E. (2016). Last millennium northern hemisphere summer temperatures from tree rings: Part I: The long term context. *Quaternary Science Reviews*, 134, 1–18.
<https://doi.org/10.1016/j.quascirev.2015.12.005>
- Wilson, R., Wilson, D., Rydval, M., Crone, A., Büntgen, U., Clark, S., Ehmer, J., Forbes, E., Fuentes, M., Gunnarson, B. E., Linderholm, H. W., Nicolussi, K., Wood, C., & Mills, C. (2017). Facilitating tree-ring dating of historic conifer timbers using Blue Intensity. *Journal of Archaeological Science*, 78, 99–111. <https://doi.org/10.1016/j.jas.2016.11.011>
- WinDendro, 2023. WinDENDRO: an image analysis system for annual tree-rings analysis.
- Wood, S. N., Goude, Y., & Shaw, S. (2015). Generalized additive models for large data sets. *Journal of the Royal Statistical Society Series C: Applied Statistics*, 64(1), 139-155.
- Wood, SN. (2011). Fast stable restricted maximum likelihood and marginal likelihood estimation of semiparametric generalised linear models. *Journal of the Royal Statistical Society: Series B (Statistical Methodology)*, 73(1), pp.3-36.

- Wright, E. A., Lucas, P. W., Cottam, D. A., & Mansfield, T. T. (1987). Physiological responses to SO₂, NO_x and O₃: implications for drought resistance. Direct effects of dry and wet deposition on forest ecosystems—in particular canopy interaction. *CEC Air Pollut. Res. Rep.*, *4*, 187-200.
- Xu, P., Zhou, T., Yi, C., Fang, W., Hendrey, G., & Zhao, X. (2018). Forest drought resistance distinguished by canopy height. *Environmental Research Letters*, *13*(7), 075003.
- Zang, C. S., Buras, A., Esquivel-Muelbert, A., Jump, A. S., Rigling, A., & Rammig, A. (2020). Standardized drought indices in ecological research: Why one size does not fit all. *Global Change Biology*, *26*(2), 322-324.
- Zang, C., & Biondi, F. (2015). Treeclim: An R package for the numerical calibration of proxy-climate relationships. *Ecography*, *38*(4), 431–436. <https://doi.org/10.1111/ecog.01335>
- Zemanová, L., Trotsiuk, V., Morrissey, R. C., Bače, R., Mikoláš, M., & Svoboda, M. (2017). Old trees as a key source of epiphytic lichen persistence and spatial distribution in mountain Norway spruce forests. *Biodiversity and Conservation*, *26*, 1943-1958.
- Zhou, M. L., Ma, J. T., Zhao, Y. M., Wei, Y. H., Tang, Y. X., & Wu, Y. M. (2012). Improvement of drought and salt tolerance in *Arabidopsis* and *Lotus corniculatus* by overexpression of a novel DREB transcription factor from *Populus euphratica*. *Gene*, *506*(1), 10–17. <https://doi.org/10.1016/j.gene.2012.06.089>
- Zielonka, T., Holeksa, J., Fleischer, P., & Kapusta, P. (2010). A tree-ring reconstruction of wind disturbances in a forest of the Slovakian Tatra Mountains, Western Carpathians. *Journal of Vegetation Science*, *21*(1), 31-42.

APPENDIX A

APPENDIX A contains the additional supporting materials for **Subsection 3.2/ 4.1/ 5.1**.

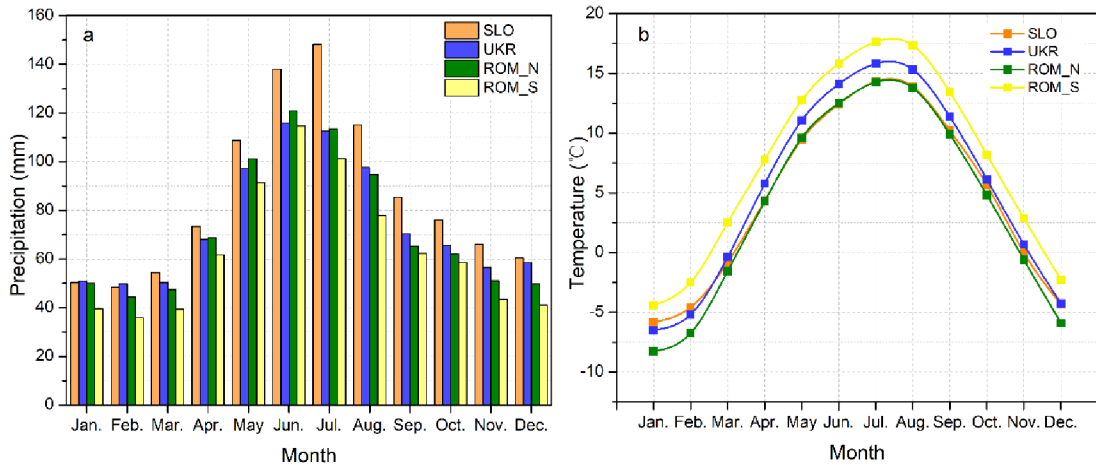


Fig. A1. Monthly climate information for the Carpathians Mountains. a) multi-year average of the monthly total precipitation for the 1901-2013 period; b) multi-year average of monthly mean temperature for the 1901-2013 period. The climate data represent the relevant CRU 0.5° TS 4.03 gridded monthly datasets covering 1901-2013 (available dataset when conducting this study) for different sub-regions, including the High Tatras (SLO) in the western Carpathians, Gorgany (UKR) and Calimani (ROM_N) in the eastern Carpathians, and Făgăraș (ROM_S) in the southern Carpathians.

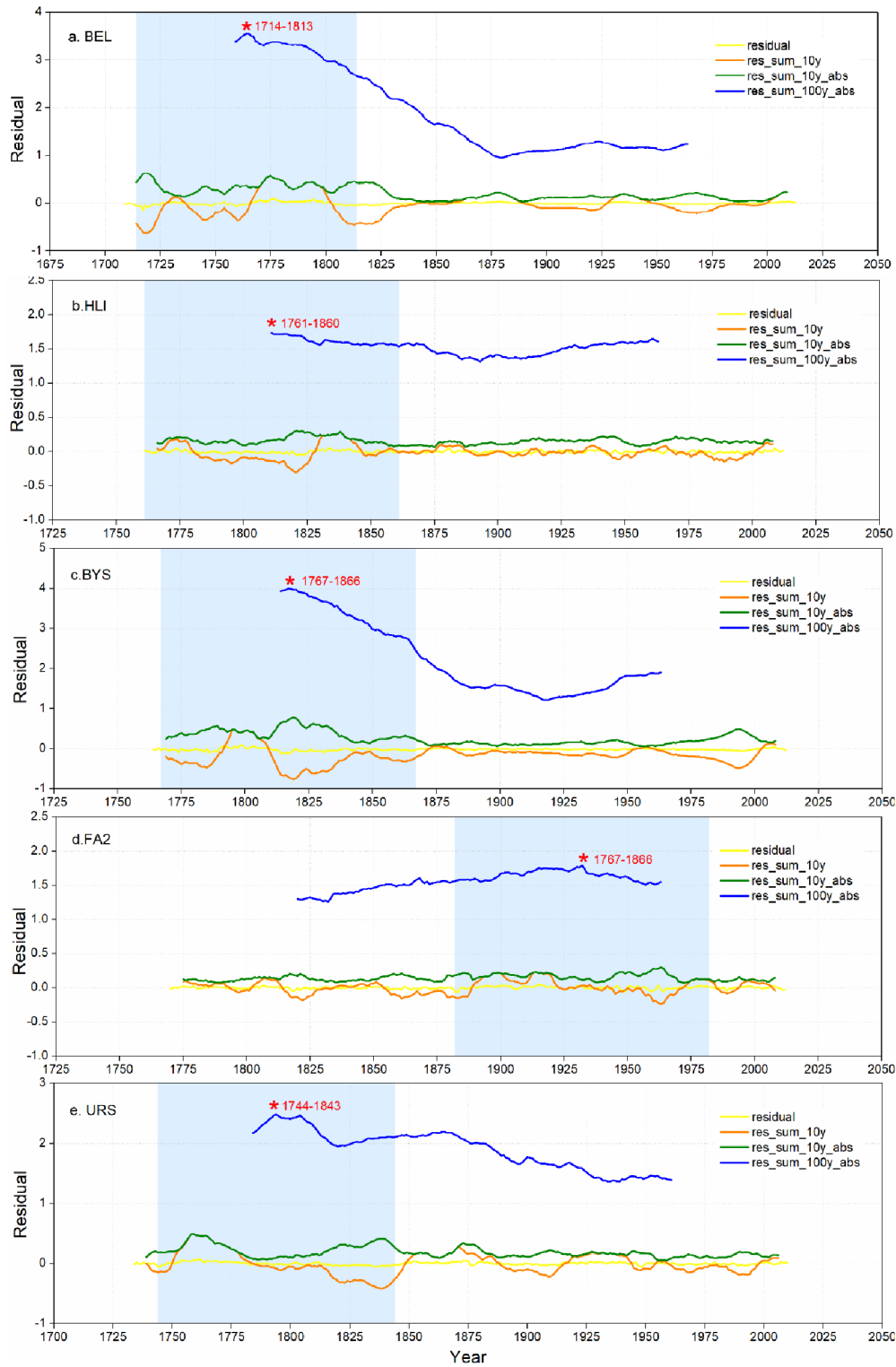


Fig. A2. Residual series of disturbance-affected (RW_dis) and disturbance-corrected (RW_dis_CID) chronologies. residual = RW_dis - RW_dis_CID; res_sum_10 = decadal residual sum; res_sum_10y_abs = absolute decadal residual sum; res_sum_100y_abs = absolute centennial residual sum. The period with the highest 'res_sum_100y_abs' was defined as 'severe disturbance period' (blue block) used in Fig. 3.

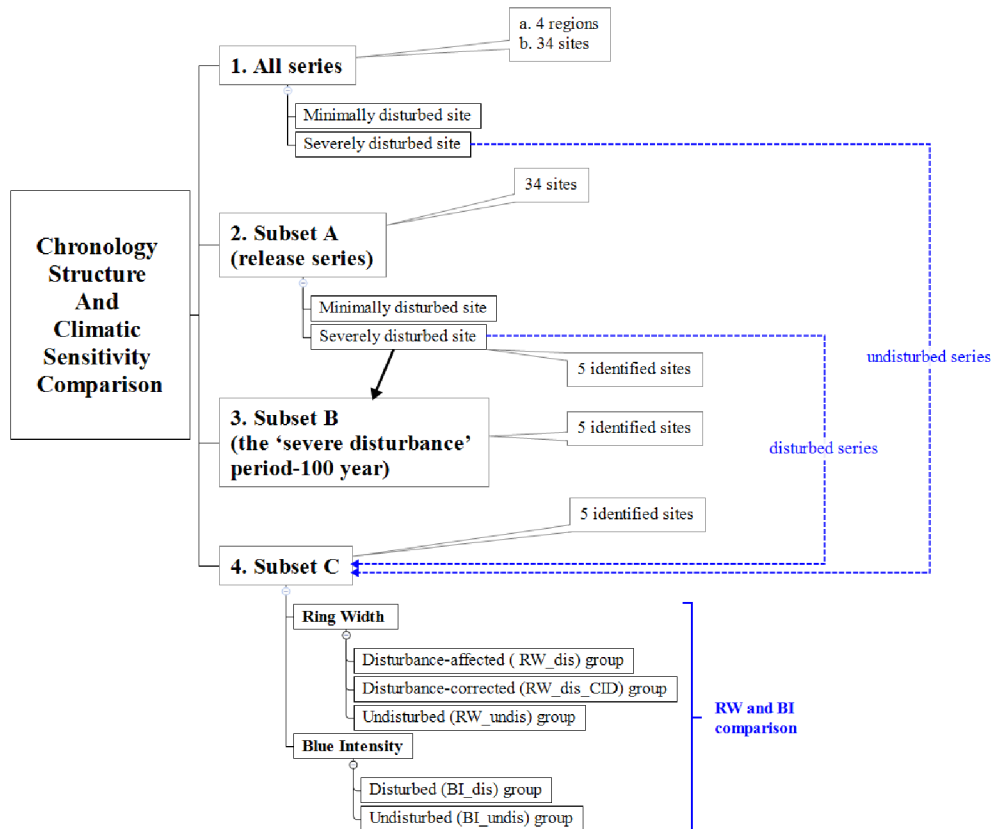


Fig. A3. Sample selection procedure for subsets A, B, and C. Steps 1-4 relate to figures 2-5 for chronology structure comparison, respectively. Dashed blue lines indicate the sources of 30 disturbed / undisturbed series of subset C for the purpose of different tree-ring parameters comparison. ‘5 identified sites’ refer to the five severely disturbed sites identified by the curve intervention detection (CID) method, incl., BEL, HLI, BYS, FA2, URS. Subset A only contains series with at least one detected release event whereas subset B only contains series with the disturbance event identified within the 100-year ‘severe disturbance’ period displayed in Fig. 3. Subset C is the generic term for the 30-series group pairs for ring width and blue intensity comparison.

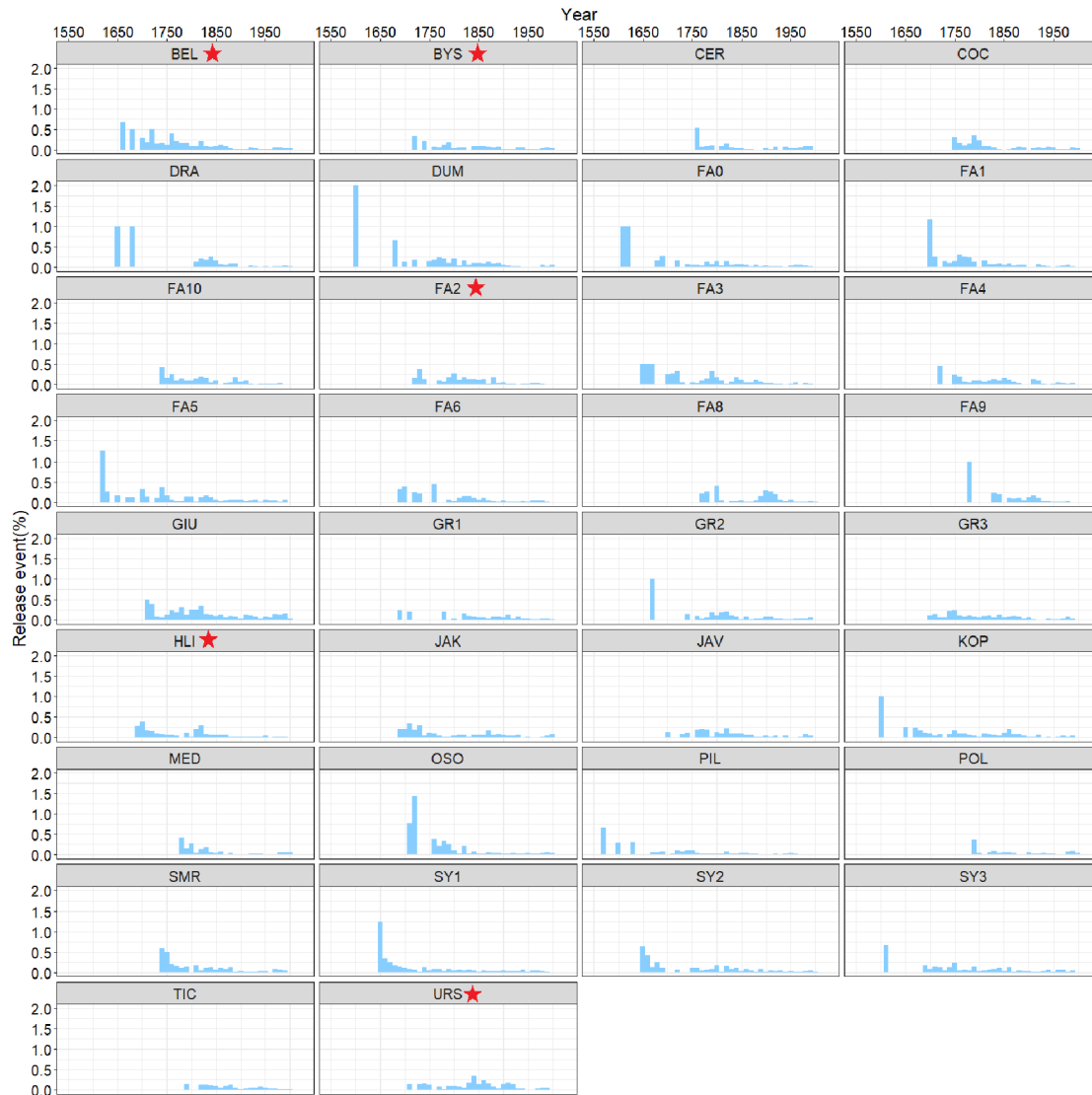


Fig. A4. Release history for all studied sites. Release event (%) was calculated using the decadal number of release events and replication [release event (%) = decadal number of release events / decadal averaged replication]. Calculation was based on release history of all series in each site. Red stars mark sites classified as ‘severely disturbed’ and selected for RW / BI disturbance trends assessment.

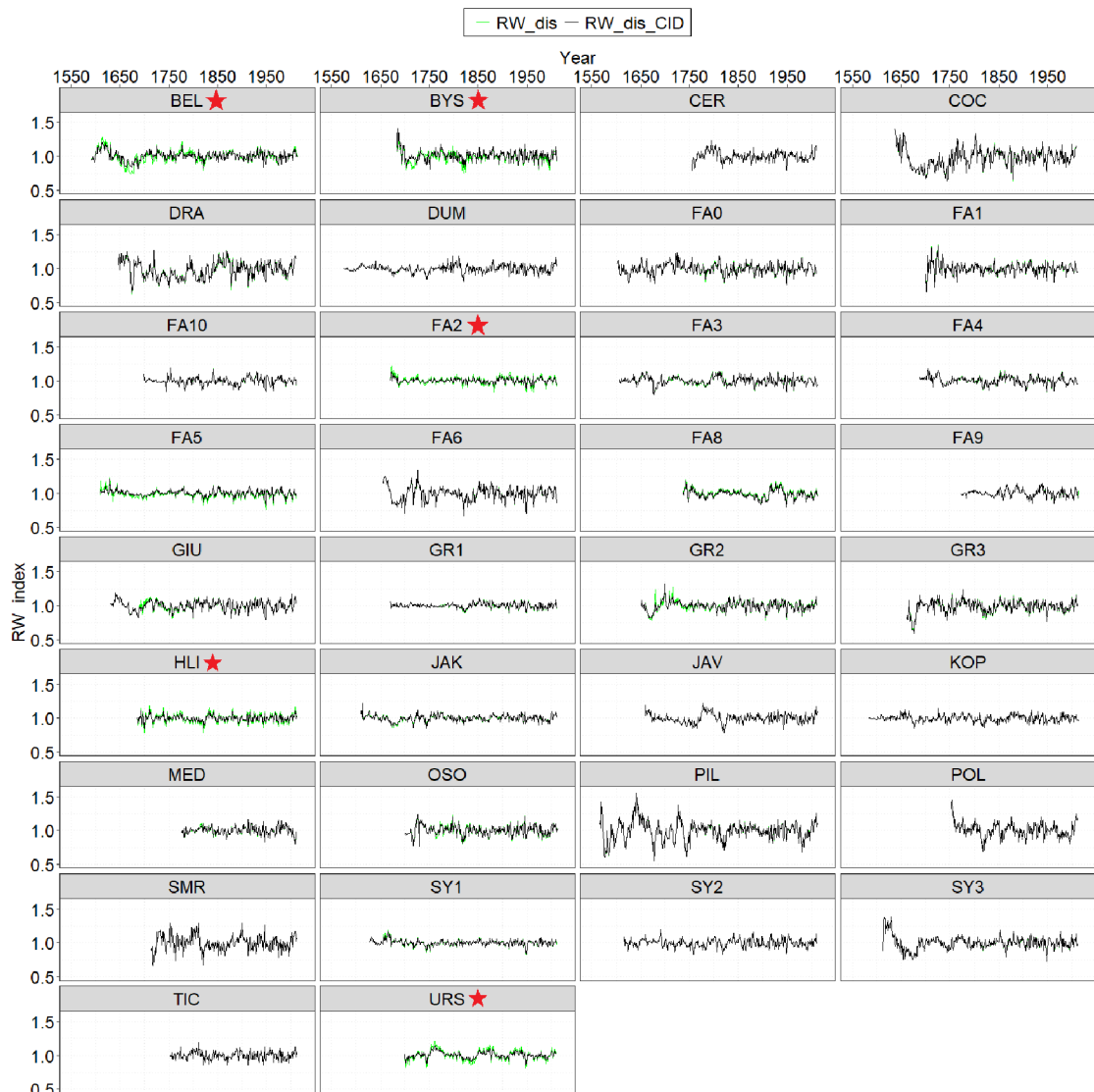


Fig. A5. Site-level (subset A) RW (RW) chronology structure comparison between disturbance-affected (RW_dis) and disturbance-corrected (RW_dis_CID) chronologies. Chronologies were developed only using disturbance-affected released series from each site. The majority of the green curve (RW_dis) and black curve (RW_dis_CID) are overlapped representing the similar growth trends. The non-overlapped parts (where the green curve overflowed from the overlapped part) indicate the disturbance trends which have been detected by curve intervention detection (CID) method. Red stars mark the selected detected severely disturbed sites for further comparison.

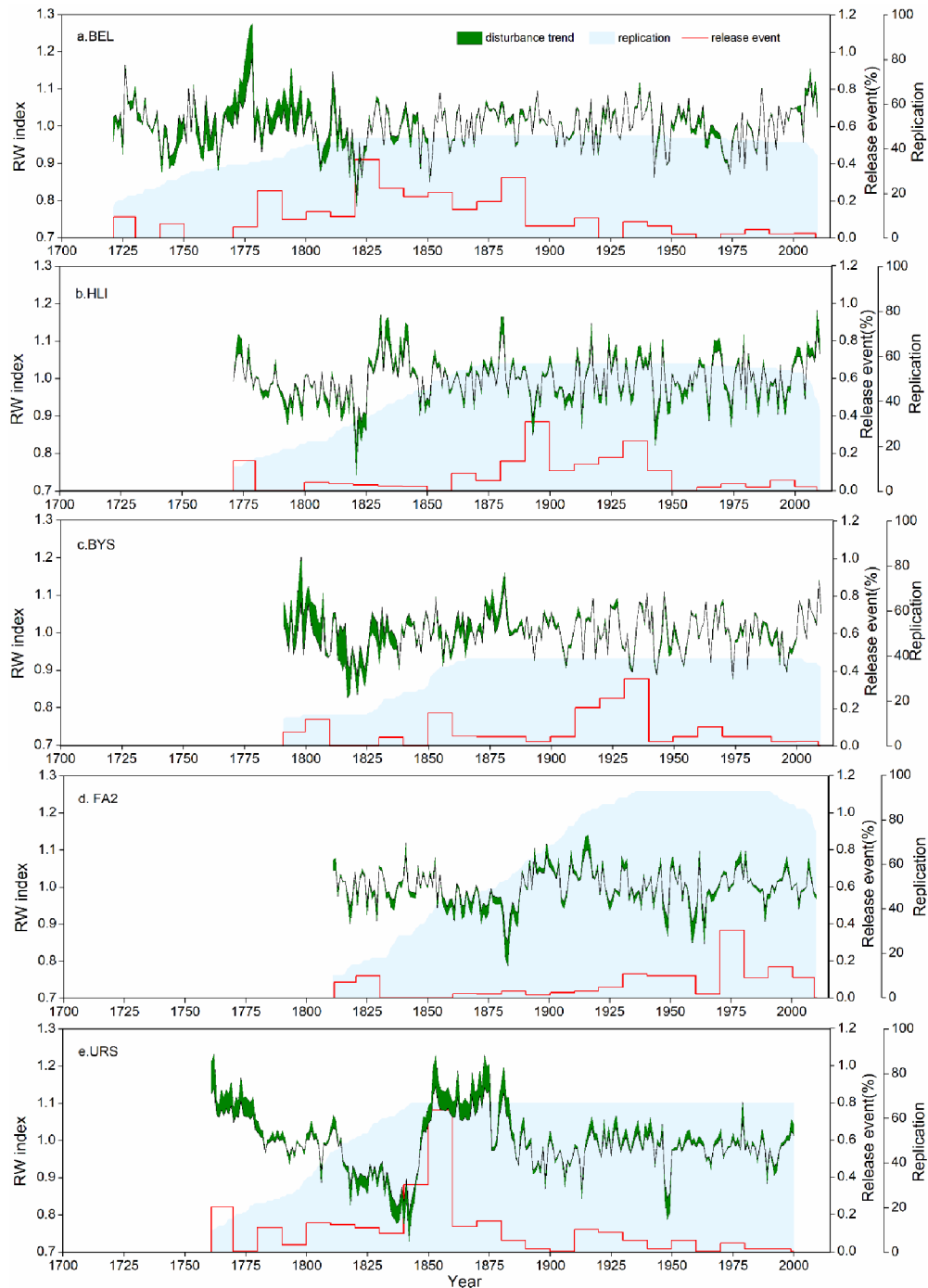


Fig. A6. RW (RW) chronology structure comparison between disturbance-affected (RW_dis) and disturbance-corrected (RW_dis_CID) chronologies composed only of series with release events which occurred within the ‘severe disturbance’ period (indicated in Fig. 3) for five sites classified as ‘severely disturbed’, highlighting the presence of disturbance trends (Subset B). Green shading indicates disturbance trends identified by the CID method and represents the difference between the RW_dis and RW_dis_CID chronologies. Release event (%) (red line) was calculated using the decadal number of release events and replication [release event (%) = decadal number of release events / decadal average replication]. Blue shading represents series replication. All chronologies were truncated to the period with replication ≥ 10 series.

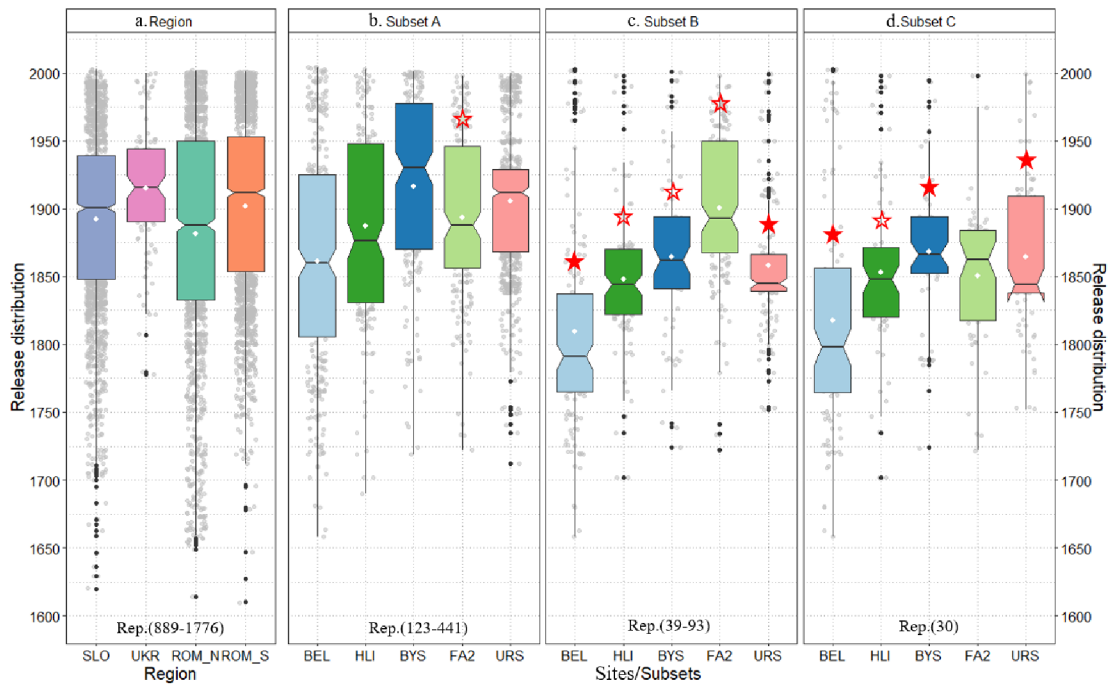


Fig. A7. Temporal release distribution for different sample subsets. The distributions represent the start year of all release events within each site / region. Changes in the distribution timeline show the coupling between timing of ‘disturbance trends’ (based on the RW_dis / RW_dis_CID comparison of each subset) and the release event disturbance history in Figs. 2-4. The filled stars mark ‘highly coupled sites/regions’; the unfilled stars mark the ‘moderately coupled sites/regions’. ‘Rep.’ represents the series replication range of each group.

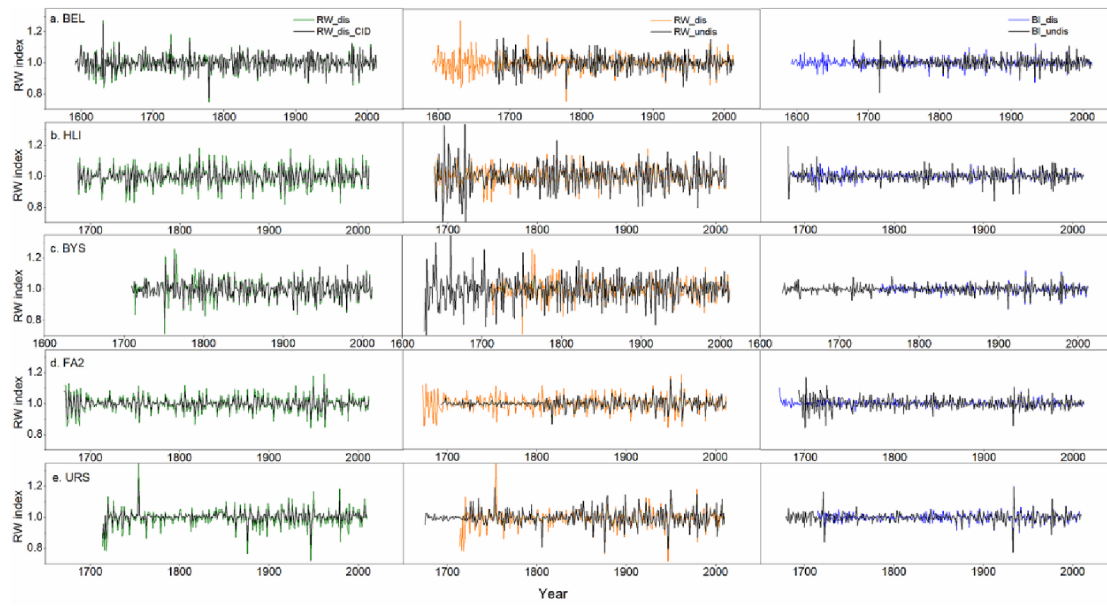


Fig. A8. High frequency (first-difference) site level RW (RW) and blue intensity (BI) chronology structure comparison between three RW subgroups (RW_dis; RW_dis_CID; RW_undis,) and two BI subgroups (BI_dis; BI_undis).

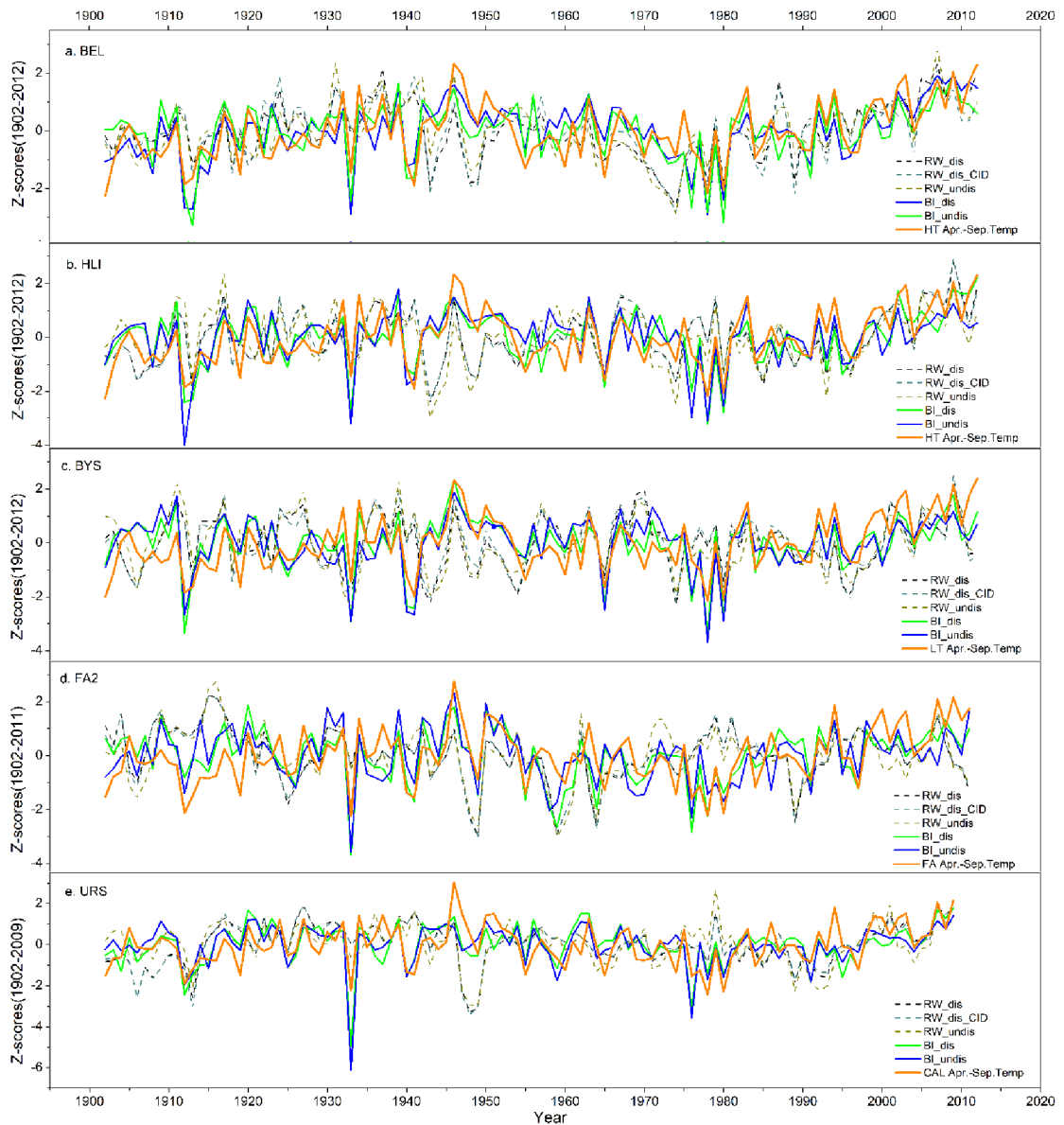


Fig. A9. Seasonal temperature (April - September) timeseries and site-level chronology structure comparisons among three RW subgroups (RW_dis; RW_dis_CID; RW_undis) and two BI subgroups (BI_dis; BI_undis) for five sites classified as ‘severely disturbed’. Temperature data correspond with the location of the respective site. HT, LT, FA and CAL represent High Tatras, Low Tatras, Fagaras and Calimani mountains, separately. Correlation coefficients between climate and chronologies are listed in Table. 3.

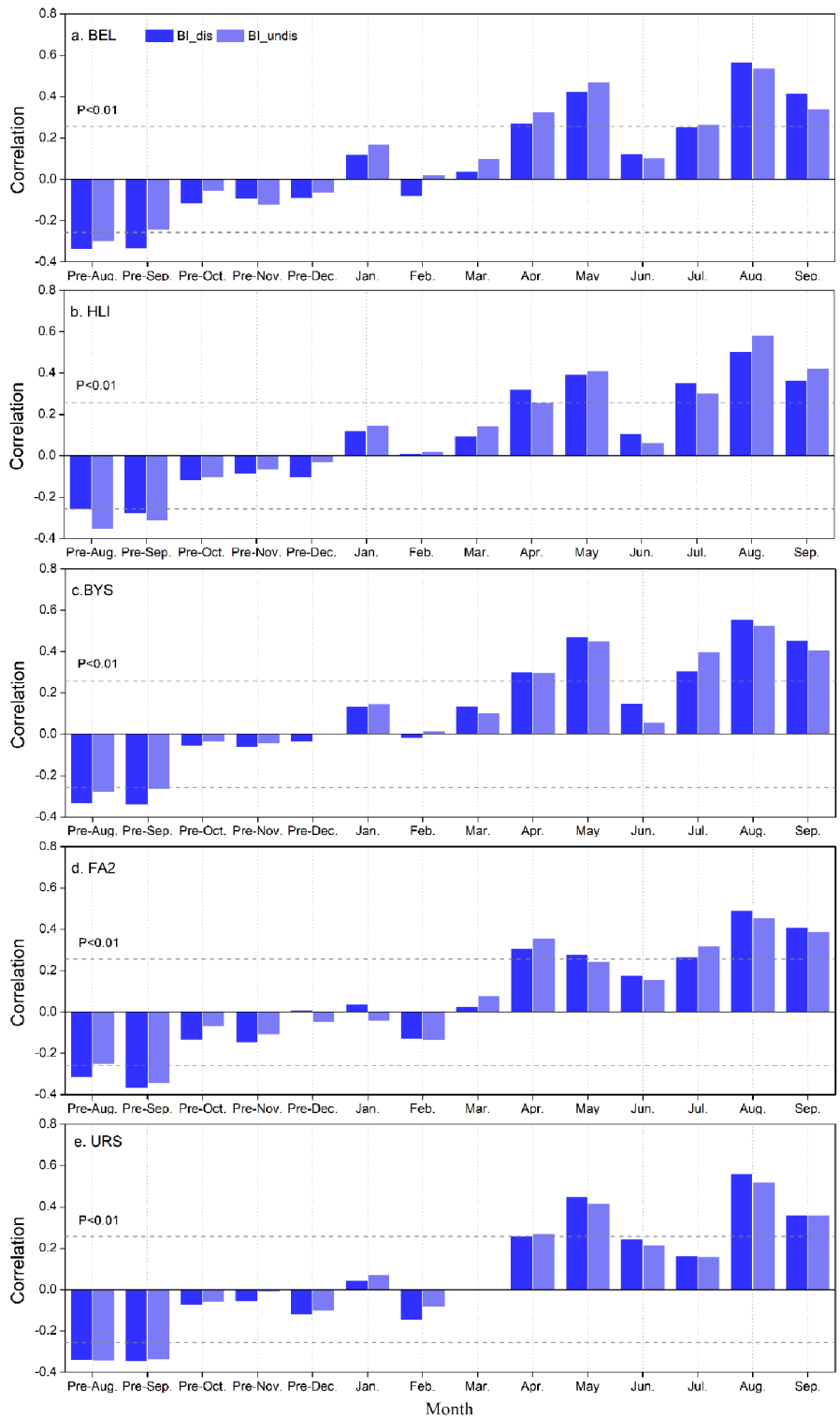


Fig. A10. Site level temperature response assessment between BI high resolution (first difference) chronologies from five sites characterized as ‘severely disturbed’, and monthly mean temperature for disturbed (dis) and undisturbed (undis) subsets for the instrumental period 1991-2013. BI chronologies represent BI series divided into the disturbed (BI_dis) and undisturbed (BI_undis) groups according to the CID disturbance assessment of RW series.

Region	Site name	Site code	Mean longitude (°)	Mean latitude (°)	Mean elevation (m a.s.l)	No. of series	No. of released series	No. of release events
Slovakia	Bielovodska dolina	BEL	20.12	49.19	1343	373	162	351
	Hlina	HLI	19.90	49.19	1432	538	125	190
	Koprova dolina	KOP	19.98	49.17	1430	449	139	249
	Osobita	OSO	19.72	49.26	1363	389	127	252
	Ticha dolina	TIC	19.95	49.22	1413	534	119	188
	Bystra	BYS	19.47	49.17	1409	462	132	194
	Dumbier	DU M	19.66	48.95	1495	517	211	383
	Janosikova Kolkaren	JAK	19.20	49.01	1308	672	210	363
	Javorova	JAV	20.16	49.22	1438	236	103	203
	Zadne Medodoly	MED	20.19	49.23	1499	216	80	120
	Pilsko	PIL	19.32	49.52	1328	335	117	216
	Polana	POL	19.49	48.64	1379	378	156	225
Smrekovica	SMR	19.43	48.95	1386	299	106	184	
South Romania	Arpaselu	FA0	24.63	45.64	1505	320	97	142
	Sambata	FA1	24.80	45.64	1496	332	126	200
	Ucisoara	FA2	24.72	45.64	1425	372	123	220
	Vistea Mare	FA3	24.74	45.64	1460	318	122	217
	Ucea Mare	FA4	24.70	45.64	1458	328	148	248
	Arpasul	FA5	24.67	45.63	1450	370	136	262
	Doamnei	FA6	24.59	45.63	1515	314	110	189
	Boia Mica	FA8	24.43	45.55	1464	379	137	236
	Capra	FA9	24.61	45.57	1573	369	80	115
	Belia	FA1 0	24.97	45.62	1476	370	151	252
North Romania	Cerbului	CER	25.28	47.14	1629	101	41	69
	Cocos	COC	25.23	47.07	1570	309	84	125
	Dragus	DRA	25.20	47.07	1586	124	42	70
	Ursul	URS	25.26	47.11	1577	889	441	794
	Giumalau	GIU	25.47	47.44	1428	2117	664	1157
Ukraine	Gropha1	GR1	23.93	48.60	1378	459	155	237
	Gropha2	GR2	23.90	48.61	1354	393	148	242
	Gropha3	GR3	23.92	48.61	1320	390	143	264
	Syvulya1	SY1	24.09	48.56	1426	537	201	395
	Syvulya2	SY2	24.16	48.54	1355	384	125	208
	Syvulya3	SY3	24.11	48.50	1298	388	117	235
Total	34 sites	-	-	-	-	14961	5178	8995

Table A1. General information for all studied sites. ‘No. of series’ refers to the number of measured time series for each site / region. ‘No. of released series’ refers to the number of

measured time series of all released cores in each site / region. 'No. of release events' refers to the number of release events that occurred in each site / region calculated from all released cores.

APPENDIX B

APPENDIX B contains the additional supporting materials for **Subsection 3.3/ 4.2/ 5.2.**

Table B1. Positive (Pos) and negative (Neg) extreme years detected by pointer year analysis.

A. RW

NB	Neg	1956	1979	1980	1981	1982			
	p-value	0.01011	0.01037	0.00013	0.00222	0.01818			
	Pos	1999	2001						
	p-value	0.97644	0.97519						
CK	Neg	1956	1974	1978	1980	1982	1983	1984	1986
	p-value	0.00292	0.02222	0.00619	0.00054	0.01705	0.01505	0.02066	0.00256
	Pos	2004	2007	2009	2012				
	p-value	0.99710	0.99341	0.99827	0.98361				
SUO	Neg	1948	1974	1980	1984	1995	1996	2003	
	p-value	0.01032	0.00540	0.00112	0.00765	0.01455	0.02178	0.01464	
	Pos	1934	1959	1963					
	p-value	0.98938	0.97797	0.99639					
SM	Neg	1948	1965	1971	1974	1980	1995	1996	
	p-value	0.00275	0.00571	0.01930	0.00290	0.00176	0.01855	0.00084	
	Pos	2009	2012	2018					
	p-value	0.97690	0.99810	0.99576					
PIL	Neg	1980	1984	1985					
	p-value	0.00003	0.00151	0.02212					
	Pos	1946							
	p-value	0.98789							
SLO	Neg	1971	1973	1974	1980	1984			
	p-value	0.02098	0.02151	0.01069	0.00470	0.02235			
	Pos	1946	1953	1954	1979				
	p-value	0.99596	0.97883	0.98492	0.98590				

B. BI

NB	Neg	1962	1967	1976	1978	2001			
	p-value	0.0208	0.0213	0.0159	0.0000	0.0065			
	Pos	5	4	7	1	1			
	p-value	/	/	/	/	/			
CK	Neg	1912	1972	1974	1976	1978	1983	1986	1988

	p-value	0.0028	0.0033	0.0154	0.0152	0.0009	0.0074	0.0000	0.0215	
		8	9	1	5	2	4	1	8	
	Pos	/								
	p-value	/								
SUO	Neg	1924	1977	1978	1980	1982	1984	1987	1993	2003
	p-value	0.0154	0.0216	0.0042	0.0051	0.0242	0.0007	0.0158	0.0148	0.0140
		5	0	9	6	4	9	3	2	9
	Pos	1934								
	p-value	0.9852								
		8								
SMR	Neg	1948	1976	1978	1984	1995				
	p-value	0.0121	0.0196	0.0139	0.0074	0.0010				
		6	7	5	5	1				
	Pos	2012	2015	2016	2017	2018	2019			
	p-value	0.9883	0.9842	0.9910	0.9949	0.9976	0.9976			
		9	3	2	8	1	1			
PIL	Neg	1978	1980	1984	1987	1988				
	p-value	0.0239	0.0000	0.0029	0.0136	0.0021				
		8	0	8	3	0				
	Pos	/								
	p-value	/								
SLO	Neg	1940	1976	1978	1980					
	p-value	0.0049	0.0005	0.0000	0.0013					
		2	0	3	4					
	Pos	1963								
	p-value	0.9754								
		4								

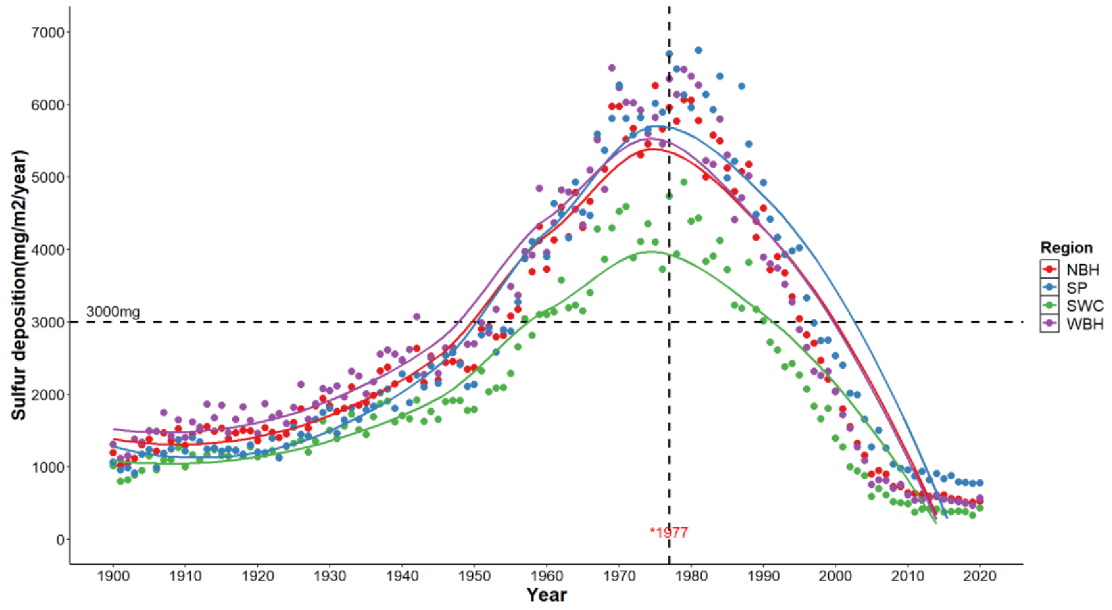
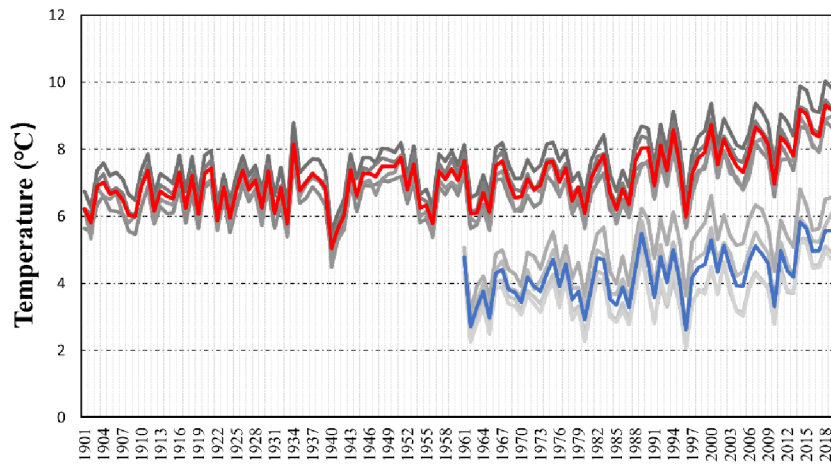


Fig. B1. Long-term trends of the modelled total sulphur deposition for the four studied locations during the 1900-2020 period. This dataset was extracted from the 1900-2050 EMEP MSC-W model. Vertical dashed lines mark the year with the highest average deposition.

A. Temperature



B. Precipitation

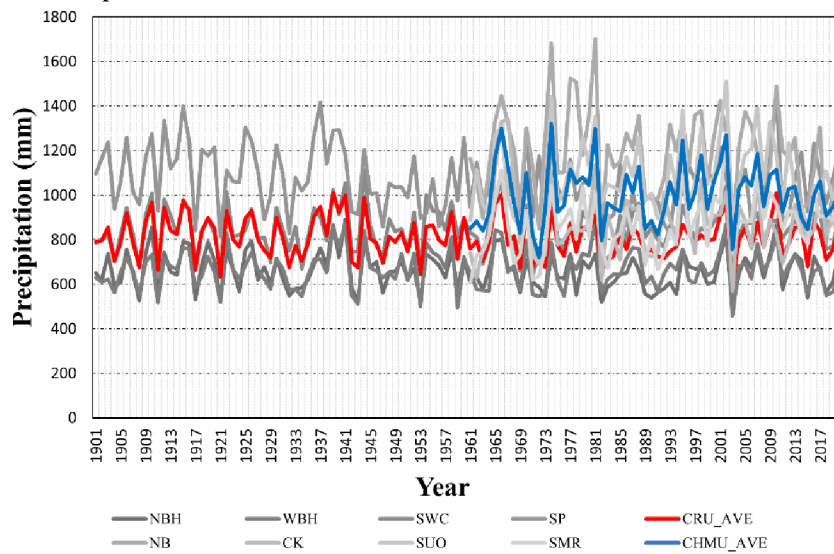
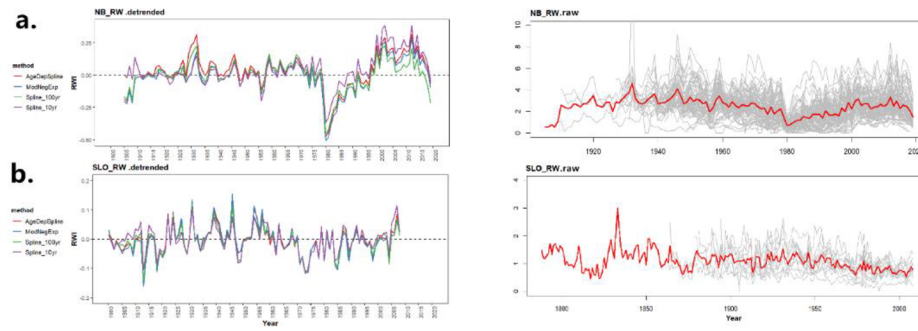


Fig. B2. Variability and trends of two sets of temperature and precipitation datasets. CRU is the Climate Research Unit TS 4.07 dataset, CHMU is the spatially interpolated meteorological station dataset of the Czech Hydrometeorological Institute. The climatic series are shown for individual sites (shades of grey) along with average conditions for all locations (AVE).

A. Ring Width



B. Blue Intensity

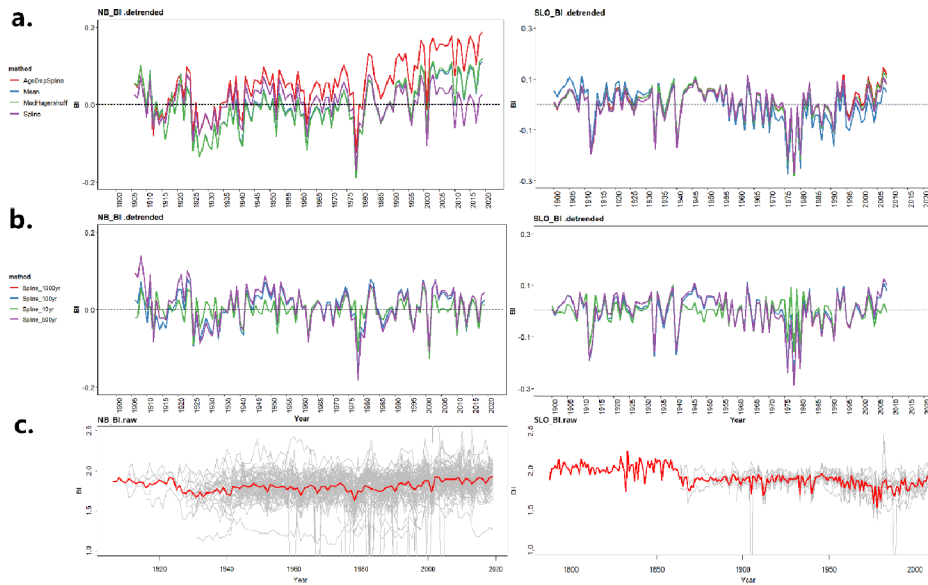


Fig. B3. Detrending method comparison for RW / BI tree ring data. For RW, three detrending methods were compared, including ‘ModNegExp’ (a modified negative exponential curve), ‘AgeDepSpline’ (an age-dependent spline), and ‘Spline’ (a smoothing spline with a 50% frequency response of 10 and 100 years). RW series were detrended using power-transformed data and residuals were computed via subtraction. For BI, the method ‘Mean’ was also included, representing a linear function through the mean with zero slope (B.(a)). Additionally, the ‘Spline’ method was used to compare smoothing splines with varying flexibility (incl. a 50% frequency response of 10, 100, 500, and 1000 years) (B.(b)). BI data were detrended using inverted BI series and residual index values were computed via subtraction. ‘raw’ represents raw measurement series without the application of any detrending method. The comparison shows that there were no major differences between the ‘AgeDepSpline’ and ‘ModNegExp’ methods for RW, while the smoothing spline flexibility influenced the retention of longer-term trends. We decided to opt for the negative exponential curve to detrend RW series in this study. As there were also no major difference between the various methods explored for detrending BI series, we opted for the method ‘spline’ with a very inflexible smoothing spline (with a 50% frequency response of 500 years) intended to represent a negative linear trend.

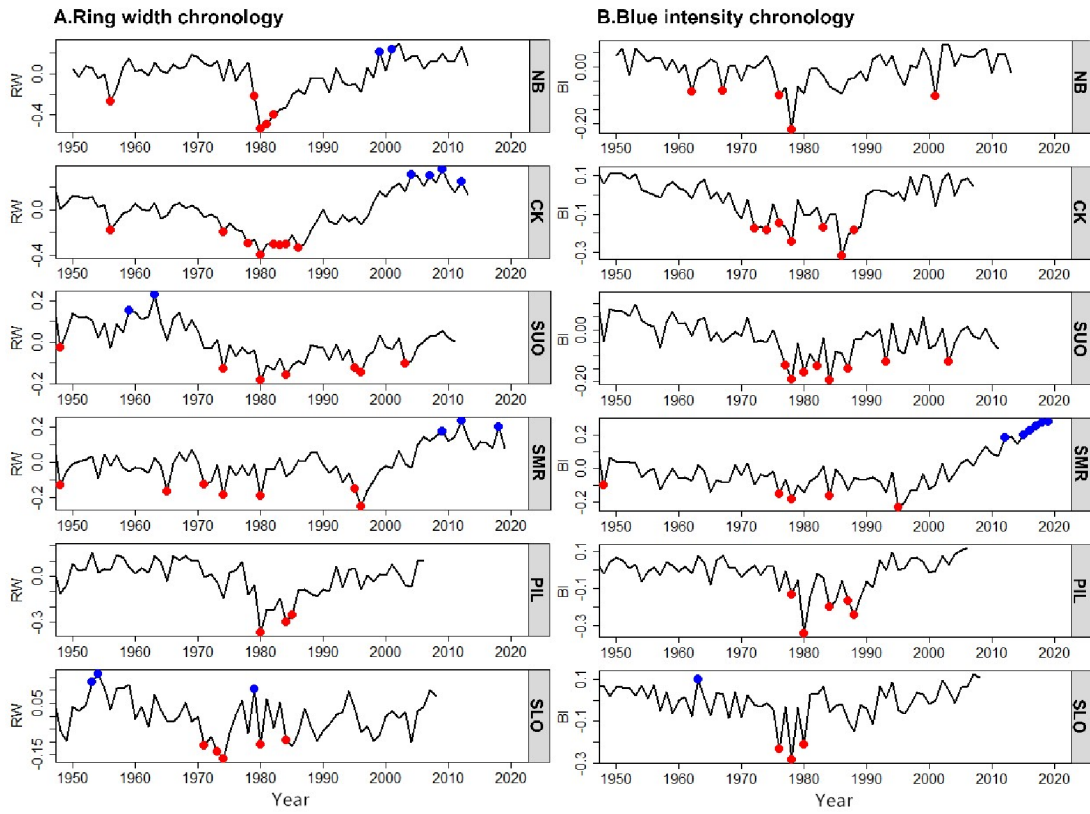


Fig. B4. Positive (Pos) and negative (Neg) extreme years detected by pointer year analysis performed for RW and BI chronologies.

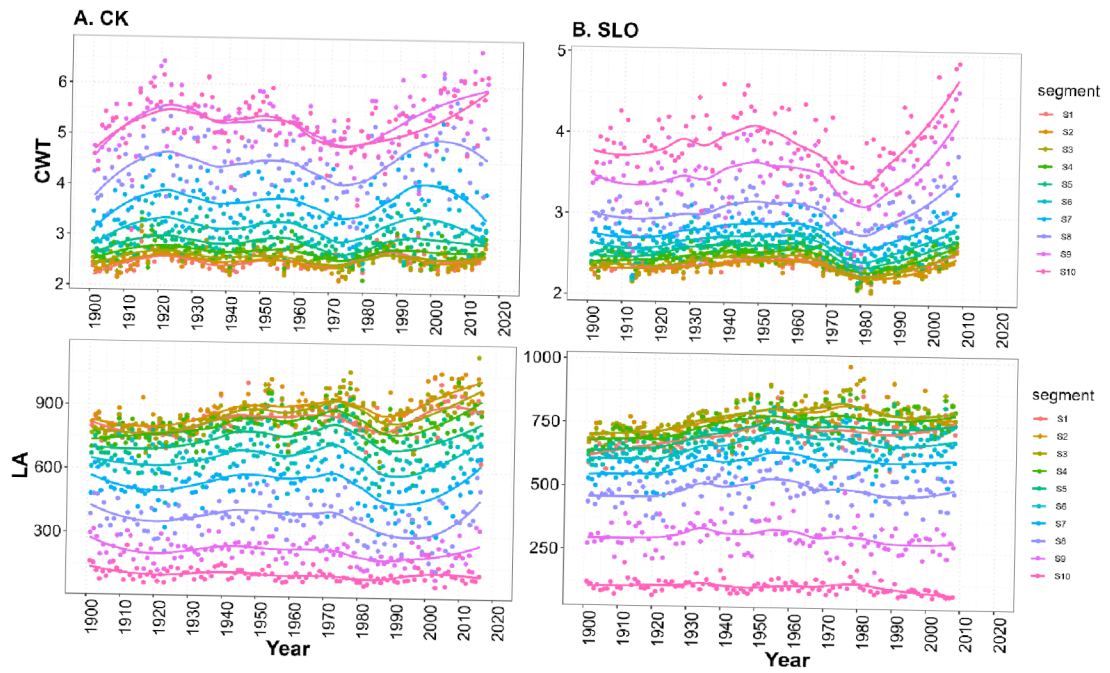


Fig. B5. Long-term trends of cell wall thickness (CWT) and lumen area (LA) of segments 1-10 (form earlywood to latewood) for site CK and SLO. Units of CWT and LA are μm . Series are truncated before 1900.

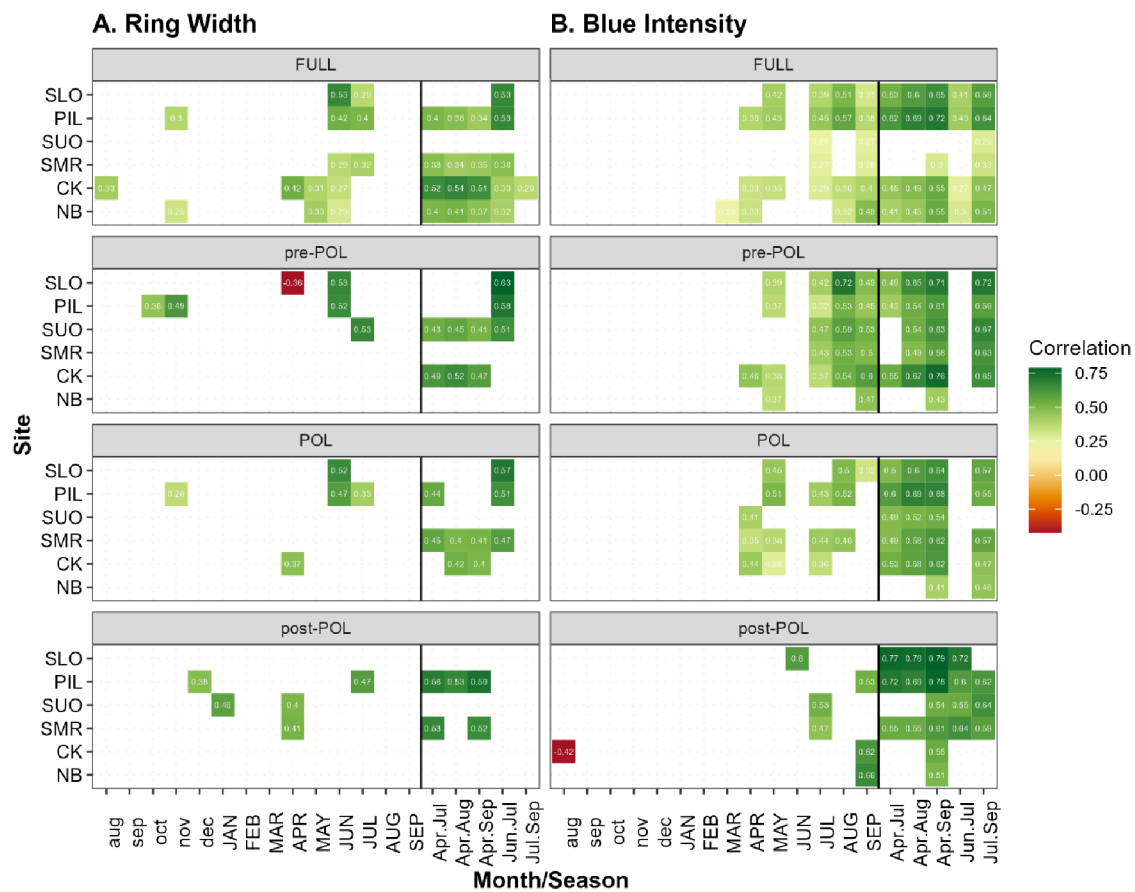


Fig. B6. Growth climate correlations between different tree ring (RW and BI) chronologies and CRU TS 4.07 monthly / seasonal temperature for different pollution periods. The FULL period represents the common period for all sites from 1902-2012 (except for NB which starts in 1928). Pre-POL, POL and post-POL represent the pre-pollution period (1911-1950), heavily polluted period (1951-1990) and post-pollution period (1991-to variable end year for each site with the temporal span based on replication with 10 or more series – see Table 2), respectively. Only significant correlations are displayed with a significance level of 0.01. Lowercase letters along the x-axis indicate months of the previous year relative to the growth year.

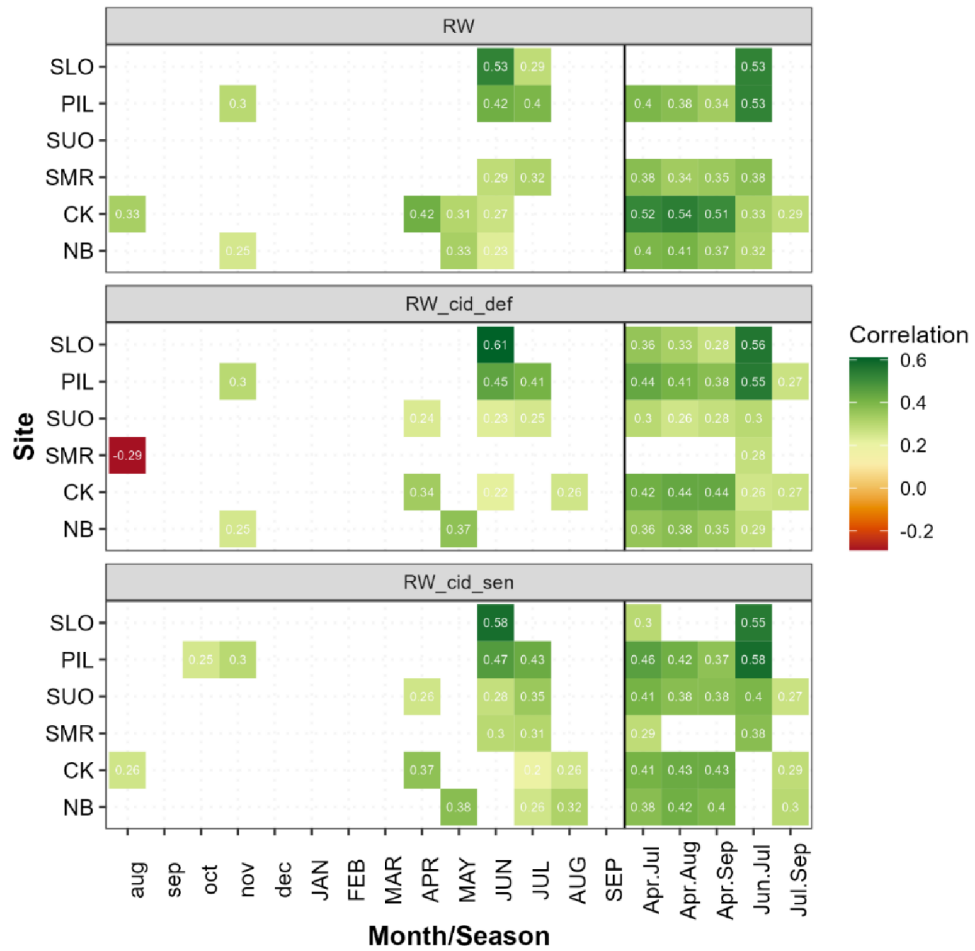


Fig. B7. Growth climate correlations between original ring width (RW) and CID-treated chronologies using standard (RW_cid_def; 3.29 st.dev.) and more sensitive (RW_cid_sen; 2.81 st.dev.) detection settings with monthly / seasonal CRU TS 4.07 temperatures for the period 1902-2012 (except for NB which starts in 1928). Only significant correlations are displayed with significance level of 0.01. Lowercase letters along the x-axis indicate months of the previous year relative to the growth year.

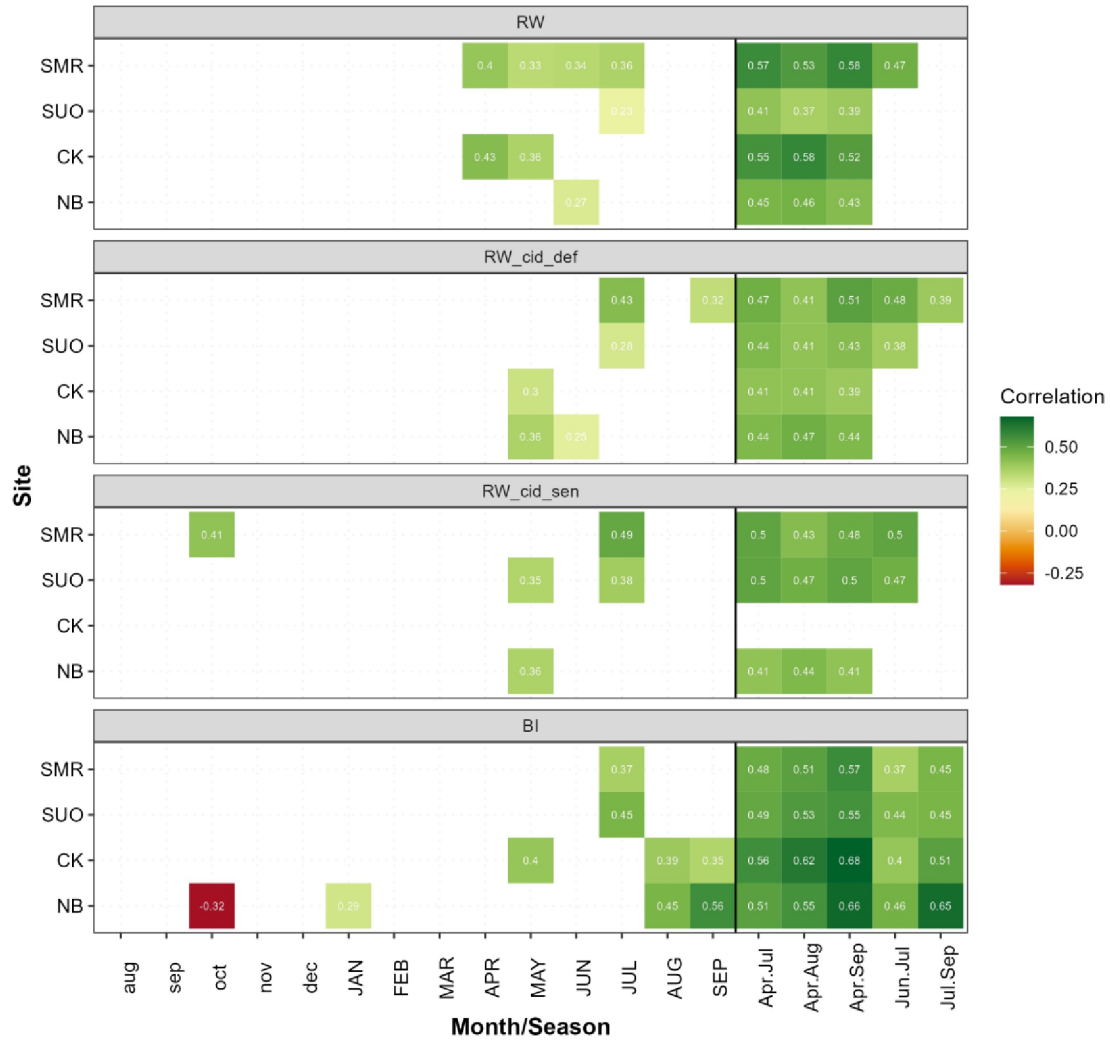


Fig. B8. Growth climate correlations between different tree ring chronologies and monthly / seasonal instrumental temperature (dataset from the CHMU meteorological stations) for the period 1962-2012. Only significant correlations are displayed with a significance level of 0.01. Sites PIL and SLO are not included as the instrumental climate data from the CHMU dataset were not available for those locations.

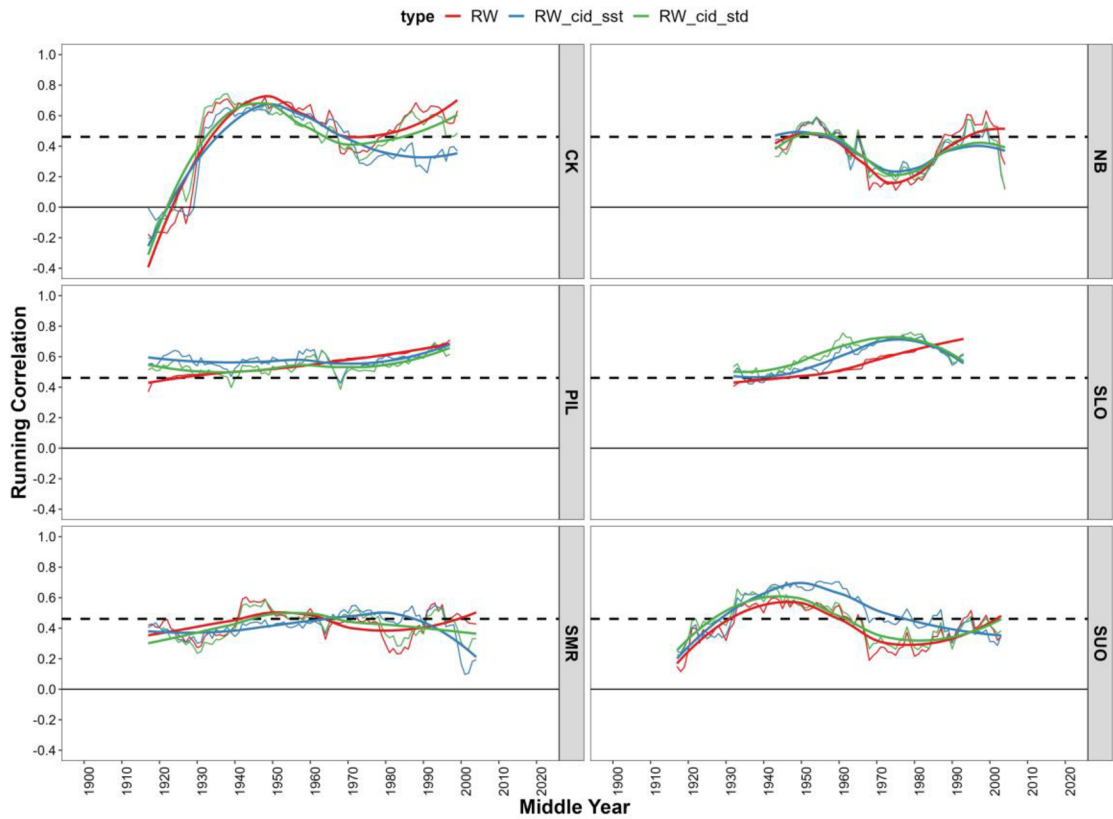


Fig. B9. 31-year running correlations between original ring width (RW), and CID-treated chronologies using standard (RW_cid_std; 3.29 st.dev.) and more sensitive (RW_cid_sst; 2.81 st.dev.) detection settings, and optimal seasonal temperatures for each parameter (selected according to seasonal correlation results in Fig. 4). The correlation periods were truncated before 1902 and replication for all sites over the entire period reached or exceeded 10 series. Chronologies were correlated with Jun-Jul (for sites SMR, SUO, SLO and PIL) and Apr-Aug (for sites NB and CK) seasonal CRU TS 4.07 temperatures. Horizontal bold dashed lines represent the 0.01 significance level. Solid curves represent smoothed values using the ‘loess’ method (with the following parameter settings: $n = 80$, $\text{span} = 0.4$) in the R package ‘ggplot2’.

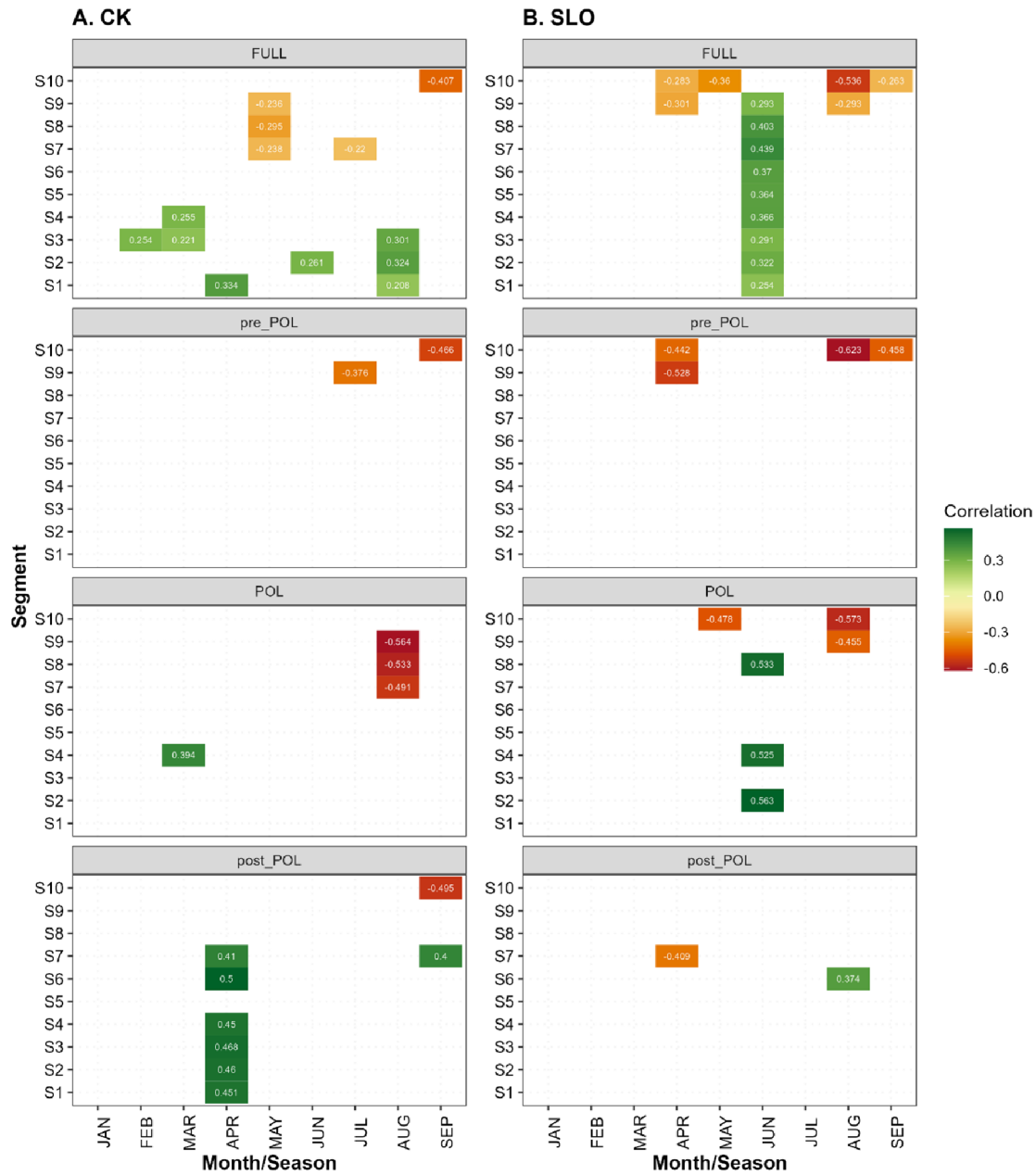


Fig. B10. Growth climate correlations between lumen area (LA) and temperature for different pollution periods of site CK and SLO, respectively. Only significant correlations are displayed with significance level of 0.01.

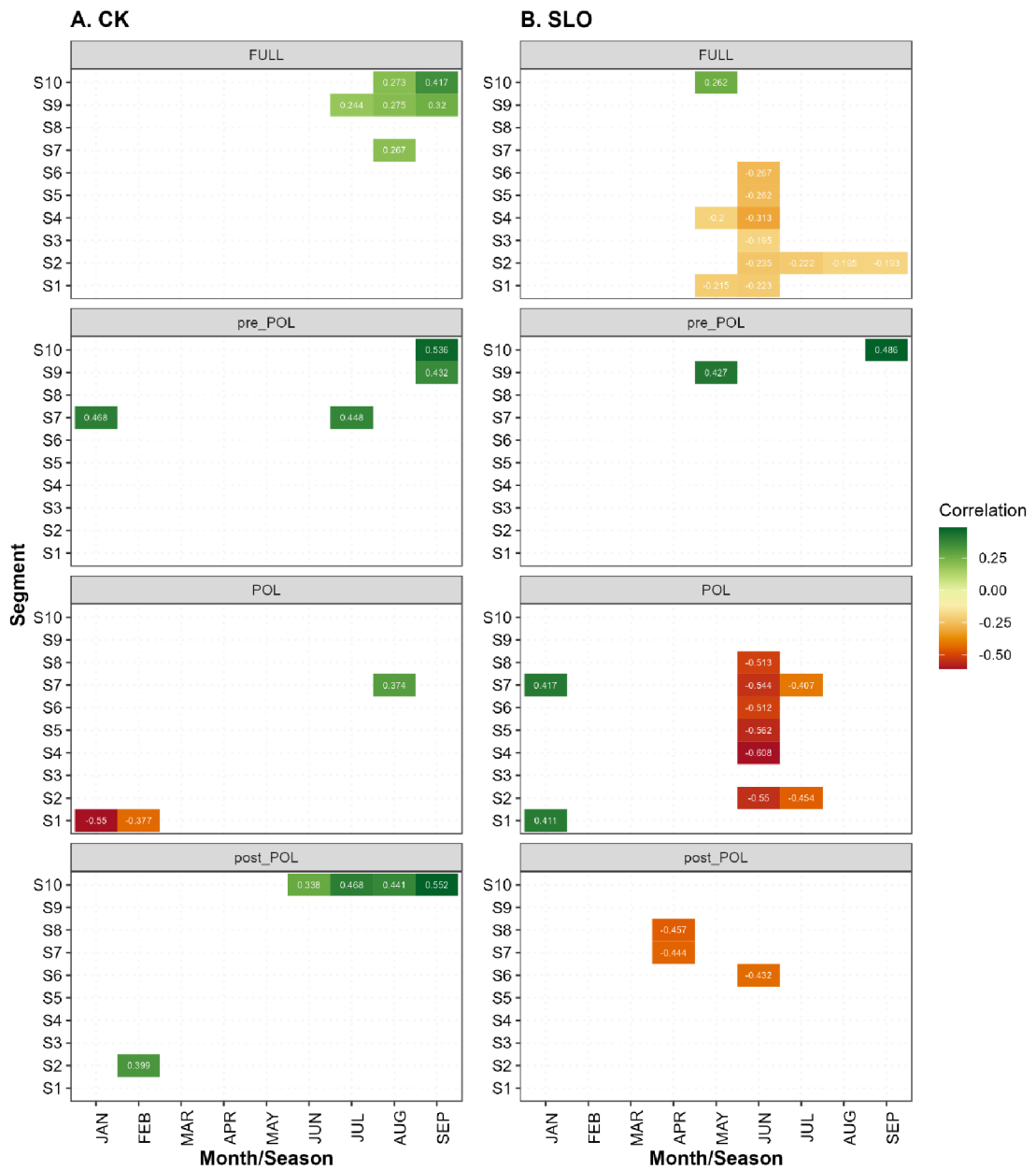


Fig. B11. Growth climate correlations between lumen area (LA) and SPEI for different pollution periods of site CK and SLO, respectively. Only significant correlations are displayed with significance level of 0.01.

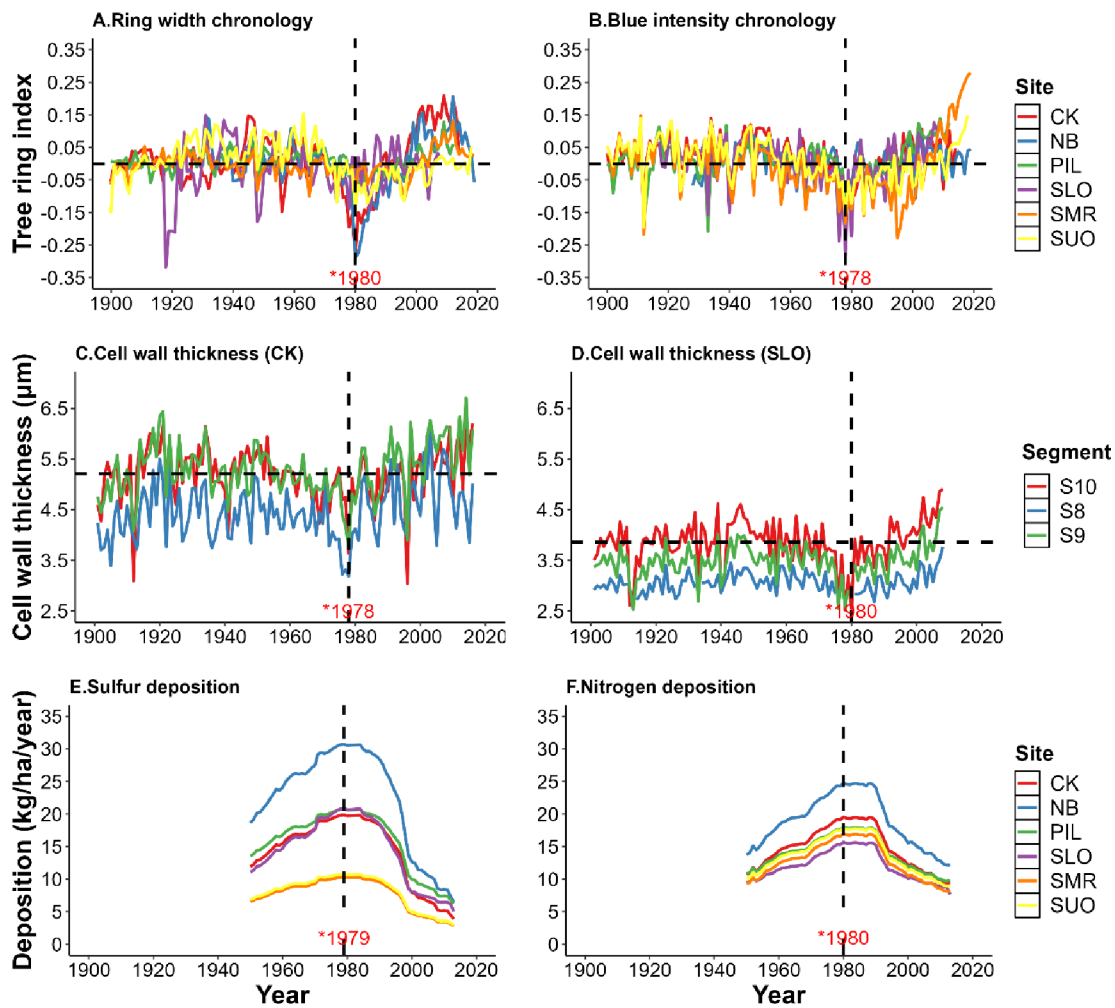


Fig. B12. Long-term trends of tree growth represented by different tree ring parameters and pollution history of all studied sites (unsmoothed). (A) and (B) display the ring width (RW) and blue intensity (BI) chronologies. (C) and (D) display the cell wall thickness (CWT) of segments 8-10 for sites CK and SLO. (E) and (F) display the sulfur and nitrogen deposition for the period 1950 to 2013. RW and BI chronologies are truncated before the year 1900 and the replication of all sites over the period 1900-2013 exceeds 10 series, except for the start year for CK and SLO are 1928 and 1917, respectively. Vertical dashed lines mark years with the highest average pollution levels (E, F) and the lowest average growth values of different parameters (A-D). Horizontal dashed lines in C and D represent the average CWT of segment 10 for site CK (for the 1900-2016 period) and SLO (for the 1900-2008 period), respectively.

APPENDIX C

APPENDIX C contains the additional supporting materials for **Subsection 3.4/ 4.3/ 5.3**.

Equation C1. Final GAMM model

$$\begin{aligned} \text{sqrt}(Rt) \sim & \text{Species} + \text{Year} + \text{Species} \times \text{Year} + s(\text{SPEI}, \text{Species}) + s(\text{Elevation}) \\ & + s(\text{Age}) + s(\text{Size}) + ti(\text{SPEI}, \text{Elevation}) + ti(\text{SPEI}, \text{Age}) + \left(\frac{\text{plotid}}{\text{treeid}} \right) \\ & + r \end{aligned} \quad (\text{Equation. S1})$$

where *Species* is the species identity (factorial variable, 5 levels, ‘*Fagus sylvatica*’ as the reference level), *Year* is the drought year (factorial variable, 3 levels, ‘2003’ as the reference level), *SPEI* is the site-specific SPEI value during the drought (unitless), *Elevation* is the elevation (in m a.s.l.), *Age* is the tree age during the drought year (based on ring count, in years), *Size* refers to accumulated tree basal area (in cm²), *plotid* and *treeid* are unique identifiers for plots and trees, respectively. ‘*s*’ indicates that a variable was fitted using a smoothing spline, and ‘*ti*’ stands for the tensor product fit of interaction terms, and ‘*r*’ is the residual error term.

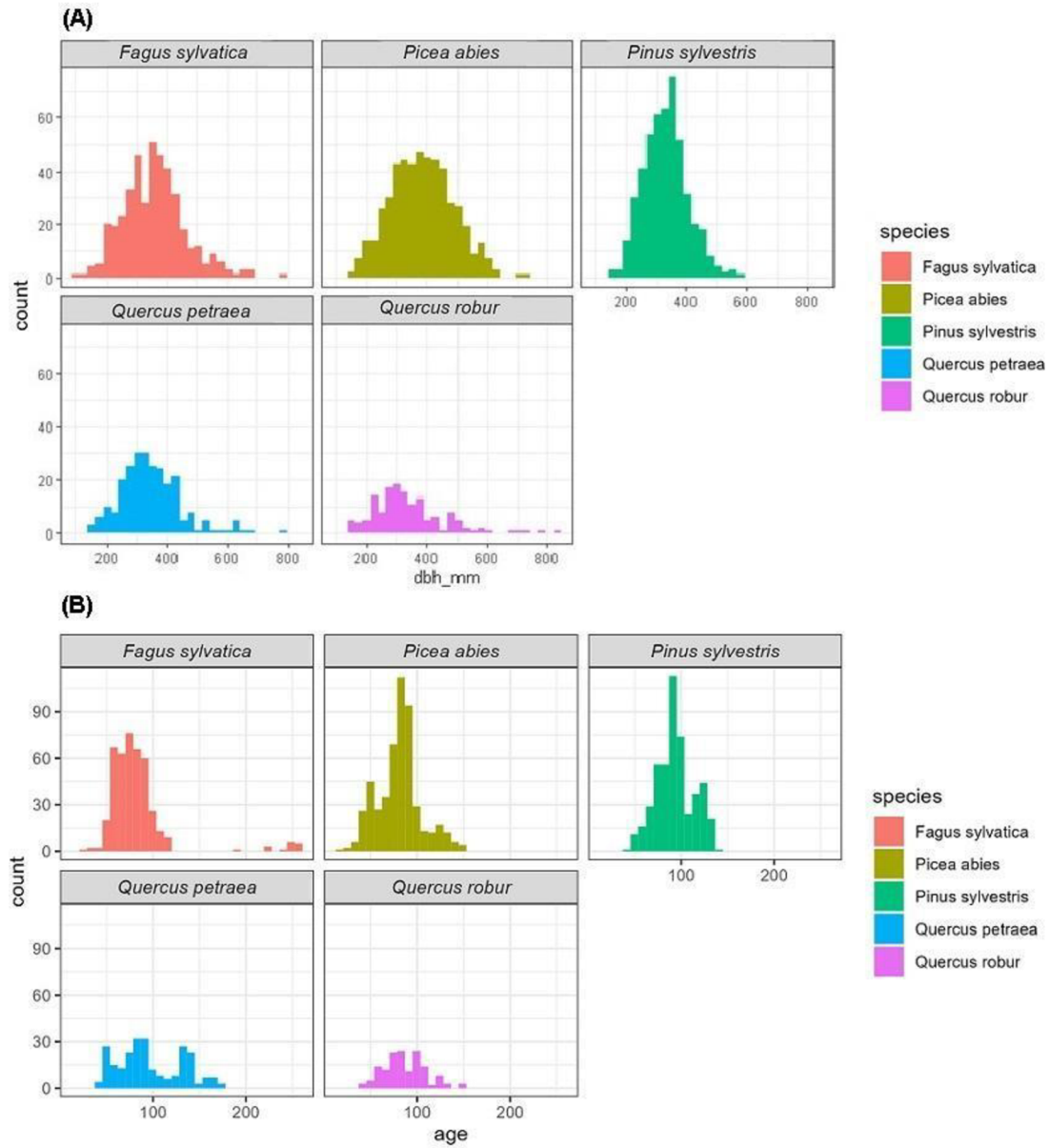


Fig. C1. DBH and age distribution of the five species. ‘dbh_mm’ is the diameter at breast height in mm. ‘age’ is the lifespan of each tree. ‘count’ is the number of trees.

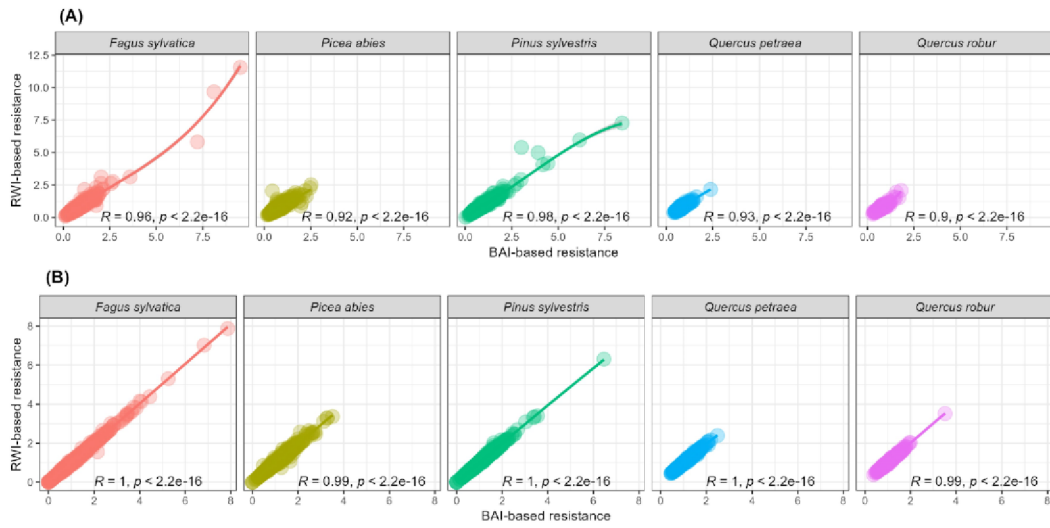


Fig. C2. RWI-based and BAI-based drought resistance comparison, of (A) two periods (2015-2019 VS 2005-2009) and (B) individual extreme drought (2003, 2015, 2018).

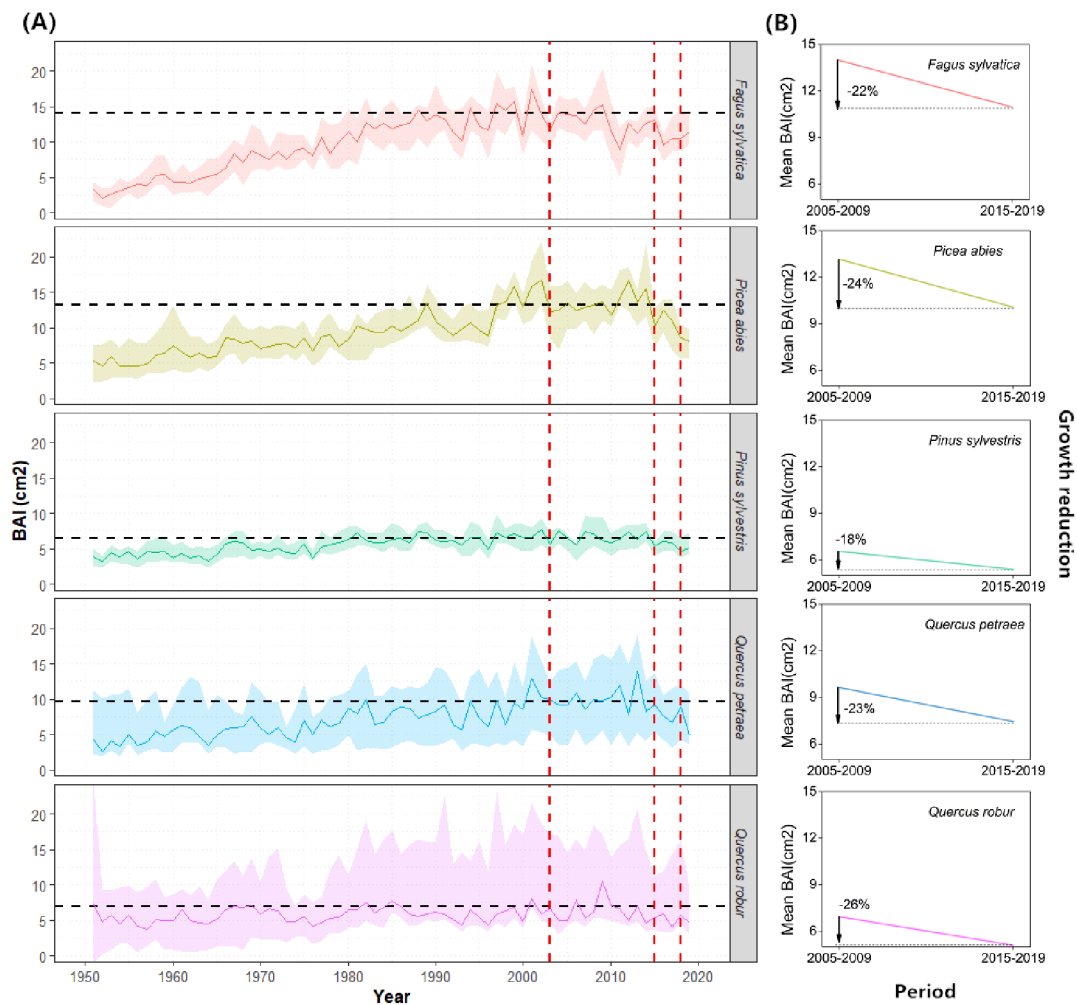


Fig. C3. Growth trajectories during the period 1950-2019. Displayed are medians (plain lines) and 95% confidence intervals of Basal Area Increment (BAI), by species. Vertical red dashed lines denote dry extremes. Horizontal black dashed lines represented the mean BAI of the “reference” period (2005-2009). In (B), medians of the mean BAI for the specified periods are displayed. Vertical black arrows and colored diagonals indicate relative growth reductions from the reference period (2005-2009) to the dry period (2015-2019).

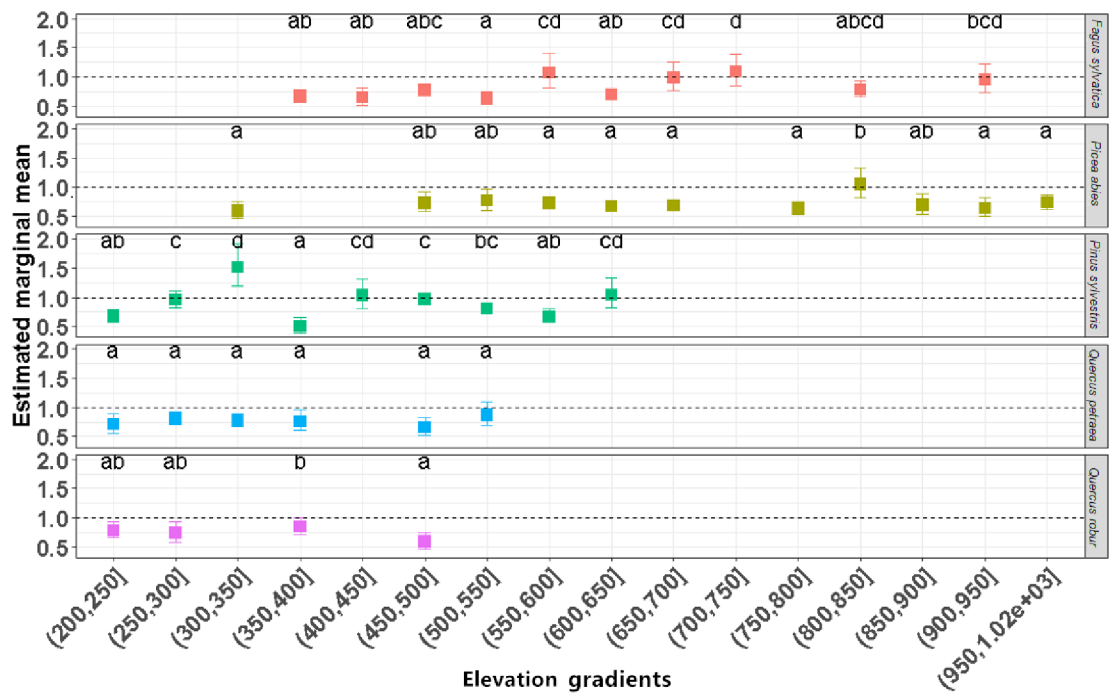


Fig. C4. Difference in impact of the 2015-2019 dry period on growth depending on the species and the elevation gradients. The x-axis presents elevation gradients in m. Different letters at the top of each panel indicate the significant difference, mean values marked by contrasting letters are significantly different ($p < 0.05$).

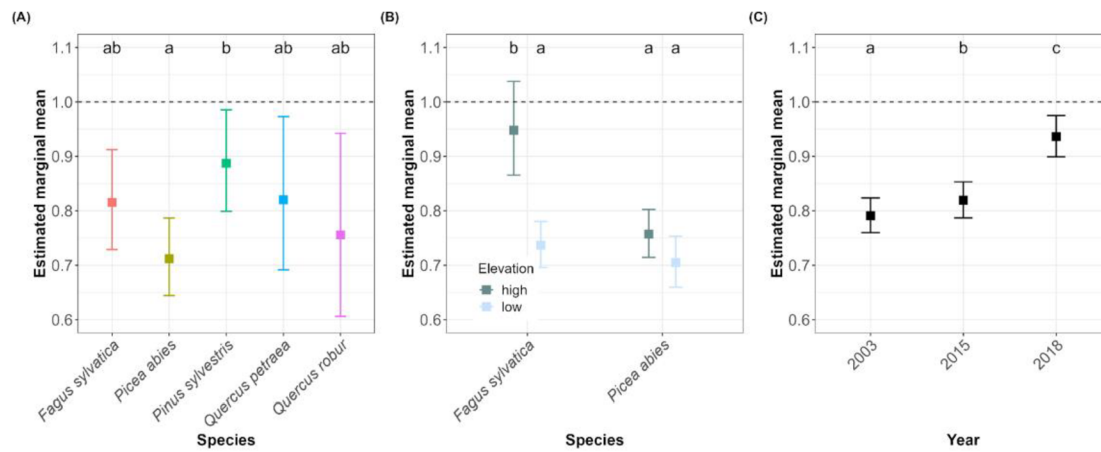


Fig. C5. Impacts of the dry period (2015-2019) and extremely dry years (2003, 2015, 2018) on tree growth (BAI-based). Panels A and B represent linear modeled logarithmic transformed least-square means of the ratio (drought resistance) between the average BAI of the 2015-2019 and 2005-2009 periods (plain squares, back transformed to the original scale) and 95% confidence intervals. Results are shown (A) by species, and (B) by elevation classes, for beech and spruce (i.e., the only two species distributed across the entire elevation gradient). In (B), elevation higher than 650 m a.s.l was defined as “high elevation”, and below or equal to 650 m a.s.l. was defined as “low elevation”. (C) Displays the logarithmic transformation least squares models of a ratio between growth rate during the individual drought year and the mean growth rates for the two years immediately preceding the dry event. Different letters at the top of each panel indicate significant differences in mean values ($p < 0.05$). The black dashed lines denote a ratio of 1, indicative of the BAI during the reference period.

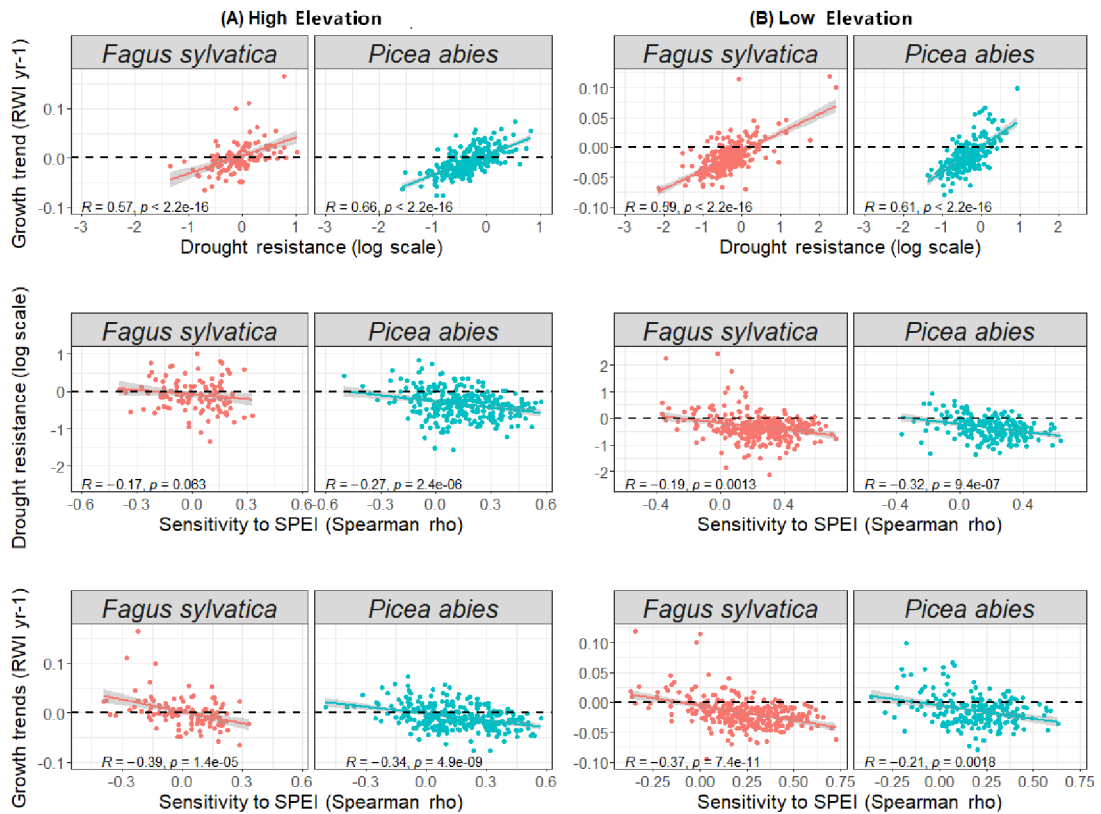


Fig. C6. Links between drought impact (Drought resistance), trees' sensitivity to variability in moisture availability (Sensitivity to SPEI, assessed by the Spearman's rank between RWI and SPEI12) and growth trends (Growth trends, Sen's slope of RWI through the 1995-2019 time-period) in high (> 650 m) and low (< = 650 m) elevations of two species (the only two species distributed over the whole elevation gradient). Dots represent observed values, lines and shadings indicate regression lines and 95% confidence intervals, respectively. Also shown are the Spearman rho ('r') and p-values.

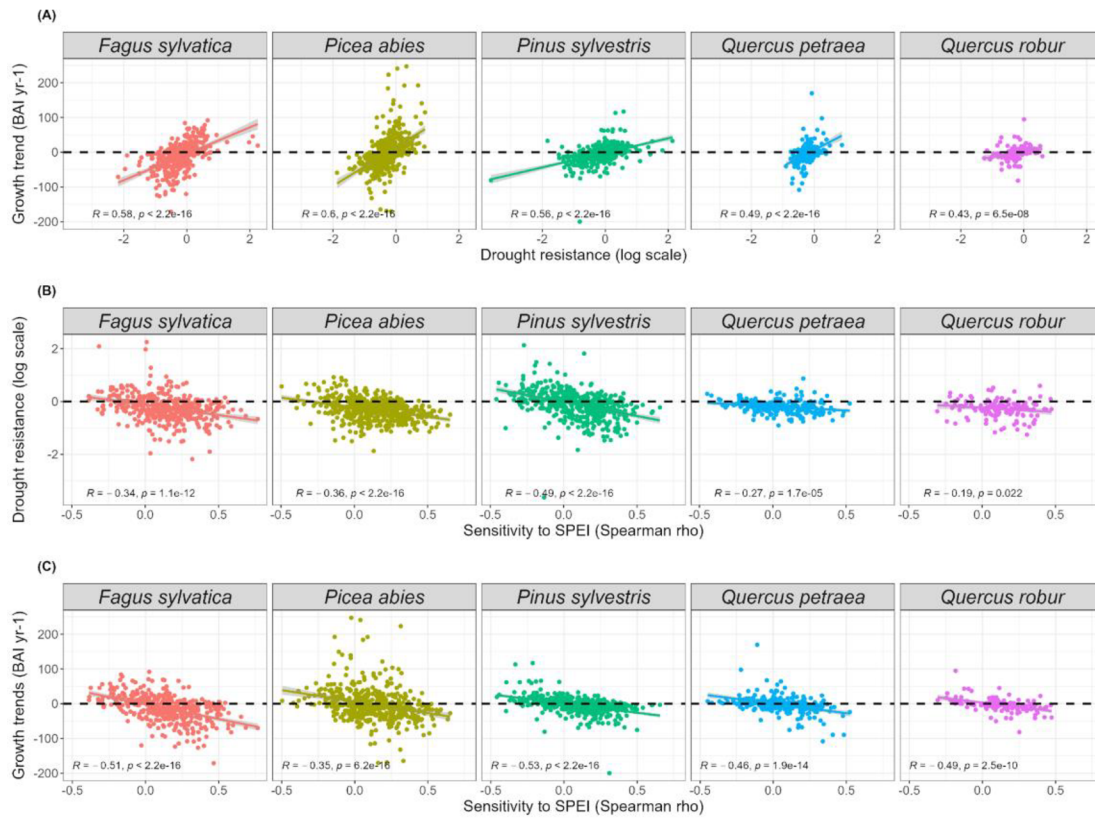


Fig. C7. Links between drought resistance, tree sensitivity to variability in moisture availability (i.e., sensitivity to SPEI, based on Spearman's rank coefficient between BAI and SPEI12) and growth trends (based on Sen's slope of BAI) during the period of 1995-2019. Dots represent observed values, and shadings indicate 95% confidence intervals. Spearman rho ('r') and p-values are also presented.

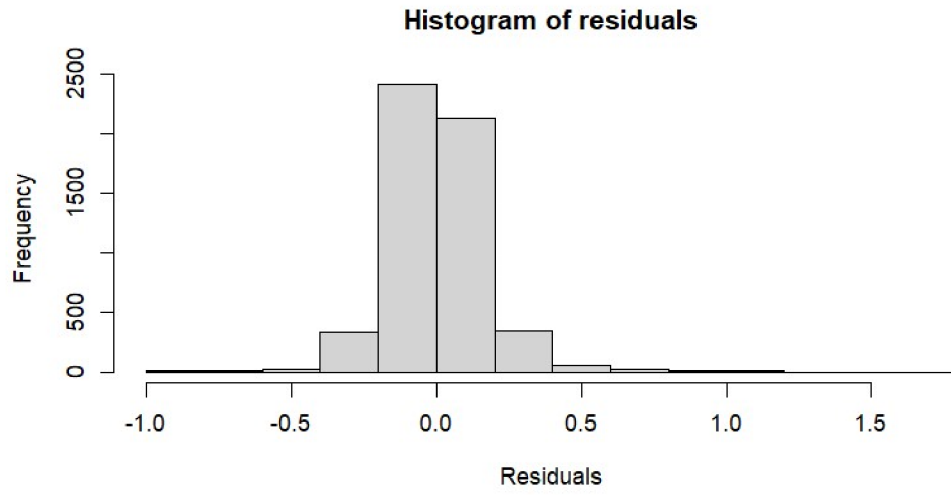


Fig. C8. Model residual diagnostics (RWI based model).

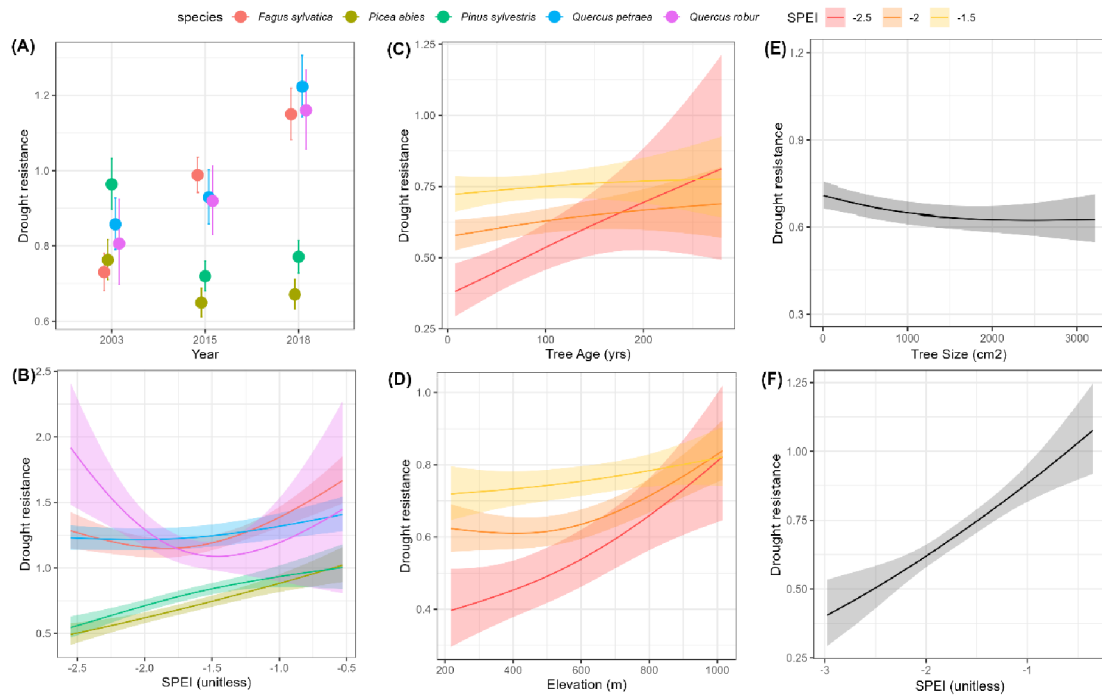


Fig. C9. Drivers of drought resistance (BAI based). Displayed are predicted mean values (dots) and their 95% confidence intervals (lines) in A, as well as functions (lines) and confidence bounds (shadings) in B - F, indicating the resistance of trees to extreme dry years. The relationships are presented between (A) SPEI, year and species, as well as functions for SPEI and (B) species, (C) tree age, (D) elevation, (E) tree size, and (F) SPEI for single species. Predictions were made based on the generalized additive mixed model (Equation 1). For each panel, explanatory variables other than the variable of interest were fixed to their mean values; in panels B-F results are based on the year 2018, and in panels C-F, results are based on the tree species Norway spruce.

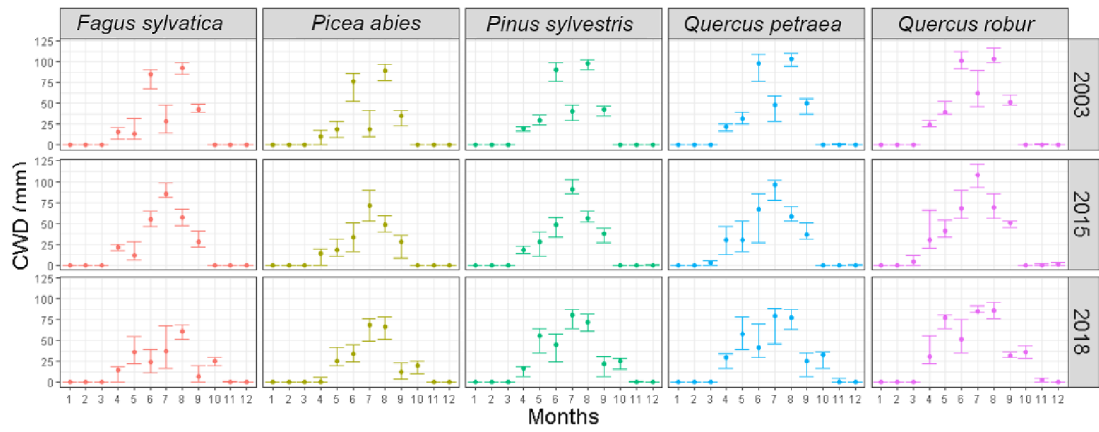


Fig. C10. Climatic Water Deficit (CWD) of dry years by species.

(A) Parametric terms					
Variable	Estimate	Std. Error	t value	p-value	Signif.
(Intercept)	0.87	0.01	62.07	0.0000	***
Species <i>Picea abies</i> (vs <i>Fagus sylvatica</i>)	0.00	0.02	-0.13	0.8958	NS
Species <i>Pinus sylvestris</i> (vs <i>Fagus sylvatica</i>)	0.11	0.02	5.62	0.0000	***
Species <i>Quercus petraea</i> (vs <i>Fagus sylvatica</i>)	0.05	0.02	2.11	0.0353	*
Species <i>Quercus robur</i> (vs <i>Fagus sylvatica</i>)	0.05	0.03	1.76	0.0792	NS
Year 2015 (vs 2003)	0.14	0.01	10.01	0.0000	***
Year 2018 (vs 2003)	0.22	0.02	12.11	0.0000	***
Species <i>Picea abies</i> : year 2015	-0.20	0.02	-9.45	0.0000	***
Species <i>Pinus sylvestris</i> : year 2015	-0.27	0.02	-11.74	0.0000	***
Species <i>Quercus petraea</i> : year 2015	-0.10	0.02	-4.90	0.0000	***
Species <i>Quercus robur</i> : year 2015	-0.07	0.03	-2.19	0.0284	*
Species <i>Picea abies</i> : year 2018	-0.27	0.02	-11.29	0.0000	***
Species <i>Pinus sylvestris</i> : year 2018	-0.32	0.02	-13.07	0.0000	***
Species <i>Quercus petraea</i> : year 2018	-0.04	0.02	-1.73	0.0832	NS
Species <i>Quercus robur</i> : year 2018	-0.03	0.03	-0.98	0.3254	NS
(B) Smooth terms					
Variable	Estimate	Std. Error	t value	p-value	Signif.
s(SPEI): Species <i>Fagus sylvatica</i>	1.80	2.00	5.26	0.0026	**
s(SPEI): Species <i>Picea abies</i>	1.67	2.00	18.89	0.0000	***
s(SPEI): Species <i>Pinus sylvestris</i>	1.78	2.00	19.78	0.0000	***
s(SPEI): Species <i>Quercus petraea</i>	0.00	2.00	0.00	0.7651	NS
s(SPEI): Species <i>Quercus robur</i>	1.70	2.00	10.00	0.0000	***
s(Elevation): Species <i>Fagus sylvatica</i>	1.02	2.00	3.55	0.0044	**
s(Elevation): Species <i>Picea abies</i>	1.17	2.00	6.41	0.0002	***
s(Elevation): Species <i>Pinus sylvestris</i>	0.00	2.00	0.00	0.7393	NS
s(Elevation): Species <i>Quercus petraea</i>	0.00	2.00	0.00	0.4670	NS
s(Elevation): Species <i>Quercus robur</i>	0.00	2.00	0.00	0.3907	NS
s(Age): Species <i>Fagus sylvatica</i>	0.00	2.00	0.00	0.3374	NS
s(Age): Species <i>Picea abies</i>	0.76	2.00	1.37	0.0521	NS
s(Age): Species <i>Pinus sylvestris</i>	0.00	2.00	0.00	0.8056	NS
s(Age): Species <i>Quercus petraea</i>	0.76	2.00	1.34	0.0495	*
s(Age): Species <i>Quercus robur</i>	0.00	2.00	0.00	0.8643	NS
s(Size): Species <i>Fagus sylvatica</i>	0.00	2.00	0.00	0.3143	NS
s(Size): Species <i>Picea abies</i>	1.55	2.00	7.22	0.0001	***
s(Size): Species <i>Pinus sylvestris</i>	0.00	2.00	0.00	0.2677	NS
s(Size): Species <i>Quercus petraea</i>	0.68	2.00	0.79	0.0976	NS
s(Size): Species <i>Quercus robur</i>	0.00	2.00	0.00	0.4319	NS
ti(SPEI, Elevation)	3.48	4.00	8.83	0.0000	***

ti(SPEI, Age)	1.99	4.00	2.69	0.0020	**
ti(SPEI, Size)	0.00	4.00	0.00	0.6168	NS
ti(Elevation, Age)	0.00	4.00	0.00	0.7969	NS
ti(Elevation, Size)	0.89	4.00	0.62	0.0586	NS
ti (Age, Size)	0.00	4.00	0.00	0.3391	NS

Table C1. Outputs from the GAMM global model (RWI based). Shown are estimated coefficients, standard errors, and t-values for parametric terms, estimated degree of freedom (edf), reference degree of freedom (Ref. df), F-value (F) for smooth terms. Significance levels (Signif.) are as follows: NS = non-significant; * = p-value < 0.05, ** = p-value < 0.01, *** = p-value < 0.001.

(A) Parametric terms					
Variable	Estimate	Std. Error	t value	p-value	Signif.
(Intercept)	0.88	0.01	65.91	0.0000	***
Species <i>Picea abies</i> (vs <i>Fagus sylvatica</i>)	0.00	0.02	0.00	0.9968	NS
Species <i>Pinus sylvestris</i> (vs <i>Fagus sylvatica</i>)	0.10	0.02	5.34	0.0000	***
Species <i>Quercus petraea</i> (vs <i>Fagus sylvatica</i>)	0.06	0.02	2.44	0.0147	**
Species <i>Quercus robur</i> (vs <i>Fagus sylvatica</i>)	0.06	0.03	1.94	0.0526	NS
Year 2015 (vs 2003)	0.14	0.01	9.80	0.0000	***
Year 2018 (vs 2003)	0.22	0.02	11.71	0.0000	***
Species <i>Picea abies</i> : year 2015	-0.21	0.02	-9.81	0.0000	***
Species <i>Pinus sylvestris</i> : year 2015	-0.27	0.02	-11.69	0.0000	***
Species <i>Quercus petraea</i> : year 2015	-0.10	0.02	-4.96	0.0000	***
Species <i>Quercus robur</i> : year 2015	-0.08	0.03	-2.45	0.0144	**
Species <i>Picea abies</i> : year 2018	-0.27	0.02	-11.55	0.0000	***
Species <i>Pinus sylvestris</i> : year 2018	-0.32	0.02	-12.90	0.0000	***
Species <i>Quercus petraea</i> : year 2018	-0.04	0.02	-1.59	0.1128	NS
Species <i>Quercus robur</i> : year 2018	-0.04	0.03	-1.12	0.2636	NS
(B) Smooth terms					
Variable	edf	Ref.df	F	p-value	Signif.
s(SPEI): Species <i>Fagus sylvatica</i>	1.82	2.00	6.18	0.0010	**
s(SPEI): Species <i>Picea abies</i>	1.68	2.00	19.61	0.0000	***
s(SPEI): Species <i>Pinus sylvestris</i>	1.78	2.00	18.80	0.0000	***
s(SPEI): Species <i>Quercus petraea</i>	0.00	2.00	0.00	0.7890	NS
s(SPEI): Species <i>Quercus robur</i>	1.66	2.00	9.29	0.0000	***
s(Elevation)	1.54	2.00	8.59	0.0000	***
s(Age)	1.13	2.00	3.78	0.0039	**
s(Size)	1.63	2.00	10.22	0.0000	***
ti(SPEI, Elevation)	3.48	4.00	9.03	0.0000	***
ti(SPEI, Age)	2.00	4.00	2.50	0.0031	**

Table C2. Outputs from the GAMM final model (BAI based). Shown are estimated coefficients, standard errors, and t-values for parametric terms, estimated degree of freedom (edf), reference degree of freedom (Ref. df), F-value (F) for smooth terms. Significance levels (Signif.) are as follows: NS = non-significant; * = p-value < 0.05, ** = p-value < 0.01, *** = p-value < 0.001. Non-significant variables have been removed from the final model based on AIC scores.